REPORT NO.
UCD/CGM-14/01

CENTER FOR GEOTECHNICAL MODELING

CPT AND SPT BASED LIQUEFACTION TRIGGERING PROCEDURES

BY

R. W. BOULANGER

I. M. IDRISS

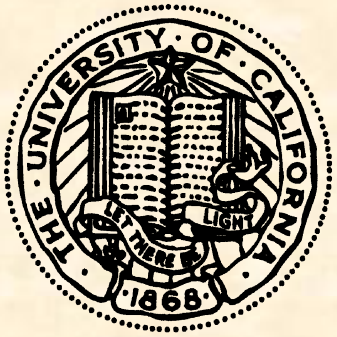

DEPARTMENT OF CIVIL & ENVIRONMENTAL ENGINEERING
COLLEGE OF ENGINEERING
UNIVERSITY OF CALIFORNIA AT DAVIS

April 2014

CPT AND SPT BASED LIQUEFACTION TRIGGERING PROCEDURES

by

Ross W. Boulanger

I. M. Idriss

Report No. UCD/CGM-14/01

Center for Geotechnical Modeling
Department of Civil and Environmental Engineering
University of California
Davis, California

April 2014

TABLE OF CONTENTS

CPT AND SPT BASED LIQUEFACTION TRIGGERING PROCEDURES

1. INTRODUCTION

1.1. Background

The Cone Penetration Test (CPT) and Standard Penetration Test (SPT) are the two most widely used indices for evaluating the liquefaction characteristics of soils. The SPT was used first in developing liquefaction correlations but the CPT has a number of advantages that have made it the primary site characterization tool in certain geologic settings. Shear wave velocity (V_s) tests, Becker Penetration Tests (BPT) and large penetrometer tests (LPT) tend to be used in special situations and thus are used less often than the SPT and CPT in liquefaction evaluations. In most situations, these different site characterization tools have complementary roles and are most effectively used in combinations.

The development of SPT-based and CPT-based liquefaction triggering procedures has progressed over the years through the efforts of countless researchers. Development of SPT-based correlations began in Japan (e.g., Kishida 1966) and progressed through to the landmark work of Seed et al. (1984, 1985) which set the standard in engineering practice for over two decades (Youd et al. 2001). Recent updates to SPT-based procedures include those by Idriss and Boulanger (2008, 2010). The SPT-based procedures from Youd et al. (2001) and Idriss and Boulanger (2010) are compared in Figure 1.1 with the case history data (from Idriss and Boulanger 2010) adjusted to the equivalent vertical effective stress of σ'_v = 1 atm (101.3 kPa, 2117 psf) and an earthquake of moment magnitude of M = 7.5. Development of CPT-based procedures began with work by Zhou (1980) using observations from the 1978 Tangshan earthquake and was followed by Seed and Idriss (1981) and Douglas et al. (1981) who proposed the use of correlations between SPT and CPT penetration resistances to convert the then available SPT-based liquefaction triggering charts for use with the CPT. Other contributions to the advancement of CPT-based liquefaction triggering procedures since the early 1980s included the work of Shibata and Teparaksa (1988), Stark and Olson (1995), Suzuki et al. (1995, 1997), Robertson and Wride (1997, 1998), Olsen (1997), Moss et al. (2006), and Idriss and Boulanger (2004, 2008). Five recent correlations are compared in Figure 1.2 with the set of clean sand case histories from Idriss and Boulanger (2008) adjusted to an equivalent σ'_v = 1 atm and M = 7.5.

The quantity and quality of CPT and SPT case histories has continued to increase with recent earthquake events, including data obtained in the 2010-2011 Canterbury earthquake sequence in New Zealand (e.g., van Ballegooy et al. 2014, Green et al. 2014) and the 2011 M_w=9.0 Tohoku earthquake in Japan (e.g., Tokimatsu et al. 2012, Cox et al. 2013). For example, Green et al. (2014) compiled 50 high-quality case histories representing cases of liquefaction and no liquefaction during the 2010-2011 Canterbury earthquake sequence with subsurface profiles for which the critical layer could be identified with relatively high confidence. The inclusion of these and other data in liquefaction triggering databases provide an opportunity for re-evaluating liquefaction triggering procedures and updating them as may be warranted.

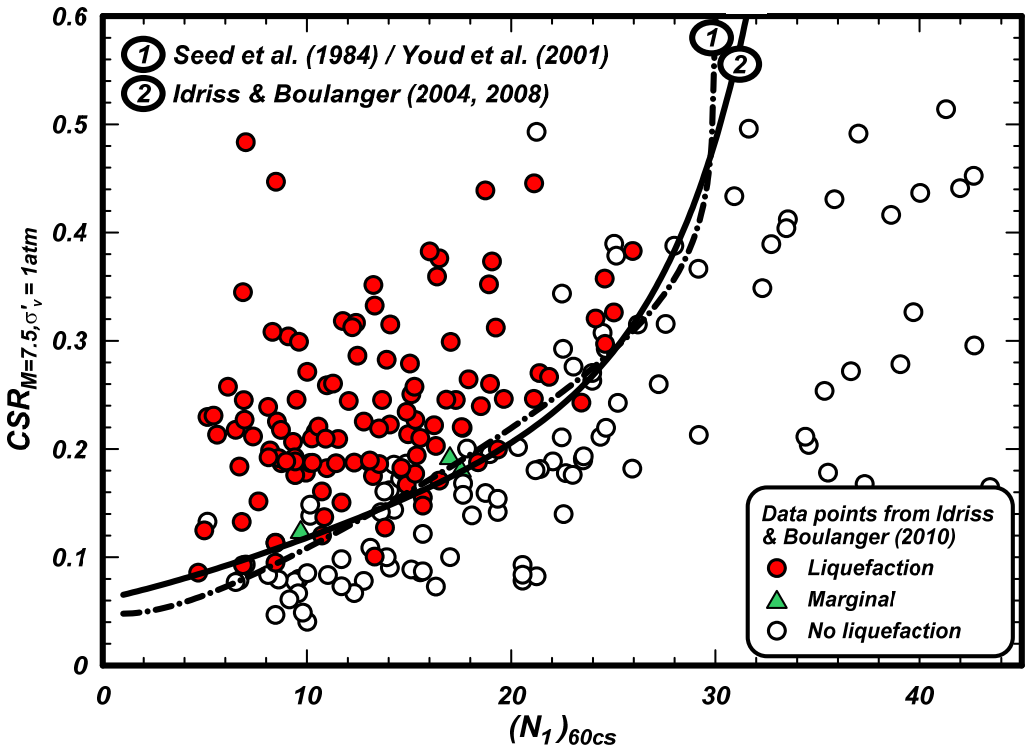

Figure 1.1. Examples of SPT-based liquefaction triggering curves with a database of case histories processed with the Idriss-Boulanger (2008) procedure (from Idriss and Boulanger 2008)

1.2. Purpose

This report presents a re-examination of CPT-based and SPT-based liquefaction triggering procedures for cohesionless soils. The primary focus of this work is on the CPT-based procedure coupled with an examination of effects of a change in the magnitude scaling factor relationship on the SPT-based procedure. Specific tasks covered by this report include the following:

- Summarize the liquefaction triggering analysis framework, including a new magnitude scaling factor relationship and a recommended procedure for estimating fines contents (FC) for use with the CPT-based procedure;
- Update the database of CPT-based case histories, including reexamining older case histories and adding data from recent earthquake events;
- Update the CPT-based liquefaction triggering correlation, as needed;
- Develop a probabilistic version of the CPT-based liquefaction triggering procedure using the updated case history database;
- Examine the SPT-based liquefaction triggering procedure using the revised magnitude scaling factor relationship and including the addition of 24 case histories to the SPT database; and
- Examine the consistency between the CPT-based and SPT-based liquefaction triggering correlations.

The process that has been used by the authors over the past decade to develop the CPT-based and SPT-based procedures has been to draw from a synthesis of experimental, theoretical, and case history

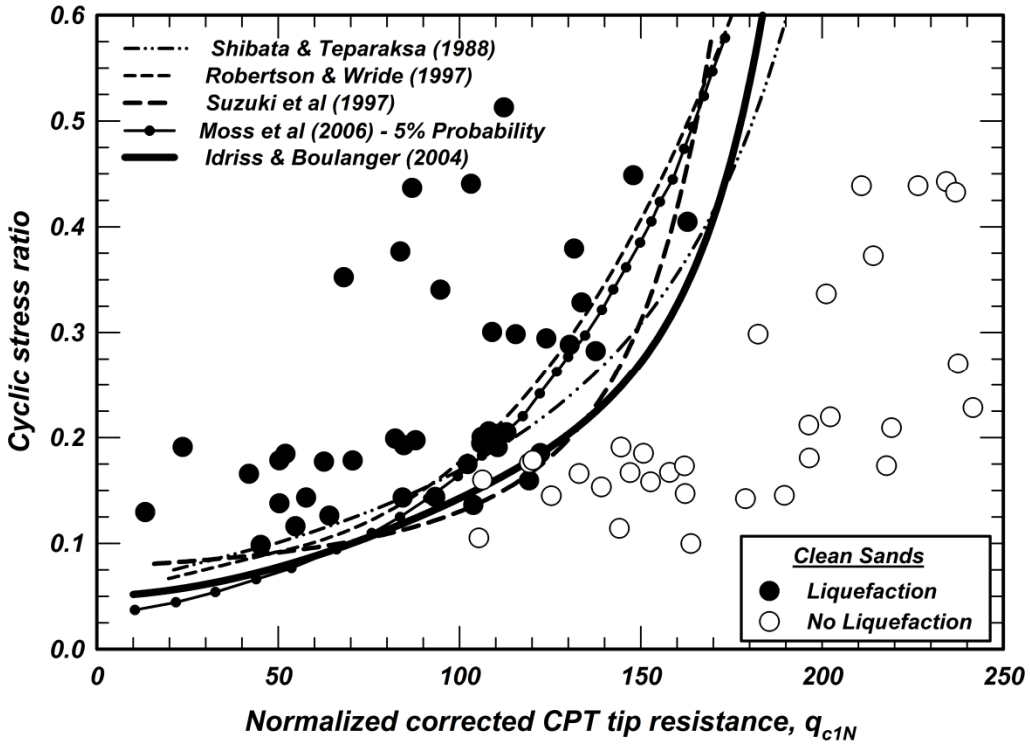

Figure 1.2. Examples of CPT-based liquefaction triggering curves for M = 7.5 and σ'_v = 1 atm with an earlier database of clean sand liquefaction case histories processed with the Idriss-Boulanger (2008) procedure (from Idriss and Boulanger 2008)

findings, rather than view each of the tasks listed above as self-contained parts. This process requires an iterative approach so that each task is informed by findings from the other tasks. It is this synthesis of information from multiple sources that is particularly valuable for arriving at reasonable correlations that are consistent with the cumulative available information while overcoming the unavoidable limitations in each individual source of information.

1.3. Organization of report

Section 2 of this report contains an overview of the liquefaction analysis framework that has been used for the CPT-based and SPT-based liquefaction triggering procedures adopted by the authors. The analysis framework is described in Idriss and Boulanger (2008) except for the revised magnitude scaling factor (MSF) developed herein that accounts for the effects of soil type and denseness. In addition, a recommended relationship and approach for estimating fines contents from CPT data is described.

Section 3 presents the updated database of CPT-based liquefaction/no liquefaction case histories. The selection of earthquake magnitudes, peak accelerations, and representative CPT data are described, and the classification of site performance discussed.

Section 4 presents the updated CPT-based liquefaction triggering correlation and summarizes the distribution of the case history data relative to the updated correlation. The distributions of the data are

examined with respect to various parameters (e.g., fines content, earthquake magnitude, overburden stress) and data sources (e.g., FC from lab data or from CPT-based correlations).

Section 5 describes the development of a probabilistic version of the CPT-based liquefaction triggering correlation using the updated case history database. Sensitivity of the derived probabilistic relationship to the key assumptions is examined, and issues affecting the application of probabilistic liquefaction triggering models in practice are discussed.

Section 6 presents an examination of the effect of the revised MSF relationship on the SPT-based liquefaction triggering procedure. In addition, the SPT-based database by Boulanger et al. (2012) was augmented with 24 additional case histories. The distributions of the case history data relative to the Idriss and Boulanger (2008) triggering correlation are examined with respect to various parameters (e.g., fines content, earthquake magnitude, overburden stress).

Section 7 examines consistency of the CPT-based and SPT-based liquefaction triggering correlations in terms of implied q_c/N_{60} ratios and CRR versus relative state parameter relationships. The derived triggering relationship is also compared to those derived by Mitchell and Tseng (1990) based on results of calibration chamber tests, cyclic laboratory tests, and cone penetration analyses.

Section 8 summarizes the major findings and provides concluding remarks.

Appendix A presents the revised magnitude scaling factor relationship.

2. ANALYSIS FRAMEWORK

2.1. A stress-based framework

The stress-based approach for evaluating the potential for liquefaction triggering, initiated by Seed and Idriss (1967), compares the earthquake-induced cyclic stress ratios (CSR) with the cyclic resistance ratios (CRR) of the soil. The soil's CRR is usually correlated to an in-situ parameter such as CPT penetration resistance, SPT blow count, or shear wave velocity, V_s. An overview of the stress-based approach that has been used with CPT or SPT data is presented in this section, followed by additional details regarding specific model components and analysis procedures in sections 2.2 – 2.7.

Earthquake-induced cyclic stress ratio (CSR)

The earthquake-induced CSR, at a given depth, z, within the soil profile, is usually expressed as a representative value (or equivalent uniform value) equal to 65% of the maximum cyclic shear stress ratio, i.e.:

$$CSR_{M,\sigma'_v} = 0.65\frac{\tau_{\max}}{\sigma'_v} \tag{2.1}$$

where τ_{max} = maximum earthquake induced shear stress, σ'_v = vertical effective stress, and the subscripts on the CSR indicate that it is computed for a specific earthquake magnitude (moment magnitude, M) and in-situ σ'_v. The choice of the reference stress level (i.e., the factor 0.65) was selected by Seed and Idriss (1967) and has been in use since. Selecting a different reference stress level would alter the values of certain parameters and relationships but would have no net significant effect on the final outcome of the derived liquefaction evaluation procedure, as long as this same reference stress level is used throughout, including forward calculations. The value of τ_{max} can be estimated from dynamic response analyses, but such analyses must include a sufficient number of input acceleration time series and adequate site characterization details to be reasonably robust. Alternatively, the maximum shear stress can be estimated using the equation, developed as part of the Seed-Idriss Simplified Liquefaction Procedure, which is expressed as,

$$CSR_{M,\sigma'_v} = 0.65\frac{\sigma_v}{\sigma'_v}\frac{a_{\max}}{g}r_d \tag{2.2}$$

where σ_v = vertical total stress at depth z, a_{max}/g = maximum horizontal acceleration (as a fraction of gravity) at the ground surface, and r_d = shear stress reduction factor that accounts for the dynamic response of the soil profile.

Cyclic resistance ratio (CRR) and penetration resistances

The CRR is correlated to CPT and SPT penetration resistances after application of procedural and overburden stress corrections. For SPTs, the various procedural corrections for arriving at a standardized, energy-corrected N_{60} value are summarized in Idriss and Boulanger (2008, 2010) and thus not repeated herein. For CPTs, a procedural aspect which warrants clarification for liquefaction applications is correction of the measured tip resistance (q_c) for unequal end area effects (Campanella et al. 1982) as,

$$q_t = q_c + (1 - a_r) u_2 \tag{2.3}$$

where q_t = the cone tip resistance corrected for unequal end area effects, a_r = area ratio for the cone tip (typical values between 0.65 and 0.85), and u_2 = pore pressure measured behind the cone tip. The magnitude of this correction can be significant for soft clays (as $u_2 > u_0$, where u_o = steady state or hydrostatic pore pressure), but is typically quite small for sands (as $u_2 \approx u_0$). Thus, the terms q_c and q_t are approximately equal in sands and often used interchangeably even if the correction for unequal area effects has been performed. The term q_c is used herein, with the understanding that the correction has been performed whenever the u_2 data are available.

CPT and SPT penetration resistances are corrected for overburden stress effects as,

$$q_{c1N} = C_N q_{cN} = C_N \frac{q_c}{P_a} \tag{2.4}$$

$$(N_1)_{60} = C_N N_{60} \tag{2.5}$$

where C_N = overburden correction factor, P_a = atmospheric pressure, $q_{cN} = q_c/P_a$, and q_{c1N} and $(N_1)_{60}$ are the penetration resistances that would be obtained in the same sand at an overburden stress of 1 atm if all other attributes remain constant (e.g., same relative density, fabric, age, degree of cementation, loading history). Maki et al. (2014) provide a review of overburden normalization frameworks for sands and clays that are based on different assumptions (i.e., same state parameter versus same void ratio); the effect of these alternative normalization schemes on liquefaction triggering correlations are currently being examined, but are not included in this report.

The soil's CRR is dependent on the duration of shaking (which is expressed through an earthquake magnitude scaling factor, MSF) and effective overburden stress (expressed through a K_σ factor). The correlation for CRR is therefore developed by adjusting the case history CSR values to a reference M = 7.5 and σ'_v = 1 atm as,

$$CSR_{M=7.5,\sigma'_v=1} = \frac{CSR_{M,\sigma'_v}}{MSF \cdot K_\sigma} \tag{2.6}$$

The resulting correlation for $CRR_{M=7.5,\sigma'=1}$ is then adjusted to other values of M and σ'_v using,

$$CRR_{M,\sigma'_v} = CRR_{M=7.5,\sigma'_v=1} \cdot MSF \cdot K_\sigma \tag{2.7}$$

The soil's CRR is further affected by the presence of sustained static shear stresses, such as may exist beneath foundations or within slopes. The effect of sustained static shear stresses, which may be expressed through a K_α factor, is generally small for nearly level ground conditions and is not included herein because the case history database is dominated by level or nearly level ground conditions.

The correlation of CRR to q_{c1N} or $(N_1)_{60}$ in cohesionless soils is also affected by the soil's fines content (FC) which can be expressed as either of,

$$CRR_{M=7.5,\sigma'_v=1} = f\left[q_{c1N}, FC\right] \tag{2.8}$$

$$CRR_{M=7.5,\sigma'_v=1} = f\left[\left(N_1\right)_{60}, FC\right] \tag{2.9}$$

For mathematical convenience, this correlation can also be expressed in terms of an equivalent clean-sand q_{c1Ncs} or $(N_1)_{60cs}$ values which are obtained using the following expressions:

$$q_{c1Ncs} = q_{c1N} + \Delta q_{c1N} \tag{2.10}$$

$$\left(N_1\right)_{60cs} = \left(N_1\right)_{60} + \Delta\left(N_1\right)_{60} \tag{2.11}$$

The adjustments Δq_{c1N} = f(FC) and $\Delta(N_1)_{60}$ = f(FC) are derived so that CRR can be expressed solely in terms of q_{c1Ncs} or $(N_1)_{60cs}$ as,

$$CRR_{M=7.5,\sigma'_{vc}=1} = f\left[q_{c1Ncs}\right] \tag{2.12}$$

$$CRR_{M=7.5,\sigma'_{vc}=1} = f\left[\left(N_1\right)_{60cs}\right] \tag{2.13}$$

A number of alternative approaches have been used to account for the effects of fines (FC and fines plasticity) on CPT-based liquefaction triggering correlations. Some frameworks utilize the CPT tip and sleeve friction ratio measurements (e.g., Robertson and Wride 1997, Moss et al. 2006) and some emphasized independent specification of fines characteristics (e.g., Idriss and Boulanger 2008). This aspect is discussed further in Section 2.3

Important attributes of a liquefaction analysis procedure

A liquefaction analysis procedure within the above stress-based framework ideally has the following two attributes:

- The liquefaction analysis procedure is applicable to the full range of conditions important to practice; e.g., shallow lateral spreads, settlement of structures, stability failures or deformations in levees or earth dams. Practice often results in the need to extrapolate outside the range of the case history experiences, requiring the framework to be supported by sound experimental and theoretical bases for guiding such extrapolations.

- The functional relationships used to describe fundamental aspects of soil behavior and site response are consistent with those used in developing companion correlations for the other in-situ tests; e.g., SPT blow count, CPT penetration resistance, and shear wave velocity, V_s. Consistency in these functional relationships facilitates the logical integration of information from multiple sources and provides a rational basis for the calibration of constitutive models for use in nonlinear dynamic analyses.

The stress-based liquefaction analysis framework for cohesionless soil includes four functions, or relationships, that describe fundamental aspects of dynamic site response, penetration resistance, and soil characteristics and behavior. These four functions, along with the major factors affecting each, are:

- r_d = f(depth; earthquake and ground motion characteristics; dynamic soil properties)

- $C_N = f(\sigma'_v; D_R; FC)$
- $K_\sigma = f(\sigma'_v; D_R; FC)$
- MSF = f(earthquake and ground motion characteristics; D_R; FC)

These functions are best developed using a synthesis of empirical, experimental and theoretical methods, as ultimately the robustness of these functions is important for guiding the application of the resulting correlations to conditions that are not well-represented in the case history database.

Statistical analyses and regression methods are valuable tools for examining liquefaction analysis methods and testing different hypotheses, but the functional relationships in the statistical models must be constrained and guided by available experimental data and theoretical considerations. In the case of liquefaction triggering correlations, the use of regression models alone to derive physical relationships is not considered adequate because: (1) the case history data are generally not sufficient to constrain the development of such relationships, as illustrated later in this report; (2) any such relationship will be dependent on the assumed forms for the other functions, given their shared dependencies on factors such as depth, soil characteristics, and ground motion characteristics; and (3) the use of regression to define functions describing fundamental behaviors does not necessarily produce a function that can be reliably used in extending the resulting correlation to conditions not well represented in the database, such as large depths.

Liquefaction triggering correlations should only be used with the same liquefaction analysis framework (and all its components) that was used to develop the correlation from the case history database. Differences in the functional components (e.g., r_d, C_N, K_σ, MSF) used by different model developers may or may not be large in different situations, such that changing a model component may or may not have a significant effect on the resulting triggering correlation. Such cases are difficult to generalize, however, and thus it is proper and prudent that correlations only be used with the same analysis framework used to develop them.

2.2. Shear stress reduction coefficient, r_d

Idriss (1999), in extending the work of Golesorkhi (1989), performed several hundred parametric site response analyses and concluded that, for the purpose of developing liquefaction evaluation procedures, the parameter r_d could be expressed as,

$$r_d = \exp\left[\alpha(z) + \beta(z) \cdot M\right] \tag{2.14a}$$

$$\alpha(z) = -1.012 - 1.126 \sin\left(\frac{z}{11.73} + 5.133\right) \tag{2.14b}$$

$$\beta(z) = 0.106 + 0.118 \sin\left(\frac{z}{11.28} + 5.142\right) \tag{2.14c}$$

where z = depth below the ground surface in meters and the arguments inside the sin terms are in radians. Details regarding the soil profiles and input motions used in developing these equations are summarized by Idriss and Boulanger (2010). The resulting variations of r_d with depth and magnitude are shown in Figure 2.1.

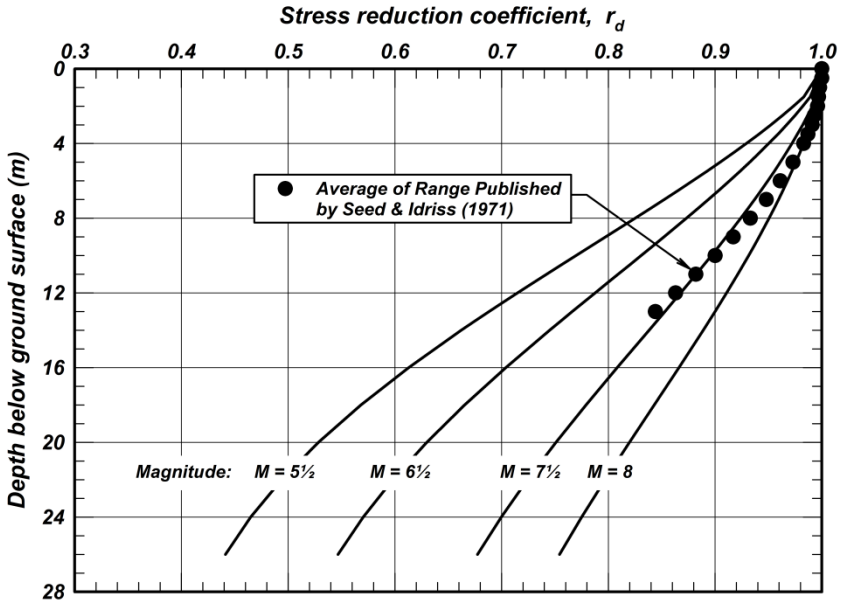

Figure 2.1. Shear stress reduction factor, r_d, relationship

Other r_d relationships have been proposed, including the probabilistic relationships by Cetin et al. (2004) and Kishida et al. (2009b). The latter two relationships were based on large numbers of site response analyses for different site conditions and ground motions, and include the effects of a site's average shear wave velocity over a specified depth and the level of shaking. Idriss and Boulanger (2010) compared these alternative r_d relationships and showed that their use in interpreting the SPT liquefaction case history database would produce relatively small differences in the derived triggering correlation; note, however, that the differences can be important for evaluations in practice when extrapolating to depths greater than covered by the database (about 10 or 12 m).

Liquefaction evaluations for depths greater than about 10 m can often benefit from site response analyses to estimate the earthquake-induced cyclic stress ratios because the uncertainty in r_d becomes large at these depths. It must be recognized, however, that a high quality site response analysis requires sufficient subsurface characterization of the site (including shear wave velocity measurements) and must account for variability in the possible input motions (e.g., seven or more time series consistent with the seismic hazard, source characteristics, and other intensity measures of importance to the project).

The extension of these r_d relationships to large magnitude subduction zone events has not been extensively studied. This extension of r_d relationships is currently being evaluated utilizing recordings from the 2011 M=9.0 Tohoku earthquake.

2.3 Overburden correction factor, C_N

The C_N relationship used was initially developed by Boulanger (2003b) based on: (1) a re-examination of published SPT calibration chamber test data covering σ'_v of 0.7 to 5.4 atm (Marcuson and Bieganousky 1977a, 1977b); and (2) results of analyses for σ'_v of 0.2 to 20 atm using the cone penetration theory of Salgado et al. (1997a, 1997b) which was shown to produce good agreement with a database of over 400 CPT calibration chamber tests with σ'_v up to 7 atm. Idriss and Boulanger (2003, 2008) subsequently

recommended that the D_R-dependence of the C_N relationship could be expressed in terms of q_{c1Ncs} or $(N_1)_{60cs}$ as follows:

$$C_N = \left(\frac{P_a}{\sigma'_v}\right)^m \leq 1.7 \tag{2.15a}$$

$$m = 1.338 - 0.249\left(q_{c1Ncs}\right)^{0.264} \tag{2.15b}$$

$$m = 0.784 - 0.0768\sqrt{\left(N_1\right)_{60cs}} \tag{2.15c}$$

with q_{c1Ncs} limited to values between 21 and 254 and $(N_1)_{60cs}$ values limited to values ≤ 46 for use in these expressions.

The use of Equation 2.15a requires iteration which is easily accomplished, for example, using the automatic iteration option in an Excel spreadsheet. The values of C_N calculated using this equation are presented in Figure 2.2a for a range of q_{c1Ncs} and $(N_1)_{60cs}$ values and for effective overburden stresses up to 10 atm, and are compared to the Liao and Whitman (1986) relationship in Figure 2.2b for effective overburden stresses up to 2 atm.

The limit of 1.7 on the maximum value of C_N is reached at σ'_v less than about 0.35 atm (~35 kPa), which would correspond to a maximum depth of about 2 to 4 m, depending on the depth to the water table. This limit is imposed because these expressions were not derived or validated for very low effective stresses,

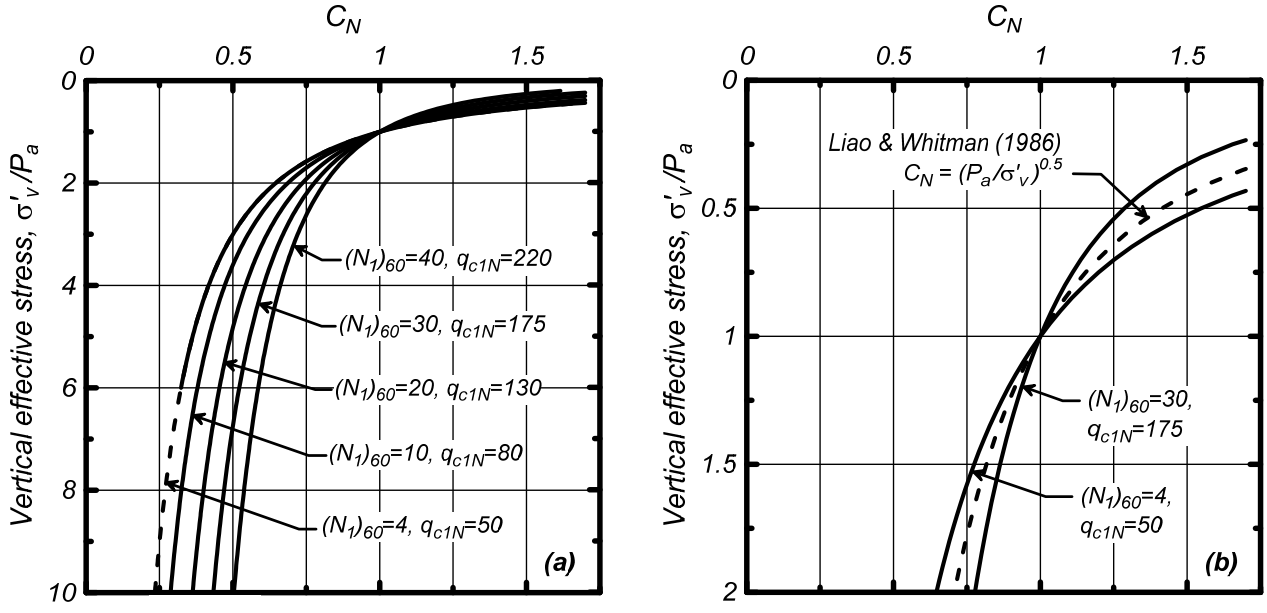

Figure 2.2. Overburden correction factor (C_N) relationship for CPT and SPT penetration resistances: (a) for σ_v'/P_a = 0 - 10, and (b) for σ_v'/P_a = 0 – 2 along with Liao and Whitman's (1986) relationship

and the assumed functional form will otherwise produce unrealistically large C_N values as the σ'_v approaches zero. Limits of 1.7 to 2.0 have been recommended by various researchers when using this function form (e.g., Robertson and Wride 1998, Youd et al. 2001). Other functional forms for C_N produce finite values at $\sigma'_v = 0$; e.g., C_N values of 1.5 to 2.4 at $\sigma'_v = 0$ are obtained using the relationships recommended for different conditions by Skempton (1986).

2.4 Overburden correction factor, K_σ

The K_σ relationship used was developed by Boulanger (2003) based on: (1) showing that the CRR for a clean reconstituted sand in the laboratory could be related to the sand's relative state parameter index, ξ_R; (2) showing that the K_σ relationship for such clean sands could be directly derived from the CRR-ξ_R relationship; and (3) deriving a K_σ relationship that was consistent with the field-based CRR-$(N_1)_{60cs}$ correlations from the corresponding field-based CRR-ξ_R relationships. Idriss and Boulanger (2008) recommended that the resulting K_σ relationship be expressed in terms of the q_{c1Ncs} or $(N_1)_{60cs}$ values as follows:

$$K_\sigma = 1 - C_\sigma \ln\left(\frac{\sigma'_v}{P_a}\right) \le 1.1 \tag{2.16a}$$

$$C_\sigma = \frac{1}{37.3 - 8.27\left(q_{c1Ncs}\right)^{0.264}} \le 0.3 \tag{2.16b}$$

$$C_\sigma = \frac{1}{18.9 - 2.55\sqrt{\left(N_1\right)_{60cs}}} \le 0.3 \tag{2.16c}$$

The coefficient C_σ can be limited to its maximum value of 0.3 by restricting q_{c1Ncs} to ≤ 211 and $(N_1)_{60cs}$ ≤ 37 for use in these expressions.

The resulting relationship is plotted in Figure 2.3 for a range of q_{c1Ncs} and $(N_1)_{60cs}$ values. The limit of 1.1 on the maximum value of K_σ is reached at a σ'_v that varies with denseness of the soil; e.g., for a soil with $(N_1)_{60cs}$ = 15 or $D_R \approx 57\%$, this limit is reached at about 0.4 atm (~40 kPa). This limit was imposed because the dependence of K_σ on σ'_v has not been measured or validated for very low effective stresses, and the assumed functional form is otherwise unbounded as the σ'_v approaches zero. The effect of omitting the limit of 1.1 for the maximum value of K_σ on the interpretation of SPT-based liquefaction case histories was shown to be essentially negligible (Idriss and Boulanger 2010).

The above relationships have been shown to be in reasonable agreement with an updated database of laboratory experimental data by Montgomery et al. (2012).

The K_σ and C_N relationships are particularly important in applications that require extrapolation for depths greater than those covered by the case history database. Different combinations of these two relationships were evaluated by Boulanger and Idriss (2012b) using the SPT test data and cyclic test results on frozen sand samples from Duncan Dam (Pillai and Byrne 1994). The K_σ and C_N relationships used in the Idriss-Boulanger (2008) SPT and CPT procedures provided good agreement with the observed variations in CRR with overburden stress for that site.

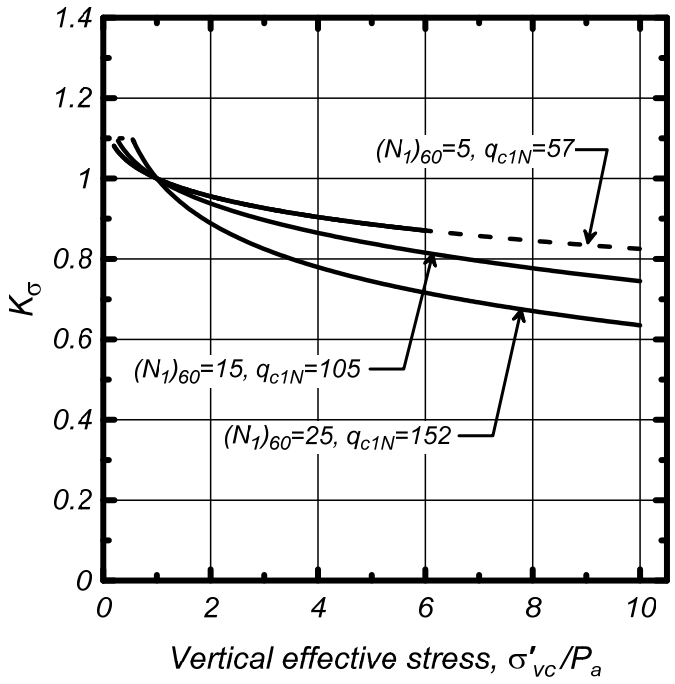

Figure 2.3. Overburden correction factor (K_σ) relationship

2.5 Magnitude scaling factor, MSF

The magnitude scaling factor (MSF) is used to account for duration effects (i.e., number and relative amplitudes of loading cycles) on the triggering of liquefaction. The MSF relationships used by Idriss and Boulanger (2008) and revised herein were derived by combining (1) laboratory-based relationships between the CRR and the number of equivalent uniform loading cycles, and (2) correlations of the number of equivalent uniform loading cycles with earthquake magnitude. The development of the MSF relationship used herein is described in detail in Appendix A. The following provides a brief summary of the MSF relationships used by Idriss and Boulanger (2008), followed by a summary of the new MSF relationship.

The MSF for sands used by Idriss and Boulanger (2008) was developed by Idriss (1999), who derived the following relationship:

$$MSF = 6.9 \cdot \exp\left(\frac{-M}{4}\right) - 0.058 \ \leq 1.8 \tag{2.17}$$

This relationship is plotted in Figure 2.4. An upper limit for the MSF is assigned to very-small-magnitude earthquakes for which a single peak stress can dominate the entire time series. The value of 1.8 is obtained by considering the time series of stress induced by a small magnitude earthquake to be dominated by single pulse of stress (i.e., ½ to 1 full cycle, depending on its symmetry), with all other stress cycles being sufficiently small to neglect. This aspect of the MSF relationship is discussed further in Appendix A.

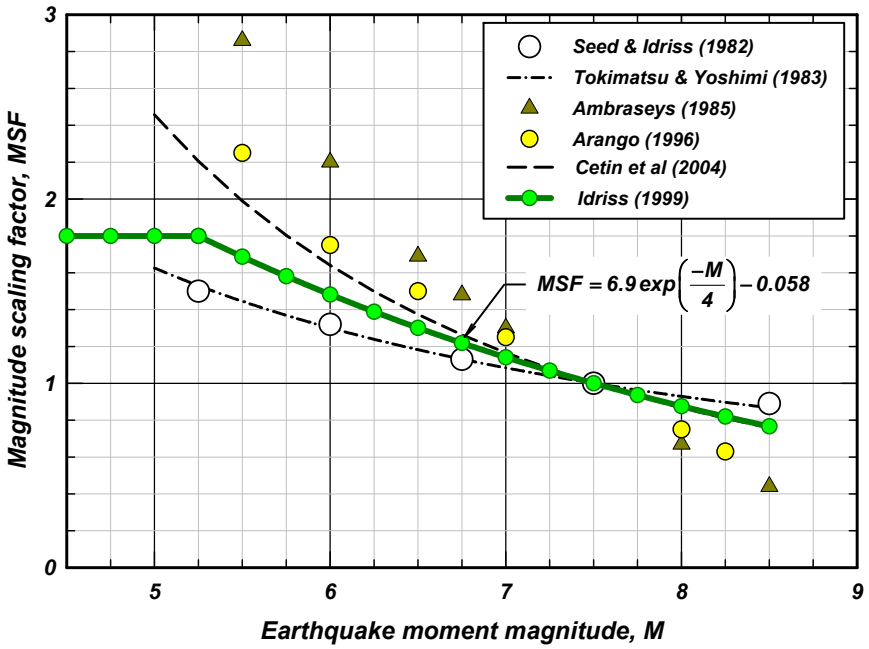

Figure 2.4. Magnitude scaling factor (MSF) relationship

The MSF for clays used by Idriss and Boulanger (2008) was developed by Boulanger and Idriss (2007) and is shown in Figure 2.5. This relationship is much flatter (less dependency on number of cycles and, hence, M) than for sands, which reflects the differences in the slopes of the cyclic strength versus number of cycles curves obtained for these soil types.

The MSF relationships used by Idriss and Boulanger (2008) for sands or clays, as shown in Figure 2.5, can be rewritten in a more general form as,

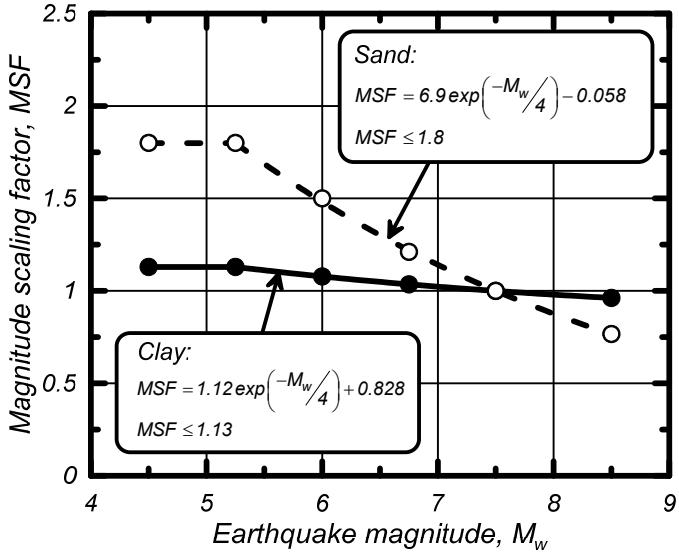

Figure 2.5. MSF relationships for clay and sand (Boulanger and Idriss 2007)

$$MSF = 1 + \left(MSF_{max} - 1\right)\left(\frac{exp\left(\frac{-M}{4}\right) - exp\left(\frac{-7.5}{4}\right)}{exp\left(\frac{-5.25}{4}\right) - exp\left(\frac{-7.5}{4}\right)}\right) \tag{2.18}$$

where MSF_{max} = 1.8 for sand and MSF_{max} = 1.09 for clay and plastic silt. With the fixed terms expressed numerically, the above equation becomes,

$$MSF = 1 + \left(MSF_{max} - 1\right)\left(8.64\, exp\left(\frac{-M}{4}\right) - 1.325\right) \tag{2.19}$$

This form of the MSF relationship was used to develop new MSF curves for a range of soil conditions as described in Appendix A. The proposed relationships relate MSF_{max} to q_{c1Ncs} and $(N_1)_{60cs}$ values as,

$$MSF_{max} = 1.09 + \left(\frac{q_{C1Ncs}}{180}\right)^3 \leq 2.2 \tag{2.20}$$

$$MSF_{max} = 1.09 + \left(\frac{(N_1)_{60cs}}{31.5}\right)^2 \leq 2.2 \tag{2.21}$$

The resulting MSF relationships for different values of q_{c1Ncs} and $(N_1)_{60cs}$ are shown in Figure 2.6. This relationship produces MSF_{max} = 1.8 at $q_{c1Ncs} \approx 160$ or $(N_1)_{60cs} \approx 27$, which matches the MSF relationship for sand by Idriss (1999), and $MSF_{max} \approx 1.10$ for $q_{c1Ncs} < 60$ $(N_1)_{60cs} < 6$, which is consistent with the

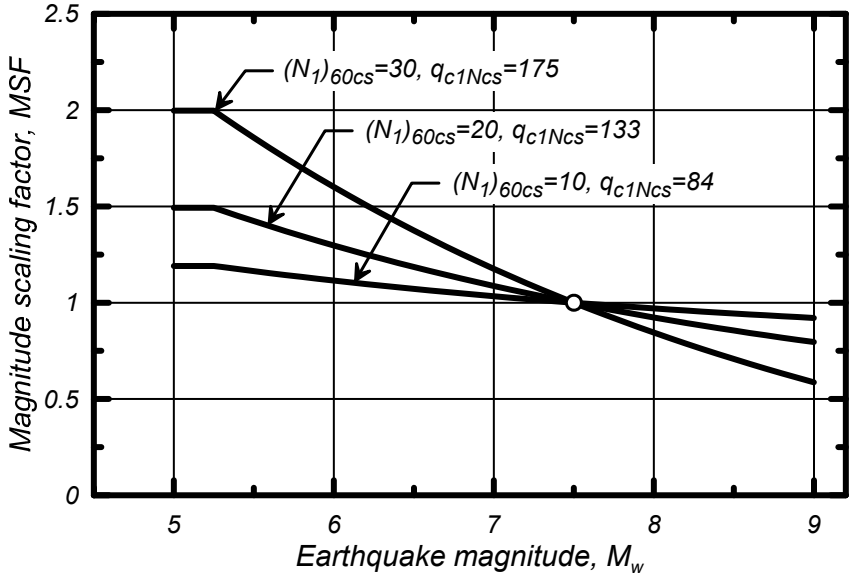

Figure 2.6. Variation in the MSF relationship with q_{c1Ncs} and with $(N_1)_{60cs}$ for cohesionless soils

expected results for very loose sands or soft low-plasticity silts.

The revised MSF relationship shown in Figure 2.6 is believed to provide an improved accounting of how this relationship should vary with soil characteristics compared to currently available MSF relationships that provide a single relationship for all cohesionless soils. Other studies have shown that the equivalent number of loading cycles and hence MSF values for different soil types will vary systematically with earthquake magnitude, distance to the fault, directivity, site conditions, and depth in a soil profile (Liu et al. 2001, Green and Terri 2005, Carter et al. 2013). Inclusion of these factors may not significantly reduce uncertainty in a MSF relationship until the cyclic loading characteristics of different soils can be estimated with greater confidence. For this reason, the revised MSF relationship, with its dependence on only M and q_{c1Ncs} or $(N_1)_{60cs}$ is considered sufficient for practical purposes.

2.6 Equivalent clean sand adjustments for fines content

The liquefaction case histories suggest that the liquefaction triggering correlations shift to the left as the fines content (FC) increases, as has been reflected in recent CPT-based and SPT-based correlations. The equivalent clean sand adjustments, Δq_{c1N} and $\Delta(N_1)_{60}$, are thus empirically derived from the liquefaction case history data, and account for the effects that fines content have on both the CRR and the CPT or SPT penetration resistances.

The equivalent clean sand adjustments for CPT, Δq_{c1N}, used herein were derived from the analyses presented later in Sections 4, 5, and 6, with their forms and limits guided in part by the trends in q_c/N_{60} ratios versus FC presented in Section 7. The adjustments are considered appropriate for nonplastic to low-plasticity silty fines, although explicit information on fines plasticity is limited in the case history database (Section 3.5). The adjustments are presented here because they are used for summarizing the case history data and examining their distributions across a range of conditions (Sections 3 and 6).

The equivalent clean sand adjustments for the CPT-based and SPT-based correlations are shown in Figures 2.7a and 2.7b, respectively. The adjustment for the SPT-based correlation is unchanged from that used by Idriss and Boulanger (2008), but the adjustment for the CPT-based correlation has changed as shown in Figure 2.7a. The proposed changes in the equivalent clean sand adjustment for the CPT are attributed to the changes in the updated case history database, the effect of the new MSF, and an increased weighting toward improving consistency with the empirical q_c/N_{60} ratios. The adjusted expression for CPT is as follows:

$$\Delta q_{c1N} = \left(11.9 + \frac{q_{c1N}}{14.6}\right) \exp\left(1.63 - \frac{9.7}{FC+2} - \left(\frac{15.7}{FC+2}\right)^2\right) \tag{2.22}$$

The expression for SPT remains as

$$\Delta\left(N_1\right)_{60} = \exp\left(1.63 + \frac{9.7}{FC+0.01} - \left(\frac{15.7}{FC+0.01}\right)^2\right) \tag{2.23}$$

where FC is the percent fines content. Both adjustments begin to plateau for FC values exceeding about 35% because the soil matrix becomes fines-dominated for any FC value greater than about this value. The percentage change in these adjustments for given FC values is different for the CPT-based and SPT-based triggering correlations, which is believed to be due to differences in the way the fines fraction affect the penetration processes; e.g., dynamic versus monotonic penetrations, full versus partial displacement

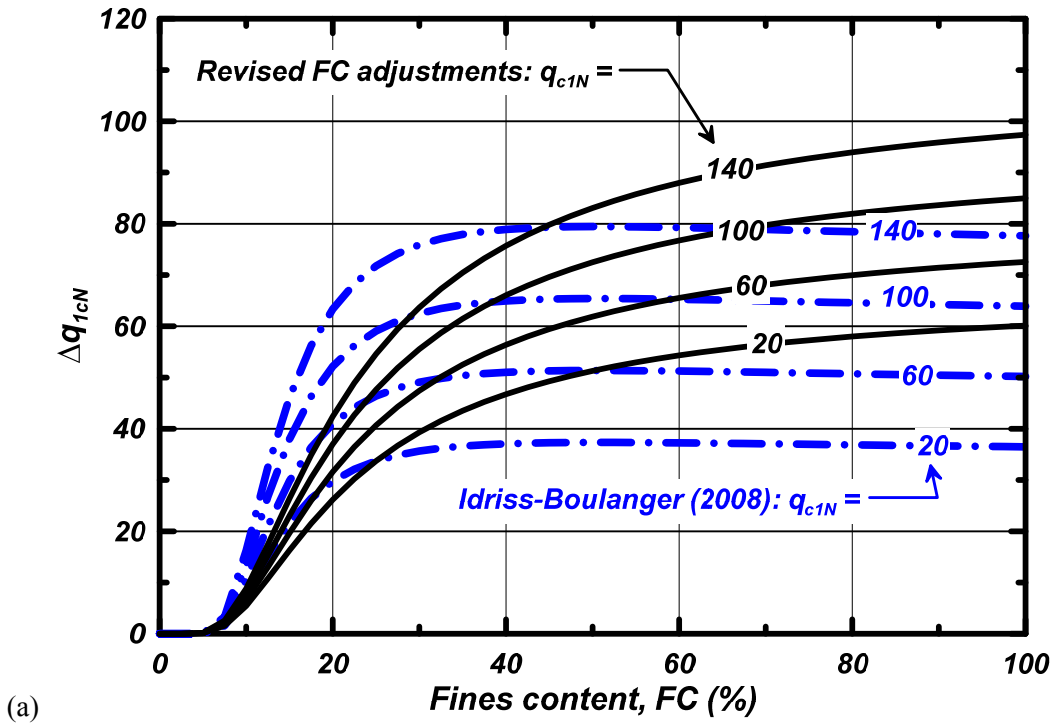

(a)

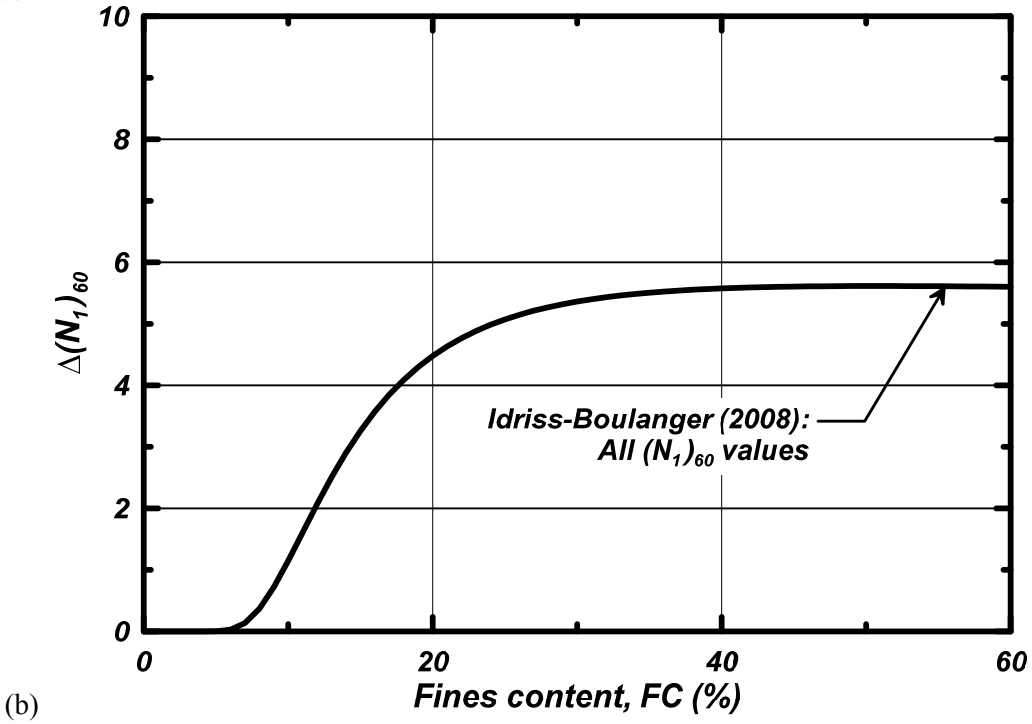

(b)

Figure 2.7. Equivalent clean sand adjustments for the (a) CPT-based and (b) SPT-based liquefaction triggering procedures

penetrometers, differences in penetration rates and associated rates of partial drainage, and other differences in the flow processes and kinematics of these penetration tests.

The deterministic version of the revised CPT-based correlation is shown in Figure 2.8a in terms of q_{c1N} for different values of FC, rather than in terms of the equivalent clean sand penetration resistances. The curves in this figure illustrate the leftward shifts in the triggering correlations as the value of FC increases. The equation for the revised deterministic CPT-based correlation is as follows:

$$CRR_{M=7.5,\sigma'_v=1atm} = \exp\left(\frac{q_{c1Ncs}}{113} + \left(\frac{q_{c1Ncs}}{1000}\right)^2 - \left(\frac{q_{c1Ncs}}{140}\right)^3 + \left(\frac{q_{c1Ncs}}{137}\right)^4 - 2.80\right) \quad (2.24)$$

The equation for the unchanged deterministic SPT-based correlation is as follows:

$$CRR_{M=7.5,\sigma'_v=1atm} = \exp\left(\frac{(N_1)_{60cs}}{14.1} + \left(\frac{(N_1)_{60cs}}{126}\right)^2 - \left(\frac{(N_1)_{60cs}}{23.6}\right)^3 + \left(\frac{(N_1)_{60cs}}{25.4}\right)^4 - 2.8\right) \quad (2.25)$$

This correlation is shown in Figure 2.8b in terms of $(N_1)_{60}$ for different values of FC, rather than in terms of the equivalent clean sand penetration resistances. These equations and figures are presented here because they are used for summarizing the case history data and examining their distributions across a range of conditions (Sections 3 and 6).

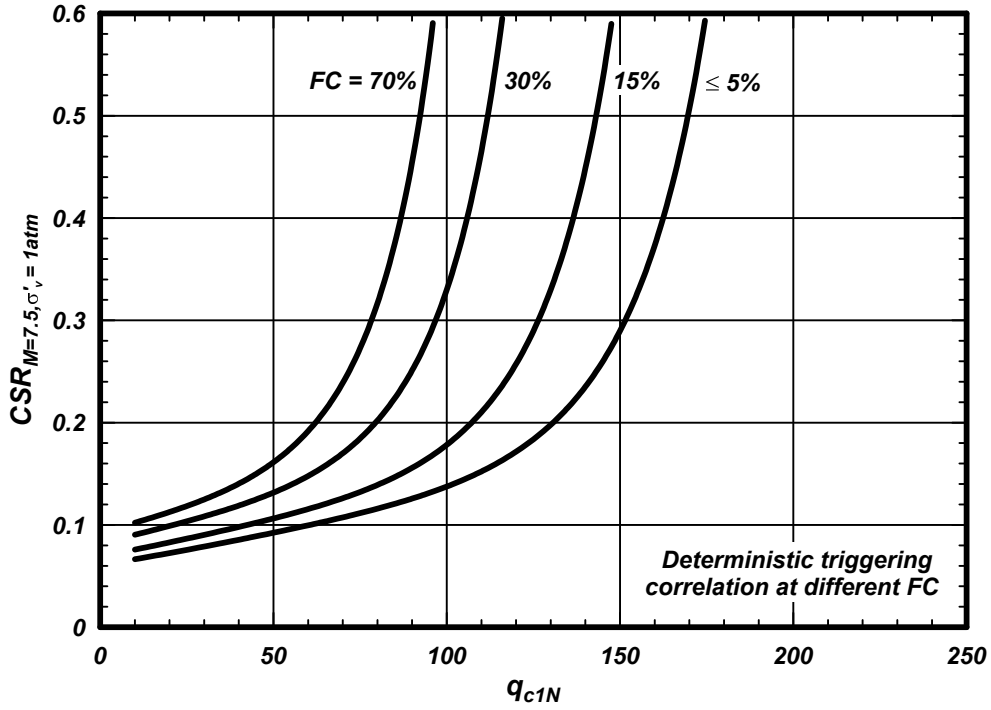

(a)

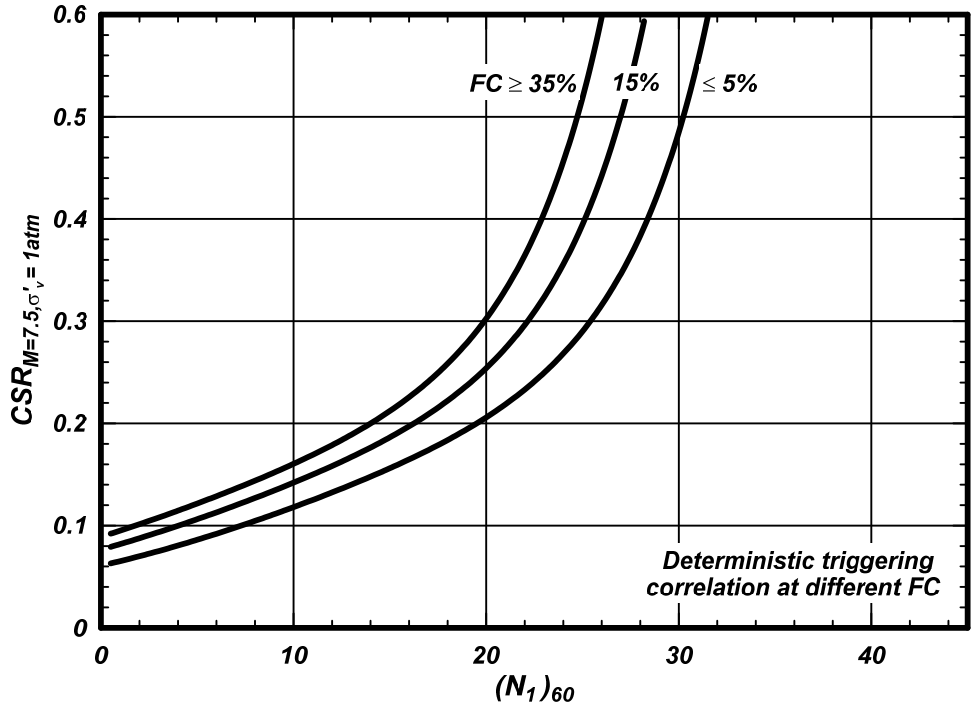

(b)

Figure 2.8. (a) Revised deterministic CPT-based triggering correlation and (b) the unchanged deterministic SPT-based triggering correlation for clean sands and for cohesionless soils having various values of FC.

2.7. Fines content and soil classification estimation using CPT data

The FC and soil classification are often correlated to a soil behavior type index (I_c) which is a function of the CPT tip resistance and sleeve friction ratio. The I_c term recommended by Robertson and Wride (1997) is computed as,

$$I_c = \left[\left(3.47 - \log\left(Q\right)\right)^2 + \left(1.22 + \log\left(F\right)\right)^2 \right]^{0.5} \tag{2.26}$$

where Q and F are normalized tip and sleeve friction ratios computed as,

$$Q = \left(\frac{q_c - \sigma_{vc}}{P_a} \right) \left(\frac{P_a}{\sigma'_{vc}} \right)^n \tag{2.27}$$

$$F = \left(\frac{f_s}{q_c - \sigma_{vc}} \right) \cdot 100\% \tag{2.28}$$

The terms Q and F are used in soil behavior type classification charts, such as the chart shown in Figure 2.9 by Robertson (1990). The exponent n varies from 0.5 in sands to 1.0 in clays (Robertson and Wride 1998). The term I_c represents the radial distance between any point on this chart and the point defined by Q = 2951 and F = 0.06026%. Circular arcs defined by constant I_c values are used to approximate the boundaries between different soil behavior types in this chart; e.g., I_c = 2.05 represents the approximate boundary between soil behavior types 5 and 6, whereas I_c = 2.60 represents the approximate boundary between soil behavior types 4 and 5 (Robertson 2009).

General correlations between FC and I_c or other CPT-based indices exhibit large scatter, such that site-specific calibration or checking of such correlations is strongly encouraged. For example, consider the datasets relating FC and I_c shown in Figure 2.10. The datasets from Suzuki et al. (1998) and the liquefaction case history database presented herein produced slightly different trends at low and high values of FC, although the differences are not large relative to the scatter in both datasets. The differences in the correlations by different investigators, such as those by Robinson et al. (2013) and Robertson and Wride (1998) shown in this figure, may therefore be partly attributable to the differences in the data sets upon which they were developed; e.g., the Robinson et al. (2013) relationship was based on soils along the Avon River in Christchurch, New Zealand.

The large uncertainty in the I_c versus FC relationship includes contributions from three major factors. One factor is the measurement uncertainty that arises from mapping FC values from samples (or some portion of a sample as is often done) in a boring to the I_c values (over some interval) from adjacent CPT soundings. Heterogeneities in the subsurface, even over short lateral or vertical distances, will contribute to the scatter. The second factor is the inherent mechanistic limitations in using the I_c parameter to predict FC across a broad range of soil types. The third factor is the unknown influence of fines plasticity. The case history data is believed to be dominated by nonplastic to low plasticity silty fines (Section 3.5), but plasticity variations in this range may still significantly contribute to the scatter in the relationship between FC and I_c. Distinguishing among these sources of uncertainty is not possible with the currently available information.

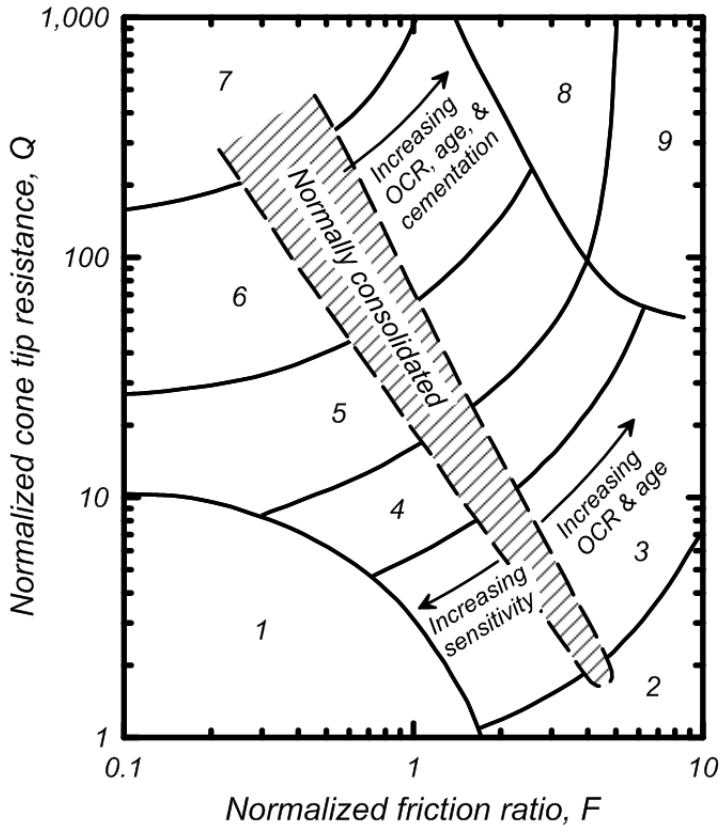

1. Sensitive, fine grained
2. Organic soils - peats
3. Clays - silty clay to clay
4. Silt mixtures - clayey silt to silty clay
5. Sand mixtures - silty sand to sandy silt
6. Sands - clean sand to silty sand
7. Gravelly sand to dense sand
8. Very stiff sand to clayey sand *
9. Very stiff, fine grained *

* Heavily overconsidated or cemented

Figure 2.9. CPT-based soil behavior type classification chart by Robertson (1990)

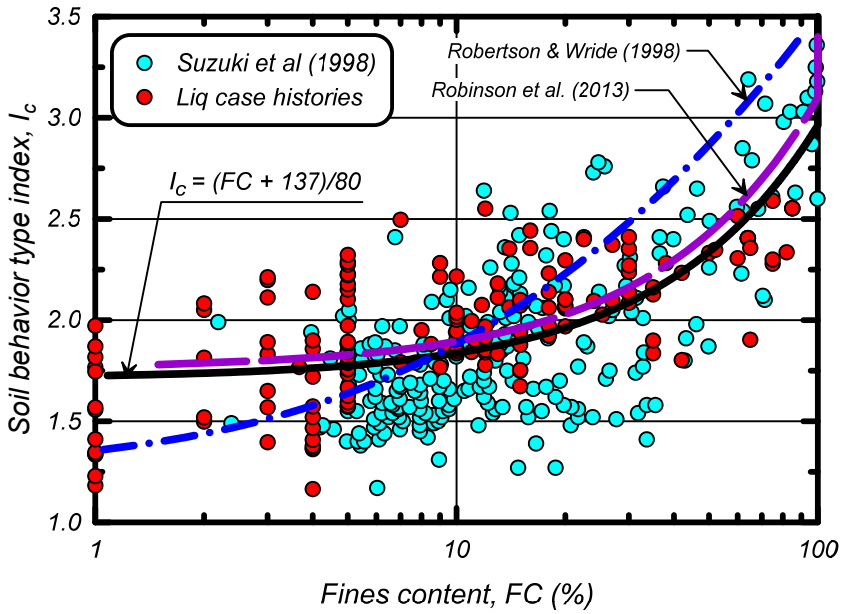

Figure 2.10. Data sets and correlations relating I_c and FC

For the present study, the relationship for estimating FC was developed by first regressing I_c against FC using the combined data sets in Figure 2.10 to obtain the least-squares fit,

$$I_C = \frac{(FC+137)}{80} + \varepsilon \tag{2.29}$$

where ε = an error term, which was found to have a mean of 0 and a standard deviation of 0.29 and be unbiased against FC. This equation can then be inverted to provide the following form for estimating FC,

$$\begin{aligned} &FC = 80(I_C + C_{FC}) - 137 \\ &0\% \le FC \le 100\% \end{aligned} \tag{2.30}$$

where C_{FC} is a fitting parameter that can be adjusted based on site-specific data when available. The sign convention for C_{FC} is set opposite to that for the error term ε in Equation 2.29 so that a positive C_{FC} corresponds to a larger estimate of FC. The regression of I_c against FC was preferred over regressing FC directly against I_c because this is a calibration or inverse regression problem (e.g., Draper and Smith 1998). This expression with C_{FC} = 0.0, -0.29, and 0.29 (i.e., +/- an amount equal to the standard deviation in the general correlation) is shown in Figure 2.11. The curves envelope approximately 2/3 of the data points, as expected. The term C_{FC} can be calibrated to site specific data by regressing I_c against FC using the equation,

$$I_C = \frac{(FC+137)}{80} - C_{FC} \tag{2.31}$$

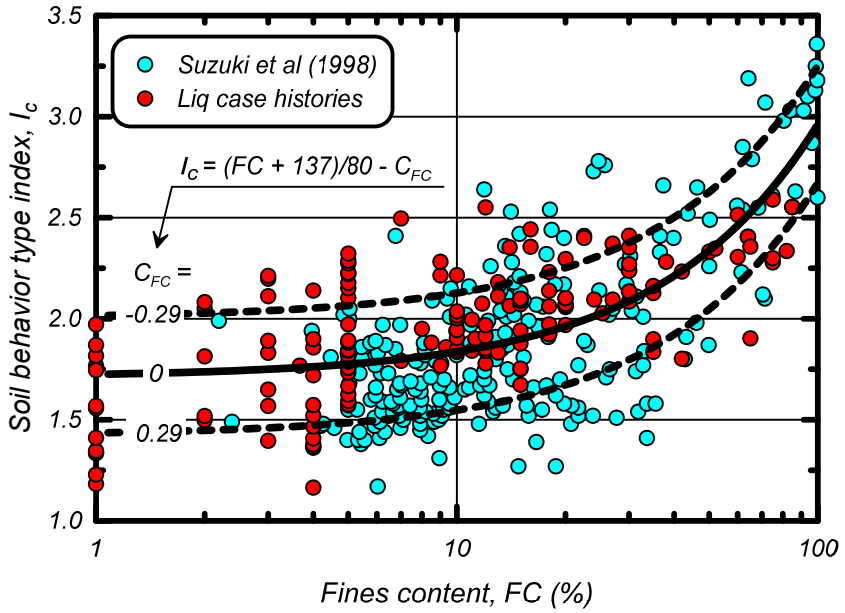

Figure 2.11. Recommended correlation between I_c and FC with plus or minus one standard deviation against the dataset by Suzuki et al. (1998) and the liquefaction database

with C_{FC} being the sole fitting parameter. This form of simple calibration will preserve the shape of the relationship developed from the database, which may aid calibration efforts when site-specific data are limited. Note that C_{FC} should be determined for individual geologic strata (common source material, deposition, etc.) and that different C_{FC} values may be obtained for different strata at any one site. For example, setting C_{FC} = 0.07 is approximately equal to the relationship developed by Robinson et al. (2013) for liquefiable soils along the Avon River in Christchurch, New Zealand.

Ground densification work has been observed to change the FC-I_c correlation at specific sites through its effects on q_c and f_s, with the result that C_{FC} may be different before and after ground densification work (e.g., Nguyen et al. 2014). Similarly, the I_c value used to distinguish clays from sands has often been observed to decrease as a result of densification. The consistency of the inferred soil profile characteristics from before to after ground densification can be used to develop site-specific adjustments in both C_{FC} and the I_c criterion for separating clay-like soils from sand-like soils.

Any CPT-based liquefaction triggering evaluation should explicitly consider the uncertainty in FC and soil classification estimates when site-specific sampling and lab testing data are not available. For analyses in the absence of site-specific soil sampling and lab testing data, it would be prudent to perform parametric analyses to determine if reasonable variations in the FC and soil classification parameters have a significant effect on the final engineering recommendations. For example, the liquefaction analyses could be repeated using C_{FC} = -0.29, 0.0, and 0.29 to evaluate the sensitivity to FC estimates. Similarly, the I_c cut-off value used to screen out clay-like soils is commonly taken as 2.6 based on Robertson and Wride (1998), but other values may be justified based on site specific sampling and testing. For this reason, liquefaction analyses could be repeated using I_c cut-off values of 2.4, 2.6, and 2.8 to evaluate sensitivity to this parameter. The results of such analyses can be used to illustrate the importance of site-specific sampling and testing for a given project, while recognizing that some amount of sampling and testing should always be required for high risk/high consequence projects.

3. CPT-BASED CASE HISTORY DATABASE

3.1. Sources of data

A database of CPT liquefaction case histories is updated, including adding data from recent earthquake events (e.g., PEER 2000a,b, Sancio 2003, Green et al. 2014, Cox et al. 2013). The individual case histories and the key references are summarized in Table 3.1. We examined the original sources for all cases, as well as interpretations by others (e.g., Moss et al. 2003), to obtain independent interpretations consistent with our current understanding and judgments. For cases where our interpretation was within a few percent of the original investigators, we retained the interpretation of the original investigator in Table 3.1.

The available information for most of the cases with I_c near 2.6 is insufficient to determine whether the soils would be best analyzed with a liquefaction triggering framework (like for sands) or a cyclic softening framework (like for clays). The cases listed in Table 3.1 are therefore limited to cases with $I_c <$ 2.6. Of the 253 cases with $I_c <$2.6, 180 cases had surface evidence of liquefaction, 71 cases had no surface evidence of liquefaction, and 2 cases were described as being at the margin between liquefaction and no liquefaction. Another notable 15 cases with $I_c \geq 2.6$ are listed in Table 3.2 for documentation purposes because they have been included in other liquefaction databases or discussed as possible liquefaction cases in the literature. Of these 15 cases with $I_c \geq 2.6$, 4 had surface evidence of ground failure (deformations) and 11 had no surface evidence of ground failure.

Most of the case histories that were used in the development of the Idriss and Boulanger (2004) CPT-based liquefaction triggering correlation are included in the current database, although the representative data for many cases have changed due to new information or revised interpretations of the site characteristics or earthquake loading. In particular, the 2004 study used case history data points from the 1995 M=6.9 Kobe earthquake based on the publication by Suzuki et al. (1997) which did not include details on the key parameters such as critical depth, water table depth, etc. The subsequent publication by Suzuki et al. (2003) included greater detail for most of those case histories from the 1995 Kobe earthquake, and thus the current database utilizes only the data from the newer publication by Suzuki et al. These case histories have since been augmented by a significant number of cases from the 1999 M=7.5 Kocaeli earthquake, 1999 M=7.6 Chi-Chi earthquake, 2010-11 Canterbury earthquake sequence, and 2011 M=9.0 Tohoku earthquake. The availability of the newer details and the significant increase in the total number of case histories offered the means to reassess the CPT-based relationships developed in 2004 as described in the remainder of this report.

Case history data points for sites without nearby strong ground motion recordings (which are the large majority) are plotted at the $CSR_{M=7.5,\sigma'=1atm}$ value expected in the absence of liquefaction, and this $CSR_{M=7.5,\sigma'=1atm}$ value may be significantly greater than the value which developed if liquefaction was triggered early in strong shaking or may be comparable to the value which developed if liquefaction was triggered late in strong shaking. Liquefaction points that fall well above the triggering curve, as well as no liquefaction data points that fall well below the triggering curve, have negligible effect on the development of the triggering correlation as discussed in Section 5.

The following sections describe the selection of earthquake magnitudes, peak accelerations, and representative soil properties (i.e., q_{c1Ncs}, I_c, FC) values, discuss the classifications of site performance, and examine the distributions of the case history data.

Table 3.1. Summary of CPT-based liquefaction case history data

Earthquake	Site	Mag (M)	a_{max} (g)	Liq (Yes, No)	Critical depth interval (m)	Avg depth (m)	Depth to GWT (m)	σ_{vc} (kPa)	σ'_{vc} (kPa)	Tip $(q_{cN})_{aver}$	Sleeve $(f_{sN})_{aver}$	Friction ratio $(F)_{aver}$ (%)	n	Q	I_c	PI	Lab FC (%)	I_c est. FC (%)	Repr. FC (%)	C_N	q_{c1N}	Δq_{c1N}	$q_{c1N,cs}$	r_d	CSR	K_σ	MSF	CSR for M=7.5, σ=1	References
1964 M=7.6 Niigata - June 16	D - Kawagisho-cho	7.60	0.162	Yes	3.0-6.0	4.4	1.1	82	49	39.8	0.39	1.00	0.5	55.8	2.11	--	3	32	3	1.54	61.2	0.0	61.2	0.97	0.170	1.06	1.00	0.161	Ishihara and Koga (1981), Farrar (1990), Moss et al. (2003)
1964 M=7.6 Niigata - June 16	E - Showa bridge (left bank)	7.60	0.162	Yes	1.6-4.6	3.1	1.4	56	40	30.0	0.30	1.02	0.5	47.0	2.18	--	5	37	5	1.70	51.0	0.1	51.1	0.98	0.147	1.07	1.00	0.138	Ishihara and Koga (1981), Farrar (1990), Moss et al. (2003)
1964 M=7.6 Niigata - June 16	F - Show Bridge (right bank)	7.60	0.162	No	5.0-6.0	5.5	1.7	98	61	124.0	1.60	1.30	0.5	158.4	1.84	--	5	10	5	1.23	152.0	0.2	152.1	0.96	0.163	1.08	0.98	0.154	Ishihara and Koga (1981), Farrar (1990), Moss et al. (2003)
1968 Inangahua, New Zealand - May 23	Three Channel Flat	7.20	0.600	Yes	2.3-3.5	2.9	3.1	50	50	20.0	0.10	0.51	0.5	27.7	2.23	--	18	41	18	1.55	31.0	23.8	54.7	0.98	0.382	1.05	1.01	0.358	Ooi (1987) as reproduced in Moss et al. (2003). Carr & Berrill (2004). Berrill et al. (1988)
1968 Inangahua, New Zealand - May 23	Reedy's Farm	7.20	0.300	Yes	1.2-1.8	1.4	1.4	24	24	8.0	0.02	0.26	0.5	15.8	2.36	--	16	51	16	1.70	13.6	17.9	31.5	0.99	0.194	1.09	1.01	0.177	Ooi (1987) as reproduced in Moss et al. (2003). Carr & Berrill (2004). Berrill et al. (1988)
1975 M=7.0 Haicheng - Feb 4	Chemical Fiber Site	7.00	0.300	Marginal	1.5-4.5	3.0	1.5	54	40	14.6	0.19	1.37	0.5	22.5	2.51	8	60	64	60	1.67	24.4	55.6	80.0	0.97	0.261	1.09	1.03	0.233	Arulanandan et al. (1986), Earth Tech (1985), Worden et al. (2010)
1975 M=7.0 Haicheng - Feb 4	17th Middle School	7.00	0.300	No	3.0-4.0	3.5	1.0	65	40	23.5	0.27	1.18	0.5	36.3	2.31	9	60	47	60	1.60	37.6	59.2	96.8	0.97	0.304	1.10	1.04	0.266	Arulanandan et al. (1986), Earth Tech (1985), Worden et al. (2010)
1976 M=7.6 Tangshan - July 27	T1 - Tangshan	7.60	0.640	Yes	5.4-6.5	6.2	3.7	109	85	64.0	1.45	2.30	0.5	68.7	2.27	--	5	45	5	1.11	70.9	0.1	71.0	0.95	0.510	1.02	1.00	0.505	Moss et al. (2009, 2011), Zhou & Zhang (1979), Shibata & Teperaska (1988)
1976 M=7.6 Tangshan - July 27	T4 - Tangshan	7.60	0.640	No	4.4-5.0	4.7	1.1	84	49	120.0	1.30	1.09	0.5	171.3	1.76	--	--	4	4	1.33	159.3	0.0	159.3	0.97	0.693	1.10	0.97	0.646	Moss et al. (2009, 2011), Zhou & Zhang (1979), Shibata & Teperaska (1988)
1976 M=7.6 Tangshan - July 27	T6 - Tangshan	7.60	0.640	Yes	2.4-3.0	2.7	1.5	48	36	76.0	0.65	0.86	0.5	126.7	1.79	--	--	6	6	1.60	121.5	0.8	122.3	0.99	0.545	1.10	0.99	0.502	Moss et al. (2009, 2011), Zhou & Zhang (1979), Shibata & Teperaska (1988)
1976 M=7.6 Tangshan - July 27	T7 - Tangshan	7.60	0.640	Yes	3.0-3.8	3.4	3.0	59	55	42.0	0.65	1.57	0.5	56.0	2.23	--	--	41	41	1.33	55.9	56.3	112.2	0.98	0.437	1.07	0.99	0.412	Moss et al. (2009, 2011), Zhou & Zhang (1979), Shibata & Teperaska (1988)
1976 M=7.6 Tangshan - July 27	T8 - Tangshan	7.60	0.640	Yes	5.2-7.4	6.3	2.2	112	72	100.0	0.90	0.91	0.5	117.1	1.83	--	3	10	3	1.17	117.1	0.0	117.1	0.95	0.615	1.04	0.99	0.598	Moss et al. (2009, 2011), Zhou & Zhang (1979), Shibata & Teperaska (1988)
1976 M=7.6 Tangshan - July 27	T9 - Tangshan	7.60	0.640	No	4.2-5.4	4.8	1.1	86	50	85.0	0.80	0.95	0.5	120.0	1.84	--	10	10	10	1.37	116.9	8.2	125.0	0.97	0.695	1.09	0.99	0.645	Moss et al. (2009, 2011), Zhou & Zhang (1979), Shibata & Teperaska (1988)
1976 M=7.6 Tangshan - July 27	T10 - Tangshan	7.60	0.640	Yes	5.0-6.6	5.3	1.5	95	57	60.0	1.00	1.69	0.5	78.6	2.14	--	4	34	4	1.37	81.9	0.0	81.9	0.96	0.664	1.05	0.99	0.635	Moss et al. (2009, 2011), Zhou & Zhang (1979), Shibata & Teperaska (1988)
1976 M=7.6 Tangshan - July 27	T11 - Tangshan	7.60	0.610	Yes	1.4-2.6	2.0	0.9	36	24	38.0	0.80	2.12	0.5	76.9	2.21	--	9	40	9	1.70	64.6	4.5	69.1	0.99	0.576	1.10	1.00	0.526	Moss et al. (2009, 2011), Zhou & Zhang (1979), Shibata & Teperaska (1988)
1976 M=7.6 Tangshan - July 27	T13 - Tangshan	7.60	0.580	Yes	4.8-6.4	5.6	1.1	104	60	113.0	1.09	0.97	0.5	145.9	1.78	--	--	5	5	1.25	141.1	0.3	141.4	0.96	0.632	1.08	0.98	0.597	Moss et al. (2009, 2011), Zhou & Zhang (1979), Shibata & Teperaska (1988)
1976 M=7.6 Tangshan - July 27	T16 - Tangshan	7.60	0.260	No	6.0-7.2	6.6	3.5	119	89	155.0	1.50	0.98	0.5	164.1	1.74	--	--	2	2	1.05	163.1	0.0	163.1	0.95	0.215	1.02	0.97	0.216	Moss et al. (2009, 2011), Zhou & Zhang (1979), Shibata & Teperaska (1988)
1976 M=7.6 Tangshan - July 27	T19 - Tangshan	7.60	0.250	Yes	2.0-4.5	3.3	1.1	60	39	41.0	0.16	0.40	0.5	65.4	1.85	--	5	11	5	1.70	69.7	0.1	69.8	0.98	0.247	1.08	1.00	0.229	Moss et al. (2003, 2011), Zhou & Zhang (1979), Shibata & Teperaska (1988)
1976 M=7.6 Tangshan - July 27	T21 - Tangshan	7.60	0.250	No	3.1-4.0	3.6	3.1	62	58	100.0	0.38	0.38	0.5	131.5	1.57	--	5	0	5	1.28	128.2	0.2	128.3	0.98	0.171	1.07	0.99	0.162	Moss et al. (2003, 2011), Zhou & Zhang (1979), Shibata & Teperaska (1988)
1976 M=7.6 Tangshan - July 27	T22 - Tangshan	7.60	0.250	Yes	0.8-1.7	2.3	0.8	42	27	45.0	0.17	0.38	0.5	85.5	1.73	--	5	2	5	1.70	76.5	0.1	76.6	0.99	0.247	1.10	0.99	0.226	Moss et al. (2003, 2011), Zhou & Zhang (1979), Shibata & Teperaska (1988)
1976 M=7.6 Tangshan - July 27	T30 - Tangshan	7.60	0.200	No	4.6-8.0	6.3	2.5	115	78	141.8	0.54	0.38	0.5	160.5	1.50	--	2	0	2	1.11	157.4	0.0	157.4	0.95	0.182	1.05	0.98	0.179	Moss et al. (2003, 2011), Zhou & Zhang (1979), Shibata & Teperaska (1988)
1976 M=7.6 Tangshan - July 27	T32 - Tangshan	7.60	0.180	Yes	2.6-3.9	3.3	2.3	58	48	33.0	0.13	0.39	0.5	46.8	1.97	--	5	21	5	1.59	52.5	0.1	52.6	0.98	0.137	1.05	1.00	0.130	Moss et al. (2003, 2011), Zhou & Zhang (1979), Shibata & Teperaska (1988)
1976 M=7.6 Tangshan - July 27	T36 - Tangshan	7.60	0.160	No	5.7-9.0	7.4	2.3	135	86	66.0	0.25	0.39	0.5	70.2	1.81	--	2	8	2	1.10	72.6	0.0	72.6	0.94	0.154	1.01	0.99	0.152	Moss et al. (2003, 2011), Zhou & Zhang (1979), Shibata & Teperaska (1988)
1976 M=7.6 Tangshan - July 27	Y24 - Tangshan	7.60	0.120	Yes	3.5-4.5	4.0	0.2	75	38	18.0	0.13	0.75	0.5	28.1	2.30	10	75	47	75	1.67	30.0	60.2	90.2	0.97	0.150	1.10	0.99	0.138	Arulanandan et al. (1982), Moss et al. (2003, 2011)
1976 M=7.6 Tangshan - July 27	Y28 - Tangshan	7.60	0.120	Yes	1.0-3.0	2.0	0.2	37	20	13.8	0.11	0.78	0.5	30.3	2.28	10	75	45	75	1.70	23.5	58.3	81.8	0.99	0.146	1.10	0.99	0.134	Arulanandan et al. (1982), Moss et al. (2003, 2011)
1976 M=7.6 Tangshan - July 27	Y29 - Tangshan	7.60	0.120	Yes	2.8-3.8	3.3	1.0	61	38	9.7	0.09	0.93	0.5	14.8	2.59	10	75	70	75	1.70	16.5	56.2	72.7	0.98	0.122	1.08	0.99	0.113	Arulanandan et al. (1982), Moss et al. (2003, 2011)
1979 M=6.5 Imperial Valley - Oct 15	Kornbloom Rd (K4)	6.53	0.130	No	2.7-5.3	3.9	2.7	69	57	21.4	0.44	2.12	0.5	27.5	2.55	--	85	67	85	1.35	28.8	61.3	90.1	0.95	0.097	1.06	1.08	0.085	Bennett et al. (1984), Moss et al. (2003)
1979 M=6.5 Imperial Valley - Oct 15	McKim Ranch - Unit A (M7)	6.53	0.510	Yes	1.6-4.8	3.2	1.5	58	41	32.2	0.25	0.80	0.5	49.4	2.10	--	20	31	20	1.62	52.1	30.5	82.7	0.96	0.448	1.08	1.07	0.388	Bennett et al. (1984), Seed et al. (1984)
1979 M=6.5 Imperial Valley - Oct 15	Radio Tower - Unit B (R2)	6.53	0.200	Yes	3.0-4.0	3.5	2.1	62	49	14.0	0.08	0.61	0.5	19.3	2.41	--	64	55	64	1.50	21.0	55.6	76.6	0.96	0.159	1.06	1.06	0.141	Bennett et al. (1984), Seed et al. (1984)
1979 M=6.5 Imperial Valley - Oct 15	Radio Tower - Unit B (R4)	6.53	0.200	No	2.1-2.7	2.4	2.1	42	39	64.0	0.69	1.08	0.5	102.3	1.92	--	18	17	18	1.52	97.4	31.5	128.9	0.98	0.137	1.10	1.17	0.106	Bennett et al. (1984), Seed et al. (1984)

Earthquake	Site	Mag (M)	a_{max} (g)	Liq (Yes, No)	Critical depth interval (m)	Avg depth (m)	Depth to GWT (m)	σ_{vc} (kPa)	σ'_{vc} (kPa)	Tip $(q_{cN})_{aver}$	Sleeve $(f_{sN})_{aver}$	Friction ratio $(F)_{aver}$ (%)	n	Q	I_c	PI	Lab FC (%)	I_c est. FC (%)	Repr. FC (%)	C_N	q_{c1N}	Δq_{c1N}	$q_{c1N,cs}$	r_d	CSR	K_σ	MSF	CSR for M=7.5, σ=1	References
1980 M=6.3 Victoria (Mexicali) - June 9	Delta Site 2	6.33	0.190	Yes	2.2-3.2	2.7	2.2	48	43	31.0	0.01	0.04	0.5	46.6	1.81	--	--	8	8	1.70	52.6	2.3	54.9	0.97	0.133	1.06	1.05	0.119	Diaz-Rodriguez (1984), Diaz-Rodriquez & and Armijo-Palacio (1991), Moss et al. (2003)
1980 M=6.3 Victoria (Mexicali) - June 9	Delta Site 3	6.33	0.190	Yes	2.0-3.8	2.9	2.0	52	43	17.0	0.13	0.79	0.5	25.2	2.35	--	--	51	51	1.59	27.0	53.6	80.6	0.97	0.144	1.08	1.08	0.123	Diaz-Rodriguez (1984), Diaz-Rodriquez & and Armijo-Palacio (1991), Moss et al. (2003)
1980 M=6.3 Victoria (Mexicali) - June 9	Delta Site 3p	6.33	0.190	Yes	1.6-4.8	3.0	2.2	54	46	19.0	0.18	0.97	0.5	27.4	2.37	--	--	52	52	1.53	29.0	54.5	83.5	0.96	0.139	1.07	1.09	0.120	Diaz-Rodriguez (1984), Diaz-Rodriquez & and Armijo-Palacio (1991), Moss et al. (2003)
1980 M=6.3 Victoria (Mexicali) - June 9	Delta Site 4	6.33	0.190	Yes	2.0-2.6	2.3	2.0	41	38	30.0	0.24	0.81	0.5	48.3	2.11	--	--	32	32	1.64	49.3	47.4	96.7	0.98	0.130	1.10	1.11	0.106	Diaz-Rodriguez (1984), Diaz-Rodriquez & and Armijo-Palacio (1991), Moss et al. (2003)
1981 M=5.9 WestMorland - April 26	Kornbloom Rd (K4)	5.90	0.320	Yes	2.7-5.3	3.9	2.7	69	57	21.4	0.44	2.12	0.5	27.5	2.55	--	85	67	85	1.35	28.8	61.3	90.1	0.94	0.235	1.06	1.14	0.195	Bennett et al. (1984), Seed et al. (1984)
1981 M=5.9 WestMorland - April 26	McKim Ranch - Unit A (M7)	5.90	0.090	No	1.6-4.8	3.2	1.5	58	41	32.2	0.25	0.80	0.5	49.4	2.10	--	20	31	20	1.62	52.1	30.5	82.7	0.95	0.078	1.08	1.12	0.064	Bennett et al. (1984), Seed et al. (1984)
1981 M=5.9 WestMorland - April 26	Radio Tower - Unit B (R2)	5.90	0.200	Yes	3.0-4.0	3.5	2.1	62	49	14.0	0.08	0.61	0.5	19.3	2.41	--	64	55	64	1.50	21.0	55.6	76.6	0.95	0.157	1.06	1.11	0.133	Bennett et al. (1984), Seed et al. (1984)
1981 M=5.9 WestMorland - April 26	Radio Tower - Unit B (R4)	5.90	0.200	No	2.1-2.7	2.4	2.1	42	39	64.0	0.69	1.08	0.5	102.3	1.92	--	18	17	18	1.52	97.4	31.5	128.9	0.97	0.136	1.10	1.30	0.095	Bennett et al. (1984), Seed et al. (1984)
1981 M=5.9 WestMorland - April 26	Wildlife B	5.90	0.260	Yes	2.6-7.0	4.8	1.2	90	54	53.3	0.79	1.50	0.5	71.6	2.13	NP	30	34	30	1.33	70.9	49.7	120.6	0.92	0.258	1.08	1.25	0.190	Bennett et al. (1984), Seed et al. (1984)
1983 M=7.7 Nihonkai-Chubu - May 26	Akita A	7.70	0.170	Yes	0.8-2.8	1.8	0.8	33	23	22.0	0.25	1.15	0.5	45.3	2.22	--	5	41	5	1.70	37.4	0.1	37.5	0.99	0.156	1.09	0.99	0.144	Farrar (1990)
1983 M=7.7 Nihonkai-Chubu - May 26	Akita B	7.70	0.170	Yes	3.4-5.6	4.5	1.0	84	49	21.0	0.15	0.74	0.5	28.8	2.29	--	5	46	5	1.66	34.8	0.1	34.9	0.97	0.182	1.04	0.99	0.175	Farrar (1990)
1983 M=7.7 Nihonkai-Chubu - May 26	Akita C	7.70	0.170	No	2.4-3.4	2.9	2.4	52	47	39.0	0.38	0.99	0.5	56.6	2.10	--	5	31	5	1.59	61.9	0.1	62.0	0.99	0.120	1.06	0.99	0.114	Farrar (1990)
1983 M=6.9 Borah Peak - Oct 28	Pence Ranch 1 & 2	6.88	0.300	Yes	1.5-4.0	2.8	1.6	50	38	49.1	0.68	1.40	0.5	79.0	2.08	--	2	30	2	1.69	83.0	0.0	83.0	0.98	0.249	1.09	1.04	0.219	Andrus et al. (1991), Moss et al. (2003)
1983 M=6.9 Borah Peak - Oct 28	Whiskey Springs Site 1	6.88	0.500	Yes	1.6-3.2	2.4	0.8	44	29	56.9	1.04	1.85	0.5	106.0	2.07	--	20	29	20	1.70	96.7	36.6	133.2	0.98	0.493	1.10	1.11	0.404	Andrus & Youd (1987), Moss et al. (2003)
1983 M=6.9 Borah Peak - Oct 28	Whiskey Springs Site 2	6.88	0.500	Yes	2.4-4.3	3.4	2.4	60	51	70.0	2.00	2.88	0.5	97.8	2.24	--	30	42	30	1.32	92.7	54.1	146.8	0.97	0.372	1.10	1.14	0.297	Andrus & Youd (1987), Moss et al. (2003)
1983 M=6.9 Borah Peak - Oct 28	Whiskey Springs Site 3	6.88	0.500	Yes	6.8-7.8	7.3	6.8	129	124	81.9	2.11	2.62	0.5	72.7	2.30	--	20	47	20	0.91	74.3	33.5	107.8	0.90	0.306	0.98	1.07	0.293	Andrus & Youd (1987), Moss et al. (2003)
1987 M=6.6 Edgecumbe, NZ - Mar 2	Awaroa Farm AWA001	6.60	0.370	Yes	2.3-3.3	2.8	1.2	51	35	67.3	0.74	1.11	0.5	113.1	1.90	--	35	15	35	1.50	100.9	61.7	162.6	0.97	0.341	1.10	1.28	0.243	Christensen (1995), Moss et al. (2003)
1987 M=6.6 Edgecumbe, NZ - Mar 2	Brady Farm BDY001	6.60	0.400	Yes	6.4-8.0	7.2	1.7	134	79	23.1	0.22	1.00	0.5	24.5	2.41	--	30	56	30	1.15	26.6	40.7	67.3	0.89	0.392	1.02	1.05	0.366	Christensen (1995), Moss et al. (2003)
1987 M=6.6 Edgecumbe, NZ - Mar 2	Brady Farm BDY004	6.60	0.400	No	3.4-5.0	4.2	1.5	77	51	75.3	0.31	0.41	0.5	104.7	1.67	--	15	0	15	1.36	102.1	23.2	125.4	0.95	0.373	1.09	1.14	0.300	Christensen (1995), Moss et al. (2003)
1987 M=6.6 Edgecumbe, NZ - Mar 2	Edgecumbe Pipe Breaks EPB001	6.60	0.390	Yes	5.0-5.9	5.5	2.5	100	71	59.5	0.23	0.39	0.5	69.9	1.82	--	5	8	5	1.22	72.9	0.1	73.0	0.93	0.331	1.03	1.05	0.305	Christensen (1995), Moss et al. (2003)
1987 M=6.6 Edgecumbe, NZ - Mar 2	Gordon Farm GDN001	6.60	0.430	Yes	1.2-4.2	2.7	0.5	50	29	33.4	0.22	0.65	0.5	61.9	1.97	--	1	21	1	1.70	56.8	0.0	56.8	0.97	0.480	1.10	1.04	0.421	Christensen (1995), Moss et al. (2003)
1987 M=6.6 Edgecumbe, NZ - Mar 2	Gordon Farm GDN002	6.60	0.370	No	1.7-2.2	1.9	0.9	35	25	92.0	0.30	0.33	0.5	184.5	1.41	--	1	0	1	1.70	156.4	0.0	156.4	0.98	0.330	1.10	1.25	0.240	Christensen (1995), Moss et al. (2003)
1987 M=6.6 Edgecumbe, NZ - Mar 2	James Street Loop JSL007	6.60	0.280	Yes	3.4-6.8	5.1	1.2	93	54	60.0	0.30	0.51	0.5	80.6	1.82	--	1	8	1	1.40	83.9	0.0	83.9	0.93	0.291	1.06	1.06	0.259	Christensen (1995), Moss et al. (2003)
1987 M=6.6 Edgecumbe, NZ - Mar 2	Keir Farm KER001	6.60	0.310	Yes	6.5-9.5	8.0	2.5	148	94	72.0	0.22	0.31	0.5	73.0	1.76	--	5	4	5	1.04	74.9	0.1	75.1	0.88	0.277	1.01	1.05	0.261	Christensen (1995), Moss et al. (2003)
1987 M=6.6 Edgecumbe, NZ - Mar 2	Landing Rd. Bridge LRB007	6.60	0.270	Yes	4.8-6.2	5.5	1.2	102	60	59.9	0.19	0.32	0.5	76.5	1.75	--	1	3	1	1.33	79.9	0.0	79.9	0.93	0.279	1.05	1.06	0.251	Christensen (1995), Moss et al. (2003)
1987 M=6.6 Edgecumbe, NZ - Mar 2	Morris Farm MRS001	6.60	0.420	Yes	7.0-8.5	7.8	1.6	144	84	75.1	0.28	0.38	0.5	80.6	1.76	--	5	3	5	1.10	82.9	0.1	83.0	0.88	0.413	1.02	1.06	0.382	Christensen (1995), Moss et al. (2003)
1987 M=6.6 Edgecumbe, NZ - Mar 2	Morris Farm MRS003	6.60	0.410	No	5.2-6.6	5.9	2.1	109	72	79.1	0.25	0.32	0.5	92.7	1.67	--	5	0	5	1.19	94.5	0.2	94.6	0.92	0.372	1.04	1.08	0.333	Christensen (1995), Moss et al. (2003)
1987 M=6.6 Edgecumbe, NZ - Mar 2	Robinson Farm East Side RBN001	6.60	0.440	Yes	2.0-5.5	3.8	0.8	70	41	36.0	0.12	0.34	0.5	55.7	1.88	--	5	13	5	1.70	61.2	0.1	61.3	0.96	0.471	1.07	1.04	0.422	Christensen (1995), Moss et al. (2003)
1987 M=6.6 Edgecumbe, NZ - Mar 2	Robinson Farm West Side RBN004	6.60	0.440	Yes	1.0-2.8	1.9	0.6	35	22	36.1	0.01	0.03	0.5	75.8	1.62	--	5	0	5	1.70	61.4	0.1	61.5	0.98	0.440	1.10	1.04	0.383	Christensen (1995), Moss et al. (2003)
1987 M=6.6 Edgecumbe, NZ - Mar 2	Sewage Pumping Station SPS001	6.60	0.260	Yes	2.0-8.2	5.0	1.3	93	56	39.8	0.12	0.31	0.5	52.0	1.89	--	5	14	5	1.43	57.0	0.1	57.1	0.94	0.260	1.04	1.04	0.239	Christensen (1995), Moss et al. (2003)
1987 M=6.6 Edgecumbe, NZ - Mar 2	Whakatane Board Mill WBM001&2	6.60	0.270	No	3.5-5.3	4.4	1.4	80	51	30.0	0.30	1.03	0.5	41.1	2.23	--	5	41	5	1.56	46.8	0.1	47.0	0.95	0.260	1.05	1.04	0.240	Christensen (1995), Moss et al. (2003)
1987 M=6.6 Edgecumbe, NZ - Mar 2	Whakatane Hospital HSP001	6.60	0.260	No	4.4-5.0	4.7	4.4	83	80	136.2	0.66	0.49	0.5	152.0	1.58	--	5	0	5	1.10	149.7	0.2	149.9	0.94	0.165	1.04	1.22	0.130	Christensen (1995), Moss et al. (2003)

Earthquake	Site	Mag (M)	a_{max} (g)	Liq (Yes, No)	Critical depth interval (m)	Avg depth (m)	Depth to GWT (m)	σ_{vc} (kPa)	σ'_{vc} (kPa)	Tip $(q_{cN})_{aver}$	Sleeve $(f_{sN})_{aver}$	Friction ratio $(F)_{aver}$ (%)	n	Q	I_c	PI	Lab FC (%)	I_c est. FC (%)	Repr. FC (%)	C_N	q_{c1N}	Δq_{c1N}	$q_{c1N,cs}$	r_d	CSR	K_σ	MSF	CSR for M=7.5, σ=1	References
1987 M=6.6 Edgecumbe, NZ - Mar 2	Whakatane Pony Club WPC001	6.60	0.270	Yes	3.6-4.6	4.1	2.4	74	57	43.0	0.12	0.28	0.5	56.1	1.85	--	10	11	10	1.40	60.0	6.6	66.6	0.95	0.217	1.05	1.05	0.198	Christensen (1995), Moss et al. (2003)
1987 M=6.2 Superstition Hills 01 - Nov 24	Radio Tower - Unit B (R2)	6.22	0.090	No	3.0-4.0	3.5	2.1	62	49	14.0	0.08	0.61	0.5	19.3	2.41	--	64	55	64	1.50	21.0	55.6	76.6	0.95	0.071	1.06	1.08	0.062	Bennett et al. (1984)
1987 M=6.2 Superstition Hills 01 - Nov 24	Wildlife B	6.22	0.133	No	2.6-7.0	4.8	1.2	90	54	53.3	0.79	1.50	0.5	71.6	2.13	NP	30	34	30	1.33	70.9	49.7	120.6	0.93	0.133	1.08	1.20	0.103	Bennett et al. (1984), Porcella et al. (1987)
1987 M=6.5 Superstition Hills 02 - Nov 24	Kornbloom Rd (K4)	6.54	0.174	No	2.7-5.3	3.9	2.7	69	57	21.4	0.44	2.12	0.5	27.5	2.55	--	85	67	85	1.35	28.8	61.3	90.1	0.95	0.129	1.06	1.08	0.114	Bennett et al. (1984), Cetin et al. (2000)
1987 M=6.5 Superstition Hills 02 - Nov 24	Radio Tower - Unit B (R2)	6.54	0.200	No	3.0-4.0	3.5	2.1	62	49	14.0	0.08	0.61	0.5	19.3	2.41	--	64	55	64	1.50	21.0	55.6	76.6	0.96	0.159	1.06	1.06	0.141	Bennett et al. (1984), Cetin et al. (2000)
1987 M=6.5 Superstition Hills 02 - Nov 24	Radio Tower - Unit B (R4)	6.54	0.180	No	2.1-2.7	2.4	2.1	42	39	64.0	0.69	1.08	0.5	102.3	1.92	--	18	17	18	1.52	97.4	31.5	128.9	0.98	0.123	1.10	1.16	0.096	Bennett et al. (1984), Cetin et al. (2000)
1987 M=6.5 Superstition Hills 02 - Nov 24	Wildlife B	6.54	0.206	Yes	2.6-7.0	4.8	1.2	90	54	53.3	0.79	1.50	0.5	71.6	2.13	NP	30	34	30	1.33	70.9	49.7	120.6	0.94	0.208	1.08	1.14	0.169	Bennett et al. (1984), Porcella et al. (1987)
1989 M=6.9 Loma Prieta - Oct 18	State Beach Kiosk	6.93	0.280	Yes	1.8-5.4	3.6	1.8	64	47	47.5	0.23	0.49	0.5	68.7	1.87	--	1	13	1	1.54	73.2	0.0	73.2	0.97	0.240	1.07	1.03	0.218	Boulanger et al. (1997)
1989 M=6.9 Loma Prieta - Oct 18	State Beach Pathway	6.93	0.280	Yes	2.3-5.0	3.3	2.5	58	50	90.0	0.30	0.34	0.5	127.0	1.56	--	1	0	1	1.37	123.5	0.0	123.5	0.97	0.206	1.09	1.08	0.174	Boulanger et al. (1997)
1989 M=6.9 Loma Prieta - Oct 18	State Beach (UC-18)	6.93	0.280	No	3.4-4.4	3.9	3.4	68	63	163.0	0.45	0.28	0.5	204.9	1.33	--	1	0	1	1.17	191.3	0.0	191.3	0.96	0.188	1.10	1.24	0.138	Boulanger et al. (1997)
1989 M=6.9 Loma Prieta - Oct 18	Sandhold Road SI-2 (deformed)	6.93	0.280	Yes	2.0-3.0	2.5	1.8	44	38	77.0	0.21	0.27	0.5	125.6	1.52	--	2	0	2	1.57	121.0	0.0	121.0	0.98	0.211	1.10	1.08	0.178	Boulanger et al. (1997)
1989 M=6.9 Loma Prieta - Oct 18	Sandhold Road SI-2 (undeformed)	6.93	0.280	No	6.0-10.0	8.0	1.8	148	87	300.0	0.81	0.27	0.5	320.7	1.16	--	4	0	4	1.04	311.8	0.0	311.9	0.89	0.276	1.04	1.24	0.213	Boulanger et al. (1997)
1989 M=6.9 Loma Prieta - Oct 18	Sandhold Road SI-4 (deformed)	6.93	0.280	Yes	1.1-1.7	1.4	1.4	24	24	30.0	0.11	0.36	0.5	60.8	1.86	--	4	12	4	1.70	51.0	0.0	51.0	0.99	0.181	1.10	1.02	0.161	Boulanger et al. (1997)
1989 M=6.9 Loma Prieta - Oct 18	Sandhold Road SI-4 (undeformed)	6.93	0.280	No	3.0-4.0	3.5	1.4	64	43	100.0	0.30	0.30	0.5	151.7	1.47	--	4	0	4	1.42	142.4	0.0	142.4	0.97	0.260	1.10	1.12	0.211	Boulanger et al. (1997)
1989 M=6.9 Loma Prieta - Oct 18	Sandhold Road SI-5 (deformed)	6.93	0.280	Yes	4.7-5.3	5.0	1.8	92	60	90.0	0.27	0.30	0.5	115.4	1.57	--	4	0	4	1.27	114.7	0.0	114.8	0.94	0.261	1.06	1.07	0.230	Boulanger et al. (1997)
1989 M=6.9 Loma Prieta - Oct 18	Sandhold Road SI-5 (undeformed)	6.93	0.280	No	6.0-8.0	7.0	1.8	129	78	190.0	0.57	0.30	0.5	214.2	1.34	--	1	0	1	1.09	206.3	0.0	206.3	0.91	0.274	1.07	1.24	0.205	Boulanger et al. (1997)
1989 M=6.9 Loma Prieta - Oct 18	Sandhold Road UC-3	6.93	0.280	No	2.0-3.0	2.5	1.7	45	37	87.0	0.30	0.35	0.5	143.6	1.52	--	4	0	4	1.55	134.6	0.0	134.6	0.98	0.216	1.10	1.10	0.178	Boulanger et al. (1997)
1989 M=6.9 Loma Prieta - Oct 18	Sandhold Road UC-2	6.93	0.280	No	1.5-2.5	2.0	1.7	35	32	104.0	0.33	0.32	0.5	183.8	1.41	--	4	0	4	1.55	161.7	0.0	161.7	0.99	0.196	1.10	1.17	0.153	Boulanger et al. (1997)
1989 M=6.9 Loma Prieta - Oct 18	Sandhold Road UC-6	6.93	0.280	No	6.0-7.0	6.5	1.7	120	73	182.0	0.31	0.17	0.5	212.6	1.23	--	1	0	1	1.11	202.5	0.0	202.5	0.92	0.275	1.09	1.24	0.204	Boulanger et al. (1997)
1989 M=6.9 Loma Prieta - Oct 18	MBARI No. 3 (RC-5)	6.93	0.280	No	3.2-3.8	3.5	1.8	63	47	155.0	0.23	0.15	0.5	227.3	1.18	--	1	0	1	1.29	200.2	0.0	200.2	0.97	0.239	1.10	1.24	0.175	Boulanger et al. (1997)
1989 M=6.9 Loma Prieta - Oct 18	MBARI No. 3 (RC-6)	6.93	0.280	No	3.8-4.4	4.1	2.6	73	59	130.0	0.26	0.20	0.5	169.7	1.35	--	1	0	1	1.24	160.6	0.0	160.6	0.96	0.218	1.10	1.16	0.171	Boulanger et al. (1997)
1989 M=6.9 Loma Prieta - Oct 18	MBARI No. 3 (RC-7)	6.93	0.280	No	4.4-5.0	4.7	3.7	83	73	92.0	0.23	0.25	0.5	107.2	1.57	--	1	0	1	1.17	107.7	0.0	107.7	0.95	0.196	1.04	1.06	0.178	Boulanger et al. (1997)
1989 M=6.9 Loma Prieta - Oct 18	MBARI Technology (RC-9)	6.93	0.280	No	3.0-4.0	3.5	2.0	63	48	124.0	0.31	0.25	0.5	178.5	1.37	--	4	0	4	1.33	164.4	0.0	164.5	0.97	0.230	1.10	1.17	0.178	Boulanger et al. (1997)
1989 M=6.9 Loma Prieta - Oct 18	MBARI No. 4 (CPT-1, 2, 3, & 4)	6.93	0.280	No	1.5-4.5	3.1	1.9	56	44	87.7	0.10	0.11	0.5	131.9	1.38	--	4	0	4	1.45	126.8	0.0	126.8	0.97	0.225	1.10	1.09	0.188	Boulanger et al. (1997)
1989 M=6.9 Loma Prieta - Oct 18	General Fish (CPT-5)	6.93	0.280	Yes	1.8-2.4	2.1	1.5	37	31	25.0	0.05	0.20	0.5	44.2	1.90	--	4	15	4	1.70	42.5	0.0	42.5	0.98	0.213	1.08	1.02	0.193	Boulanger et al. (1997)
1989 M=6.9 Loma Prieta - Oct 18	General Fish (CPT-6)	6.93	0.280	No	2.3-2.9	2.6	1.7	46	38	100.0	0.20	0.20	0.5	163.2	1.36	--	4	0	4	1.49	149.3	0.0	149.3	0.98	0.220	1.10	1.13	0.176	Boulanger et al. (1997)
1989 M=6.9 Loma Prieta - Oct 18	Harbor Office (UC-12)	6.93	0.280	Yes	3.8-4.4	4.1	1.9	74	53	62.0	0.56	0.91	0.5	84.7	1.94	--	15	18	15	1.37	84.9	21.8	106.7	0.96	0.246	1.07	1.06	0.216	Boulanger et al. (1997)
1989 M=6.9 Loma Prieta - Oct 18	Harbor Office (UC-13)	6.93	0.280	Yes	3.8-4.4	4.1	1.9	74	53	43.0	0.43	1.02	0.5	58.4	2.10	--	15	31	15	1.42	61.2	19.8	81.0	0.96	0.246	1.06	1.04	0.224	Boulanger et al. (1997)
1989 M=6.9 Loma Prieta - Oct 18	Harbor Office (UC-20)	6.93	0.280	Yes	4.4-5.0	4.7	3.0	84	67	41.0	0.24	0.59	0.5	49.2	2.04	--	10	26	10	1.28	52.5	6.4	58.9	0.95	0.215	1.03	1.03	0.204	Boulanger et al. (1997)
1989 M=6.9 Loma Prieta - Oct 18	Harbor Office (UC-21)	6.93	0.280	Yes	3.9-4.5	4.2	2.7	75	60	49.0	0.24	0.49	0.5	62.4	1.90	--	10	15	10	1.34	65.7	6.7	72.5	0.96	0.217	1.04	1.03	0.201	Boulanger et al. (1997)
1989 M=6.9 Loma Prieta - Oct 18	Woodward Marine (UC-9)	6.93	0.280	Yes	2.6-3.2	2.9	1.2	53	36	66.0	0.20	0.30	0.5	109.3	1.59	--	5	0	5	1.64	108.2	0.2	108.3	0.97	0.259	1.10	1.06	0.222	Boulanger et al. (1997)
1989 M=6.9 Loma Prieta - Oct 18	Woodward Marine (UC-10)	6.93	0.280	Yes	1.7-2.3	2.0	1.0	36	26	31.0	0.12	0.40	0.5	59.9	1.88	--	5	14	5	1.70	52.7	0.1	52.8	0.99	0.246	1.10	1.02	0.219	Boulanger et al. (1997)

Earthquake	Site	Mag (M)	a_{max} (g)	Liq (Yes, No)	Critical depth interval (m)	Avg depth (m)	Depth to GWT (m)	σ_{vc} (kPa)	σ'_{vc} (kPa)	Tip $(q_{cN})_{aver}$	Sleeve $(f_{sN})_{aver}$	Friction ratio $(F)_{aver}$ (%)	n	Q	I_c	PI	Lab FC (%)	I_c est. FC (%)	Repr. FC (%)	C_N	q_{c1N}	Δq_{c1N}	$q_{c1N,cs}$	r_d	CSR	K_σ	MSF	CSR for M=7.5, σ=1	References
1989 M=6.9 Loma Prieta - Oct 18	Woodward Marine (UC-11)	6.93	0.280	Yes	1.9-2.5	2.2	1.0	40	28	31.0	0.11	0.36	0.5	57.9	1.88	--	15	13	15	1.70	52.7	19.1	71.8	0.98	0.254	1.10	1.03	0.224	Boulanger et al. (1997)
1989 M=6.9 Loma Prieta - Oct 18	Woodward Marine (15-A)	6.93	0.280	Yes	2.6-3.2	2.9	1.3	53	37	51.0	0.11	0.22	0.5	83.4	1.65	--	3	0	3	1.70	86.7	0.0	86.7	0.97	0.253	1.10	1.04	0.221	Boulanger et al. (1997)
1989 M=6.9 Loma Prieta - Oct 18	Woodward Marine (14-A)	6.93	0.280	Yes	3.3-3.9	3.6	1.2	66	43	78.0	0.04	0.05	0.5	119.1	1.40	--	3	0	3	1.49	116.6	0.0	116.6	0.97	0.273	1.10	1.07	0.231	Boulanger et al. (1997)
1989 M=6.9 Loma Prieta - Oct 18	Marine Lab (UC-1)	6.93	0.280	Yes	10.7-11.3	11.0	2.4	204	120	46.0	0.46	1.05	0.5	40.4	2.24	--	30	42	30	0.92	42.1	43.8	85.9	0.84	0.260	0.98	1.04	0.254	Boulanger et al. (1997)
1989 M=6.9 Loma Prieta - Oct 18	Marine Lab (UC-7)	6.93	0.280	Yes	8.0-8.6	8.3	1.4	155	87	43.0	0.77	1.87	0.5	44.7	2.35	--	30	51	30	1.08	46.5	44.7	91.2	0.89	0.288	1.02	1.04	0.271	Boulanger et al. (1997)
1989 M=6.9 Loma Prieta - Oct 18	Marine Lab (UC-8)	6.93	0.280	Yes	8.3-8.9	8.6	1.3	160	89	43.0	0.56	1.35	0.5	44.2	2.27	--	30	45	30	1.07	46.0	44.6	90.6	0.88	0.290	1.01	1.04	0.275	Boulanger et al. (1997)
1989 M=6.9 Loma Prieta - Oct 18	Marine Lab (C2)	6.93	0.280	Yes	9.5-10.1	9.8	2.2	182	107	38.0	0.53	1.47	0.5	35.1	2.37	--	27	53	27	0.97	36.8	39.3	76.1	0.86	0.266	1.00	1.03	0.259	Boulanger et al. (1997)
1989 M=6.9 Loma Prieta - Oct 18	Marine Lab (C3)	6.93	0.280	Yes	4.1-4.7	4.4	1.5	81	52	82.0	0.23	0.28	0.5	112.8	1.57	--	3	0	3	1.37	112.1	0.0	112.1	0.95	0.268	1.08	1.07	0.233	Boulanger et al. (1997)
1989 M=6.9 Loma Prieta - Oct 18	Marine Lab (C4)	6.93	0.280	Yes	5.2-5.8	5.5	2.8	99	73	19.0	0.04	0.21	0.5	21.2	2.21	--	3	40	3	1.28	24.4	0.0	24.4	0.94	0.232	1.02	1.02	0.224	Boulanger et al. (1997)
1989 M=6.9 Loma Prieta - Oct 18	Model Airport (AIR-18)	6.93	0.260	Yes	2.0-3.6	2.8	2.4	50	47	18.0	0.18	1.03	0.5	25.8	2.40	--	23	55	23	1.60	28.7	31.6	60.3	0.98	0.177	1.06	1.03	0.163	Bennett & Tinsley (1995), Toprak & Holzer (2003)
1989 M=6.9 Loma Prieta - Oct 18	Model Airport (AIR-21)	6.93	0.260	Yes	2.0-3.2	2.6	2.4	47	45	21.0	0.08	0.41	0.5	30.7	2.15	--	5	35	5	1.70	35.7	0.1	35.8	0.98	0.173	1.05	1.02	0.161	Bennett & Tinsley (1995), Toprak & Holzer (2003)
1989 M=6.9 Loma Prieta - Oct 18	Miller Farm (CMF-3)	6.93	0.360	Yes	4.3-7.3	5.8	4.9	105	97	35.7	0.14	0.41	0.5	35.4	2.10	--	27	31	27	1.03	36.6	39.3	75.9	0.93	0.237	1.00	1.03	0.229	Bennett & Tinsley (1995), Toprak & Holzer (2003)
1989 M=6.9 Loma Prieta - Oct 18	Miller Farm (CMF-5)	6.93	0.360	Yes	5.5-8.0	6.7	4.9	117	100	78.0	0.39	0.51	0.5	77.3	1.83	--	13	10	13	1.01	78.6	15.5	94.1	0.92	0.253	1.00	1.05	0.241	Bennett & Tinsley (1995), Toprak & Holzer (2003)
1989 M=6.9 Loma Prieta - Oct 18	Miller Farm (CMF-8)	6.93	0.360	Yes	4.3-8.0	6.0	4.9	110	99	47.3	0.24	0.51	0.5	46.7	2.03	--	25	25	25	1.01	47.9	39.1	87.0	0.93	0.242	1.00	1.04	0.231	Bennett & Tinsley (1995), Toprak & Holzer (2003)
1989 M=6.9 Loma Prieta - Oct 18	Miller Farm (CMF-10)	6.93	0.360	No	6.9-9.6	8.2	3.0	153	102	68.0	0.68	1.03	0.5	66.3	2.06	--	20	28	20	1.00	67.9	32.7	100.6	0.89	0.313	1.00	1.05	0.297	Bennett & Tinsley (1995), Toprak & Holzer (2003)
1989 M=6.9 Loma Prieta - Oct 18	Farris Farm (FAR-58)	6.93	0.360	Yes	5.0-9.5	7.4	4.8	136	111	110.7	0.55	0.51	0.5	104.5	1.72	--	4	1	4	0.96	106.1	0.0	106.1	0.90	0.261	0.99	1.06	0.248	Bennett & Tinsley (1995), Toprak & Holzer (2003)
1989 M=6.9 Loma Prieta - Oct 18	Farris Farm (FAR-59)	6.93	0.360	Yes	5.5-10.5	8.0	4.8	147	116	94.0	0.47	0.51	0.5	86.4	1.79	--	7	6	7	0.93	87.6	1.5	89.1	0.89	0.266	0.99	1.04	0.258	Bennett & Tinsley (1995), Toprak & Holzer (2003)
1989 M=6.9 Loma Prieta - Oct 18	Farris Farm (FAR-61)	6.93	0.360	Yes	5.0-10.0	7.4	4.2	136	105	77.5	0.50	0.65	0.5	74.8	1.90	--	11	15	11	0.98	76.2	10.3	86.5	0.91	0.275	1.00	1.04	0.265	Bennett & Tinsley (1995), Toprak & Holzer (2003)
1989 M=6.9 Loma Prieta - Oct 18	Leonardini (LEN-37)	6.93	0.220	No	2.5-7.5	4.9	2.5	91	67	34.5	0.17	0.51	0.5	41.2	2.08	--	12	29	12	1.29	44.6	10.2	54.8	0.95	0.183	1.03	1.02	0.173	Bennett & Tinsley (1995), Toprak & Holzer (2003)
1989 M=6.9 Loma Prieta - Oct 18	Leonardini (LEN-39)	6.93	0.220	Yes	1.9-4.5	2.9	1.9	53	43	24.7	0.06	0.24	0.5	36.8	2.00	--	11	23	11	1.70	41.9	8.3	50.2	0.97	0.171	1.06	1.02	0.158	Bennett & Tinsley (1995), Toprak & Holzer (2003)
1989 M=6.9 Loma Prieta - Oct 18	Leonardini (LEN-51)	6.93	0.220	Yes	3.7-5.7	4.7	1.8	87	59	45.0	0.23	0.51	0.5	57.8	1.94	--	10	19	10	1.37	61.6	6.6	68.2	0.95	0.201	1.04	1.03	0.187	Bennett & Tinsley (1995), Toprak & Holzer (2003)
1989 M=6.9 Loma Prieta - Oct 18	Leonardini (LEN-52a)	6.93	0.220	No	2.9-3.6	3.2	2.7	58	53	60.0	0.36	0.61	0.5	81.7	1.85	--	12	11	12	1.38	83.0	12.8	95.8	0.97	0.152	1.07	1.05	0.136	Bennett & Tinsley (1995), Toprak & Holzer (2003)
1989 M=6.9 Loma Prieta - Oct 18	Leonardini (LEN-53)	6.93	0.220	Yes	2.1-6.5	4.3	2.1	79	58	52.0	0.26	0.51	0.5	67.9	1.88	--	9	14	9	1.37	71.4	3.6	75.0	0.96	0.187	1.05	1.03	0.172	Bennett & Tinsley (1995), Toprak & Holzer (2003)
1989 M=6.9 Loma Prieta - Oct 18	Sea Mist (SEA-31)	6.93	0.220	Yes	1.5-5.5	3.5	0.8	66	39	25.0	0.13	0.51	0.5	39.2	2.09	--	24	31	24	1.69	42.3	36.1	78.4	0.97	0.232	1.09	1.04	0.206	Bennett & Tinsley (1995), Toprak & Holzer (2003)
1989 M=6.9 Loma Prieta - Oct 18	Jefferson Ranch (JRR-141)	6.93	0.210	Yes	3.8-8.0	6.0	2.1	112	73	42.0	0.21	0.51	0.5	48.0	2.02	--	10	24	10	1.22	51.1	6.3	57.5	0.93	0.193	1.02	1.02	0.184	Bennett & Tinsley (1995), Toprak & Holzer (2003)
1989 M=6.9 Loma Prieta - Oct 18	Jefferson Ranch (JRR-148)	6.93	0.210	Yes	6.4-8.0	7.3	3.0	135	93	85.0	0.43	0.51	0.5	87.2	1.79	--	5	6	5	1.05	88.9	0.2	89.1	0.91	0.179	1.01	1.04	0.171	Bennett & Tinsley (1995), Toprak & Holzer (2003)
1989 M=6.9 Loma Prieta - Oct 18	Pajaro Dunes (PD1-44)	6.93	0.220	Yes	3.4-5.5	4.5	3.4	82	72	78.0	0.39	0.51	0.5	91.7	1.77	--	4	4	4	1.20	93.3	0.0	93.3	0.95	0.157	1.04	1.05	0.145	Bennett & Tinsley (1995), Toprak & Holzer (2003)
1989 M=6.9 Loma Prieta - Oct 18	Radovich (RAD-98)	6.93	0.380	No	3.5-7.5	5.3	3.5	97	79	77.3	0.52	0.67	0.5	86.1	1.86	--	9	12	9	1.13	87.6	5.7	93.3	0.94	0.283	1.02	1.05	0.264	Bennett & Tinsley (1995), Toprak & Holzer (2003)
1989 M=6.9 Loma Prieta - Oct 18	Radovich (RAD-99)	6.93	0.380	Yes	4.6-7.2	6.0	4.1	110	91	50.0	0.35	0.72	0.5	51.4	2.06	--	18	28	18	1.06	52.9	26.3	79.2	0.93	0.276	1.01	1.04	0.264	Bennett & Tinsley (1995), Toprak & Holzer (2003)
1989 M=6.9 Loma Prieta - Oct 18	Marinovich (MRR-65)	6.93	0.400	Yes	6.5-10.5	8.5	5.6	156	128	76.0	0.53	0.71	0.5	66.2	1.97	--	12	20	12	0.88	66.9	12.0	78.9	0.89	0.281	0.98	1.04	0.278	Bennett & Tinsley (1995), Toprak & Holzer (2003)
1989 M=6.9 Loma Prieta - Oct 18	Marinovich (MRR-67)	6.93	0.400	No	5.8-7.0	6.5	6.2	118	115	144.0	1.15	0.81	0.5	133.9	1.75	--	15	3	15	0.95	137.2	26.2	163.4	0.92	0.245	0.98	1.17	0.215	Bennett & Tinsley (1995), Toprak & Holzer (2003)
1989 M=6.9 Loma Prieta - Oct 18	Tanimura (TAN-103)	6.93	0.130	Yes	8.0-9.4	8.7	5.0	160	124	40.0	0.24	0.62	0.5	34.6	2.18	--	13	38	13	0.88	35.1	12.8	47.9	0.88	0.096	0.99	1.02	0.096	Bennett & Tinsley (1995), Toprak & Holzer (2003)

Earthquake	Site	Mag (M)	a_{max} (g)	Liq (Yes, No)	Critical depth interval (m)	Avg depth (m)	Depth to GWT (m)	σ_{vc} (kPa)	σ'_{vc} (kPa)	Tip $(q_{cN})_{aver}$	Sleeve $(f_{sN})_{aver}$	Friction ratio $(F)_{aver}$ (%)	n	Q	I_c	PI	Lab FC (%)	I_c est. FC (%)	Repr. FC (%)	C_N	q_{c1N}	Δq_{c1N}	$q_{c1N,cs}$	r_d	CSR	K_σ	MSF	CSR for M=7.5, σ=1	References
1989 M=6.9 Loma Prieta - Oct 18	Tanimura (TAN-105)	6.93	0.130	No	4.2-6.4	5.3	4.2	97	86	38.0	0.19	0.51	0.5	40.1	2.09	--	30	30	30	1.09	41.5	43.7	85.1	0.94	0.089	1.02	1.04	0.085	Bennett & Tinsley (1995), Toprak & Holzer (2003)
1989 M=6.9 Loma Prieta - Oct 18	McGowan Farm (MCG-136)	6.93	0.260	No	2.4-5.5	4.0	2.4	74	58	40.0	0.32	0.81	0.5	51.8	2.09	--	15	30	15	1.37	54.7	19.2	74.0	0.96	0.206	1.05	1.03	0.190	Bennett & Tinsley (1995), Toprak & Holzer (2003)
1989 M=6.9 Loma Prieta - Oct 18	McGowan Farm (MCG-138)	6.93	0.260	No	1.8-4.5	2.9	1.8	53	43	21.7	0.15	0.72	0.5	32.6	2.23	--	42	42	42	1.59	34.3	51.4	85.7	0.97	0.206	1.08	1.04	0.183	Bennett & Tinsley (1995), Toprak & Holzer (2003)
1989 M=6.9 Loma Prieta - Oct 18	Granite (GRA-123)	6.93	0.340	Yes	7.0-8.0	7.5	5.0	138	113	44.0	0.29	0.67	0.5	40.3	2.14	--	18	34	18	0.94	41.2	25.0	66.2	0.90	0.243	0.99	1.03	0.238	Bennett & Tinsley (1995), Toprak & Holzer (2003)
1989 M=6.9 Loma Prieta - Oct 18	Southern Pacific Bridge (SPR-48)	6.93	0.330	Yes	5.4-9.0	7.0	5.3	129	112	51.3	0.39	0.79	0.5	47.6	2.11	--	13	32	13	0.94	48.4	13.6	62.0	0.91	0.225	0.99	1.03	0.221	Bennett & Tinsley (1995), Toprak & Holzer (2003)
1989 M=6.9 Loma Prieta - Oct 18	Silliman (SIL-68)	6.93	0.380	Yes	3.5-7.0	5.2	3.5	95	79	56.0	0.36	0.66	0.5	62.3	1.97	--	18	21	18	1.14	63.8	27.6	91.4	0.94	0.282	1.02	1.04	0.263	Bennett & Tinsley (1995), Toprak & Holzer (2003)
1989 M=6.9 Loma Prieta - Oct 18	KETT (KET-74)	6.93	0.470	Yes	2.2-3.2	2.7	1.5	50	38	48.0	0.62	1.31	0.5	77.4	2.07	--	15	29	15	1.63	78.3	21.2	99.5	0.98	0.391	1.10	1.05	0.338	Bennett & Tinsley (1995), Toprak & Holzer (2003)
1989 M=6.9 Loma Prieta - Oct 18	Martella (MAR-110)	6.93	0.130	No	3.4-5.7	4.5	1.8	84	57	36.0	0.22	0.61	0.5	46.8	2.06	--	14	28	14	1.40	50.3	16.3	66.6	0.95	0.118	1.05	1.03	0.109	Bennett & Tinsley (1995), Toprak & Holzer (2003)
1989 M=6.9 Loma Prieta - Oct 18	Martella (MAR-111)	6.93	0.130	No	1.7-6.5	4.0	1.7	74	52	40.0	0.24	0.61	0.5	54.9	2.00	--	10	23	10	1.48	59.3	6.6	65.9	0.96	0.116	1.05	1.03	0.107	Bennett & Tinsley (1995), Toprak & Holzer (2003)
1989 M=6.9 Loma Prieta - Oct 18	Salinas River Bridge (SRB-116)	6.93	0.120	No	6.4-7.4	6.9	6.4	125	120	40.0	0.92	2.37	0.5	35.5	2.50	--	7	63	7	0.89	35.5	1.2	36.7	0.91	0.074	0.99	1.02	0.074	Bennett & Tinsley (1995), Moss et al. (2006)
1989 M=6.9 Loma Prieta - Oct 18	Salinas River Bridge (SRB-117)	6.93	0.120	No	6.4-8.0	7.2	6.4	131	123	56.0	0.90	1.64	0.5	49.5	2.28	--	9	46	9	0.89	49.6	4.2	53.8	0.91	0.075	0.99	1.02	0.075	Bennett & Tinsley (1995), Moss et al. (2006)
1989 M=6.9 Loma Prieta - Oct 18	Alameda Bay Farm Isl. (HBI-P6)	6.93	0.240	Yes	3.0-4.5	3.8	3.0	66	59	60.0	0.22	0.37	0.5	77.8	1.77	--	0	4	4	1.35	80.7	0.0	80.8	0.96	0.169	1.05	1.04	0.155	Mitchell et al. (1994)
1989 M=6.9 Loma Prieta - Oct 18	Alameda Bay Farm Isl. (Dike)	6.93	0.240	No	5.5-6.8	6.2	5.5	108	102	105.0	2.94	2.83	0.5	103.7	2.22	--	10	40	10	1.00	104.9	7.8	112.7	0.93	0.154	1.00	1.07	0.144	Mitchell et al. (1994)
1989 M=6.9 Loma Prieta - Oct 18	POO7-2	6.93	0.280	Yes	5.5-7.0	6.3	3.0	116	84	55.0	0.22	0.41	0.5	59.1	1.89	--	3	14	3	1.12	61.6	0.0	61.6	0.92	0.232	1.01	1.03	0.223	Mitchell et al. (1994), Kayen et al. (1998)
1989 M=6.9 Loma Prieta - Oct 18	POO7-3	6.93	0.280	Marginal	5.5-7.0	6.3	3.0	116	84	56.0	0.84	1.53	0.5	60.2	2.20	--	3	39	3	1.12	62.7	0.0	62.7	0.92	0.232	1.01	1.03	0.223	Mitchell et al. (1994), Kayen et al. (1998)
1989 M=6.9 Loma Prieta - Oct 18	POR-2&3&4	6.93	0.180	Yes	4.0-7.5	5.5	3.5	89	70	19.0	0.11	0.58	0.5	21.8	2.35	--	52	51	52	1.23	23.4	52.9	76.3	0.94	0.140	1.03	1.03	0.131	Mitchell et al. (1994), Kayen et al. (1998)
1989 M=6.9 Loma Prieta - Oct 18	SFOBB-1	6.93	0.280	Yes	5.0-7.5	6.3	3.0	117	84	52.0	0.25	0.49	0.5	55.7	1.95	--	8	19	8	1.12	58.1	2.6	60.7	0.92	0.233	1.01	1.03	0.224	Mitchell et al. (1994), Kayen et al. (1998)
1989 M=6.9 Loma Prieta - Oct 18	SFOBB-2	6.93	0.280	Yes	6.0-9.0	7.5	3.0	139	95	81.0	0.35	0.44	0.5	82.0	1.78	--	12	5	12	1.03	83.6	12.8	96.4	0.90	0.241	1.01	1.05	0.228	Mitchell et al. (1994), Kayen et al. (1998)
1989 M=6.9 Loma Prieta - Oct 18	Treasure Island Fire Station	6.93	0.160	Yes	3.0-7.0	5.0	1.5	93	59	40.0	0.28	0.72	0.5	51.1	2.06	--	20	28	20	1.34	53.4	30.7	84.2	0.94	0.155	1.05	1.04	0.142	Pass (1994), Youd and Carter (2005)
1994 M=6.7 Northridge - Jan 17	Balboa Blvd Unit C (BAL-10)	6.69	0.840	Yes	8.2-9.7	8.9	7.2	164	147	76.0	1.86	2.50	0.5	61.7	2.33	--	50	50	50	0.85	64.5	63.1	127.5	0.86	0.526	0.95	1.13	0.488	Bennett et al. (1998), Holzer et al. (1999), Moss et al. (2003)
1994 M=6.7 Northridge - Jan 17	Rory Lane (M-27)	6.69	0.800	Yes	3.4-4.4	3.9	3.4	71	66	80.0	0.95	1.20	0.5	97.8	1.97	--	20	21	20	1.20	96.0	36.5	132.5	0.96	0.534	1.06	1.15	0.440	Abdel-Haq & Hryciw (1998)
1995 M=6.9 Hyogoken-Nambu - Jan 16	Dust Management Center	6.90	0.370	Yes	6.0-8.0	7.0	2.0	125	76	75.0	0.28	0.38	0.5	85.0	1.74	--	--	2	2	1.16	87.3	0.0	87.3	0.91	0.360	1.03	1.04	0.336	Suzuki et al. (2003)
1995 M=6.9 Hyogoken-Nambu - Jan 16	Fukuzumi Park	6.90	0.650	No	11.0-12.5	11.8	3.1	210	125	178.7	2.54	1.44	0.5	158.5	1.87	--	--	13	13	0.93	165.9	20.3	186.2	0.82	0.583	0.95	1.26	0.487	Suzuki et al. (2003)
1995 M=6.9 Hyogoken-Nambu - Jan 16	Hamakoshienn Housing Area	6.90	0.500	Yes	2.5-5.0	3.8	2.0	67	50	45.9	0.30	0.66	0.5	64.6	1.96	--	--	20	20	1.43	65.8	31.6	97.4	0.96	0.421	1.07	1.05	0.372	Suzuki et al. (2003)
1995 M=6.9 Hyogoken-Nambu - Jan 16	Honjyo Central Park	6.90	0.700	No	4.0-6.0	5.0	2.5	93	68	140.4	0.84	0.60	0.5	170.0	1.59	--	--	0	0	1.16	163.5	0.0	163.5	0.94	0.584	1.07	1.18	0.462	Suzuki et al. (2003)
1995 M=6.9 Hyogoken-Nambu - Jan 16	Imazu Elementary School	6.90	0.600	Yes	4.0-5.2	4.6	1.4	86	54	100.0	0.15	0.15	0.5	135.1	1.40	--	--	0	0	1.31	131.1	0.0	131.1	0.95	0.584	1.08	1.10	0.489	Suzuki et al. (2003)
1995 M=6.9 Hyogoken-Nambu - Jan 16	Kobe Art Institute	6.90	0.500	No	3.0-3.8	3.4	3.0	62	58	128.3	1.98	1.55	0.5	168.9	1.88	--	--	13	13	1.22	157.0	21.6	178.6	0.97	0.335	1.10	1.23	0.248	Suzuki et al. (2003)
1995 M=6.9 Hyogoken-Nambu - Jan 16	Kobe Customs Maya Office A	6.90	0.600	Yes	4.0-9.0	6.5	1.8	121	75	23.2	0.09	0.42	0.5	25.5	2.23	--	--	41	41	1.18	27.3	49.3	76.7	0.92	0.578	1.03	1.04	0.544	Suzuki et al. (2003)
1995 M=6.9 Hyogoken-Nambu - Jan 16	Kobe Customs Maya Office B	6.90	0.600	Yes	3.0-6.0	4.5	1.8	84	57	50.2	0.44	0.89	0.5	65.7	2.02	--	--	25	25	1.32	66.2	41.6	107.8	0.95	0.543	1.06	1.07	0.479	Suzuki et al. (2003)
1995 M=6.9 Hyogoken-Nambu - Jan 16	Kobe Port Const. Office	6.90	0.600	Yes	3.0-5.0	4.0	2.5	72	57	37.9	0.11	0.30	0.5	49.6	1.91	--	--	15	15	1.39	52.5	20.3	72.8	0.96	0.471	1.05	1.03	0.434	Suzuki et al. (2003)
1995 M=6.9 Hyogoken-Nambu - Jan 16	Kobe Wharf Public Co.	6.90	0.450	Yes	4.0-5.5	4.8	2.1	86	60	42.8	0.33	0.79	0.5	54.3	2.06	--	--	28	28	1.29	55.4	44.3	99.8	0.95	0.396	1.05	1.06	0.356	Suzuki et al. (2003)
1995 M=6.9 Hyogoken-Nambu - Jan 16	Koyo Pump Station	6.90	0.450	Yes	5.0-7.0	6.0	2.6	109	76	20.0	0.34	1.80	0.5	21.8	2.59	--	--	70	70	1.17	23.4	57.5	80.9	0.93	0.391	1.03	1.04	0.366	Suzuki et al. (2003)

Earthquake	Site	Mag (M)	a_{max} (g)	Liq (Yes, No)	Critical depth interval (m)	Avg depth (m)	Depth to GWT (m)	σ_{vc} (kPa)	σ'_{vc} (kPa)	Tip $(q_{cN})_{aver}$	Sleeve $(f_{sN})_{aver}$	Friction ratio $(F)_{aver}$ (%)	n	Q	I_c	PI	Lab FC (%)	I_c est. FC (%)	Repr. FC (%)	C_N	q_{c1N}	Δq_{c1N}	$q_{c1N,cs}$	r_d	CSR	K_σ	MSF	CSR for M=7.5, σ=1	References
1995 M=6.9 Hyogoken-Nambu - Jan 16	Mizukasa Park	6.90	0.650	Yes	4.0-4.5	4.3	2.0	77	55	88.0	0.40	0.46	0.5	118.2	1.65	--	--	0	0	1.33	116.7	0.0	116.7	0.96	0.565	1.07	1.08	0.488	Suzuki et al. (2003)
1995 M=6.9 Hyogoken-Nambu - Jan 16	Nagashi Park	6.90	0.650	No	1.1-1.8	1.4	1.0	25	21	79.0	0.31	0.39	0.5	173.0	1.48	--	--	0	0	1.70	134.3	0.0	134.3	0.99	0.498	1.10	1.11	0.409	Suzuki et al. (2003)
1995 M=6.9 Hyogoken-Nambu - Jan 16	New Port No. 6 Pier	6.90	0.600	Yes	3.5-5.5	4.5	2.5	81	61	62.1	0.27	0.44	0.5	78.6	1.79	--	--	7	7	1.31	81.4	1.0	82.3	0.95	0.490	1.05	1.04	0.450	Suzuki et al. (2003)
1995 M=6.9 Hyogoken-Nambu - Jan 16	New Wharf Const. Offices	6.90	0.450	Yes	3.2-3.8	3.5	2.6	62	53	23.0	0.22	0.96	0.5	30.9	2.32	--	--	48	48	1.41	32.4	53.9	86.3	0.97	0.329	1.06	1.04	0.298	Suzuki et al. (2003)
1995 M=6.9 Hyogoken-Nambu - Jan 16	Nisseki Kobe Oil Tank A	6.90	0.600	Yes	4.8-6.1	5.5	2.4	99	69	40.2	0.24	0.62	0.5	47.3	2.06	--	--	28	28	1.22	48.9	42.7	91.6	0.94	0.523	1.04	1.05	0.481	Suzuki et al. (2003)
1995 M=6.9 Hyogoken-Nambu - Jan 16	Nisseki Kobe Oil Tank B	6.90	0.600	Yes	5.0-6.0	5.5	2.4	99	69	47.9	0.35	0.75	0.5	56.6	2.04	--	--	26	26	1.21	57.9	41.8	99.7	0.94	0.523	1.04	1.06	0.476	Suzuki et al. (2003)
1995 M=6.9 Hyogoken-Nambu - Jan 16	Shimonakajima Park	6.90	0.650	No	3.2-4.5	3.8	2.0	68	51	126.8	0.94	0.75	0.5	178.4	1.64	--	--	0	0	1.30	165.1	0.0	165.1	0.96	0.545	1.10	1.18	0.418	Suzuki et al. (2003)
1995 M=6.9 Hyogoken-Nambu - Jan 16	Shiporex Kogyo Osaka Factory	6.90	0.400	Yes	4.0-7.0	5.5	1.5	102	62	24.8	0.10	0.43	0.5	30.3	2.17	--	--	36	36	1.30	32.3	47.2	79.5	0.94	0.396	1.04	1.04	0.366	Suzuki et al. (2003)
1995 M=6.9 Hyogoken-Nambu - Jan 16	Sumiyoshi Elementary	6.90	0.600	No	2.4-3.2	2.8	1.9	50	41	110.0	0.67	0.61	0.5	171.8	1.59	--	--	0	0	1.43	156.8	0.0	156.8	0.98	0.462	1.10	1.16	0.362	Suzuki et al. (2003)
1995 M=6.9 Hyogoken-Nambu - Jan 16	Taito Kobe Factory	6.90	0.450	Yes	3.2-4.2	3.7	1.6	67	47	25.0	0.10	0.41	0.5	35.7	2.09	--	--	30	30	1.52	38.0	43.1	81.1	0.96	0.406	1.07	1.04	0.365	Suzuki et al. (2003)
1995 M=6.9 Hyogoken-Nambu - Jan 16	Tokuyama Concrete Factory	6.90	0.500	Yes	4.0-6.2	5.2	2.0	95	64	29.6	0.13	0.44	0.5	36.1	2.10	--	--	31	31	1.29	38.0	44.0	82.0	0.94	0.456	1.04	1.04	0.421	Suzuki et al. (2003)
1995 M=6.9 Hyogoken-Nambu - Jan 16	Yoshida Kogyo Factory	6.90	0.500	No	3.6-4.2	4.1	3.0	73	62	128.0	3.70	2.91	0.5	162.6	2.10	--	--	31	31	1.16	149.0	67.3	216.3	0.96	0.365	1.10	1.26	0.264	Suzuki et al. (2003)
1999 M=7.5 Kocaeli - Aug 17	Hotel Sapanca SH-4	7.51	0.370	Yes	0.8-2.4	1.6	0.5	30	19	9.4	0.04	0.46	0.5	21.1	2.32	NP	5	49	5	1.70	15.9	0.1	16.1	0.99	0.376	1.08	1.00	0.347	PEER (2000a), Moss et al. (2003)
1999 M=7.5 Kocaeli - Aug 17	Soccer Field SF-5	7.51	0.370	Yes	1.2-2.4	1.8	1.0	33	25	12.8	0.15	1.20	0.5	25.2	2.44	NP	16	58	16	1.70	21.8	18.6	40.5	0.99	0.314	1.09	1.00	0.288	PEER (2000a), Moss et al. (2003)
1999 M=7.5 Kocaeli - Aug 17	Police Station Site, PS-1	7.51	0.400	Yes	1.8-2.8	2.3	1.0	42	29	11.4	0.21	1.95	0.7	25.9	2.55	NP	12	67	12	1.70	19.3	9.6	28.9	0.99	0.368	1.07	1.00	0.344	PEER (2000a), Moss et al. (2003)
1999 M=7.5 Kocaeli - Aug 17	Yalova Harbor YH-3	7.51	0.370	Yes	1.2-6.0	3.6	1.0	67	41	54.0	0.23	0.43	0.5	83.5	1.77	NP	9	4	9	1.59	86.1	4.9	91.0	0.98	0.380	1.09	1.00	0.349	PEER (2000a), Moss et al. (2003)
1999 M=7.5 Kocaeli - Aug 17	Adapazari Site B	7.51	0.400	Yes	3.3-4.3	3.8	3.3	68	63	62.0	0.32	0.52	0.5	77.9	1.84	--	35	10	35	1.23	76.4	56.2	132.5	0.97	0.273	1.07	1.00	0.257	PEER (2000a), Sancio (2003), Moss et al. (2003), Bray et al. (2004)
1999 M=7.5 Kocaeli - Aug 17	Adapazari Site C2	7.51	0.400	Yes	3.3-4.0	3.7	0.4	69	37	29.0	0.23	0.81	0.5	46.5	2.13	--	35	33	35	1.65	47.9	49.8	97.7	0.98	0.470	1.10	1.00	0.428	PEER (2000a), Sancio (2003), Moss et al. (2003), Bray et al. (2004)
1999 M=7.5 Kocaeli - Aug 17	Adapazari Site D	7.51	0.400	Yes	1.8-2.5	2.2	1.5	39	32	12.5	0.07	0.59	0.5	21.5	2.36	--	65	52	65	1.70	21.3	55.8	77.2	0.99	0.308	1.10	1.00	0.280	PEER (2000a), Sancio (2003), Moss et al. (2003), Bray et al. (2004)
1999 M=7.5 Kocaeli - Aug 17	Adapazari Site E	7.51	0.400	Yes	1.5-3.0	2.3	0.5	42	25	20.0	0.08	0.41	0.5	39.7	2.05	--	2	27	2	1.70	34.1	0.0	34.1	0.99	0.436	1.09	1.00	0.401	PEER (2000a), Sancio (2003), Moss et al. (2003), Bray et al. (2004)
1999 M=7.5 Kocaeli - Aug 17	Adapazari Site F	7.51	0.400	Yes	1.8-3.0	2.4	0.5	45	26	33.2	0.10	0.30	0.5	64.4	1.80	--	42	7	42	1.70	56.4	56.8	113.2	0.99	0.440	1.10	1.00	0.401	PEER (2000a), Sancio (2003), Moss et al. (2003), Bray et al. (2004)
1999 M=7.5 Kocaeli - Aug 17	Adapazari Site G	7.51	0.400	Yes	1.5-2.7	2.1	0.5	39	23	24.9	0.08	0.32	0.5	51.4	1.90	--	65	15	65	1.70	42.3	61.8	104.1	0.99	0.439	1.10	1.00	0.400	PEER (2000a), Sancio (2003), Moss et al. (2003), Bray et al. (2004)
1999 M=7.5 Kocaeli - Aug 17	Adapazari Site H	7.51	0.400	Yes	2.0-3.0	2.5	1.7	45	37	26.0	0.15	0.59	0.5	42.0	2.10	--	15	31	15	1.70	44.1	18.3	62.5	0.99	0.311	1.08	1.00	0.288	PEER (2000a), Sancio (2003), Moss et al. (2003), Bray et al. (2004)
1999 M=7.5 Kocaeli - Aug 17	Adapazari Site J	7.51	0.400	Yes	1.5-3.5	2.5	0.6	46	28	15.0	0.13	0.87	0.5	27.7	2.34	3	82	50	82	1.70	25.5	59.9	85.4	0.99	0.428	1.10	1.00	0.390	PEER (2000a), Sancio (2003), Moss et al. (2003), Bray et al. (2004)
1999 M=7.5 Kocaeli - Aug 17	Degirmendere DN-1	7.51	0.400	Yes	1.7-2.6	2.2	1.7	38	34	71.1	0.70	0.99	0.5	122.5	1.84	--	12	10	12	1.62	115.3	14.4	129.6	0.99	0.291	1.10	1.00	0.265	Youd et al. (2009)
1999 M=7.5 Kocaeli - Aug 17	Degirmendere DN-2	7.51	0.400	No	2.7-3.7	3.2	2.5	57	50	78.0	0.88	1.13	0.5	110.3	1.91	--	12	16	12	1.38	107.6	14.0	121.6	0.98	0.290	1.09	1.00	0.266	Youd et al. (2009)
1999 M=7.5 Kocaeli - Aug 17	Yalova Harbor	7.51	0.300	Yes	3.4-6.4	4.9	0.8	92	51	52.3	0.24	0.47	0.5	72.4	1.84	--	11	10	11	1.44	75.5	9.6	85.1	0.96	0.338	1.07	1.00	0.317	Cetin et al. (2004b)
1999 M=7.6 Chi-Chi - Sept 20	Nantou Site C, NCC-1,2,&3	7.62	0.380	Yes	2.0-3.0	2.5	1.0	46	31	20.0	0.20	1.02	0.5	35.3	2.28	--	38	46	38	1.70	34.0	48.8	82.8	0.99	0.360	1.10	0.99	0.330	PEER (2000b), Moss et al. (2003)
1999 M=7.6 Chi-Chi - Sept 20	Nantou Site C-7	7.62	0.380	Yes	2.5-4.5	3.5	1.0	65	40	11.0	0.06	0.58	0.5	16.5	2.46	--	--	60	60	1.69	18.6	53.9	72.5	0.98	0.390	1.08	0.99	0.364	PEER (2000b), Moss et al. (2003)
1999 M=7.6 Chi-Chi - Sept 20	Nantou Site C-8	7.62	0.380	Yes	5.0-9.0	7.0	1.0	131	72	27.2	0.56	2.16	0.5	30.7	2.52	--	--	65	65	1.19	32.5	58.9	91.4	0.94	0.423	1.03	0.99	0.413	PEER (2000b), Moss et al. (2003)
1999 M=7.6 Chi-Chi - Sept 20	WuFeng Site B	7.62	0.600	Yes	2.0-4.0	3.0	1.1	55	36	30.0	0.30	1.02	0.5	49.0	2.16	--	35	36	35	1.66	49.9	50.2	100.1	0.98	0.578	1.10	0.99	0.531	PEER (2000b), Moss et al. (2003)
1999 M=7.6 Chi-Chi - Sept 20	WuFeng Site C	7.62	0.600	Yes	4.0-5.0	4.5	1.2	83	51	35.0	0.70	2.05	0.5	48.2	2.35	--	14	51	14	1.49	52.2	16.4	68.6	0.97	0.619	1.06	0.99	0.589	PEER (2000b), Moss et al. (2003)

Earthquake	Site	Mag (M)	a_{max} (g)	Liq (Yes, No)	Critical depth interval (m)	Avg depth (m)	Depth to GWT (m)	σ_{vc} (kPa)	σ'_{vc} (kPa)	Tip $(q_{cN})_{aver}$	Sleeve $(f_{sN})_{aver}$	Friction ratio $(F)_{aver}$ (%)	n	Q	I_c	PI	Lab FC (%)	I_c est. FC (%)	Repr. FC (%)	C_N	q_{c1N}	Δq_{c1N}	$q_{c1N,cs}$	r_d	CSR	K_σ	MSF	CSR for M=7.5, σ=1	References
1999 M=7.6 Chi-Chi - Sept 20	Yuanlin C-4	7.62	0.250	Yes	3.0-6.0	4.5	0.7	84	46	30.0	0.38	1.30	0.5	43.1	2.27	--	--	45	45	1.48	44.3	55.3	99.6	0.97	0.286	1.08	0.99	0.266	PEER (2000b), Moss et al. (2003)
1999 M=7.6 Chi-Chi - Sept 20	Yuanlini C-19	7.62	0.250	Yes	4.5-5.5	5.0	0.6	94	50	20.0	0.20	1.05	0.5	27.1	2.39	--	--	54	54	1.46	29.1	55.1	84.2	0.96	0.293	1.07	0.99	0.276	PEER (2000b), Moss et al. (2003)
1999 M=7.6 Chi-Chi - Sept 20	Yuanlin C-22	7.62	0.250	Yes	2.8-4.2	3.5	1.1	64	41	27.0	0.12	0.46	0.5	41.3	2.05	--	--	27	27	1.62	43.7	40.7	84.5	0.98	0.249	1.08	0.99	0.231	PEER (2000b), Moss et al. (2003)
1999 M=7.6 Chi-Chi - Sept 20	Yuanlin C-24	7.62	0.250	Yes	5.2-7.8	6.5	1.2	121	69	38.0	0.23	0.62	0.5	44.5	2.09	--	--	30	30	1.22	46.4	44.5	90.9	0.95	0.270	1.04	0.99	0.263	PEER (2000b), Moss et al. (2003)
1999 M=7.6 Chi-Chi - Sept 20	Yuanlin C-25	7.62	0.250	Yes	4.0-7.0	5.5	3.5	98	79	20.0	0.20	1.05	0.5	21.5	2.47	--	--	61	61	1.15	23.0	55.3	78.3	0.96	0.195	1.02	0.99	0.192	PEER (2000b), Moss et al. (2003)
1999 M=7.6 Chi-Chi - Sept 20	Yuanlin C-32	7.62	0.250	Yes	4.5-7.5	6.0	0.7	112	61	34.0	0.21	0.64	0.5	42.5	2.11	--	--	32	32	1.31	44.4	46.0	90.4	0.95	0.287	1.05	0.99	0.275	PEER (2000b), Moss et al. (2003)
2010 M=7.1 Darfield - Sept 4	SHY-09	7.00	0.187	No	4.3-5.4	4.8	2.0	88	61	37.0	0.07	0.19	0.5	46.5	1.87	--	--	4	4	1.38	51.1	0.0	51.1	0.95	0.167	1.04	1.02	0.158	Green et al. (2014)
2011 M-6.2 Christchurch - Feb 22	SHY-09	6.20	0.347	Yes	4.3-5.4	4.8	2.0	88	61	37.0	0.07	0.19	0.5	46.5	1.87	--	--	4	4	1.38	51.1	0.0	51.1	0.93	0.303	1.04	1.06	0.276	Green et al. (2014)
2010 M=7.1 Darfield - Sept 4	AVD-07	7.00	0.183	No	2.9-4.5	3.7	1.7	66	48	69.0	0.44	0.64	0.5	99.1	1.80	--	--	7	7	1.45	99.9	1.3	101.2	0.97	0.158	1.08	1.05	0.140	Green et al. (2014)
2011 M-6.2 Christchurch - Feb 22	AVD-07	6.20	0.396	Yes	2.9-4.5	3.7	1.7	66	48	69.0	0.44	0.64	0.5	99.1	1.80	--	--	7	7	1.45	99.9	1.3	101.2	0.95	0.336	1.08	1.14	0.274	Green et al. (2014)
2010 M=7.1 Darfield - Sept 4	BUR-46	7.00	0.167	Yes	5.75-8.75	7.3	1.3	138	80	73.7	0.44	0.61	0.5	81.3	1.85	--	--	4	4	1.14	83.7	0.0	83.8	0.91	0.171	1.02	1.03	0.162	Green et al. (2014)
2011 M-6.2 Christchurch - Feb 22	BUR-46	6.20	0.323	Yes	5.75-8.75	7.3	1.3	138	80	73.7	0.44	0.61	0.5	81.3	1.85	--	--	4	4	1.14	83.7	0.0	83.8	0.88	0.318	1.02	1.10	0.284	Green et al. (2014)
2010 M=7.1 Darfield - Sept 4	CBD-21	7.00	0.219	No	4.5-6.5	5.5	1.4	104	64	120.9	0.69	0.58	0.5	151.2	1.62	--	--	0	0	1.21	146.3	0.0	146.3	0.94	0.218	1.07	1.11	0.183	Green et al. (2014)
2011 M-6.2 Christchurch - Feb 22	CBD-21	6.20	0.460	Yes	4.5-6.5	5.5	1.4	104	64	120.9	0.69	0.58	0.5	151.2	1.62	--	--	0	0	1.21	146.3	0.0	146.3	0.91	0.446	1.07	1.32	0.315	Green et al. (2014)
2010 M=7.1 Darfield - Sept 4	FND-01	7.00	0.199	Yes	3.6-3.9	3.8	1.8	67	48	28.0	0.19	0.69	0.5	39.8	2.15	--	--	24	24	1.51	42.3	36.4	78.7	0.96	0.173	1.07	1.03	0.157	Green et al. (2014)
2011 M-6.2 Christchurch - Feb 22	FND-01	6.20	0.382	Yes	3.6-3.9	3.8	1.8	67	48	28.0	0.19	0.69	0.5	39.8	2.15	--	--	24	24	1.51	42.3	36.4	78.7	0.95	0.327	1.07	1.09	0.281	Green et al. (2014)
2010 M=7.1 Darfield - Sept 4	KAN-03	7.00	0.237	Yes	3.75-6.7	5.2	1.0	100	58	82.1	0.31	0.39	0.5	107.1	1.65	--	--	3	3	1.31	107.5	0.0	107.5	0.94	0.249	1.06	1.05	0.223	Green et al. (2014)
2011 M-6.2 Christchurch - Feb 22	KAN-03	6.20	0.188	No	3.75-6.7	5.2	1.0	100	58	82.1	0.31	0.39	0.5	107.1	1.65	--	--	3	3	1.31	107.5	0.0	107.5	0.92	0.193	1.06	1.15	0.157	Green et al. (2014)
2010 M=7.1 Darfield - Sept 4	KAN-05	7.00	0.227	Yes	3.15-4.1	3.6	2.0	66	50	37.8	0.17	0.46	0.5	53.0	1.96	--	--	8	8	1.54	58.0	2.6	60.6	0.97	0.189	1.06	1.02	0.175	Green et al. (2014)
2011 M-6.2 Christchurch - Feb 22	KAN-05	6.20	0.183	Yes	3.15-4.1	3.6	2.0	66	50	37.8	0.17	0.46	0.5	53.0	1.96	--	--	8	8	1.54	58.0	2.6	60.6	0.95	0.150	1.06	1.07	0.133	Green et al. (2014)
2010 M=7.1 Darfield - Sept 4	KAN-09	7.00	0.239	Yes	1.25-2.45	1.9	0.9	34	25	28.9	0.10	0.33	0.5	58.0	1.86	--	--	9	9	1.70	49.1	4.8	53.9	0.99	0.212	1.10	1.02	0.189	Green et al. (2014)
2011 M-6.2 Christchurch - Feb 22	KAN-09	6.20	0.186	No	1.25-2.45	1.9	0.9	34	25	28.9	0.10	0.33	0.5	58.0	1.86	--	--	9	9	1.70	49.1	4.8	53.9	0.98	0.164	1.10	1.06	0.141	Green et al. (2014)
2010 M=7.1 Darfield - Sept 4	KAN-19	7.00	0.234	Yes	2.35-5.00	3.7	0.8	70	42	77.5	0.41	0.53	0.5	119.9	1.68	--	--	2	2	1.51	117.1	0.0	117.1	0.97	0.247	1.10	1.06	0.211	Green et al. (2014)
2011 M-6.2 Christchurch - Feb 22	KAN-19	6.20	0.187	No	2.35-5.00	3.7	0.8	70	42	77.5	0.41	0.53	0.5	119.9	1.68	--	--	2	2	1.51	117.1	0.0	117.1	0.95	0.194	1.10	1.19	0.149	Green et al. (2014)
2010 M=7.1 Darfield - Sept 4	KAN-23	7.00	0.216	Yes	4.3-5.3	4.8	0.5	92	50	93.3	0.58	0.63	0.5	131.0	1.69	--	--	0	0	1.36	127.3	0.0	127.3	0.95	0.245	1.09	1.08	0.208	Green et al. (2014)
2011 M-6.2 Christchurch - Feb 22	KAN-23	6.20	0.186	No	4.3-5.3	4.8	0.5	92	50	93.3	0.58	0.63	0.5	131.0	1.69	--	--	0	0	1.36	127.3	0.0	127.3	0.93	0.207	1.09	1.23	0.154	Green et al. (2014)
2010 M=7.1 Darfield - Sept 4	KAN-26d	7.00	0.231	Yes	4.9-8.0	6.5	1.5	122	74	78.5	0.33	0.43	0.5	90.6	1.74	--	--	3	3	1.18	92.6	0.0	92.6	0.92	0.230	1.03	1.04	0.215	Green et al. (2014)
2011 M-6.2 Christchurch - Feb 22	KAN-26c	6.20	0.181	Yes	1.5-2.4	2.0	1.5	34	30	25.1	0.14	0.56	0.5	45.6	2.05	--	--	22	22	1.70	42.7	32.4	75.1	0.98	0.132	1.10	1.08	0.111	Green et al. (2014)
2010 M=7.1 Darfield - Sept 4	KAN-28	7.00	0.231	Yes	2.0-3.15	2.6	1.4	47	35	41.7	0.14	0.34	0.5	69.9	1.79	--	--	5	5	1.70	70.9	0.1	71.0	0.98	0.195	1.09	1.03	0.174	Green et al. (2014)
2011 M-6.2 Christchurch - Feb 22	KAN-28	6.20	0.182	Yes	2.0-3.15	2.6	1.4	47	35	41.7	0.14	0.34	0.5	69.9	1.79	--	--	5	5	1.70	70.9	0.1	71.0	0.97	0.152	1.09	1.08	0.130	Green et al. (2014)
2010 M=7.1 Darfield - Sept 4	KAS-08	7.00	0.204	Yes	1.3-2.65	2.0	1.3	35	29	23.9	0.13	0.56	0.5	44.2	2.07	--	--	20	20	1.70	40.6	29.5	70.1	0.99	0.161	1.10	1.03	0.143	Green et al. (2014)
2011 M-6.2 Christchurch - Feb 22	KAS-08	6.20	0.186	Yes	1.3-2.65	2.0	1.3	35	29	23.9	0.13	0.56	0.5	44.2	2.07	--	--	20	20	1.70	40.6	29.5	70.1	0.98	0.146	1.10	1.08	0.123	Green et al. (2014)

Earthquake	Site	Mag (M)	a_{max} (g)	Liq (Yes, No)	Critical depth interval (m)	Avg depth (m)	Depth to GWT (m)	σ_{vc} (kPa)	σ'_{vc} (kPa)	Tip $(q_{cN})_{aver}$	Sleeve $(f_{sN})_{aver}$	Friction ratio $(F)_{aver}$ (%)	n	Q	I_c	PI	Lab FC (%)	I_c est. FC (%)	Repr. FC (%)	C_N	q_{c1N}	Δq_{c1N}	$q_{c1N,cs}$	r_d	CSR	K_σ	MSF	CSR for M=7.5, σ=1	References
2010 M=7.1 Darfield - Sept 4	KAS-11	7.00	0.211	Yes	2.0-3.1	2.6	1.2	47	34	39.0	0.23	0.60	0.5	67.0	1.92	--	--	10	10	1.70	66.4	7.2	73.6	0.98	0.187	1.10	1.03	0.166	Green et al. (2014)
2011 M-6.2 Christchurch - Feb 22	KAS-11	6.20	0.186	Yes	2.0-3.1	2.6	1.2	47	34	39.0	0.23	0.60	0.5	67.0	1.92	--	--	10	10	1.70	66.4	7.2	73.6	0.97	0.164	1.10	1.08	0.138	Green et al. (2014)
2010 M=7.1 Darfield - Sept 4	KAS-20	7.00	0.211	Yes	3.5-5.0	4.3	1.6	79	53	45.9	0.15	0.33	0.5	62.4	1.83	--	--	6	6	1.46	67.0	0.4	67.4	0.96	0.196	1.05	1.03	0.181	Green et al. (2014)
2011 M-6.2 Christchurch - Feb 22	KAS-20	6.20	0.172	Yes	3.5-5.0	4.3	1.6	79	53	45.9	0.15	0.33	0.5	62.4	1.83	--	--	6	6	1.46	67.0	0.4	67.4	0.94	0.157	1.05	1.07	0.139	Green et al. (2014)
2010 M=7.1 Darfield - Sept 4	KAS-40	7.00	0.224	Yes	1.9-2.75	2.3	1.9	41	36	35.2	0.12	0.35	0.5	57.9	1.87	--	--	8	8	1.70	59.8	2.2	62.0	0.98	0.160	1.08	1.02	0.144	Green et al. (2014)
2011 M-6.2 Christchurch - Feb 22	KAS-40	6.20	0.177	Yes	1.9-2.75	2.3	1.9	41	36	35.2	0.12	0.35	0.5	57.9	1.87	--	--	8	8	1.70	59.8	2.2	62.0	0.97	0.125	1.08	1.07	0.109	Green et al. (2014)
2010 M=7.1 Darfield - Sept 4	SNB-01	7.00	0.170	Yes	2.25-5.0	3.6	2.0	66	50	53.7	0.34	0.65	0.5	75.6	1.90	--	--	9	9	1.47	78.7	4.8	83.5	0.97	0.141	1.07	1.03	0.128	Green et al. (2014)
2011 M-6.2 Christchurch - Feb 22	SNB-01	6.20	0.351	Yes	2.25-5.0	3.6	2.0	66	50	53.7	0.34	0.65	0.5	75.6	1.90	--	--	9	9	1.47	78.7	4.8	83.5	0.95	0.287	1.07	1.10	0.245	Green et al. (2014)
2010 M=7.1 Darfield - Sept 4	NBT-02	7.00	0.170	Yes	4.8-6.7	5.8	2.0	107	70	48.6	0.25	0.53	0.5	57.0	1.96	--	--	12	12	1.23	59.8	11.6	71.5	0.93	0.157	1.03	1.03	0.149	Green et al. (2014)
2011 M-6.2 Christchurch - Feb 22	NBT-02	6.20	0.354	Yes	4.8-6.7	5.8	2.0	107	70	48.6	0.25	0.53	0.5	57.0	1.96	--	--	12	12	1.23	59.8	11.6	71.5	0.91	0.318	1.03	1.08	0.287	Green et al. (2014)
2010 M=7.1 Darfield - Sept 4	NBT-03	7.00	0.168	Yes	7.0-10.2	8.6	2.4	162	101	60.2	0.32	0.54	0.5	58.7	1.95	--	--	11	11	1.00	60.4	10.1	70.4	0.89	0.155	1.00	1.03	0.151	Green et al. (2014)
2011 M-6.2 Christchurch - Feb 22	NBT-03	6.20	0.346	Yes	7.0-10.2	8.6	2.4	162	101	60.2	0.32	0.54	0.5	58.7	1.95	--	--	11	11	1.00	60.4	10.1	70.4	0.84	0.304	1.00	1.08	0.283	Green et al. (2014)
2010 M=7.1 Darfield - Sept 4	RCH-14	7.00	0.183	No	3.5-5.5	4.5	2.3	81	60	23.8	0.01	0.03	0.5	29.8	2.01	--	--	7	7	1.45	34.4	0.9	35.3	0.95	0.154	1.03	1.02	0.146	Green et al. (2014)
2011 M-6.2 Christchurch - Feb 22	RCH-14	6.20	0.339	Yes	3.5-5.5	4.5	2.3	81	60	23.8	0.01	0.03	0.5	29.8	2.01	--	--	7	7	1.45	34.4	0.9	35.3	0.93	0.279	1.03	1.05	0.257	Green et al. (2014)
2010 M=7.1 Darfield - Sept 4	Z1-3	7.00	0.217	Yes	4.0-8.25	6.1	1.4	116	70	51.5	0.57	1.13	0.5	60.7	2.11	--	--	26	26	1.20	61.9	42.2	104.1	0.93	0.218	1.04	1.05	0.200	Green et al. (2014)
2011 M-6.2 Christchurch - Feb 22	Z1-3	6.20	0.455	Yes	4.0-8.25	6.1	1.4	116	70	51.5	0.57	1.13	0.5	60.7	2.11	--	--	26	26	1.20	61.9	42.2	104.1	0.90	0.444	1.04	1.14	0.372	Green et al. (2014)
2010 M=7.1 Darfield - Sept 4	Z2-11	7.00	0.210	No	2.2-3.3	2.8	1.0	51	34	64.2	0.69	1.09	0.5	109.7	1.90	--	--	11	11	1.66	106.4	10.2	116.6	0.98	0.201	1.10	1.06	0.171	Green et al. (2014)
2011 M-6.2 Christchurch - Feb 22	Z2-11	6.20	0.447	Yes	2.2-3.3	2.8	1.0	51	34	64.2	0.69	1.09	0.5	109.7	1.90	--	--	11	11	1.66	106.4	10.2	116.6	0.97	0.422	1.10	1.18	0.324	Green et al. (2014)
2010 M=7.1 Darfield - Sept 4	Z2-6	7.00	0.214	No	2.0-2.85	2.4	2.0	42	38	47.0	0.42	0.90	0.5	75.9	1.98	--	--	16	16	1.63	76.5	23.8	100.3	0.98	0.152	1.10	1.05	0.132	Green et al. (2014)
2011 M-6.2 Christchurch - Feb 22	Z2-6	6.20	0.451	Yes	2.0-2.85	2.4	2.0	42	38	47.0	0.42	0.90	0.5	75.9	1.98	--	--	16	16	1.63	76.5	23.8	100.3	0.97	0.317	1.10	1.13	0.254	Green et al. (2014)
2010 M=7.1 Darfield - Sept 4	Z4-4	7.00	0.215	No	2.0-3.25	2.6	2.0	46	40	41.2	0.37	0.91	0.5	64.7	2.03	--	--	18	18	1.60	66.2	28.4	94.5	0.98	0.158	1.09	1.04	0.138	Green et al. (2014)
2011 M-6.2 Christchurch - Feb 22	Z4-4	6.20	0.450	Yes	2.0-3.25	2.6	2.0	46	40	41.2	0.37	0.91	0.5	64.7	2.03	--	--	18	18	1.60	66.2	28.4	94.5	0.97	0.327	1.09	1.12	0.267	Green et al. (2014)
2010 M=7.1 Darfield - Sept 4	Z8-11	7.00	0.219	Yes	1.4-2.0	1.7	1.4	30	27	23.0	0.17	0.75	0.5	43.9	2.13	--	--	39	39	1.70	39.1	50.7	89.8	0.99	0.157	1.10	1.04	0.137	Green et al. (2014)
2011 M-6.2 Christchurch - Feb 22	Z8-11	6.20	0.453	Yes	1.4-2.0	1.7	1.4	30	27	23.0	0.17	0.75	0.5	43.9	2.13	--	--	39	39	1.70	39.1	50.7	89.8	0.98	0.322	1.10	1.11	0.264	Green et al. (2014)
2011 M=9.0 Tohoku - Mar 11	Hinode Minami ES	9.00	0.170	No	4.0-5.6	4.8	1.1	89	53	101.0	0.82	0.8	0.5	138.1	1.75	--	--	3	3	1.32	133.5	0.0	133.5	1.01	0.187	1.09	0.79	0.216	Cox et al. (2013)
2011 M=9.0 Tohoku - Mar 11	Hosoyama Nekki	9.00	0.18	No	3.8-4.6	4.2	2.5	76	60	66.0	0.29	0.4	0.5	84.9	1.77	--	--	5	5	1.32	87.2	0.1	87.3	1.01	0.150	1.05	0.92	0.156	Cox et al. (2013)
2011 M=9.0 Tohoku - Mar 11	Takasu Chuou Park	9.00	0.21	Yes	6.3-7.3	6.8	1.1	127	71	67.0	0.46	0.7	0.5	78.3	1.90	--	--	15	15	1.19	79.7	21.9	101.6	1.01	0.245	1.04	0.89	0.266	Cox et al. (2013)
2011 M=9.0 Tohoku - Mar 11	Takasu Kaihin Park	9.00	0.22	Yes	8.4-9.6	9.0	1.3	169	93	95.0	0.45	0.5	0.5	97.3	1.74	--	--	2	2	1.04	99.1	0.0	99.1	1.01	0.261	1.01	0.89	0.289	Cox et al. (2013)
2011 M=9.0 Tohoku - Mar 11	Akemi ES	9.00	0.169	No	7.5-14	10.1	1.2	189	102	83.0	0.48	0.6	0.5	80.7	1.85	--	--	11	11	1.00	82.7	10.2	92.9	1.00	0.205	1.00	0.91	0.226	Cox et al. (2013)
2011 M=9.0 Tohoku - Mar 11	Hinode ES	9.00	0.199	Yes	2.0-3.6	2.8	1.2	51	36	34.0	0.24	0.7	0.5	56.3	2.03	--	--	25	25	1.69	57.4	40.6	98.0	1.00	0.187	1.10	0.90	0.190	Cox et al. (2013)
2011 M=9.0 Tohoku - Mar 11	Irifune NS	9.00	0.256	Yes	5.5-7.1	6.3	1.6	117	71	20.0	0.28	1.5	0.5	22.5	2.53	--	--	66	66	1.21	24.3	56.9	81.1	1.01	0.276	1.03	0.92	0.289	Cox et al. (2013)

Table 3.2. Examples of case histories involving potential cyclic softening of clays or plastic silts

Earthquake	Site	Magnitude (M)	a_{max} (g)	Ground failure (Yes, No)	Critical depth interval (m)	Avg depth (m)	Depth to GWT (m)	σ_{vc} (kPa)	σ'_{vc} (kPa)	Tip $(q_{cN})_{aver}$	Sleeve $(f_{sN})_{aver}$	Friction ratio $(F)_{aver}$ (%)	n	Q	I_c	PI	Lab FC (%)	I_c est. FC (%)	Repr. FC (%)	References
1975 M=7.0 Haicheng - Feb 4	Construction Building Site	7.00	0.300	Yes	3.0-7.4	5.3	1.5	97	60	5.7	0.11	2.41	1.0	7.9	3.03	10	60	100	60	Arulanandan et al. (1986), Earth Tech (1985), Worden et al. (2010)
1975 M=7.0 Haicheng - Feb 4	Guest House	7.00	0.300	No	2.8-4.2	3.5	1.5	64	44	8.0	0.10	1.4	1.00	16.9	2.62	--	--	73	73	Arulanandan et al. (1986), Earth Tech (1985), Worden et al. (2010)
1975 M=7.0 Haicheng - Feb 4	Paper Mill	7.00	0.300	Yes	3.0-5.0	4.0	1.0	74	45	6.8	0.10	1.72	1.0	13.6	2.75	14.5	60	83	60	Arulanandan et al. (1986), Earth Tech (1985), Worden et al. (2010)
1976 M=7.6 Tangshan - July 27	F13 - Tangshan	7.60	0.120	No	3.1-5.1	4.1	0.7	76	43	9.5	0.23	2.63	1.0	20.5	2.71	10	75	80	75	Arulanandan et al. (1982), Moss et al. (2003, 2011)
1981 M=5.9 WestMorland - April 26	Kornbloom Rd (K3)	5.90	0.320	No	2.7-5.3	4.2	2.7	75	60	11.0	0.34	3.30	1.0	17.1	2.83	--	85	90	85	Bennett et al. (1984), Seed et al. (1984)
1989 M=6.9 Loma Prieta - Oct 18	Model Airport (AIR-16)	6.93	0.260	No	2.8-4.0	3.4	2.1	62	49	3.1	0.00	0.12	1	5.2	2.78	--	89	85	89	Bennett & Tinsley (1995), Toprak & Holzer (2003)
1989 M=6.9 Loma Prieta - Oct 18	Miller Farm (CMF-1)	6.93	0.360	No	4.0-8.0	6.0	3.5	111	86	6.9	0.27	4.54	1	6.9	3.23	--	77	100	77	Bennett & Tinsley (1995), Toprak & Holzer (2003)
1989 M=6.9 Loma Prieta - Oct 18	Miller Farm (CMF-2)	6.93	0.360	No	6.5-9.5	8.0	4.9	147	117	14.0	0.32	2.57	1	10.8	2.93	--	95	97	95	Bennett & Tinsley (1995), Toprak & Holzer (2003)
1989 M=6.9 Loma Prieta - Oct 18	Farris Farm (FAR-55)	6.93	0.360	No	2.0-4.0	3.0	2.3	55	48	10.8	0.62	6.00	1	21.6	2.92	25	80	97	80	Bennett & Tinsley (1995), Toprak & Holzer (2003)
1989 M=6.9 Loma Prieta - Oct 18	Sea Mist (SEA-29)	6.93	0.220	No	3.0-7.1	4.6	2.0	86	60	4.3	0.04	1.17	1	5.7	3.00	9	72	100	72	Bennett & Tinsley (1995), Toprak & Holzer (2003)
1989 M=6.9 Loma Prieta - Oct 18	Pajaro Dunes (PD1-43)	6.93	0.220	No	2.6-3.3	2.9	2.6	53	50	3.0	0.06	2.42	1	5.0	3.20	35	71	100	71	Bennett & Tinsley (1995), Toprak & Holzer (2003)
1999 M=7.5 Kocaeli - Aug 17	Cark Canal site	7.51	0.400	No	2.9-4.5	3.7	2.9	66	58	10.4	0.16	1.70	1	17.0	2.67	8	74	76	74	Youd et al. (2009)
1999 M=7.5 Kocaeli - Aug 17	Cumhuriyet Avenue site	7.51	0.400	No	3.1-4.5	3.8	1.0	68	41	6.9	0.15	2.38	1	15.4	2.78	12	80	86	80	Youd et al. (2009)
1999 M=7.6 Chi-Chi - Sept 20	Nantou Site C-3 & C-16	7.62	0.380	Yes	4.0-6.0	5.0	1.0	93	54	12.0	0.40	3.61	1	20.9	2.79	--	--	86	86	PEER (2000b), Moss et al. (2003)
1999 M=7.6 Chi-Chi - Sept 20	Yuanlin C-2	7.62	0.250	Yes	5.0-8.0	6.5	0.6	122	64	15.0	0.35	2.54	1	21.9	2.68	--	--	77	77	PEER (2000b), Moss et al. (2003)

3.2. Earthquake magnitudes and peak accelerations

Moment magnitudes (M or M_w) are used for all earthquakes in the updated liquefaction database (Tables 3.1 and 3.2). The moment magnitudes were obtained from the Next Generation Attenuation (NGA and NGA-2) projects flatfile (Chiou et al. 2008; Ancheta et al. 2014) and the USGS Centennial Earthquake Catalog (Engdahl and Villasenor 2002, and online catalog 2010). Preference was given to the NGA values if the USGS Catalog gave a different value for M.

Estimates of peak horizontal ground accelerations (PGA or a_{max}) are listed for each site in Table 3.1. PGA estimates by the original site investigators or from the Moss et al. (2003) database were used in all cases except as noted below.

USGS ShakeMaps (Worden et al. 2010) were used to check PGA estimates for a number of sites with no nearby recordings. The new ShakeMaps incorporate a weighted-average approach for combining different types of data (e.g., recordings, intensities, ground motion prediction equations) to arrive at best estimates of peak ground motion parameters. With one exception, the ShakeMaps confirmed that existing estimates of PGA were reasonable, such that no changes to these estimates were warranted.

The ShakeMap for the 1975 Haicheng earthquake, however, indicated that significant changes to PGA estimates were warranted for some sites affected by the earthquake. The ShakeMap for the 1975 Haicheng earthquake indicated that the five sites in the database for this earthquake experienced PGAs of about 0.3 g, compared to the value of 0.15g assumed by the original investigators (Arulanandan et al. 1986). The value of 0.3 g was used for these cases in the present database.

The specification of an a_{max} value for either the interpretation of case histories or the evaluation of liquefaction in practice includes the issue of exactly how this parameter should be defined; e.g., as the geometric mean of the horizontal components, as the maximum of the two horizontal components, as some rotated resultant of the recorded horizontal components, or as some orientation-independent measure of the geometric mean of the ground motions? The major considerations involved in addressing this issue can be grouped in three categories: (1) the potential magnitudes of the differences in definitions and how any inconsistencies may manifest themselves in practice, (2) our understanding of the soil mechanics of liquefaction behavior, and (3) the need for consistency between how the liquefaction triggering correlations are developed and how they are applied in practice.

The differences between the geometric mean a_{max} and the maximum of the two recorded horizontal components is most often in the range of 10% based on a review of records in the NGA-2 database for the range of soil and shaking conditions of most interest; e.g., the 16^{th}, 50^{th}, and 84^{th} percentile ratios are 1.03, 1.10, and 1.24, respectively, for all records with site classes of C-E, moment magnitudes of 5.0-7.9, and geometric mean a_{max} values of 0.05-1.0g. For example, the geometric mean a_{max} at the Wildlife B site, which is included in the CPT-based database in Table 3.1, was only 1% and 5% smaller than the maximum of the recorded horizontal components for the two 1987 Superstition Hills earthquakes. Differences between the maximum rotated component and the geometric mean can be larger, but maximum rotated measures of a_{max} have not been used in the systematic examination of case histories to date. The orientation-independent measures of the geometric mean of the ground motion used in development of GMPEs as part of the NGA research programs are systematically larger than the as-recorded geometric means, but usually by less than about 3% (Boore et al. 2006).

Our understanding of the soil mechanics of liquefaction behavior would suggest that the maximum of the two horizontal acceleration components could be preferred over the geometric mean as a representation of the seismic loading for level ground conditions, whereas the preferred measure for non-level ground conditions is less clear. For example, the results of uni- and bi-directional cyclic direct simple shear tests

without any static shear stress bias (mimicking level ground conditions) show that the CRR for bi-directional loading with two equally-strong horizontal components is only about 10-20% smaller than for uni-directional loading. A geometric mean of two horizontal components may not be applicable to uni-directional loading, but it illustrates that a geometric mean will have less meaning than a maximum component if the two horizontal components ever have greatly different magnitudes. For non-level ground conditions, such as near channel slopes or around embankments, the ground deformations associated with liquefaction in the subsurface could be driven more by the component of motion in the weaker direction of the soil or soil-structure system. An estimate of the geometric mean a_{max} may be a more appropriate measure for non-level ground sites, given that the directionality of the motion relative to the weaker axis of a soil or soil-structure system are generally not known. Overall, a geometric mean a_{max} may be a reasonable representation in practice given the above considerations and the fact that the differences between the two horizontal components are often not large.

The sources of a_{max} estimates in the case history database involve a number of approaches. Some a_{max} values come from ground motion prediction equations (GMPEs) or from the use of GMPEs to interpolate between surrounding recordings (e.g., Green et al. 2014). In such cases, the a_{max} value generally represents an estimate of the geometric mean. Many other a_{max} values in the literature were estimated by unspecified means, and thus their basis is not as clear. A small number of a_{max} values come from strong ground motion recordings immediately at the site of interest (Niigata, Wildlife B and seven sites from Urayasu), and these have been interpreted in terms of the maximum of the two horizontal components. As noted above, the maximum horizontal component at Wildlife B was only 1% and 5% greater than the geometric mean a_{max} for the two 1987 Superstition Hills earthquakes, such that the choice of either measure has little effect on the interpretation of those two cases. For the seven sites from Urayasu, the strong motion recordings from the 2011 Tohoku earthquake have not yet been released and thus the currently available information is limited to the maximum of the two horizontal components. .

In practice, an estimate of a_{max} is generally obtained from seismic hazard maps or GMPEs, such that the estimate represents a geometric mean. An adjustment could be applied to the geometric mean to obtain an estimate for a maximum horizontal component, but many geotechnical structures have strong/weak directions (e.g., levees, dam, embankments, bridge foundations) and the application of maximum-direction motions to the weak axis of a structure can correspond to a lower probability of occurrence than is intended under many design practices (Stewart et al. 2011). For this reason, the use of a geometric mean a_{max} in assessing liquefaction hazards is considered to be a reasonable engineering approach for many geotechnical structures or soil-structure systems.

It is, therefore, recommended that the application of these triggering correlations be used in conjunction with the geometric mean value for a_{max}. This approach is the most consistent with how the case history database was developed and is considered appropriate for geotechnical structures that have direction-dependent response characteristics.

3.3. Selection and computation of q_{c1Ncs} values

A number of CPT-based case histories are discussed in detail to illustrate several issues important to the interpretation of case histories, including the importance of a geologic understanding of the site and the methodology used for selecting representative CPT q_{c1Ncs} values from critical strata. In general, the appropriateness of any averaging of q_{cN} values for a specific stratum in case history interpretations or forward analyses depends on the spatial characteristics of the stratum (e.g., thickness, lateral extent, continuity), the mode of deformation (e.g., reconsolidation settlement, lateral spreading, slope instability), and the spatial dimensions of the potential deformation mechanisms relative to the strata of concern. A

familiarity with how representative q_{c1Ncs} values are selected for the database is important for guiding the forward application of these correlations in a manner consistent with their development.

The timing of CPT soundings relative to the earthquake loading is not clear in all case histories. In most cases, the CPTs were performed after earthquake loading or were likely performed after earthquake loading. There are, however, many cases where the CPT data were from site investigations performed before the earthquake in combination with some performed after the earthquake. For example, Chameau et al. (1998) compared CPT data performed at several San Francisco waterfront sites before and after the 1989 Loma Prieta. They concluded that q_{cN} values increased in loose to medium dense dune sand fills in areas that experienced liquefaction-induced ground failure during the earthquake, whereas q_{cN} values initially in a denser state did not exhibit such an increase. Boulanger et al. (1995) compared pre- and post-earthquake CPT data at a site in Moss Landing that did not show surface evidence of liquefaction in the 1989 Loma Prieta earthquake. They reported an apparent slight increase in the q_{cN} values (less than about 15%) in the critical depth intervals, while also noting that these differences were not large relative to the natural spatial variability in q_{cN} values. Case histories from the Christchurch area in the Canterbury earthquake sequence are particularly unique in that there were sites where CPTs were performed before or after one of the major shaking events, including some sites which experienced liquefaction three or four times. CPTs and Swedish Weight Sounding tests performed before and after some of these events did not indicate any significant change in penetration resistance (M. Cubrinovski 2014, personal communication). The effects of earthquake loading on CPT data can be expected to vary with the pre-earthquake state of the soil, the severity of the earthquake loading or induced liquefaction, other soil characteristics (e.g., FC, fines plasticity, age, presence of cementation), and the time elapsed between earthquake loading and penetration testing. The presently available data are not sufficient for discriminating these effects on the q_{cN} values listed in the case history database, but they do suggest that including pre- and post-earthquake CPT data in the database may only introduce a small amount of additional conservatism in the resulting correlations, particularly given that the effects of earthquake loading are likely smaller for data points close to the boundaries of the triggering correlation.

The selected critical depth intervals and the associated representative parameters are summarized in Table 3.1.

Moss Landing State Beach

The Moss Landing State Beach case history is illustrative of cases where the stratigraphy is relatively uniform and selection of critical intervals is reasonably straight-forward. Liquefaction occurred along the access road to the Moss Landing State Beach during the 1989 M=6.9 Loma Prieta earthquake (Boulanger et al. 1997). The estimated PGA at the site is 0.28 g. A profile along the access road is shown in Figure 3.1. At the Entrance Kiosk, the upper few meters of sand were mostly Holocene alluvial and estuarine deposits in the abandoned Salinas River channel. West of the Beach Path, the upper few meters of sand are instead thought to be primarily the beach deposits which separated the abandoned river channel from Monterey Bay. Ground surface displacements ranged from about 30-60 cm at the Entrance Kiosk to about 10-30 cm at the Beach Path. Ground displacements were not observed farther up the road (near CPT sounding UC-18).

At the Entrance Kiosk, the q_{cN} values below the water table in soundings UC-15 and UC-14 averaged about 33 and 43 (q_{c1Ncs} of 56 and 72), respectively, between depths of 1.8 and about 4.0 m. The soils became only slightly denser for depths up to about 5.4 m, with the average q_{cN} values being about 42 and 53 (q_{c1Ncs} of 66 and 81), respectively, for depths of 1.8 to about 5.4 m. The representative value was taken as $q_{cN} = 48$ ($q_{c1Ncs} = 73$) because it is the mean value for both soundings over depths of 1.8 to 5.4 m, it ensures that liquefaction is predicted to occur over a significant portion of the stratum thickness at both

CPT locations, and the large deformations at this location would be consistent with liquefaction over the thicker interval.

At the Beach Path, the q_{cN} values in sounding UC-16 averaged about 87 (q_{c1Ncs} = 126) between depths of 2.3 and 3.3 m, and then increased with depth such that the average q_{cN} was about 112 (q_{c1Ncs} = 145) over depths of 2.3 and 5.4 m. The q_{cN} values in sounding UC-17 averaged about 93 (q_{c1Ncs} = 122) between depths of 2.6 and 5.0 m, with the looser soils between depths of 4.0 and 5.0 m having an average q_{cN} of 66 (q_{c1Ncs} = 86) . The lateral spreading displacement of 10-30 cm would represent a shear strain of about 10-30% over a 1.0-m thick zone or 4-12% over a 2.4-m thick zone. The representative value was taken as q_{cN} = 90 (q_{c1Ncs} = 124) because it is about the mean value in the critical 1.0-m interval in UC-16 and the mean value in the critical 2.4-m interval in UC-17, and the modest deformations at this location would seem consistent with this extent of liquefaction. This interpretation produces a point that lies just below the deterministic triggering correlation.

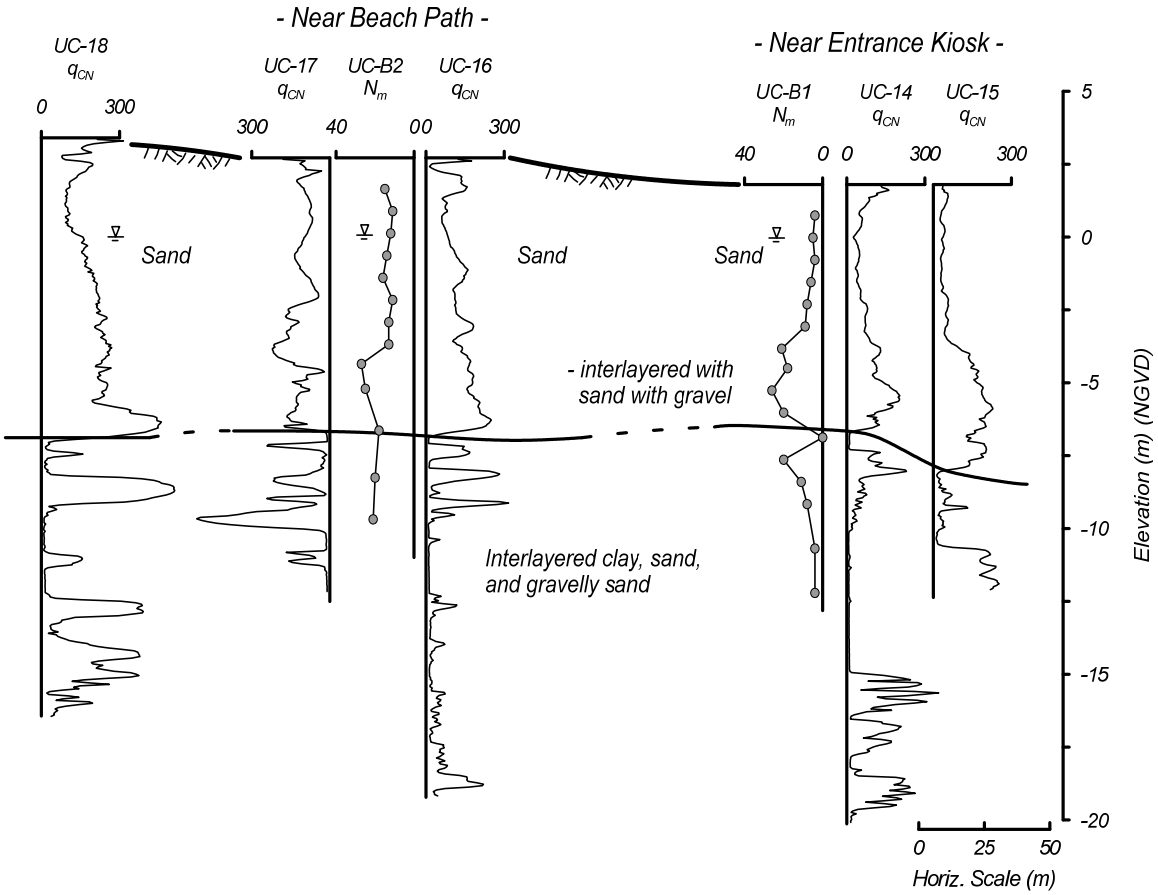

Figure 3.1: Profile at the Moss Landing State Beach (Boulanger et al. 1997)

At sounding UC-18, the q_{cN} averaged about 163 (q_{c1Ncs} = 191) between depths of 3.4 and 4.4 m, after which they increase significantly with increasing depth. This 1-m thick interval is already sufficient dense that it plots well below the deterministic triggering correlation.

Consider the forward analysis of these three sites based on this method for selecting representative q_{cN} values. If there was an earthquake that was just strong enough to produce a computed $FS_{liq} = 1.0$ for the representative q_{cN} value at the Beach Path, then the FS_{liq} would be less than 1.0 over intervals of 0.5 to 1.2 m at the two soundings. Since ground deformations may develop over thinner intervals within the identified strata, this approach for selecting representative q_{cN} values should result in the liquefaction correlation being conservative for forward applications that analyze CPT soundings point-by-point. In other instances, such as applications involving embankment dams, use of an average q_{cN} for a stratum may be more appropriate if the potential failure surfaces are extensive relative to the stratum's dimensions. In general, the appropriateness of any averaging of q_{cN} values for a specific stratum in forward analyses or case history interpretations depends on the spatial characteristics of the stratum (e.g., thickness, lateral extent, continuity), the mode of deformation (e.g., reconsolidation settlement, lateral spreading, slope instability), and the spatial dimensions of the potential deformation mechanisms relative to the strata of concern.

Wildlife Liquefaction Array

The Wildlife Liquefaction Array site is illustrative of cases where the stratigraphy is more complex and the selection of critical intervals is more subjective. Liquefaction occurred at the Wildlife Liquefaction Array in the 1981 Westmoreland and in the 1987 Superstition Hills earthquakes. Several CPT soundings were performed in an area that spans a distance of about 30 m in the area of liquefaction (boils and modest lateral spreading). Results of CPT, SPT, and laboratory index tests were obtained from Youd and Bennett (1983), Holzer and Youd (2007), and Bennett (2010, personal communication). Two cross-sections of the site are shown in Figures 3.2 (Bennett et al. 1984) and 3.3 (data courtesy T. Holzer). The site is approximately level, but the center of the array is only about 23 m from the west bank of the Alamo River. The site stratigraphy consists of about 7 m of Holocene flood plain sediments ($\approx$ 2.5 m of silt overlying $\approx$ 4.4 m of silty sand and sandy silt; Figures 3.2 and 3.3) deposited in an old incised river channel and overlying denser sedimentary deposits (Holzer and Youd 2007).

Liquefaction was triggered in the silty sand layer between depths of about 2.6 and 7.0 m, as evidenced by the pore pressure transducer records and inclinometer readings. The upper 1 m of this layer includes portions that are sandy silt and silt with an average fines content of about 78%, whereas the lower portion is predominantly silty sand with an average fines content of about 30%. The three CPT soundings (C1, C2, and C3) shown in Figure 3.3 formed a triangle around the location of the slope inclinometer that recorded the lateral movements at the site (Holzer and Youd 2007). At CPT C1, the critical interval would appear to be loose silty sands near a depth of about 5.0 m with q_{cN} values of about 33 (q_{c1Ncs} of 89), whereas the average q_{cN} for the full layer is about 47 (q_{c1Ncs} of 113). At CPT C2, the critical interval would appear to be loose sandy silts near a depth of about 3.8 m with q_{cN} values of about 41 (q_{c1Ncs} of 110), whereas the average q_{cN} for the full layer is about 58 (q_{c1Ncs} of 129). At CPT C3, the critical interval would again appear to be loose sandy silts near a depth of about 3.0 m with q_{cN} values of about 16 (q_{c1Ncs} of 67), whereas the average q_{cN} for the full layer is about 55 (q_{c1Ncs} of 128). The overall averages for the silty sand and sandy silt layers from these three soundings were $q_{cN} = 53$ and $q_{c1Ncs} = 123$.

The representative q_{c1Ncs} for this site was taken as 123 because it is the average value for the suspect stratum, it would ensure that liquefaction was predicted to occur over a significant portion of the stratum thickness at all three CPT locations, the close spacing of these three CPTs suggests that liquefaction had to have developed over sufficiently thick intervals at all three locations to produce the observed ground deformations, and the weakest zones in each of the CPTs did not all occur at the same depths. This approach is also consistent with the approach used by Idriss and Boulanger (2010) to interpret the SPT data at this site. Note that this selection produces a point for the 1987 Superstition Hills earthquake that, like the SPT interpretation, plots slightly below the deterministic liquefaction triggering correlation.

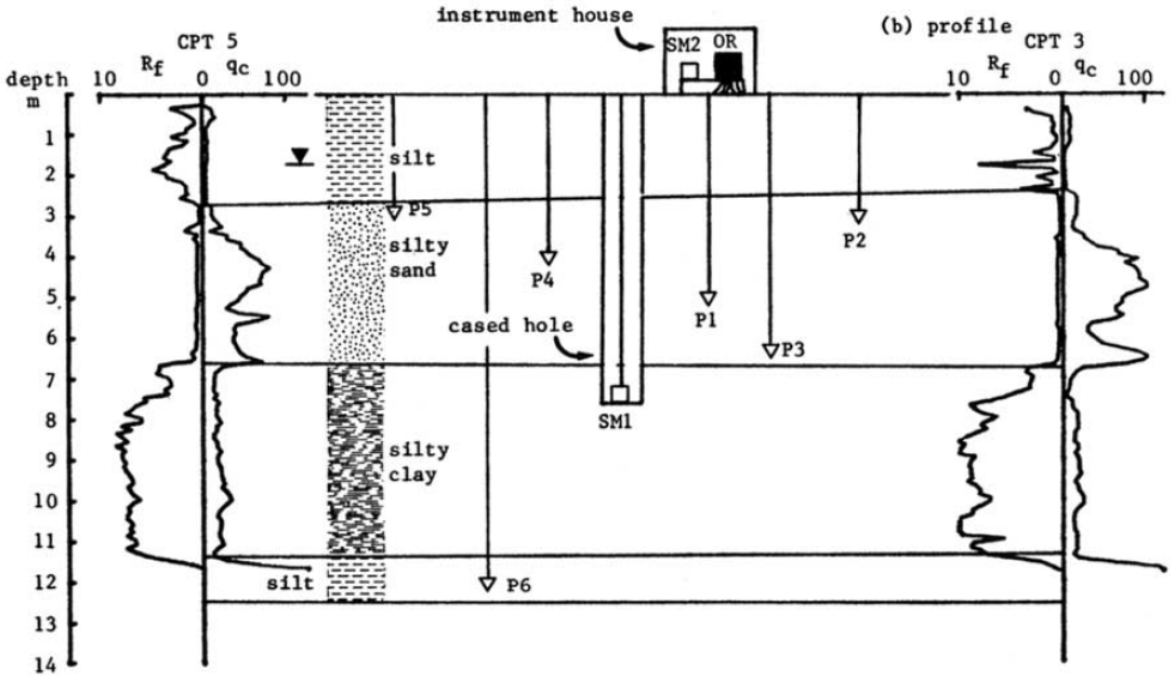

Figure 3.2: Profile at the Wildlife Liquefaction Array (Bennett et al. 1984)

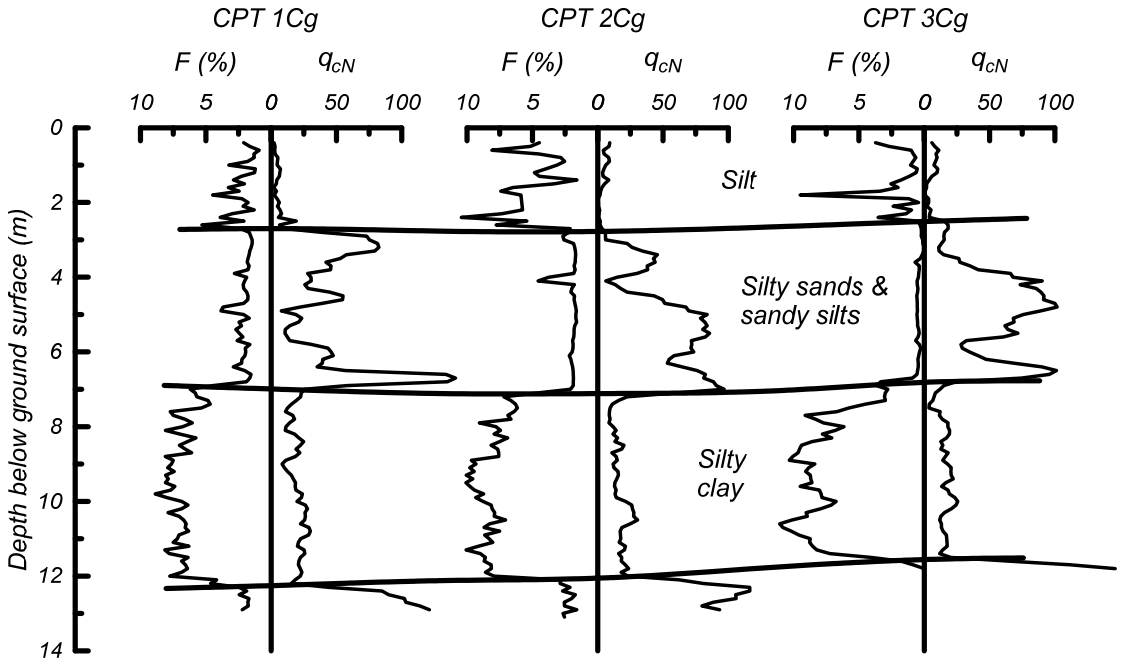

Figure 3.3. Three CPT soundings around the slope inclinometer at the Wildlife Liquefaction array (data courtesy of T. Holzer)

Miller and Farris Farms

The Miller and Farris Farms site is illustrative of cases where the boundaries of liquefaction and lateral spreading effects are controlled by changes in geologic facies (Holzer and Bennett 2007). Liquefaction and ground failure developed along the Pajaro River between the Miller and Farris Farms during the 1989 Loma Prieta earthquake. A cross-section across the zone of ground failure is shown in Figure 3.4. Exploration data from the site are described in Bennett and Tinsley (1995) and discussed in Holzer et al. (1994) and Holzer and Bennett (2007).

They concluded that the zone of ground failure was restricted to the areas underlain by the younger (Q_{yf}) floodplain deposit, which fills an old river channel that was incised into the older (Q_{of}) floodplain deposit. Three of the CPT soundings (CMF-3, 5, & 8) that encountered the younger Q_{vf} deposit were interpreted as having representative q_{cN} values of 36, 76, and 47 at critical depths of about 6 m; the corresponding q_{c1Ncs} values were 78, 102, and 82, which is a relatively minor variation given that these soundings span a distance of about 550 m with the failure zone parallel to the river.

The areas of no liquefaction or ground failure were characterized by a relatively thick surface deposit of high-plasticity silt. This silt has sufficiently high I_c values that it would normally be identified as clay-like; e.g., I_c averaged about 2.9 to 3.3 in CMF-1 and CMF-2. The deeper older sands that underlay the high-plasticity silt deposits were not that much denser than the younger floodplain deposits, with the representative q_{cN} value for the older sands being about 68 (q_{c1Ncs} values of 111) at depths of about 7-10 m at CMF-10. The potential for the relatively thick silt layer to have masked any effects of liquefaction in these deeper older sands is an example of how potential false negatives may be expected to exist in the database.

This site is one of several examples used by Holzer and Bennett (2007) to illustrate how the boundaries of a lateral spread are often controlled by changes in geologic facies. It also illustrates how borings located short distances outside of a ground failure zone may, or may not, be representative of the soils that have liquefied. For this reason, the interpretation of liquefaction case histories using borings located outside the failure zone have the potential to be misinterpreted unless the geologic conditions are fully understood and taken into consideration. It also emphasizes the need for investigators to incorporate and include the geologic conditions in the description of the case histories investigated.

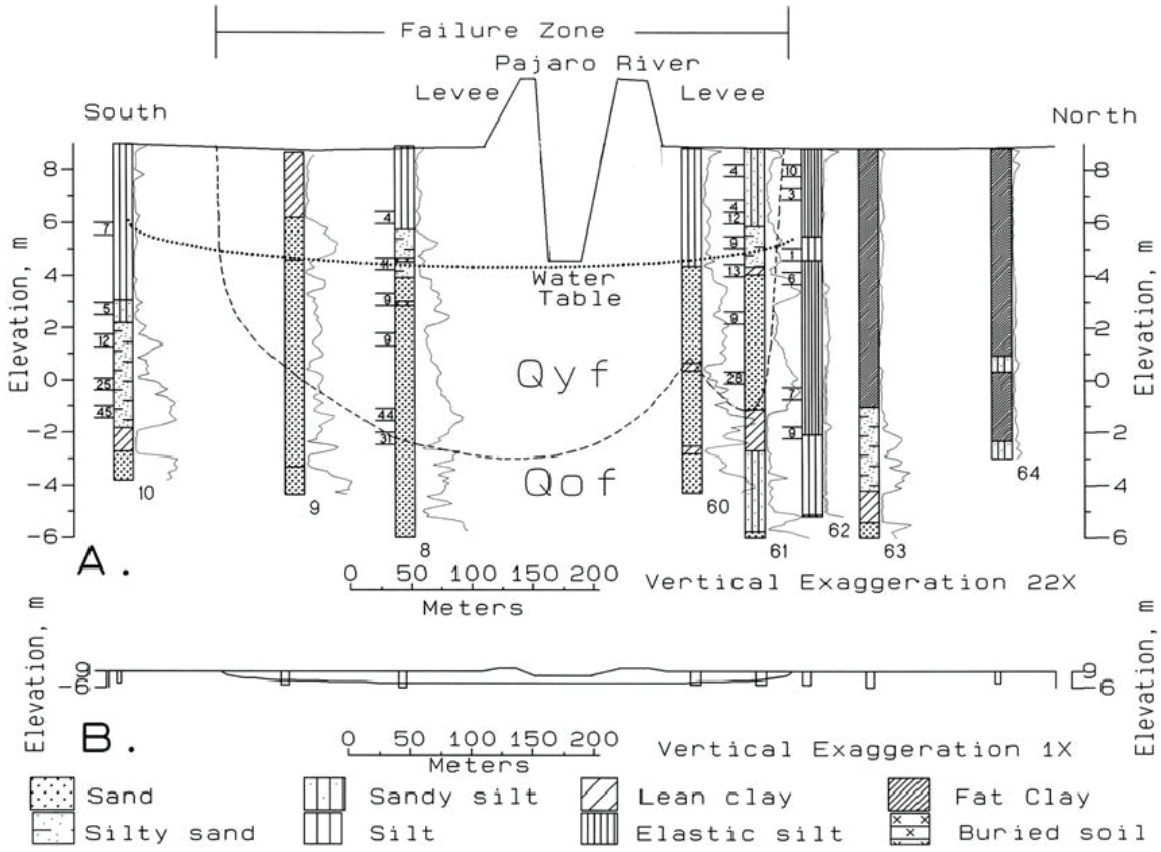

Figure 3.4. Profile across the failure zone at the Miller (south side of Pajaro River) and Farris Farms (north side of Pajaro River) during the 1989 Loma Prieta Earthquake (Holzer et al. 1994)

Malden Street

Ground failure along Malden Street in the San Fernando Valley during the 1994 Northridge earthquake is an example of ground failure due to lurching in soft clays (O'Rourke 1998, Holzer et al. 1999). The estimated PGA at this location was 0.51 g. A cross-section across the ground failure zone is shown in Figure 3.5. The failure zone is underlain by an 8.5-m-thick stratum of Holocene alluvial lean to sandy lean clay (Units A and B), which is underlain by Pleistocene silty sand (Unit D). The Holocene alluvium in the San Fernando Valley was deposited primarily by floodwaters coming out of the surrounding mountain canyons, with the texture of the sediments being primarily determined by the source materials in the surrounding mountains. The ground water table in the failure zone at the Malden Street site was at a depth of 3.9 m, and no Holocene sands were encountered below the water table. The fine grained soils of Unit B typically had FC > 70% with an average PI of 18. Undrained shear strengths (s_u) for Units A and B were determined from field vane shear tests and CPT data. The s_u in Unit B was generally less than 50 kPa, compared to about 120 kPa for Unit A, and it decreased to an average value of s_u = 26 kPa in the 1.5-m-thick interval between depths 4.3 and 5.8 m in the area of ground failure. Holzer et al. (1999) computed peak dynamic shear stresses, based on the estimated PGA of 0.51 g, that were about twice the fine-grained soil's undrained shear strength. For the underlying Pleistocene sediment (Unit D), Holzer et al. (1999) obtained 8 SPT N values, of which 2 were in silty sands and 6 were in clayey sands; they reported an average $(N_1)_{60cs}$ value of 43 (using the procedures from Youd et al. 2001) with an average FC = 27% based on the two tests in silty sands. Holzer et al. (1999) and O'Rourke (1998) both concluded that cyclic softening/failure of the soft clay along Malden Street caused the observed ground deformations. In fact, O'Rourke used this site as a key example of ground failure due to lurching in soft clays, and not liquefaction of a cohesionless deposit.

This case history illustrates the importance of recognizing that ground failures that mimic those caused by liquefaction can develop in soft clays under strong earthquake shaking, which is important to the interpretation of ground failure case histories and to the forward prediction of ground failures in practice. Additional case histories from the 1999 Chi-Chi and Kocaeli earthquakes have provided several examples regarding the behavior of low-plasticity fine grained soils, including cases of ground failure attributed to cyclic softening of silty clays beneath strongly loaded foundations (e.g., Chu et al. 2008) and cases where the low but measurable plasticity of the fines fraction was identified as one of the characteristics associated with lateral spreading displacements being significantly smaller than would be predicted by the application of current liquefaction analysis procedures (e.g., Chu et al. 2006, Youd et al. 2009).

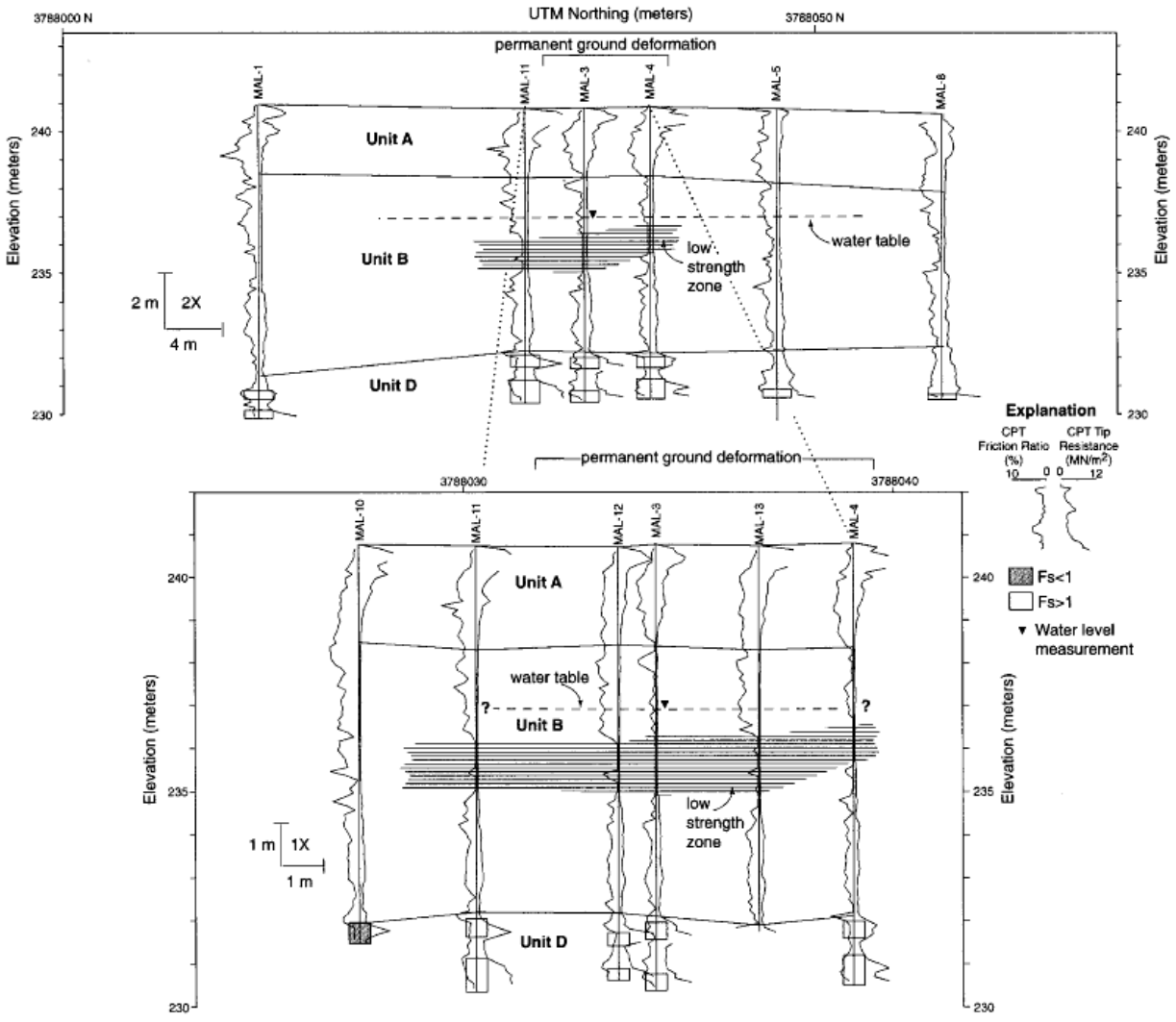

Figure 3.5. Profile across the failure zone at the Malden Street site during the 1994 Northridge Earthquake (Holzer et al. 1999)

3.4. Classification of site performance

Site performance during an earthquake is classified as a "liquefaction", "no liquefaction", or "marginal" case; some databases designate these cases as "yes", "no", or "no/yes", respectively. In this report, the classification of site performance was based on the classification assigned by the original investigator, except for the Seventh Street Wharf site at the Port of Oakland (discussed below). Cases described as "liquefaction" were generally accompanied with reports of sand boils and/or visible ground surface settlements, cracks, or lateral spreading movements. Cases described as "no liquefaction" were either accompanied with reports of no visible surface manifestations (i.e., no sand boils, ground surface settlements, cracks, or lateral movements) or can be inferred as having corresponded to such conditions when not explicitly stated.

A case may be described as "marginal" if the available information suggests that conditions at the site are likely at, or very near, the boundary of conditions that separate the physical occurrence of liquefaction from non-liquefaction. Only two cases are classified as marginal in the database because it is very difficult to define a marginal case in most field conditions. Areas of liquefaction and non-liquefaction in the field are often separated by distinct geologic boundaries (e.g., Holzer and Bennett 2007) such that borehole data can be used to describe liquefaction and no liquefaction cases, but not the marginal condition. Thus explicit information is typically not available for marginal conditions. The two marginal cases in the database are, therefore, discussed below.

The Seventh Street Wharf site at the Port of Oakland and its performance in the 1989 Loma Prieta earthquake are described in Kayen et al. (1998) and Kayen and Mitchell (1998). Boring POO7-2 was intentionally located in an area with surface manifestations of liquefaction, whereas boring POO7-3 was in an area with no surface manifestations. The two borings, POO7-2 and POO7-3, were characterized as "liquefaction" and "no liquefaction" sites, respectively, in Kayen et al. (1998). The following additional information and updated interpretation of the performance of these sites was provided by Kayen (2010, personal communication).

The two borings, POO7-2 and POO7-3, were separated by 70-100 m. At the location of POO7-3, there were no sand boils in the immediate 15-20 meters. This site was at the back of the park (now converted to container yard) at the farthest distance from the dike. In the zone along the bay margin, perhaps 20 m wide, there were ample fissures and sand boils, deformations toward the free-face, and a small lateral spread into the bay. The distance from this zone to POO7-3 was about 20-30 m. Kayen (2010, personal communication) indicated that, at this time, he would classify the location at POO7-3 as a liquefaction site because it was too close to the park perimeter deformations to be classified as a non-liquefaction site based on surface observations alone. This site was listed as a "marginal" case in the database presented herein because the soil conditions at POO7-3 had similar stratigraphy but slightly denser conditions than at POO7-2.

The other marginal case in the database is the Chemical Fiber Plant during the 1975 Haicheng earthquake (Arulanandan et al. 1986). The original investigators described the site as a marginal case, and the available information is not sufficient to modify that judgment.

3.5. Distribution of data

The distributions of q_{cN}, F, I_c, and FC (by lab only) are plotted versus the representative depth of the critical zone in Figure 3.6. These figures indicate that the database is limited to average critical depths less than 12 m with very few points for average depths greater than about 9 m.

The distributions of M, a_{max}, $CSR_{M,\sigma}$, and the depth to the water table are plotted versus the representative depth of the critical zone in Figure 3.7. The current database includes relatively few cases for M less than 6 or greater than 7.6.

The distributions of the data are further illustrated in Figure 3.8 showing a_{max} versus M (two parameters which enter the calculation of $CSR_{M=7.5,\sigma=1}$) and q_{cN} versus FC (two parameters which enter the calculation of q_{c1Ncs}).

The distribution of the liquefaction and no-liquefaction case histories are plotted on the CPT classification chart of Robertson (1990) in Figure 3.9. The liquefaction and no-liquefaction cases span across soil behavior types 4, 5, and 6, and plot both to the left and right of the zone expected for normally-consolidated soils.

The distribution of the analysis parameters C_N, K_σ, r_d, and MSF for the liquefaction and no-liquefaction case histories are plotted versus σ'_v in Figure 3.10. The parameter C_N varies the most over the range of conditions covered by the case histories, whereas the K_σ, r_d, and MSF parameters vary by much smaller amounts.

Explicit statements regarding the plasticity of the fines fraction [e.g., a plasticity index (PI) or statement that the fines are nonplastic] are not provided for most case histories. For example, consider the 35 case history data points for FC > 35%. No explicit statement regarding the plasticity index or nonplastic nature of the fines fraction was provided for 29 of these sites, although the visual descriptions and classifications of the soils (e.g., SM, ML) implied either nonplastic or low-plasticity silty fines. The PIs reported for the other 6 sites were 3, 8, 9, 10, 10, and 10, which also correspond to low plasticity fines. Ideally, the case history data would include more accurate details regarding fines plasticity so that possible effects of varying fines plasticity could be evaluated. In the meantime, the available information does suggest that the database presented herein corresponds primarily to soils with nonplastic or low plasticity silty fines.

Liquefaction analyses should explicitly evaluate how the conditions of a specific project compare to the conditions covered by the case history database, as illustrated by the distributions shown in this section. If project conditions fall outside the range of conditions that are well constrained by case history data, then the results of liquefaction triggering analyses using different correlations can be strongly dependent on the functional relationships used within those correlations. In such cases, a clear understanding of the bases behind the functional relationships can be important for guiding judgments regarding the applicability of the results so obtained.

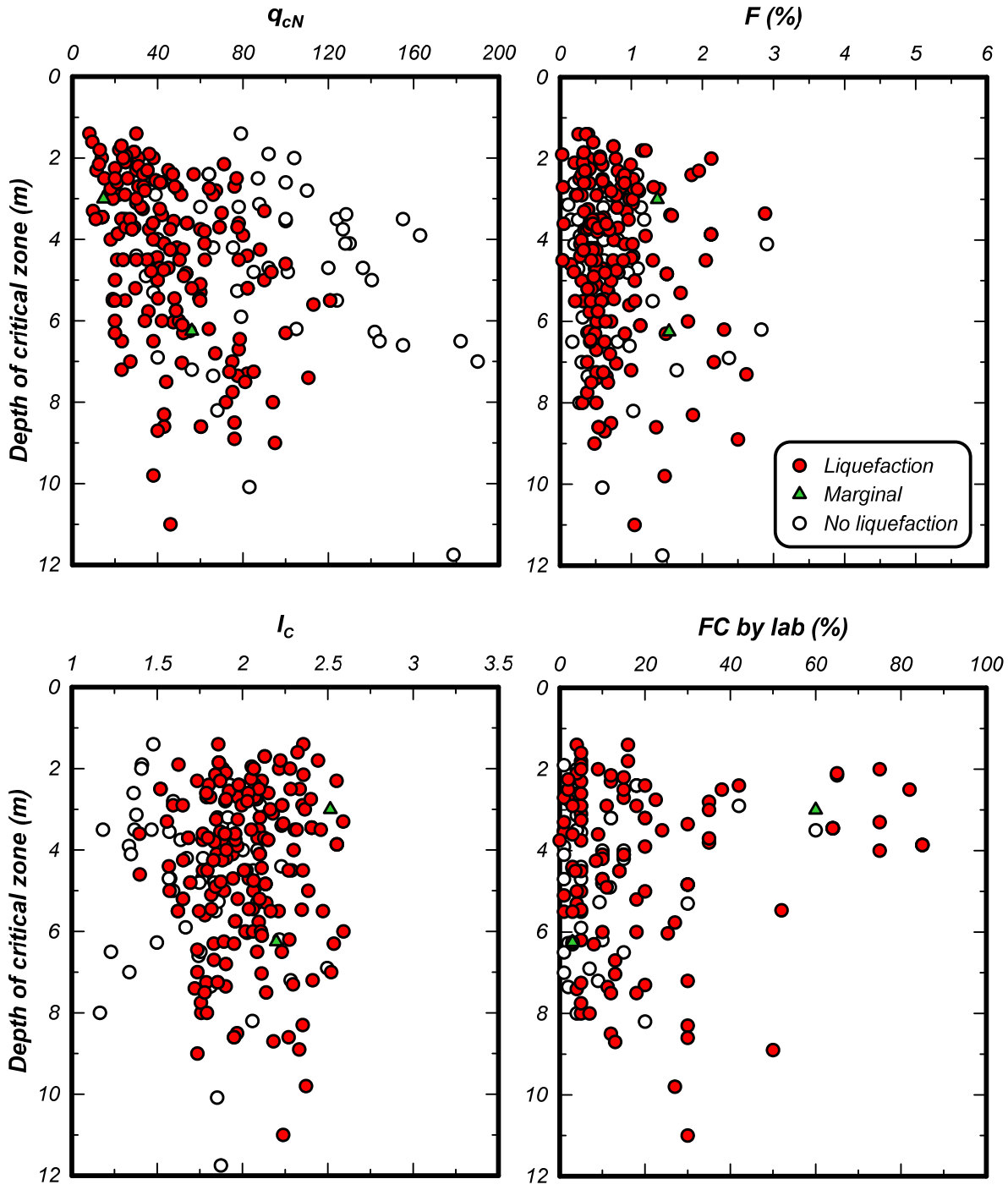

Figure 3.6. Distributions of the parameters q_{cN}, F, I_c, and FC versus the representative depth of the critical zone

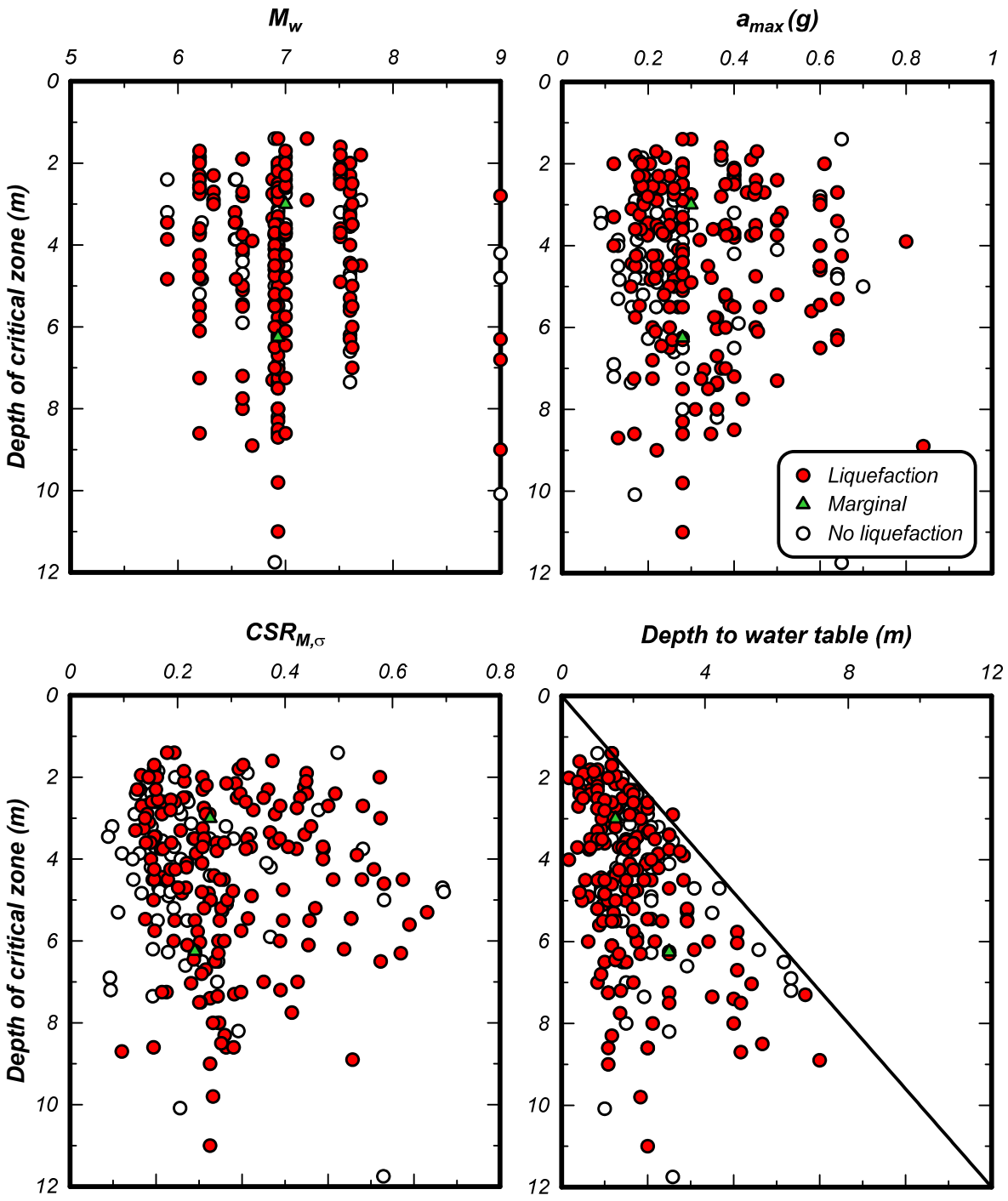

Figure 3.7. Distributions of the parameters M_w, a_{max}, $CSR_{M,\sigma}$, and depth to water table versus the representative depth of the critical zone

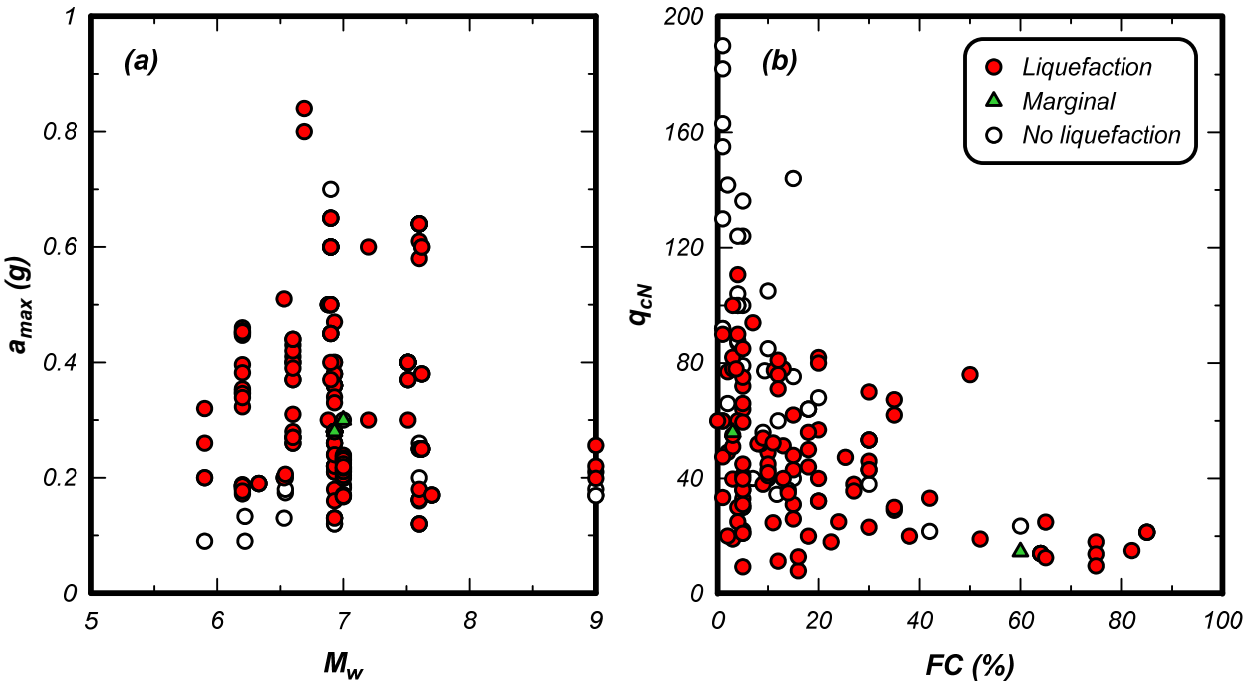

Figure 3.8. Distributions of: (a) a_{max} versus M and (b) q_{cN} versus FC for cases with FC determining by laboratory testing

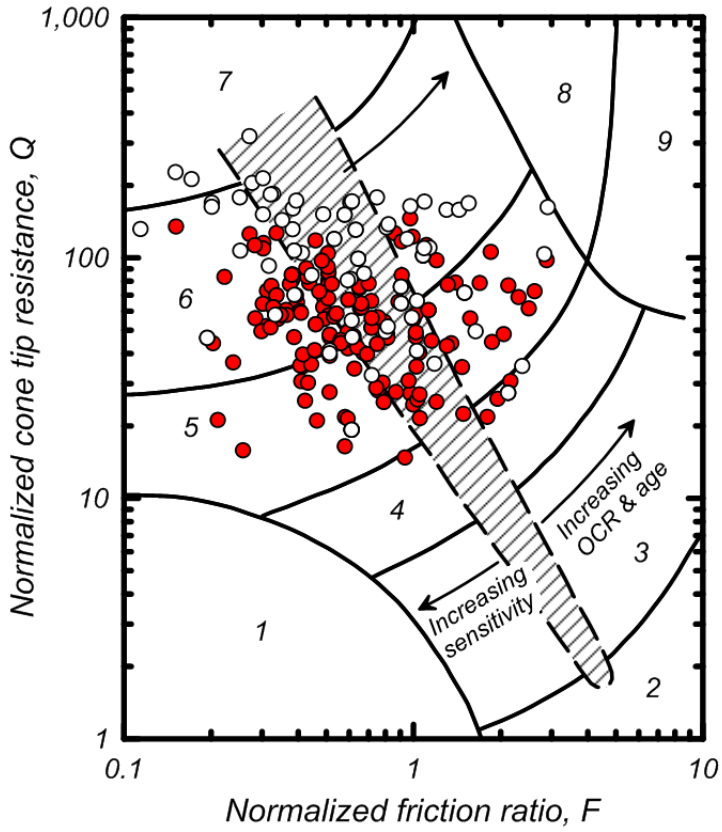

1. Sensitive, fine grained
2. Organic soils - peats
3. Clays - silty clay to clay
4. Silt mixtures - clayey silt to silty clay
5. Sand mixtures - silty sand to sandy silt
6. Sands - clean sand to silty sand
7. Gravelly sand to dense sand
8. Very stiff sand to clayey sand *
9. Very stiff, fine grained *

* Heavily overconsidated or cemented

Figure 3.9. Distributions of liquefaction (red bullets) and no-liquefaction (open bullets) case histories on the Robertson (1990) CPT classification chart

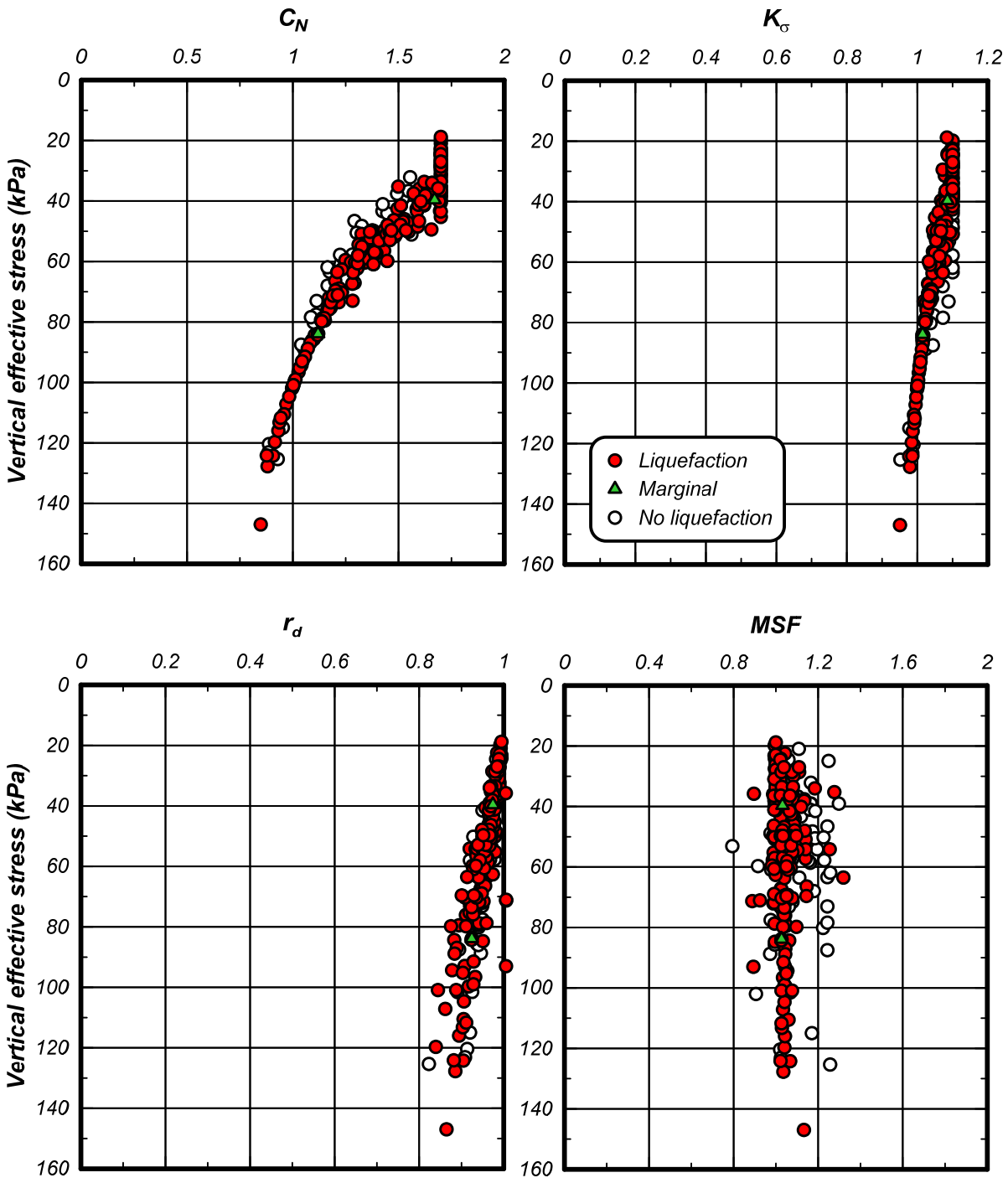

Figure 3.10. Distributions of the parameters C_N, K_σ, r_d, and MSF versus the σ'_v in the critical zone

4. UPDATED CPT-BASED TRIGGERING PROCEDURE

This section presents the updated deterministic CPT-based liquefaction triggering correlation and the distribution of the updated case history data (Section 3) against the correlation for a range of different parameter bins. The updated correlation's development and comparison to the full database are described first, following by examination of the data for bins of varying FC, M, and σ'_v. These comparisons are presented in terms of q_{c1Ncs} so that the entire data (clean sands, silty sands and nonplastic sandy silts) can be combined in different data bins. The data, as listed in Table 3.1, were all processed using the equations and analysis framework presented in Section 2.

4.1. Correlation with updated database

The full, updated case history database is shown in Figure 4.1 in terms of equivalent $CSR_{M=7.5,\sigma'=1}$ versus equivalent clean sand q_{c1Ncs} values along with the deterministic triggering correlation by Idriss and Boulanger (2008) and the revised deterministic triggering correlation derived as part of this study. The revised triggering curve closely follows the Idriss-Boulanger (2008) triggering curve for q_{c1Ncs} values of 80 to 130, but curves upward at both lower and higher values of q_{c1Ncs} where the case history data are more sparse. These adjustments at the higher and lower end of q_{c1Ncs} values were guided by consideration of the case history data, consistency with empirical trends in q_c/N_{60} ratios (Section 7), and consistency with the SPT-based triggering correlation in terms of equivalent relationships between CRR and the relative state parameter index. The revised deterministic triggering curve was also developed as part of the probabilistic analyses presented in Section 5 and corresponds to a probability of liquefaction of about 16% (model uncertainty alone). The revised deterministic triggering correlation is expressed as,

$$CRR_{M=7.5,\sigma'_v=1atm} = \exp\left(\frac{q_{c1Ncs}}{113} + \left(\frac{q_{c1Ncs}}{1000}\right)^2 - \left(\frac{q_{c1Ncs}}{140}\right)^3 + \left(\frac{q_{c1Ncs}}{137}\right)^4 - 2.8\right) \quad (4.1)$$

There are 5 liquefaction points that fall below the revised deterministic triggering correlations (Table 4.1) and 32 no-liquefaction points that fall above it. Three of the points below the curve are less than a vertical distance of 0.005 from the curve, such that they are basically on the curve. The two points located well below the curve are the cases for the Awaroa Farm and KAN-26c sites.

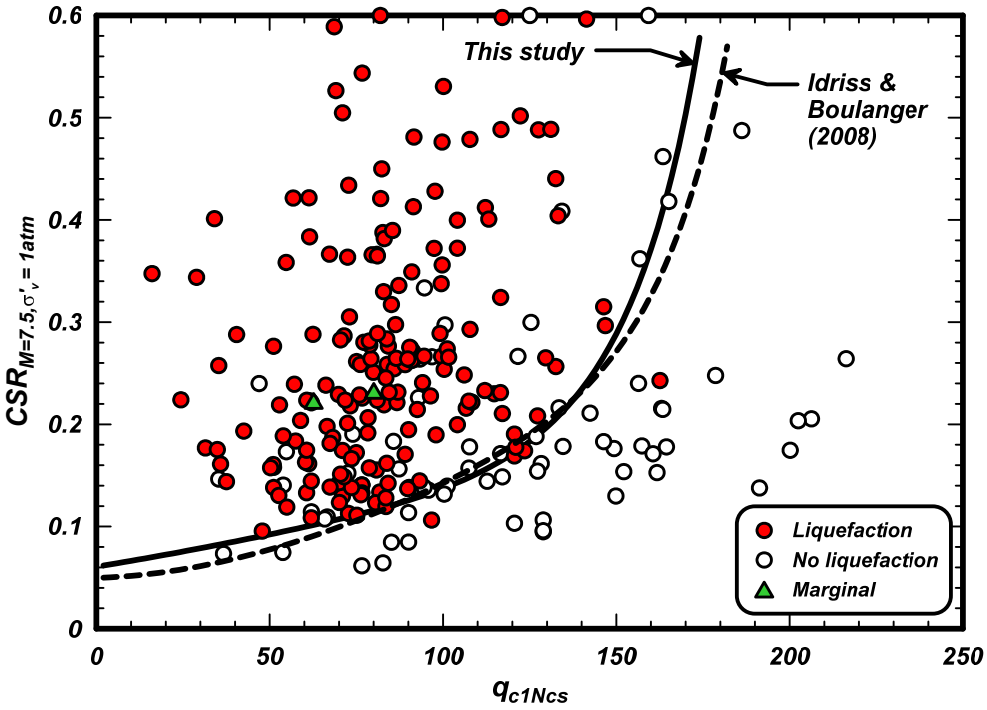

Figure 4.1. Updated CPT case history database of liquefaction in cohesionless soils with various fines contents in terms of equivalent CSR for M = 7.5 and σ'_v = 1 atm and equivalent clean sand q_{c1Ncs}

Table 4.1. Liquefaction data points falling below the deterministic triggering curve

Earthquake	Site	Magnitude (M)	σ'_{vc} (kPa)	Lab FC (%)	Repr. FC (%)	$q_{c1N,cs}$
1980 M=6.3 Victoria (Mexicali) - June 9	Delta Site 4	6.33	38	--	32	96.7
1987 M=6.5 Superstition Hills 02 - Nov 24	Wildlife B	6.54	54	30	30	120.6
1987 M=6.6 Edgecumbe, NZ - Mar 2	Awaroa Farm AWA001	6.60	35	35	35	162.6
1989 M=6.9 Loma Prieta - Oct 18	State Beach Pathway	6.93	50	1	1	123.5
2011 M-6.2 Christchurch - Feb 22	KAN-26c	6.20	30	--	22	75.1

4.2. Variation with fines content

The distribution of data points for different values of FC is presented in Figures 4.2a through 4.2d showing the data for cases with the representative FC binned for the ranges of ≤ 5%, 5-15%, 15-35%, and >35%, respectively. For these respective bins, there are 1, 0, 4, and 0 liquefaction points below the triggering curve and 13, 14, 2, and 3 no-liquefaction points above the triggering curve. The liquefaction and no-liquefaction data points show no apparent bias with respect to FC.

The data for all sands with the FC determined by laboratory test are shown in Figure 4.3a, whereas the data for all sands with the FC determined by I_c-based correlation are shown in Figure 4.3b. There are 3 liquefaction data points that fall below the triggering curve and 18 no-liquefaction data points above the triggering curve when FC is determined by laboratory test. There are 2 liquefaction data points that fall below the triggering curve and 14 no-liquefaction data points above the triggering curve when FC is determined by I_c-based correlation.

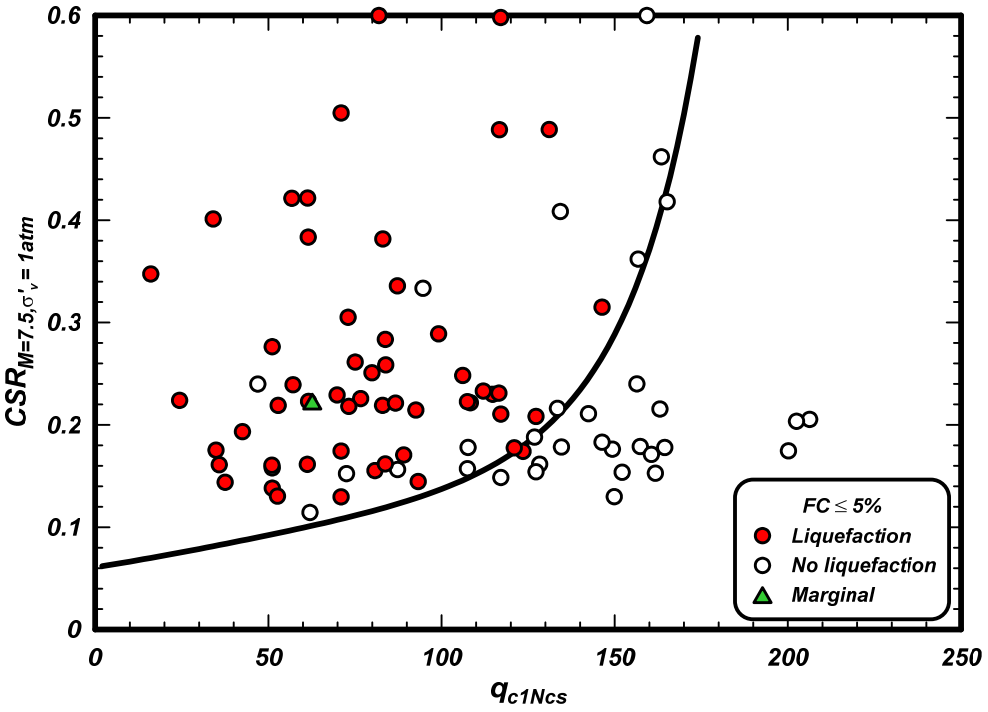

(a)

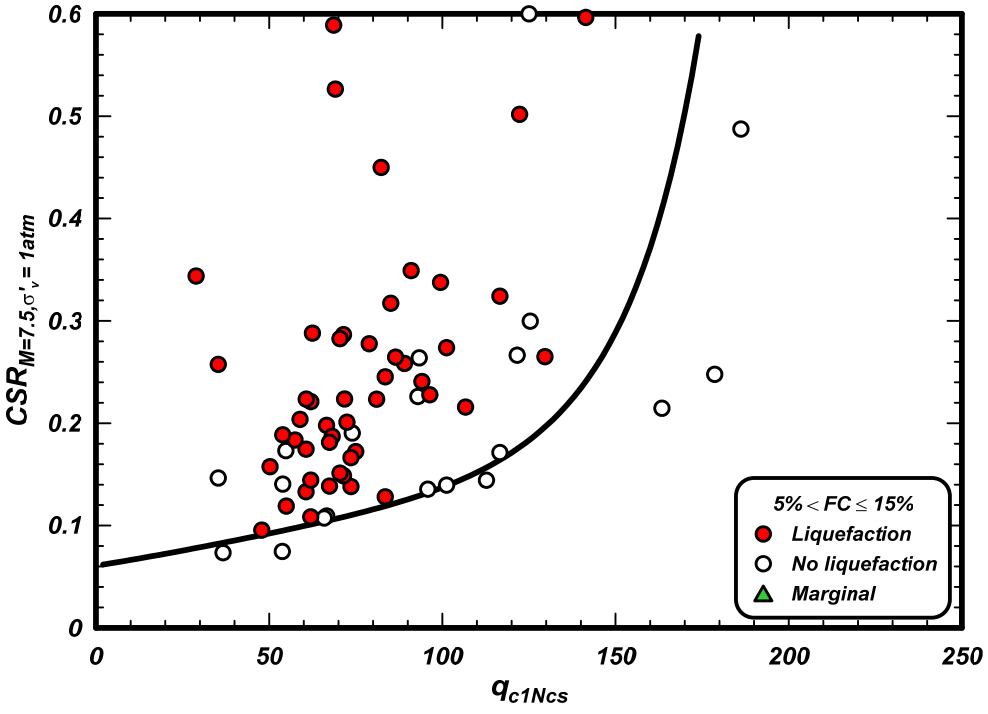

(b)

Figure 4.2a-b. Distribution of case history data with different fines contents and processed with the revised MSF relationship

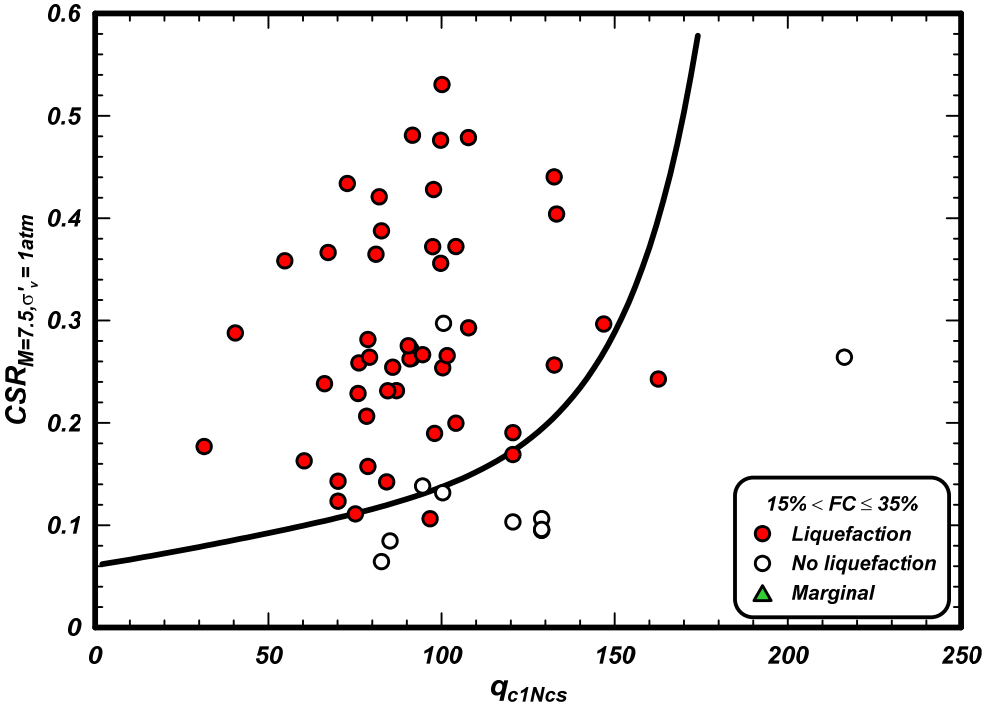

(c)

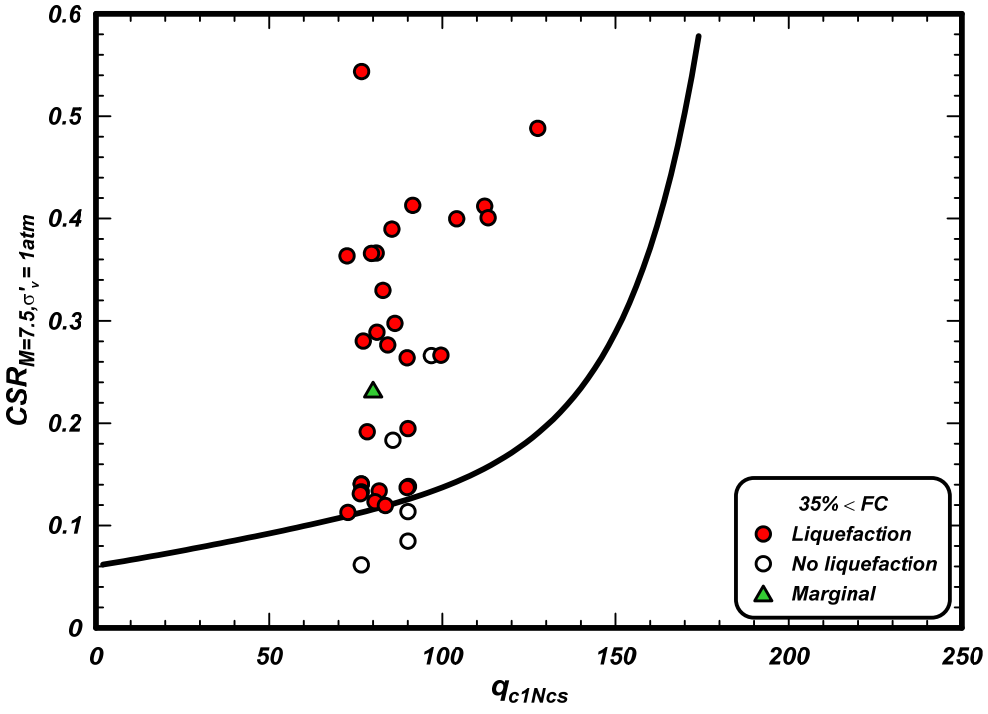

(d)

Figure 4.2c-d. Distribution of case history data with different fines contents and processed with the revised MSF relationship

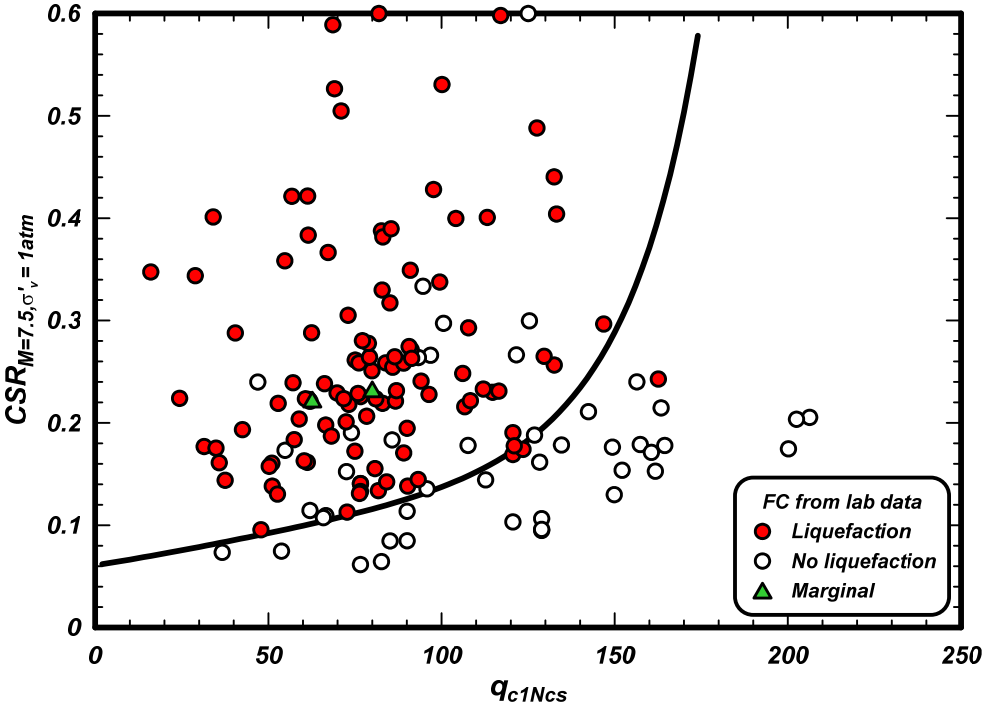

(a)

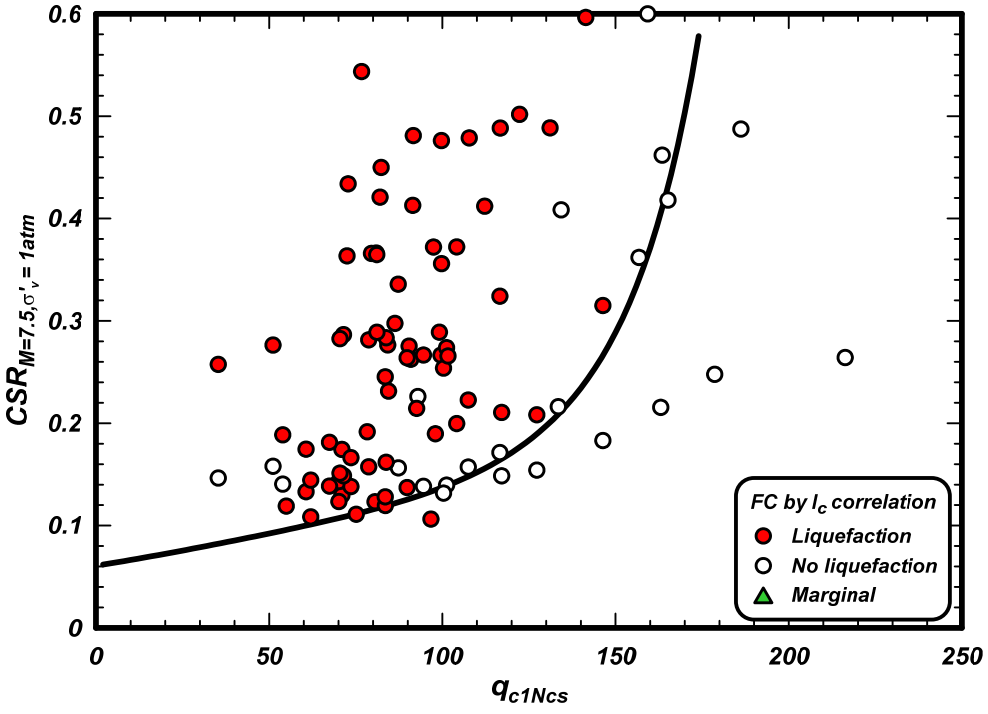

(b)

Figure 4.3. Distribution of case history data for: (a) FC determined by laboratory testing, and (b) FC determined by I_c correlation. Processed with the revised MSF relationship

4.3. Variation with earthquake magnitude

The distribution of data points for different earthquake magnitudes is presented in Figures 4.4a through 4.4e showing the data for cases with M binned for the ranges of M <6.25, 6.25-6.75, 6.75-7.25, 7.25-7.75, and M > 7.75, respectively. There are 1, 3, 1, 0, and 0 liquefaction points below the triggering curve in these five bins, and 2, 4, 18, 5, and 3 no-liquefaction points above the triggering curve, respectively. The liquefaction and no-liquefaction data points show no apparent bias with respect to M in the first four bins (i.e., M up to values of 7.75). The few data points for M > 7.75 are high relative to the triggering curve but they are not sufficient in quantity to suggest any changes to the correlation.

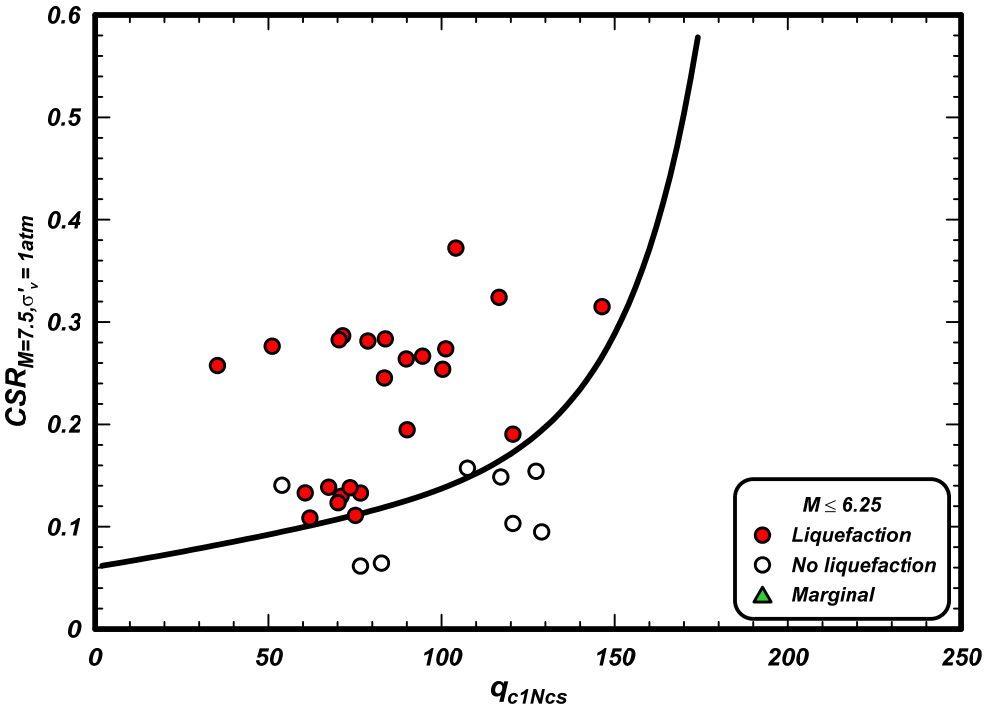

(a)

Figure 4.4a. Distribution of case history data with different earthquake magnitudes and processed with the revised MSF relationship

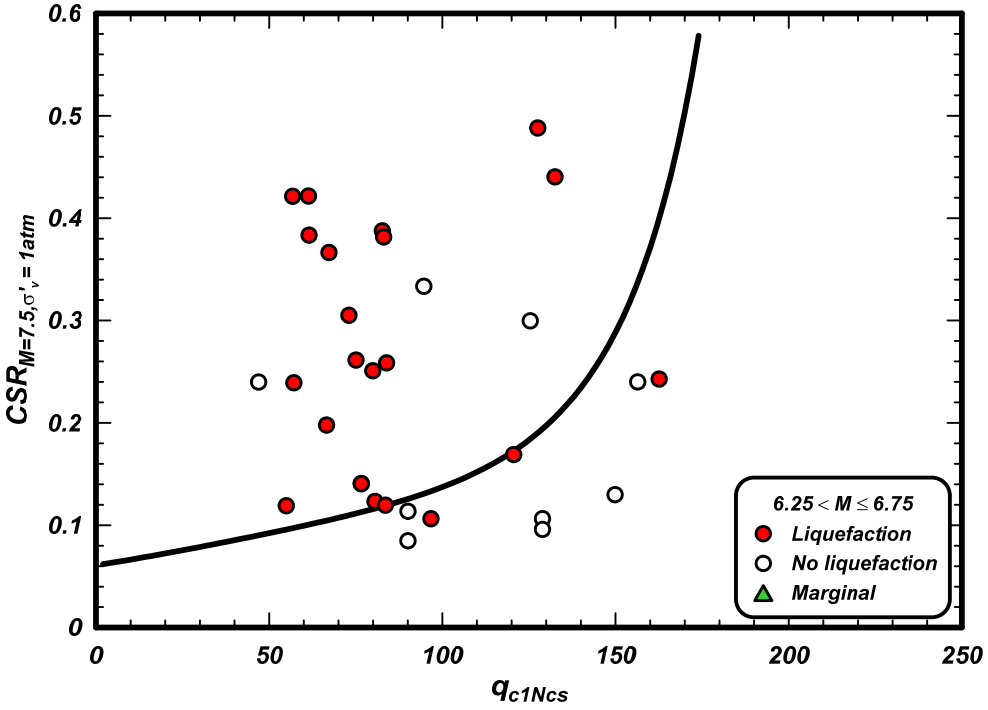

(b)

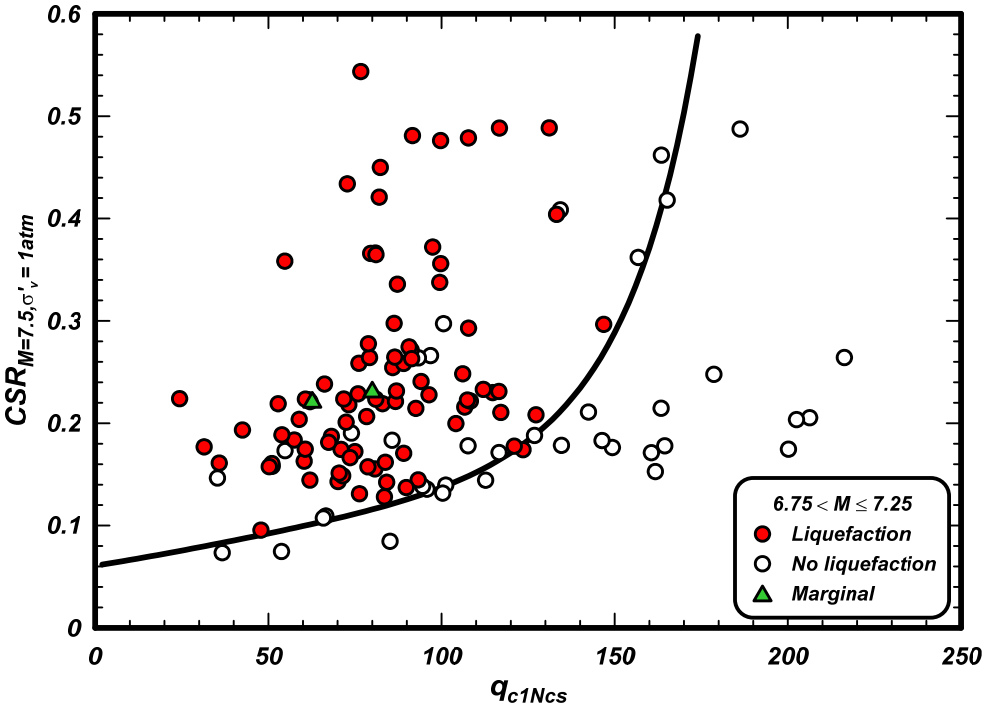

(c)

Figure 4.4b-c. Distribution of case history data with different earthquake magnitudes and processed with the revised MSF relationship

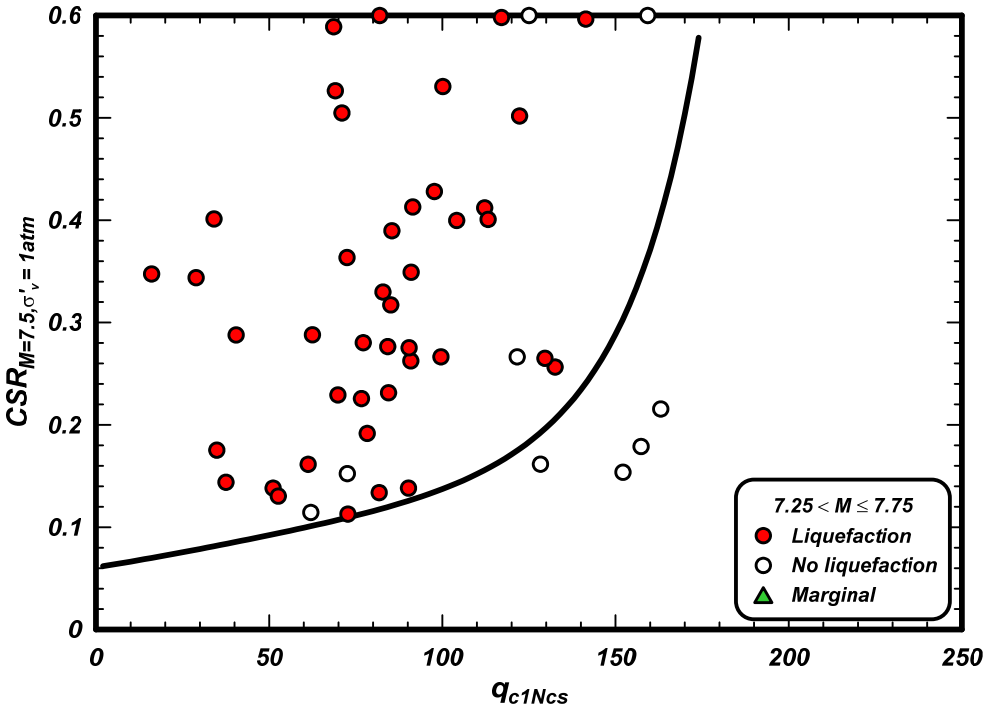

(d)

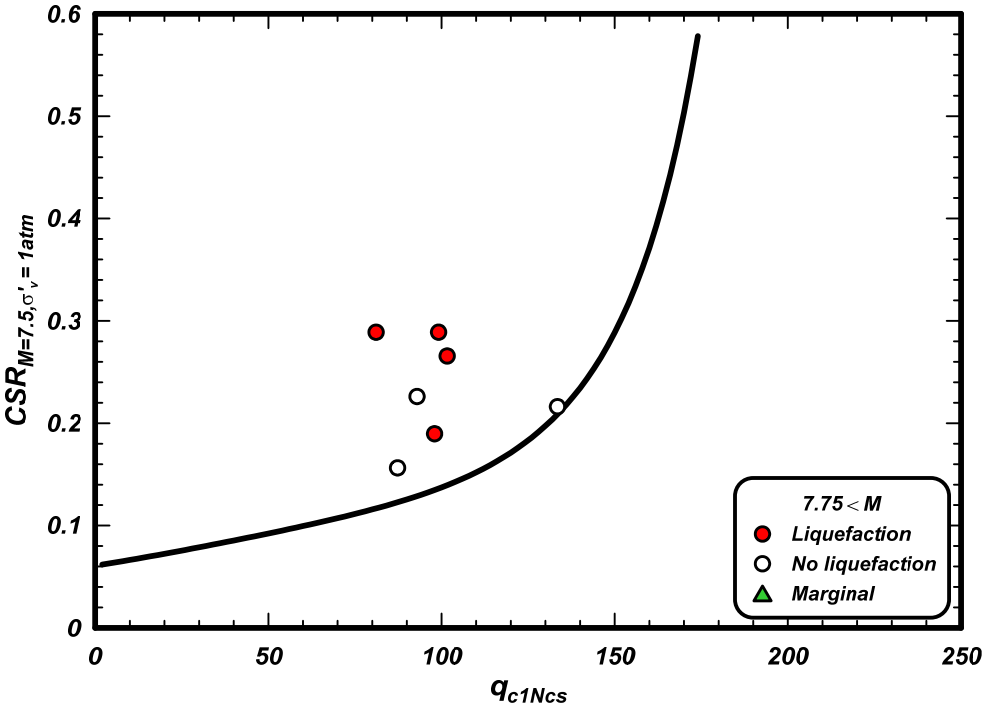

(e)

Figure 4.4d-e. Distribution of case history data with different earthquake magnitudes and processed with the revised MSF relationship

4.4. Variation with effective overburden stress

The distribution of data points for different σ'_v is presented in Figures 4.5a through 4.5d showing the data for cases with σ'_v binned between 0-0.4 atm, 0.4-0.8 atm, 0.8-1.2 atm, and >1.2 atm, respectively. There are 3, 2, 0, and 0 liquefaction points below the triggering curve in these four bins, respectively, and there are 5, 24, 3, and 0 no-liquefaction points above the triggering curve, respectively. The bins with σ'_v between ≤ 0.4 atm and 0.4-0.8 atm have the most data, including the majority of the liquefaction cases that lie close to and along the liquefaction triggering curve. The bin with σ'_v > 1.2 atm has the fewest data. Thus, the case histories do not constrain the triggering curve equally well across these stress bins. Nonetheless, the overall distribution of both the liquefaction and no-liquefaction data points relative to the triggering curve across these stress bins appears reasonably balanced.

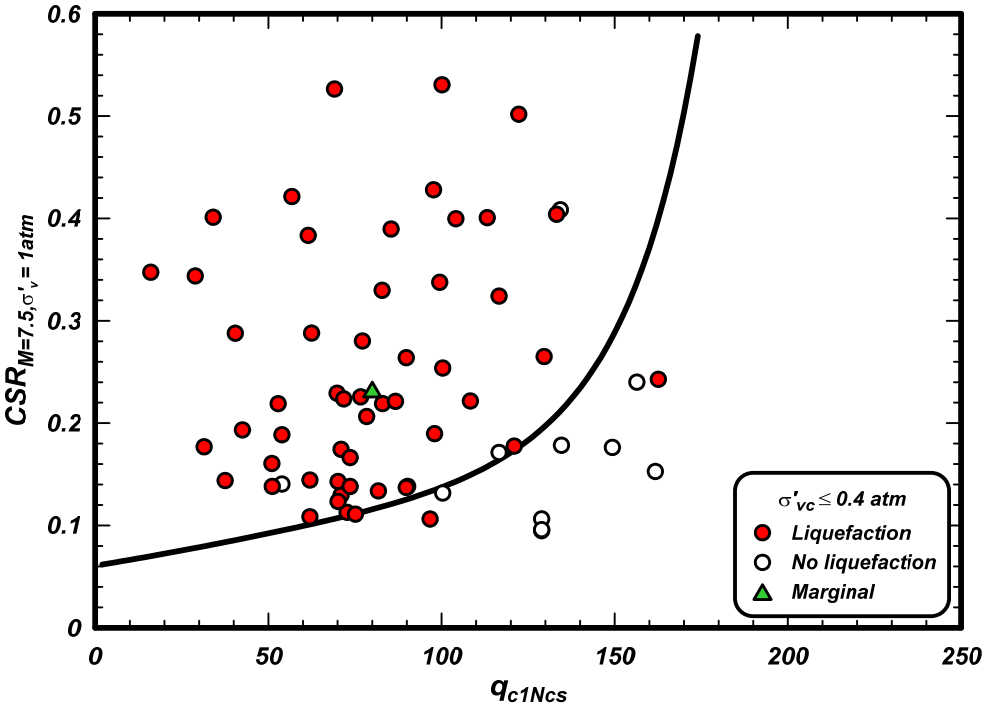

(a)

Figure 4.5a. Distribution of case history data with different effective overburden stresses and processed with the revised MSF relationship

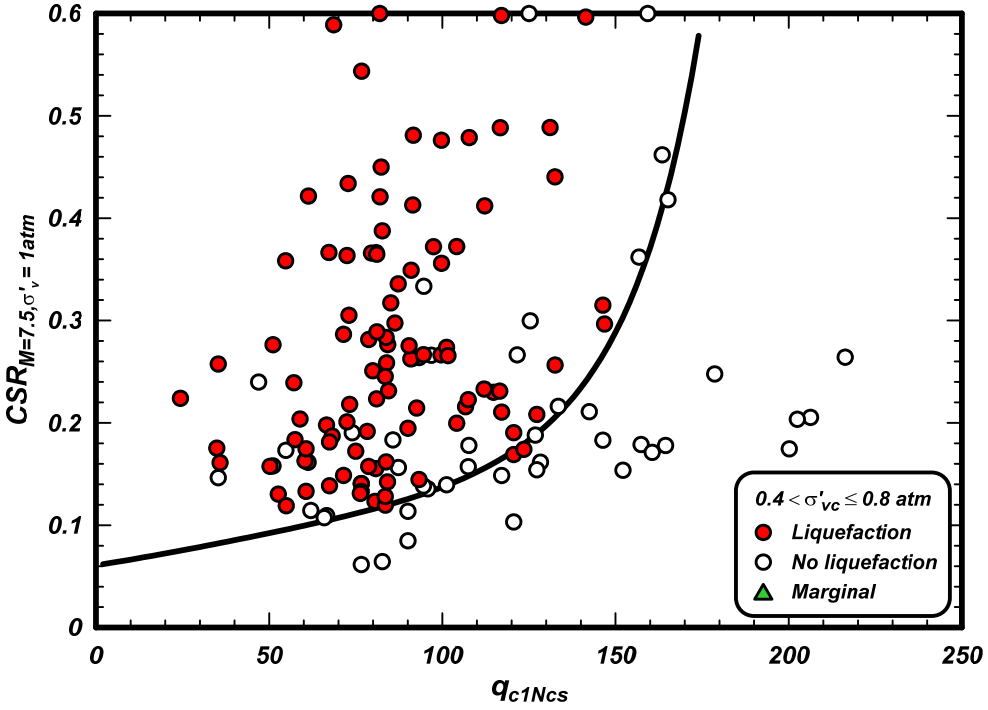

(b)

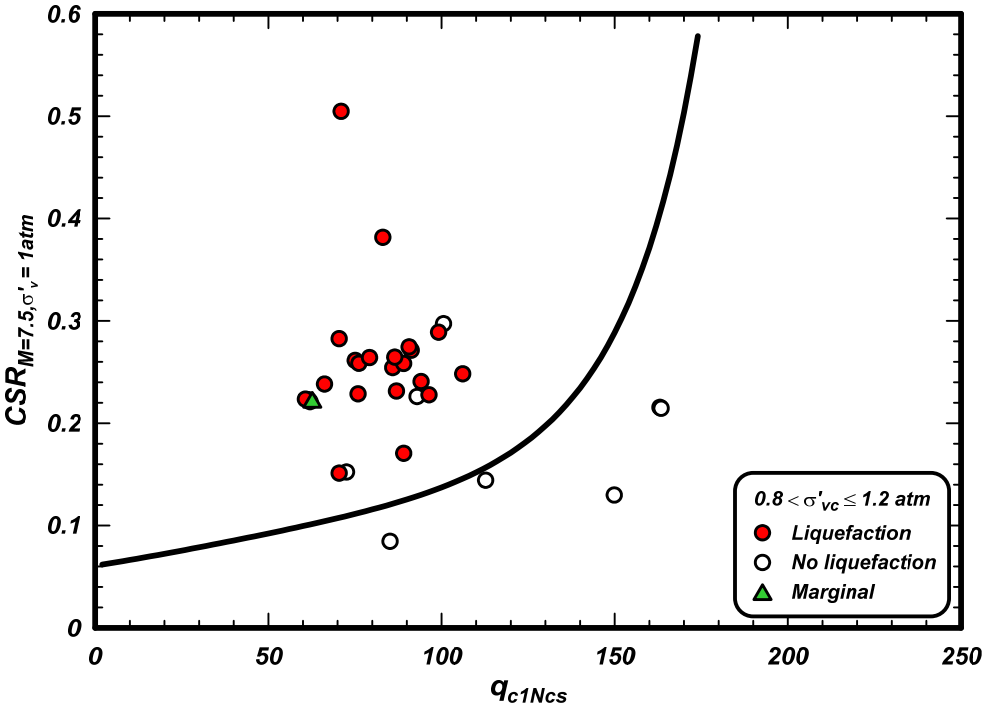

(c)

Figure 4.5b-c. Distribution of case history data with different effective overburden stresses and processed with the revised MSF relationship

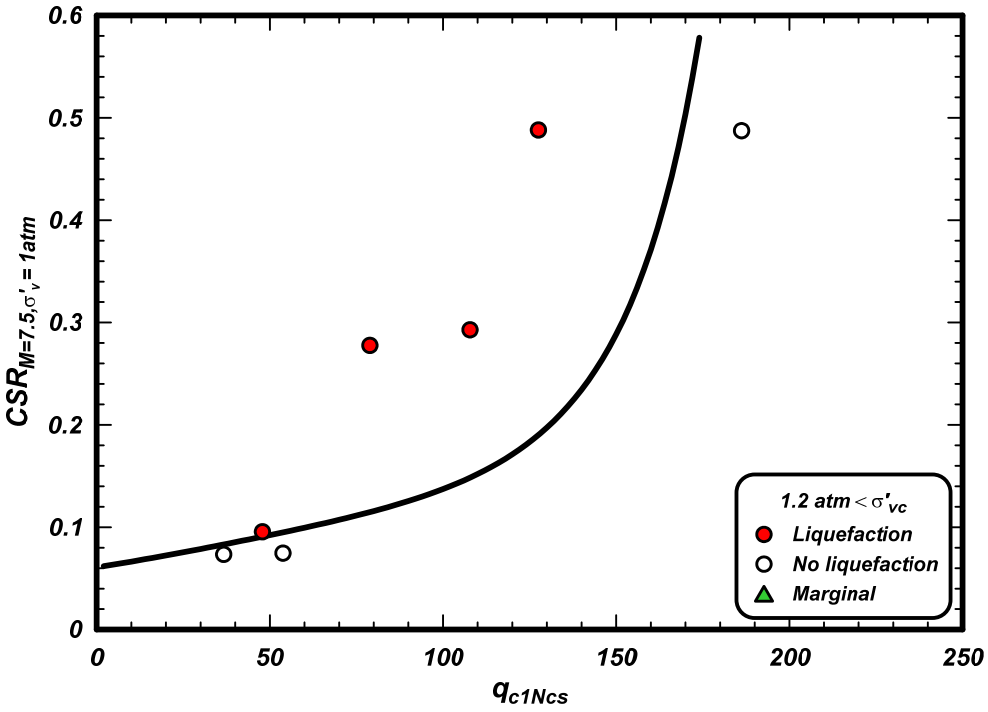

(d)

Figure 4.5d. Distribution of case history data with different effective overburden stresses and processed with the revised MSF relationship

4.5. Summary

The revised deterministic CPT-based triggering correlation closely follows the Idriss-Boulanger (2008) triggering curve for q_{c1Ncs} values of 80 to 130, but curves slightly upward at both lower and higher values of q_{c1Ncs}. The new adjustments, which include the new MSF and FC correction relationships, are later shown tin Section 7 to improve consistency with empirical trends in q_c/N_{60} ratios while maintaining consistency with the SPT-based triggering correlation in terms of equivalent relationships between CRR and the relative state parameter index.

The distribution of the case history data was examined relative to the revised deterministic triggering curve. The case history data were shown to be in reasonable agreement with the liquefaction triggering correlation across bins of varying FC, M, and σ'_v and found to show no evident biases with regard to these or other case history parameters.

The case history distributions provide a valuable basis for understanding how various components of the analysis framework may or may not affect the triggering correlation. For example, the C_N and K_σ parameters become less certain at confining stresses less than about 30 or 40 kPa for a number of technical reasons, and thus their expressions include maximum values that are reached in this stress range. If those maximum value limits were increased, then many data points in the bin for σ'_v between 0-0.4 atm will move slightly downward or to the right. The reverse is true if the maximum limits were decreased. The position of the triggering curve is, however, better constrained by the case history data for σ'_v greater than 0.4 atm and thus these data are given more weight in determining the final correlation. The r_d parameter, on the other hand, becomes more uncertain as the depth increases and thus variations in this parameter only has significant effects on the data points for σ'_v greater than about 0.8 atm. The data for the σ'_v bins of 0.8-1.2 atm and >1.2 atm, as shown in Figure 4.5, are relatively limited and scattered, such that changes in the r_d relationship had no significant effect on the final triggering correlation. In contrast, variations in the MSF parameter were found to have a more significant effect on the triggering correlation because it affected data across all bins. The revised MSF relationship presented in Section 2 improved the fit of the data points across the various bins of M compared to the use of an MSF relationship that did not include dependence on soil properties.

5. PROBABILISTIC RELATIONSHIP FOR CPT-BASED PROCEDURE

5.1. Probabilistic relationships for liquefaction triggering

SPT- and CPT-based probabilistic correlations for the triggering of liquefaction in sands and silty sands have been developed by a number of investigators, including Christian and Swiger (1975), Liao et al. (1988), Liao and Lum (1998), Youd and Nobel (1997), Toprak et al. (1999), Juang et al. (2002), Cetin et al. (2002, 2004), and Moss et al. (2006). Some relationships represent the total uncertainty in the evaluation of the case history database; i.e., they include the uncertainty in the triggering relationship (model uncertainty) and the uncertainty in the representative $(N_1)_{60cs}$ or q_{c1Ncs} and $CSR_{M=7.5,\sigma'=1}$ values determined for the case histories (measurement or parameter uncertainty). The relationship by Cetin et al. (2002, 2004) was developed using a statistical approach that allowed a separate accounting of the model and measurement uncertainties. For applications, the total uncertainty will include contributions from the liquefaction triggering model and the input parameters. The parameter uncertainties in an application are not the same as the measurement uncertainties in the case history database, and thus it is important to have separately quantified the model uncertainty so that it can be more rationally combined with the parameter uncertainties in a full probabilistic liquefaction evaluation.

A probabilistic version of the Idriss and Boulanger (2008) CPT-based liquefaction triggering correlation is developed using the updated case history database, the revised MSF relationship from Section 2, and a maximum likelihood method that utilizes the forms of the limit state and likelihood functions used by Cetin et al. (2002). This is the same procedure used by Boulanger and Idriss (2012a) to develop their SPT-based liquefaction triggering correlation. Emphasis is placed on developing a reasonable first-order estimate of the total and model uncertainties given that the available case history data are insufficient for quantifying the components of uncertainty on a site-by-site basis. Measurement or estimation uncertainties in $CSR_{M=7.5,\sigma'=1}$ and q_{c1Ncs} for the case histories and choice-based sampling bias are accounted for. Sensitivity of the maximum likelihood solution to the assumptions regarding uncertainties in $CSR_{M=7.5,\sigma'=1}$ and q_{c1Ncs}, the correction for sampling bias, and potential effects of false positives or false negatives in the database are examined. Sensitivity of the solution to the use of only clean sand case histories versus all case histories is examined. A probabilistic correlation is then proposed and issues regarding its use in practice are discussed.

5.2. Limit state function

The model for the limit state function (g) was taken as the difference between the natural logs of the $CRR_{M=7.5,\sigma'=1atm}$ and $CSR_{M=7.5,\sigma'=1atm}$ values, such that liquefaction is assumed to have occurred if $g \leq 0$ and to have not occurred if $g > 0$. The $CRR_{M=7.5,\sigma'=1atm}$ value was estimated using the following relationship,

$$CRR_{M=7.5,\sigma'_v=1atm} = \exp\left(\frac{q_{c1Ncs}}{113} + \left(\frac{q_{c1Ncs}}{1000}\right)^2 - \left(\frac{q_{c1Ncs}}{140}\right)^3 + \left(\frac{q_{c1Ncs}}{137}\right)^4 - C_o\right) \tag{5.1}$$

where C_o is an unknown fitting parameter that serves to scale the relationship while maintaining its shape; note that the shape of the relationship was constrained based on considerations discussed in Section 7 and that the deterministic version shown in Section 4 corresponds to $C_o = 2.80$. The use of a single fitting parameter provides a means for examining the uncertainty in the Idriss-Boulanger relationship. The $CSR_{M=7.5,\sigma'=1atm}$ value represents the loading that would be expected to be induced by the shaking, and it

was estimated using the relationships from Idriss and Boulanger (2008) with the revised MSF relationship presented in Section 2.5.

$$CSR_{M=7.5,\sigma'_v=1atm} = 0.65\frac{\sigma_v}{\sigma'_v}\frac{a_{\max}}{g}r_d\frac{1}{MSF}\frac{1}{K_\sigma} \tag{5.2}$$

The limit state function can then be written as,

$$\hat{g}\left(q_{c1Ncs}, C_o, CSR_{M=7.5,\sigma'_v=1atm}\right) = \ln\left(CRR_{M=7.5,\sigma'_v=1atm}\right) - \ln\left(CSR_{M=7.5,\sigma'_v=1atm}\right) \tag{5.3}$$

where the hat on g indicates that the limit state function is imperfect in its prediction of liquefaction behavior. This form is similar to that used by Cetin et al. (2002), although it is considerably simpler because most of the liquefaction triggering analysis components considered herein are based on experimental and theoretical considerations in lieu of including some of them as unknown fitting parameters.

The uncertainties in the limit state function are represented by three contributors. Measurement or estimation uncertainties in the case history data points are assumed to be adequately represented by including uncertainties in the q_{c1Ncs} and $CSR_{M=7.5,\sigma'=1atm}$ values. The uncertainty in q_{c1Ncs} is assumed to be normally distributed with a constant coefficient of variation (COV) (e.g., Baecher and Christian 2003). The uncertainty in $CSR_{M=7.5,\sigma'=1atm}$ is assumed to be log-normally distributed, which is consistent with log-normal distributions for the uncertainty in predictions of peak ground accelerations (e.g., Abrahamson et al. 2008). Uncertainty in the $CRR_{M=7.5,\sigma'=1atm}$ expression is represented by inclusion of a random model error term, which is also assumed to be log normally distributed with mean of zero.

The uncertainty in the representative q_{c1Ncs} value assigned to any case history includes contributions from three major sources. One major source of uncertainty is the degree to which the available CPT data are truly representative of the critical strata, which depends on the degree to which the geologic conditions are understood, the heterogeneity of the deposits, the number of soundings, and the placement of the soundings relative to the strata of concern. A second major source of uncertainty is the CPT-based estimation of soil types (e.g., fines content and fines plasticity), which depends on the availability and quality of site-specific sampling and index testing data. A third main source of uncertainty is variability in the CPT equipment and procedures used at different case history sites. The large majority of the liquefaction case histories lack sufficient information to justify attempting to develop site-specific estimates of these uncertainties for each case history. For this reason, the value of COV was taken as being the same for all case histories where fines content and fines plasticity are based on site-specific sampling and index testing and to be 50% greater when site-specific sampling and index testing data are not available. The 50% increase in the uncertainty for cases without site-specific sampling and index test data is a subjective adjustment based on considering how potential differences in fines content adjustments (Δq_{c1N}) would affect estimates of q_{c1Ncs}. Parametric analyses were then used to assess the sensitivity of the solution to the assumed values for the COV.

The uncertainty in the $CSR_{M=7.5,\sigma'=1atm}$ values estimated for any case history similarly depends on numerous factors, including the proximity of strong ground motion recordings, potential variability in site responses, availability and quality of indirect measures of shaking levels (e.g., eye witness reports, damage to structures, disruption of nonstructural contents), variability in the ground motion characteristics (e.g., duration of shaking), and the overburden stress. The estimates of a_{max} at liquefaction and no-liquefaction sites by various researchers are often based on a combination of these types of information, and can be expected to have smaller variances than estimates obtained from ground motion

prediction equations alone. The uncertainty in estimates of a_{max} for each case history depends on the quality of information available, but it was found that quantifying these uncertainties on a case-history specific basis was generally not justified, except for those few cases that had a strong ground motion recording directly at the site. Additional uncertainties come from variations in the duration of shaking and other ground motion characteristics which are approximately accounted for by the MSF term and in the effects of overburden stress which are approximately accounted for by the K_σ term. For this reason, the standard deviation in $\ln(CSR_{M=7.5,\sigma'=1atm})$ was set to one of two values – a relatively small value for the few sites that had strong ground motion recordings directly at the site and a relatively greater value for all other sites – and then parametric analyses were used to assess the sensitivity of the solution to these assumed values.

It is convenient to simplify the notation as follows,

$$Q = q_{c1Ncs} \tag{5.4}$$

$$S = CSR_{M=7.5,\sigma'_v=1atm} \tag{5.5}$$

$$R = CRR_{M=7.5,\sigma'_v=1atm} \tag{5.6}$$

The limit state function can be written using a total error term ε_T, to account for both the inability of $\hat{g}$ to predict liquefaction perfectly and the uncertainty in the parameters used to compute $\hat{g}$.

$$g\left(Q,S,C_o,\varepsilon_{\ln(R)}\right) = \hat{g}\left(\hat{Q},\hat{S},C_o\right) + \varepsilon_T \tag{5.7}$$

The ε_T is normally distributed with a mean value of zero, and it includes the effects of uncertainty in the parameters, which can be expressed as,

$$Q = \hat{Q} + \varepsilon_Q \tag{5.8}$$

$$\sigma_Q = COV_Q \cdot Q \tag{5.9}$$

$$\ln\left(S\right) = \ln\left(\hat{S}\right) + \varepsilon_{\ln(S)} \tag{5.10}$$

$$\ln\left(R\right) = \ln\left(\hat{R}\right) + \varepsilon_{\ln(R)} \tag{5.11}$$

The limit state function with inclusion of the uncertainties can then be written as,

$$g\left(Q,S,C_o,\varepsilon_{\ln(R)}\right) = \ln\left(R\right) - \ln\left(S\right) \tag{5.12}$$

$$g\left(Q,S,C_o,\varepsilon_{\ln(R)}\right) = \left(\frac{\hat{Q}+\varepsilon_Q}{113} + \left(\frac{\hat{Q}+\varepsilon_Q}{1000}\right)^2 - \left(\frac{\hat{Q}+\varepsilon_Q}{140}\right)^3 + \left(\frac{\hat{Q}+\varepsilon_Q}{137}\right)^4 - C_o\right) + \varepsilon_{\ln(R)} - \ln\left(\hat{S}\right) - \varepsilon_{\ln(S)} \tag{5.13}$$

This expression can be simplified by multiplying out the polynomial terms and then neglecting the higher order terms with ε_Q squared or cubed. The resulting expression is,

$$g\left(Q,S,C_o,\varepsilon_{\ln(R)}\right)=\left(\frac{\hat{Q}}{113}+\left(\frac{\hat{Q}}{1000}\right)^2-\left(\frac{\hat{Q}}{140}\right)^3+\left(\frac{\hat{Q}}{137}\right)^4-C_o\right)$$
$$+\left(\frac{1}{113}+\frac{2\hat{Q}}{1000^2}-\frac{3\hat{Q}^2}{140^3}+\frac{4\hat{Q}^3}{137^4}\right)\varepsilon_Q+\varepsilon_{\ln(R)} \tag{5.14}$$
$$-\ln\left(\hat{S}\right)-\varepsilon_{\ln(S)}$$

$$g\left(Q,S,C_o,\varepsilon_{\ln(R)}\right)=\hat{g}\left(\hat{Q},\hat{S},C_o\right)$$
$$+\left(\frac{1}{113}+\frac{2\hat{Q}}{1000^2}-\frac{3\hat{Q}^2}{140^3}+\frac{4\hat{Q}^3}{137^4}\right)\varepsilon_Q+\varepsilon_{\ln(R)}-\varepsilon_{\ln(S)} \tag{5.15}$$

The total error is thus the sum of the above three error terms as,

$$\varepsilon_T=\left(\frac{1}{113}+\frac{2\hat{Q}}{1000^2}-\frac{3\hat{Q}^2}{140^3}+\frac{4\hat{Q}^3}{137^4}\right)\varepsilon_Q+\varepsilon_{\ln(R)}-\varepsilon_{\ln(S)} \tag{5.16}$$

The standard deviation in ε_T can be expressed as,

$$\left(\sigma_T\right)^2=\left(\frac{1}{113}+\frac{2\hat{Q}}{1000^2}-\frac{3\hat{Q}^2}{140^3}+\frac{4\hat{Q}^3}{137^4}\right)^2\left(\sigma_Q\right)^2+\left(\sigma_{\ln(R)}\right)^2+\left(\sigma_{\ln(S)}\right)^2 \tag{5.17}$$

5.3. Likelihood function

The likelihood function is the product of the probabilities of the individual case history observations, assuming that the case history observations are statistically independent. For a liquefaction case ($g \le 0$), the probability of having observed liquefaction can be expressed as,

$$P\left[g\left(Q,S,C_o,\varepsilon_{\ln(R)}\right)\le 0\right]=\Phi\left[-\frac{\hat{g}\left(\hat{Q},\hat{S},C_o\right)}{\sigma_T}\right] \tag{5.18}$$

where Φ is the standard normal cumulative probability function. For example, the probability of having observed liquefaction becomes greater than 0.84 if the case history data point plots more than one σ_T above the triggering curve. In this regard, it is important to recognize that case history data points for sites without strong ground motion recordings (which are the large majority) are plotted at the $CSR_{M=7.5,\sigma'=1atm}$ value expected in the absence of liquefaction, and that this $CSR_{M=7.5,\sigma'=1atm}$ value may be significantly greater than the value which developed if liquefaction was triggered early in strong shaking. For this reason, the case history data points that fall well above the triggering curve have probabilities close to unity, and thus they have very little influence on the overall likelihood function. The same is true for the no-liquefaction cases that fall well below the triggering curve. The likelihood function can now be written as,

$$L\left(C_o,\varepsilon_{\ln(R)}\right)=\prod_{Liquefied\ sites}P\left[g\left(Q,S,C_o,\varepsilon_{\ln(R)}\right)\le 0\right]\prod_{Noniquefied\ sites}P\left[g\left(Q,S,C_o,\varepsilon_{\ln(R)}\right)>0\right] \quad (5.19)$$

$$L\left(C_o,\varepsilon_{\ln(R)}\right)=\prod_{Liquefied\ sites}\Phi\left[-\frac{\hat{g}\left(\hat{Q},\hat{S},C_o\right)}{\sigma_T}\right]\prod_{Noniquefied\ sites}\Phi\left[\frac{\hat{g}\left(\hat{Q},\hat{S},C_o\right)}{\sigma_T}\right] \quad (5.20)$$

The case history database is, however, believed to contain an uneven sampling of liquefaction and no-liquefaction case histories because researchers more often have chosen to investigate liquefaction sites. Manski and Leman (1977) suggest that the bias from an uneven choice-based sampling process can be corrected for by weighting the observations to better represent the actual population. Cetin et al. (2002) noted that this amounted to rewriting the likelihood function as,

$$L\left(C_o,\varepsilon_{\ln(R)}\right)=\prod_{Liquefied\ sites}\Phi\left[-\frac{\hat{g}\left(\hat{Q},\hat{S},C_o\right)}{\sigma_T}\right]^{w_{liquefied}}\prod_{Noniquefied\ sites}\Phi\left[\frac{\hat{g}\left(\hat{Q},\hat{S},C_o\right)}{\sigma_T}\right]^{w_{nonliquefied}} \quad (5.21)$$

where the exponents $w_{liquefied}$ and $w_{nonliquefied}$ used to weight the observations are computed as,

$$w_{liquefied}=\frac{Q_{liq,true}}{Q_{liq,sample}} \quad (5.22)$$

$$w_{nonliquefied}=\frac{1-Q_{liq,true}}{1-Q_{liq,sample}} \quad (5.23)$$

where $Q_{liq,true}$ is the true proportion of the occurrences of liquefaction in the population, and $Q_{liq,sample}$ is the proportion of occurrences of liquefaction in the sample set. Cetin et al. (2002) reported that a panel of eight experts agreed that the ratio $w_{nonliquefied}/w_{liquefied}$ should be greater than 1.0 and less than 3.0 for the SPT-based case history database, with the most common estimate being between 1.5 and 2.0. They further allowed this ratio to be a parameter in the Bayesian updating analyses, and found that a ratio of 1.5 minimized their overall model variance. Accordingly, they adopted weighting values of $w_{liquefied} = 0.8$ and $w_{nonliquefied} = 1.2$, producing the ratio $w_{nonliquefied}/w_{liquefied} = 1.5$. Moss et al. (2006) used these same weighting parameters in their application of this procedure to their CPT-based liquefaction triggering database.

The case history database likely contains a number of false negatives and false positives because the true site performance is either masked or mischaracterized. A scenario of greatest concern for false negatives is when liquefaction at depth does not produce any visible surface manifestation, such as may occur when a thick crust of non-liquefiable soil overlays a relatively thin zone of liquefaction and there is no significant slope or heavy structure to drive deformations. A design chart for such conditions was presented by Ishihara (1985) based on a number of case history observations. False positives are not expected to be as common, but it is possible that ground surface cracking or settlement could result from seismic compression of unsaturated loose soils or yielding of soft clays (e.g., bearing failures around buildings), and that such movements could be interpreted as having been caused by liquefaction of a different strata at the site. The potential exists for false positives or false negatives to produce points that fall far from the triggering correlation, which would be incorrectly treated as a highly unlikely case in the

maximum likelihood solution. The potentially strong influence of such outliers was minimized in the present analyses by limiting the probability of any one observation to be no smaller than a specified minimum value, P_{min}. Sensitivity analyses considered values of P_{min} equal to 0, 0.05, 0.075, and 0.10, as well as an alternative approach where outlier points were omitted.

5.4. Results of parameter estimation and sensitivity studies

There are six parameters that can be either estimated or left as fitting parameters in determining the maximum likelihood solution: C_o, $\sigma_{ln(R)}$, $\sigma_{ln(S)}$, COV_Q, $w_{nonliquefied}/w_{liquefied}$, and P_{min}. Cetin et al. (2002) estimated uncertainties in S for the individual case histories that were used in their Bayesian analyses, and then suggested that $\sigma_{ln(S)}$ would be about 0.2 in applications with good practices. The value of COV_Q can range from 0.20 to 0.60 in sand with a mean of about 0.38 (Kulhawy and Trautmann 1996, Phoon and Kulhawy 1999). Ground motion prediction equations have standard deviations of about 0.45-0.55 in the natural log of the peak ground acceleration (Abrahamson et al. 2008), which suggest that $\sigma_{ln(S)}$ could be around 0.45-0.55 if it was estimated solely on the basis of a ground motion prediction equation; smaller values of $\sigma_{ln(S)}$ would be expected for most case histories given the additional information provided by strong ground motion recordings and site-specific observations (e.g., eye witness reports, damage to structures, disruption of nonstructural contents). As previously discussed, the data available for most sites in the liquefaction database are inadequate to quantify the site-specific uncertainty in Q or S, and thus the approach adopted in this study was to solve for C_o and $\sigma_{ln(R)}$ using a range of estimated values for $\sigma_{ln(S)}$, COV_Q, $w_{nonliquefied}/w_{liquefied}$, and P_{min}.

Clean sand case histories

Maximum likelihood solutions for C_o and $\sigma_{ln(R)}$ using only the clean sand (FC ≤ 5%) case histories are listed in Tables 5.1 and 5.2 for six cases with different assumptions regarding the values for $\sigma_{ln(S)}$, COV_Q, $w_{nonliquefied}/w_{liquefied}$, and P_{min}. The three cases listed in Table 5.1 involve varying the values for $\sigma_{ln(S)}$ from 0.20 to 0.10 and COV_Q from 0.20 to 0.10 while keeping $w_{nonliquefied}/w_{liquefied} = 1.5$ and $P_{min} = 0.0$. The three cases listed in Table 5.2 are the same as for Table 5.1, except that $P_{min} = 0.05$. The value of COV_Q list in these tables is for cases where the FC is based on laboratory test data. Recall that the COV_Q was increased by 50% for sites with fines characteristics determined by correlation rather than laboratory test data and that a reduced value for $\sigma_{ln(S)}$ of 0.05 was used for the sites that had strong ground motion recordings directly at the site. The reduced $\sigma_{ln(S)}$ of 0.05 for sites with strong ground motion recordings allows for uncertainties associated with the duration of shaking (as represented by the MSF), the overburden stress effect (represented by the K_σ factor), and the variation of shear stresses with depth (as represented by the r_d factor) even when the peak ground surface acceleration is known.

Curves for probabilities of liquefaction [P_L] equal to 15%, 50%, and 85%, with inclusion of the estimation errors in $CSR_{M=7.5,\sigma'=1atm}$ and q_{c1Ncs}, for the cases listed in Tables 5.1 and 5.2 are plotted together with the clean sand case history data in Figures 5.1 ($P_{min} = 0.0$) and 5.2 ($P_{min} = 0.05$), respectively. The solutions for the three cases with $P_{min} = 0.0$ were all similar, with the median curves (i.e., $P_L = 50\%$) being almost identical (with $C_o = 2.51$-2.52) and the total uncertainty terms (e.g., positions of the $P_L = 15\%$ and 85% curves) and model uncertainty terms (e.g., $\sigma_{ln(R)} = 0.42$-0.44) were also similar. The solutions for the three cases with $P_{min} = 0.05$ produced a slightly lower median curve (i.e., $C_o = 2.55$-2.56) than was obtained for the first three cases (i.e., $C_o = 2.55$-2.56 produces about 4% smaller R values than $C_o = 2.51$-2.52) and much smaller estimates for the total uncertainty terms (e.g., $P_L = 15\%$ and 85% curves are located closer together) and model uncertainty terms(i.e., $\sigma_{ln(R)}$ is reduced to 0.0-0.13). Setting P_{min} equal to 0.05 rather than to 0.0 reduced the influence of the two or three no-liquefaction data points located well above the

expected triggering correlation (Figure 5.1 or 5.2), which is why the most likely triggering curve shifted down slightly and the most likely uncertainty terms were greatly reduced.

Table 5.1. Effect of $\sigma_{ln(S)}$ and COV_Q on parameter estimations for clean sand (FC ≤ 5%) case histories with P_{min} = 0.0

Parameters	Case 1a	Case 2a	Case 3a
$\sigma_{ln(S)}$	0.20	0.15	0.10
COV_Q	0.20	0.15	0.10
$w_{nonliquefied}/w_{liquefied}$	1.5	1.5	1.5
P_{min}	0.0	0.0	0.0
C_o	2.52	2.51	2.52
$\sigma_{ln(R)}$	0.44	0.42	0.44

Table 5.2. Effect of $\sigma_{ln(S)}$ and COV_Q on parameter estimations for clean sand (FC ≤ 5%) case histories with P_{min} = 0.05

Parameters	Case 1b	Case 2b	Case 3b
$\sigma_{ln(S)}$	0.20	0.15	0.10
COV_Q	0.20	0.15	0.10
$w_{nonliquefied}/w_{liquefied}$	1.5	1.5	1.5
P_{min}	0.05	0.05	0.05
C_o	2.55	2.55	2.56
$\sigma_{ln(R)}$	0.0	0.0	0.13

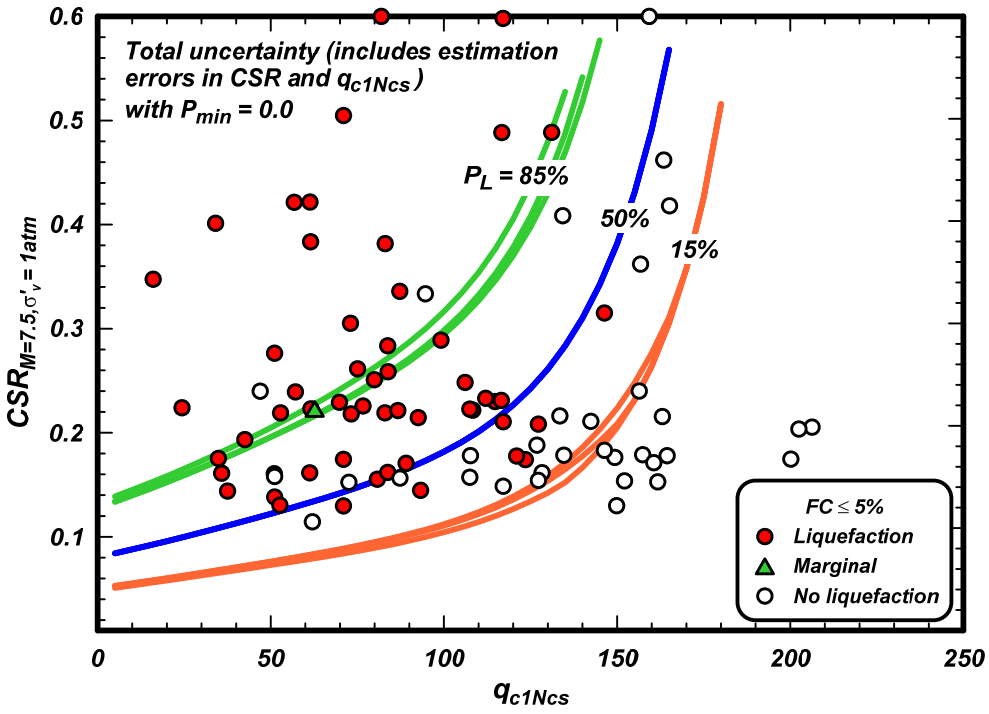

Figure 5.1. $CRR_{M=7.5,\sigma'v=1atm}$ versus q_{c1Ncs} for P_L = 15, 50, and 85% in clean sands with inclusion of estimation errors in $CSR_{M=7.5,\sigma'v=1atm}$ and q_{c1Ncs} and using P_{min} = 0.0. Solutions for cases listed in Table 5.1

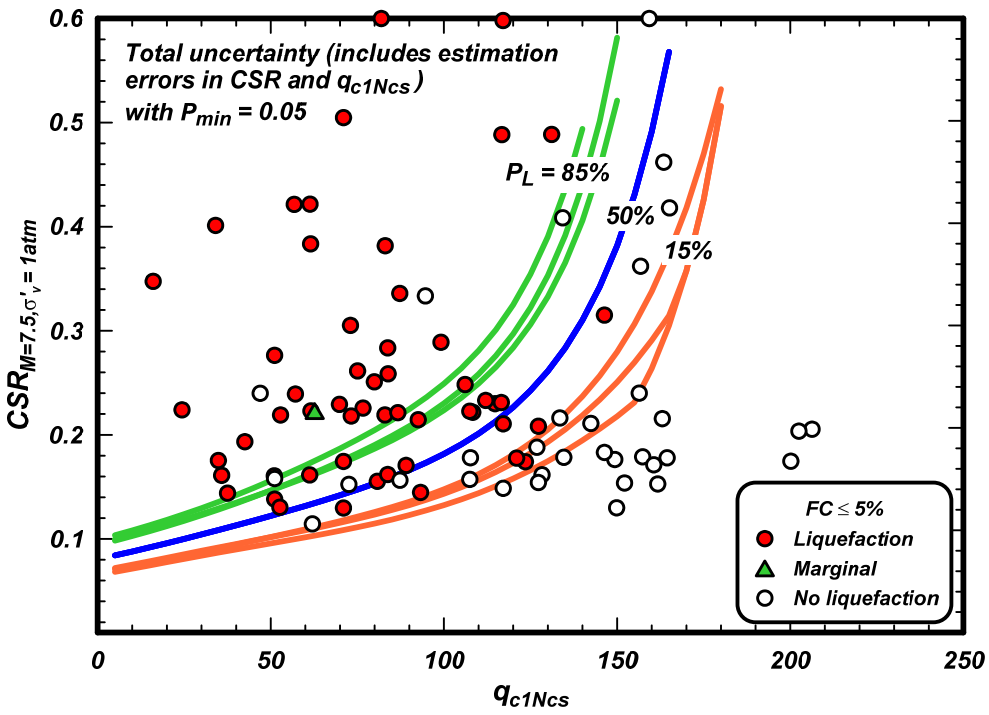

Figure 5.2. $CRR_{M=7.5,\sigma'v=1atm}$ versus q_{c1Ncs} for P_L = 15, 50, and 85% in clean sands with inclusion of estimation errors in $CSR_{M=7.5,\sigma'v=1atm}$ and q_{c1Ncs} and using P_{min} = 0.05. Solutions for cases listed in Table 5.2

Case histories for all FC based on laboratory test data

Maximum likelihood solutions for C_o and $\sigma_{ln(R)}$ using all the case histories (any FC) where the FC is based on laboratory test data are listed in Tables 5.3 and 5.4 for six cases with different assumptions regarding the values for $\sigma_{ln(S)}$, COV_Q, $w_{nonliquefied}/w_{liquefied}$, and P_{min}. The three cases listed in Table 5.3 involve varying the values for $\sigma_{ln(S)}$ from 0.20 to 0.10 and COV_Q from 0.20 to 0.10 while keeping $w_{nonliquefied}/w_{liquefied}$ = 1.5 and P_{min} = 0.05. The three cases listed in Table 5.4 are the same as for Table 5.3, except that P_{min} = 0.075.

The variation in P_{min} had a larger effect on the maximum likelihood solutions than did the other parameter variations, as was observed for the clean sand case histories. For P_{min} = 0.05, the median triggering curves were about equal (C_o = 2.59-2.60) and the model uncertainties were similar ($\sigma_{ln(R)}$ = 0.29-0.37). Increasing P_{min} to 0.075 shifted the median triggering curves downward by about 6% (C_o = 2.65-2.66) and strongly reduced the model uncertainty terms ($\sigma_{ln(R)}$ = 0.0-0.21).

Curves for probabilities of liquefaction [P_L] equal to 15%, 50%, and 85% for cases 5a (P_{min} = 0.05) and 5b (P_{min} = 0.075) are plotted together with the case history data: (1) in Figure 5.3 with the total uncertainty, which means with inclusion of the estimation errors in $CSR_{M=7.5,\sigma'=1atm}$ and q_{c1Ncs}, and (2) in Figure 5.4 with the model uncertainty alone, which means excluding the estimation errors in $CSR_{M=7.5,\sigma'=1atm}$ and q_{c1Ncs}. In both figures, the curves for P_{min} = 0.075 are located closer together because the larger P_{min} value reduced the most likely values for both model uncertainty and total uncertainty. These figures also show that there are more no-liquefaction cases above the P_L = 85% curve than liquefaction cases below the P_L = 15% curve. To the extent that these few no-liquefaction cases lying above the P_L = 85% curve may

include some false negatives, the larger P_{min} value serves to reduce their potentially adverse influence on the most likely solution.

Table 5.3. Effect of $\sigma_{ln(S)}$ and COV_Q on parameter estimations for all FC based on laboratory test data with P_{min} = 0.05

Parameters	Case 4a	Case 5a	Case 6a
$\sigma_{ln(S)}$	0.20	0.15	0.10
COV_Q	0.20	0.15	0.10
$w_{nonliquefied}/w_{liquefied}$	1.5	1.5	1.5
P_{min}	0.05	0.05	0.05
C_o	2.59	2.60	2.60
$\sigma_{ln(R)}$	0.29	0.34	0.37

Table 5.4. Effect of $\sigma_{ln(S)}$ and COV_Q on parameter estimations for all FC based on laboratory test data with P_{min} = 0.075

Parameters	Case 4b	Case 5b	Case 6b
$\sigma_{ln(S)}$	0.20	0.15	0.10
COV_Q	0.20	0.15	0.10
$w_{nonliquefied}/w_{liquefied}$	1.5	1.5	1.5
P_{min}	0.075	0.075	0.075
C_o	2.65	2.65	2.66
$\sigma_{ln(R)}$	0.0	0.14	0.21

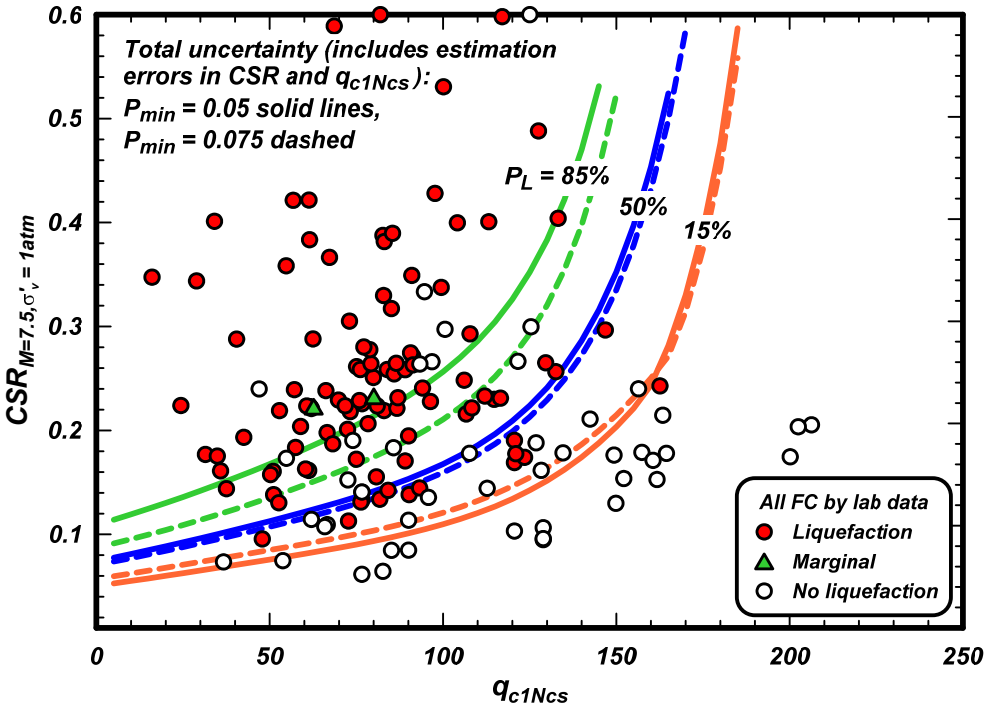

Figure 5.3. $CRR_{M=7.5,\sigma'v=1atm}$ versus q_{c1Ncs} for P_L = 15, 50, and 85% for all sands with FC based on laboratory test data, with inclusion of estimation errors in $CSR_{M=7.5,\sigma'v=1atm}$ and q_{c1Ncs}, and using P_{min} = 0.05 or 0.075. Solutions for cases 5a and 5b from Tables 5.3 and 5.4

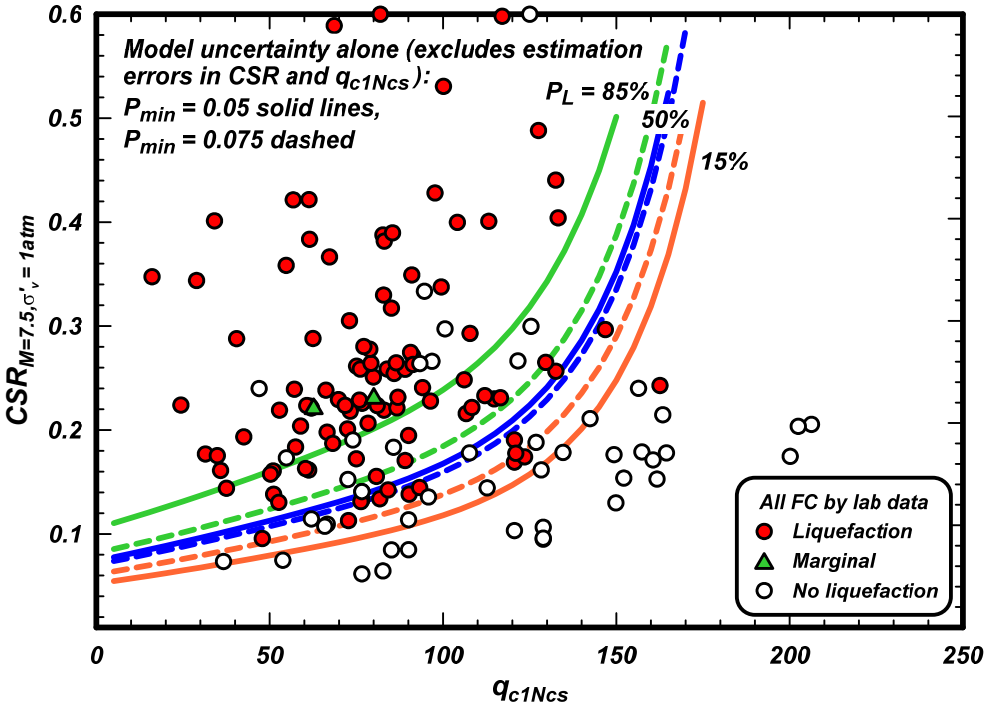

Figure 5.4. $CRR_{M=7.5,\sigma'v=1atm}$ versus q_{c1Ncs} for P_L = 15, 50, and 85% for all sands with FC based on laboratory test data, with model uncertainty alone (excluding estimation errors in $CSR_{M=7.5,\sigma'v=1atm}$ and q_{c1Ncs}), and using P_{min} = 0.05 or 0.075. Solutions for cases 5a and 5b from Tables 5.3 and 5.4

The differences in the solutions for the total uncertainty (σ_T) are illustrated in Figure 5.5 showing results for cases 4a and 5a (P_{min} = 0.05) and cases 4b and 5b (P_{min} = 0.075). Cases 4a and 4b have similar total uncertainties despite their differences in the assumed values for $\sigma_{ln(S)}$ and COV_Q, and likewise cases 5a and 5b have similar total uncertainties. The total uncertainty for cases 5a and 5b are, however, much lower than for cases 4a and 4b because of the strong effects that P_{min} has on reducing the influence of the few no-liquefaction case history points located above the P_L = 85% curves.

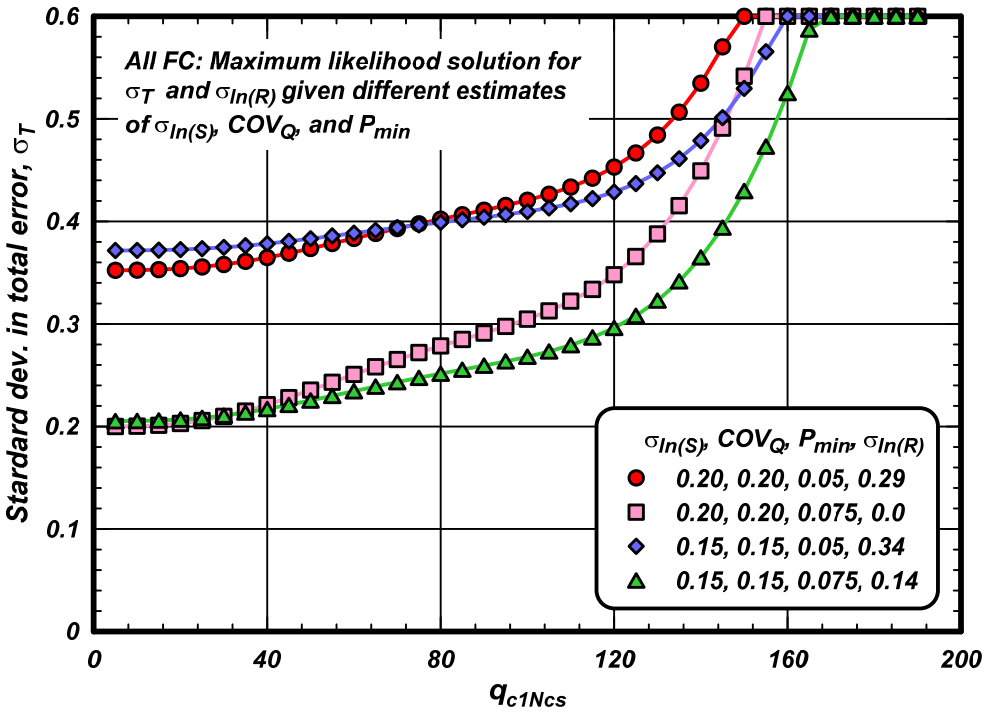

Figure 5.5. Standard deviation in the total error term (σ_T) and CRR relationship ($\sigma_{ln(R)}$) from the maximum likelihood solution for different estimates of $\sigma_{ln(S)}$ and COV_Q in any FC sand. Solutions for cases 4a and 5a (Table 5.3) and 4b and 5b (Table 5.4)

Case histories for all FC based on laboratory test data or I_c correlation

Maximum likelihood solutions for C_o and $\sigma_{ln(R)}$ using all the case histories (any FC – by laboratory data or correlation with I_c) are listed in Table 5.5 for three cases with values for $\sigma_{ln(S)}$ from 0.20 to 0.10 and COV_Q from 0.20 to 0.10 while keeping $w_{nonliquefied}/w_{liquefied} = 1.5$ and $P_{min} = 0.075$. The three cases (7a – 9a) listed in Table 5.5 are the same as for Table 5.4, except that the analyses now include case histories where the FC was determined by correlation to I_c as well.

Table 5.5. Effect of $\sigma_{ln(S)}$ and COV_Q on parameter estimations for all FC with $P_{min} = 0.075$

Parameters	Case 7a	Case 8a	Case 9a
$\sigma_{ln(S)}$	0.20	0.15	0.10
COV_Q	0.20	0.15	0.10
$w_{nonliquefied}/w_{liquefied}$	1.5	1.5	1.5
P_{min}	0.075	0.075	0.075
C_o	2.67	2.68	2.68
$\sigma_{ln(R)}$	0.05	0.18	0.24

Curves for probabilities of liquefaction [P_L] equal to 15%, 50%, and 85% for cases 7a-9a are plotted together with the case history data: (1) in Figure 5.6 with the total uncertainty, which means with inclusion of the estimation errors in $CSR_{M=7.5,\sigma'=1atm}$ and q_{c1Ncs}, and (2) in Figure 5.7 with the model uncertainty alone, which means excluding the estimation errors in $CSR_{M=7.5,\sigma'=1atm}$ and q_{c1Ncs}. The curves based on total uncertainty (Figure 5.6) are very similar despite the assumed values for $\sigma_{ln(S)}$ and COV_Q ranging from 0.20 to 0.10. The total uncertainties for these cases were similar, as shown in Figure 5.8, because decreasing the assumed values for $\sigma_{ln(S)}$ and COV_Q was offset by increases in the most likely values for $\sigma_{ln(R)}$; e.g., decreasing $\sigma_{ln(S)}$ and COV_Q from 0.2 to 0.1 caused $\sigma_{ln(R)}$ to increase from 0.05 to 0.24 as listed in Table 5.5. At the same time, the curves for P_L = 15% and 85% based on model uncertainty alone (Figure 5.7) are significantly affected by the differences in the assumed values for $\sigma_{ln(S)}$ and COV_Q. These results illustrate how the maximum likelihood analysis of the case history data provides insight on the total uncertainty, but does not provide clear guidance on the appropriate partitioning of that uncertainty into the components of Q, S, and R.

The effect of including the case histories with FC determined by correlation with I_c can be evaluated by comparing the solution results in Table 5.5 with those in Table 5.4. Including the case histories with FC determined by correlation with Ic caused the median triggering curve to shift downward by about 2% (Co = 2.67-2.68 versus 2.65-2.66) while slightly increasing the estimated model uncertainty ($\sigma_{ln(R)}$ = 0.05-0.24 versus 0.0-0.21).

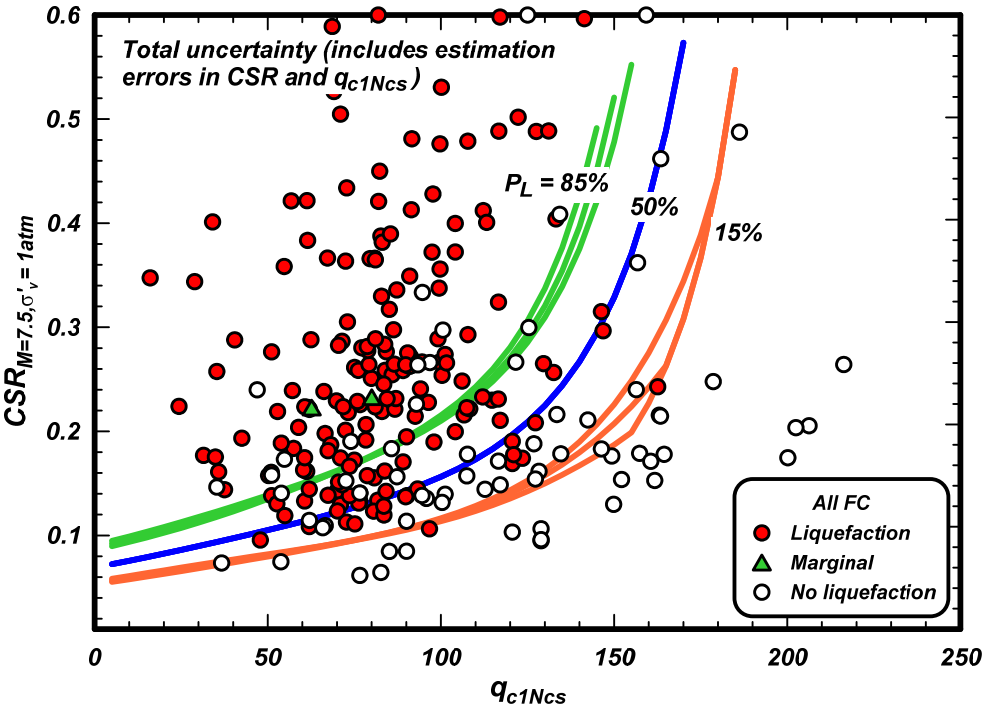

Figure 5.6. $CRR_{M=7.5,\sigma'v=1atm}$ versus q_{c1Ncs} for P_L = 15, 50, and 85% for all sands with inclusion of estimation errors in $CSR_{M=7.5,\sigma'v=1atm}$ and q_{c1Ncs}. Solutions for cases 7a – 9a from Table 5.5

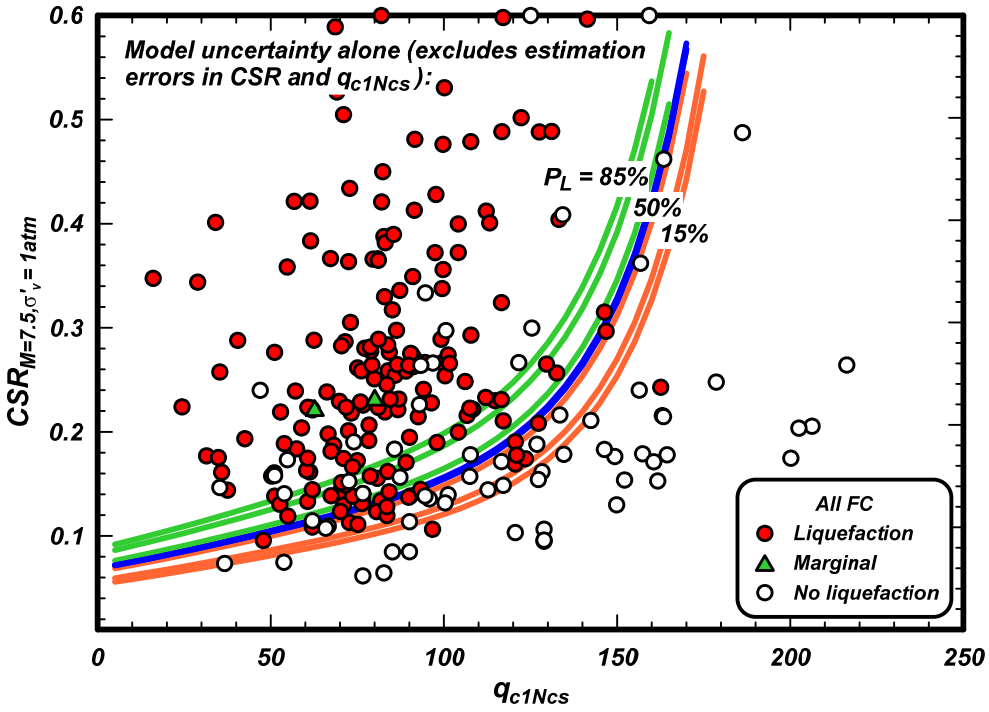

Figure 5.7. $CRR_{M=7.5,\sigma'v=1atm}$ versus q_{c1Ncs} for P_L = 15, 50, and 85% for all sands with model uncertainty alone (excluding estimation errors in $CSR_{M=7.5,\sigma'v=1atm}$ and q_{c1Ncs}). Solutions for cases 7a – 9a Table 5.5

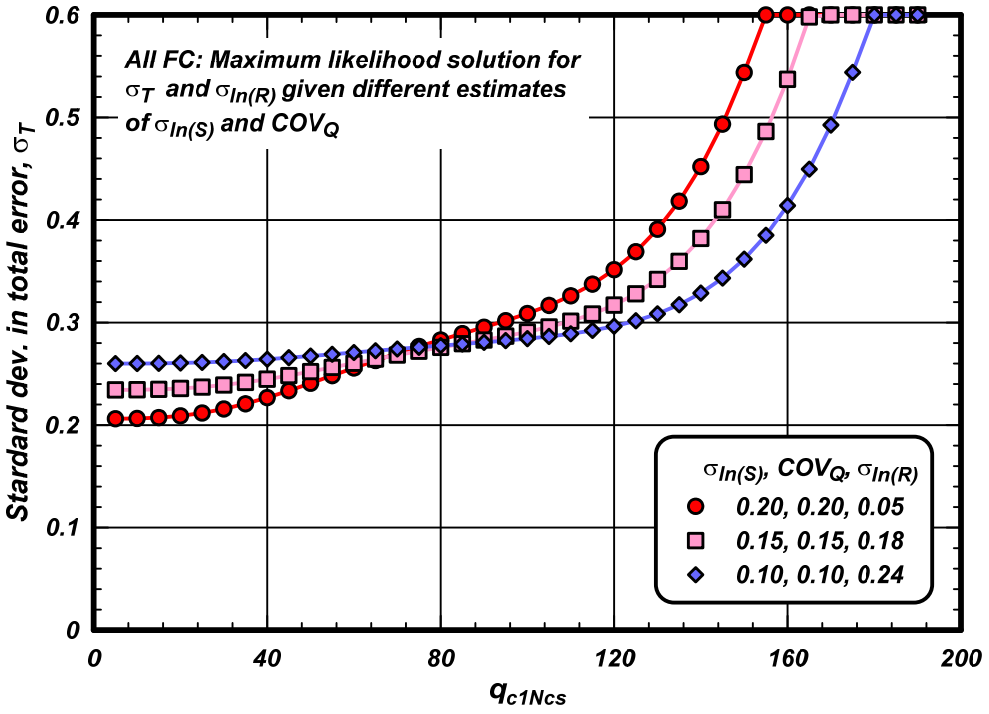

Figure 5.8. Standard deviation in the total error term (σ_T) and CRR relationship ($\sigma_{ln(R)}$) from the maximum likelihood solution for different estimates of $\sigma_{ln(S)}$ and COV_Q in any FC sand. Solution for cases 7a – 9a in Table 5.5

Case histories for σ'_v greater than 40 kPa

Maximum likelihood solutions for C_o and $\sigma_{ln(R)}$ using all the case histories (any FC) with σ'_v greater than 40 kPa are listed in Table 5.6 for three cases involving various assumptions for the values of $\sigma_{ln(S)}$, COV_Q, $w_{nonliquefied}/w_{liquefied}$, and P_{min}. The three cases (10a – 12a) listed in Table 5.6 are the same as for Table 5.5, except that the analyses now exclude case histories where the σ'_v was less than 40 kPa. The reason for examining the effect of excluding case histories involving very shallow depths (e.g., less than about 2 m) is that the K_σ and C_N relationships are not as well defined at these low stresses and upper limits on their values have been imposed based on judgment and other considerations.

Table 5.6. Effect of $\sigma_{ln(S)}$ and COV_Q on parameter estimations for all FC with σ'_v greater than 40 kPa

Parameters	Case 10a	Case 11a	Case 12a
$\sigma_{ln(S)}$	0.20	0.15	0.10
COV_Q	0.20	0.15	0.10
$w_{nonliquefied}/w_{liquefied}$	1.5	1.5	1.5
P_{min}	0.075	0.075	0.075
C_o	2.55	2.55	2.55
$\sigma_{ln(R)}$	0.30	0.33	0.36

The solutions for the case histories with σ'_v greater than 40 kPa (cases 10a-12a) indicate a median triggering curve that is about 12-13% higher than obtained using all the case history data (cases 7a-9a) and a larger model uncertainty ($\sigma_{ln(R)}$ of 0.30-0.26 versus 0.05-0.24). In examining these differences, it is useful to consider the position of the P_L = 15% curves for these two sets of analysis cases. The P_L = 15% curves are located approximately one $\sigma_{ln(R)}$ below the median curves, so their relative positions can be expressed in terms of the sum of the C_o and $\sigma_{ln(R)}$ values. For example, the P_L = 15% curve for case 11a (data for σ'_v greater than 40 kPa) is actually about 2% lower than for case 8a (with all data); i.e., 2.55+0.33 = 2.88 versus 2.68+0.18 = 2.86. Thus, excluding the shallower case histories had very little effect on the P_L = 15% curve (about a 2% shift downward) but a relatively large effect on the P_L = 85% curve (about a 28% shift upward), with the effects attributed to a complex combination of factors such as the changes in the relative number of outliers, numbers of case histories, and additional uncertainties in the analysis framework.

Effect of other solution parameters

The potential effects of false negatives and false positives in the case history database was further examined using the alternative approach of excluding any case histories that fall more than 1.5 standard deviations from the expected triggering curve; i.e., no-liquefaction cases falling more than 1.5 σ_T above the P_L = 50% curve and any liquefaction cases falling more than 1.5 σ_T below the P_L = 50% curve. Using all case histories (any FC), this criteria only affected one or two liquefaction cases compared to several no-liquefaction cases (e.g., Figure 5.7). Maximum likelihood solutions for C_o and $\sigma_{ln(R)}$ using all the case histories (any FC) with this alternative approach of excluding outlier points are listed in Table 5.7. These are the same three cases listed in Table 5.5 which was based on imposing a P_{min} = 0.075 on such outliers. Excluding outliers by this approach cause the most likely median triggering curve to shift downward by 8-16% (C_o of 2.76 -2.83 versus 2.67-2.68) and significantly reduced the estimated model uncertainty ($\sigma_{ln(R)}$ of 0.0-0.04 versus 0.05-0.24), but had a relatively neutral effect on the position of the P_L = 15% curve (i.e., sum of $C_o + \sigma_{ln(R)}$ equal to 2.76-2.85 versus 2.72-2.96).

Table 5.7. Effect of $\sigma_{ln(S)}$ and COV_Q on parameter estimations for all FC and excluding points more than 1.5 standard deviations from expected triggering curve [P < 0.067%]

Parameters	Case 7b	Case 8b	Case 9b
$\sigma_{ln(S)}$	0.20	0.15	0.10
COV_Q	0.20	0.15	0.10
$w_{nonliquefied}/w_{liquefied}$	1.5	1.5	1.5
P_{min}	n/a	n/a	n/a
C_o	2.83	2.78	2.76
$\sigma_{ln(R)}$	0.02	0.04	0.0

The effect of varying the weighting ratio $w_{nonliquefied}/w_{liquefied}$ from 1.0 to 2.0 while keeping $\sigma_{ln(S)}$, COV_Q, and P_{min} constant was evaluated using the full case history dataset. The solutions for one set of assumptions are summarized in Table 5.8. The smaller weighting ratio caused the solution for the most likely triggering curve to shift downward by about 10% (i.e., C_o = 2.77 versus 2.67) and the most likely value for $\sigma_{ln(R)}$ to decrease (i.e., $\sigma_{ln(R)}$ reduces to 0.0 from 0.05), while the greater weighting ratio causes the most likely triggering curve to shift upward by about 11% (i.e., C_o = 2.56 versus to 2.67) and the most likely value for $\sigma_{ln(R)}$ to increase (i.e., $\sigma_{ln(R)}$ increases to 0.32 from 0.05).

Table 5.8. Effect of varying the weighting ratio for the full case history dataset (any FC)

Parameters	Case 7c	Case 7a	Case 7e
$\sigma_{ln(S)}$	0.20	0.20	0.20
COV_Q	0.20	0.20	0.20
$w_{nonliquefied}/w_{liquefied}$	1.0	1.5	2.0
P_{min}	0.075	0.075	0.075
C_o	2.77	2.67	2.56
$\sigma_{ln(R)}$	0.0	0.05	0.32

The effect of limiting the total uncertainty σ_T at high q_{c1Ncs} values (Figures 5.5 and 5.8) was also investigated parametrically. The previous solutions limited σ_T to a maximum value of 0.60. Solutions were obtained with no upper limit imposed and with a lower limit of 0.50. These changes only affect the influence of the data points near the upper limit of the triggering curve. The effects of these changes were smaller than those observed for the above variations in weighting ratio or P_{min}. For example, repeating case 7a with a lower limit on σ_T of 0.5 caused no change in C_o or $\sigma_{ln(R)}$ and with no lower limit on σ_T caused C_o to increase from 2.67 to 2.68 and $\sigma_{ln(R)}$ to increase from 0.05 to 0.06.

5.5. Recommended relationships

Selecting the most appropriate values for C_o and $\sigma_{ln(R)}$ from the results of these maximum likelihood solutions involves subjective evaluation of the most appropriate partitioning of the total uncertainty in the liquefaction case history database. This evaluation must also consider the limitations of the statistical models and case history database, including uncertainties that are not explicitly accounted for. Of the

various analysis cases considered, the cases with $\sigma_{ln(S)} = 0.20$, $COV_Q = 0.20$, and $P_{min} = 0.05$-0.075 are considered more realistic than the other cases; e.g., $\sigma_{ln(S)} = 0.10$, $COV_Q = 0.10$ and $P_{min} = 0.0$ are lower than would be reasonably estimated based on established literature. The solutions with these larger $\sigma_{ln(S)}$, COV_Q, and P_{min} terms, however, often result in estimated model uncertainties closer to zero than seem reasonable. This apparent discrepancy arises from limitations in the case history database, the analysis method, and the ability to define parameter uncertainties accurately. Taking these factors into consideration, the results presented in the preceding sections are considered reasonable bounds of different interpretations, from which values of $C_o = 2.60$ and $\sigma_{ln(R)} = 0.20$ are recommended as reasonable for use in practice.

The liquefaction triggering correlation derived from the maximum likelihood solution can then be expressed as,

$$CRR_{M=7.5,\sigma'_v=1atm} = \exp\left(\frac{q_{c1Ncs}}{113} + \left(\frac{q_{c1Ncs}}{1000}\right)^2 - \left(\frac{q_{c1Ncs}}{140}\right)^3 + \left(\frac{q_{c1Ncs}}{137}\right)^4 - 2.60 + \varepsilon_{\ln(R)} \right) \tag{5.24}$$

where $\varepsilon_{ln(R)}$ is normally distributed with a mean of 0.0 and a standard deviation of $\sigma_{ln(R)} = 0.20$. This expression can also be written as,

$$CRR_{M=7.5,\sigma'_v=1atm} = \exp\left(\frac{q_{c1Ncs}}{113} + \left(\frac{q_{c1Ncs}}{1000}\right)^2 - \left(\frac{q_{c1Ncs}}{140}\right)^3 + \left(\frac{q_{c1Ncs}}{137}\right)^4 - 2.60 + \sigma_{\ln(R)} \cdot \Phi^{-1}(P_L) \right) \tag{5.25}$$

where Φ^{-1} is the inverse of the standard cumulative normal distribution, and P_L is the probability of liquefaction. Alternatively, the conditional probability of liquefaction for known values of $CSR_{M=7.5,\sigma'=1atm}$ and q_{c1Ncs} can be computed as,

$$P_L\left(q_{c1Ncs}, CSR_{M=7.5,\sigma'_v=1atm}\right) = \Phi\left[-\frac{\frac{q_{c1Ncs}}{113} + \left(\frac{q_{c1Ncs}}{1000}\right)^2 - \left(\frac{q_{c1Ncs}}{140}\right)^3 + \left(\frac{q_{c1Ncs}}{137}\right)^4 - 2.60 - \ln\left(CSR_{M=7.5,\sigma'_v=1atm}\right)}{\sigma_{\ln(R)}} \right] \tag{5.26}$$

The recommended triggering curves for probabilities of liquefaction [P_L] equal to 15%, 50%, and 85% with model uncertainty alone [i.e., conditional on known values of $CSR_{M=7.5,\sigma'=1atm}$ and q_{c1Ncs}] are plotted together with the clean sand (FC ≤ 5%) case history data in Figure 5.9a and the full case history database in Figure 5.9b. The above probabilistic triggering relationship (equation 5.24) is equal to the deterministic triggering correlation in Section 4 when $\varepsilon_{ln(R)} = -0.20$. The deterministic relationship is therefore 1 standard deviation below the expected triggering curve and accordingly corresponds to a probability of liquefaction of about 16%.

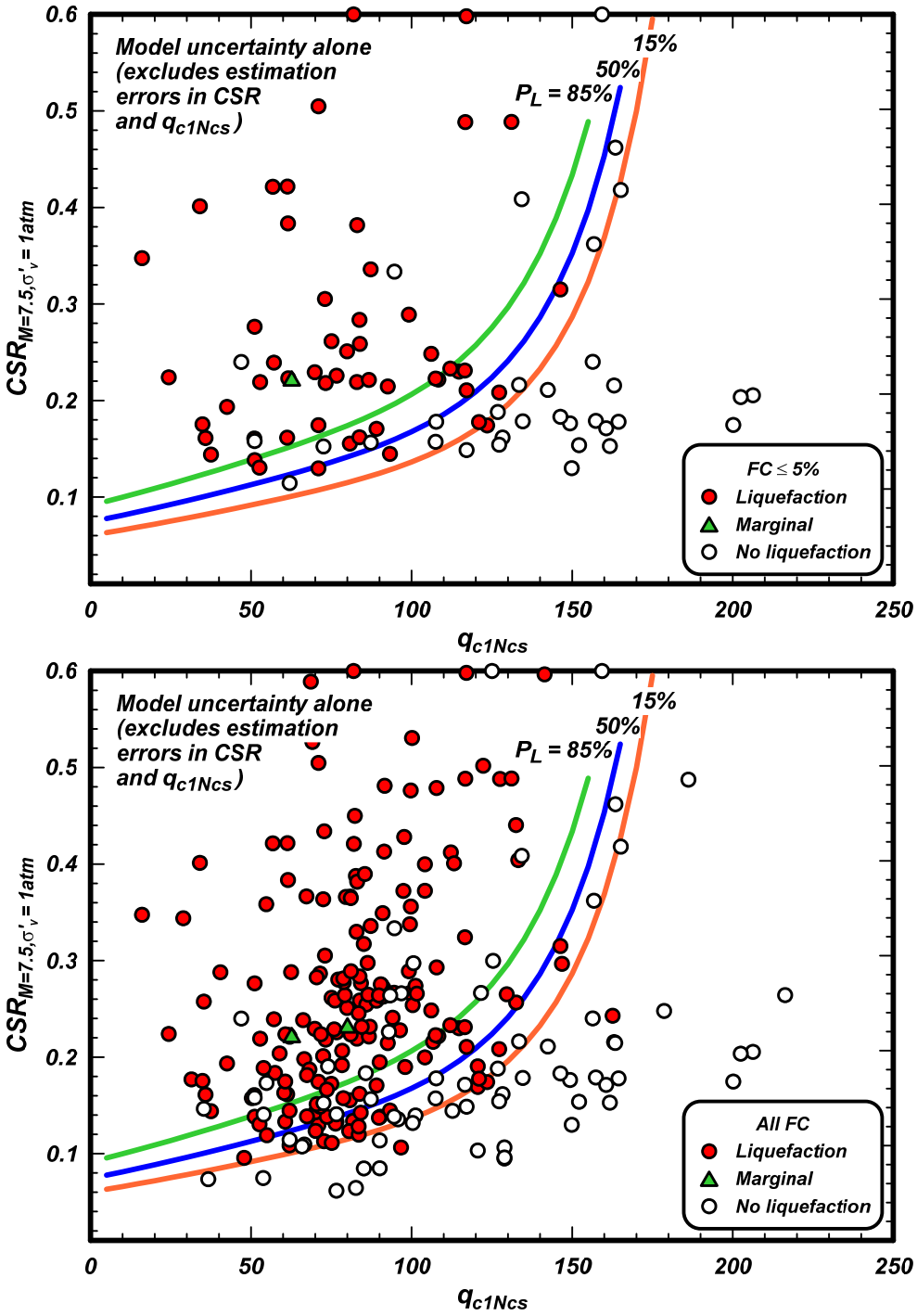

Figure 5.9. Curves of $CRR_{M=7.5,\sigma'v=1atm}$ versus q_{c1Ncs} for probabilities of liquefaction of 15%, 50%, and 85%: (a) clean sands, (b) all sands

The probabilistic triggering relationship expressed in Equations 5.24-5.26 must be recognized as being conditional on known values for $CSR_{M=7.5,\sigma'=1atm}$ and q_{c1Ncs} values; i.e., these equations only include the model uncertainty. To assess the probability of liquefaction in a liquefaction hazard evaluation, the conditional probability of liquefaction provided by these equations needs to be combined with the probabilities of the $CSR_{M=7.5,\sigma'=1atm}$ and q_{c1Ncs} values; i.e., the parameter uncertainties. In most situations, the uncertainties in estimating the latter parameters are much greater than the uncertainty in the liquefaction triggering model. For this reason, the formal treatment of uncertainties in the seismic hazard analysis and a detailed site characterization effort are generally more important to a liquefaction evaluation analysis than the uncertainty in the liquefaction triggering model.

For example, a probabilistic liquefaction hazard analysis can be structured so that it sequentially branches through a range of seismic hazards (which would account for the majority of the uncertainty in the $CSR_{M=7.5,\sigma'=1atm}$ values) and a range of site characterizations (which should account for the majority of the uncertainty in the q_{c1Ncs} values) before it gets to the liquefaction triggering analysis. In that scenario, it may be reasonable to only include model uncertainty in the liquefaction triggering analysis because the parameter uncertainties were already accounted for in the previous branches of the analysis.

5.6. Summary

A probabilistic version of the CPT-based liquefaction triggering correlation was developed using the updated case history database, the revised MSF relationship, and a maximum likelihood approach. Measurement and estimation uncertainties in CSR and q_{c1Ncs}, the effects of the choice-based sampling bias in the case history database, and the effects of false positives and false negatives in the case history database are accounted for. The results of sensitivity analyses showed that the position of the most likely triggering curve was well constrained by the data and that the magnitude of the total error term was also reasonably constrained. The most likely value for the standard deviation of the error term in the triggering correlation was, however, found to be dependent on the uncertainties assigned to CSR and q_{c1Ncs}. Despite this and other limitations, the results of the sensitivity study appear to provide reasonable bounds on the effects of different interpretations on the positions of the triggering curves for various probabilities of liquefaction. The probabilistic relationship for liquefaction triggering proposed herein is considered a reasonable approximation in view of these various findings.

The deterministic liquefaction triggering correlation presented in Section 4 corresponds to a probability of liquefaction of 16% considering model uncertainty alone.

A full probabilistic liquefaction hazard analysis will need to consider the uncertainties in the seismic hazard, the site characterization, and the liquefaction triggering model. The uncertainty in the liquefaction triggering model is much smaller than the uncertainty in the seismic hazard, and will often also be smaller than the uncertainty in the site characterization. For this reason, the seismic hazard analysis and the site characterization efforts are often the most important components of any probabilistic assessment of liquefaction hazards.

6. UPDATE AND EXAMINATION OF SPT-BASED DATABASE AND PROCEDURE

6.1. Introduction

The effect of the revised MSF relationship (Section 2.4 and Appendix A) on the Idriss-Boulanger (2008) SPT-based liquefaction triggering correlations is briefly examined in this section. The purpose of this examination is to evaluate how the revised MSF, as implemented in the examination of the CPT-based case histories, affects the distribution of the SPT-based case history data relative to the triggering correlation.

The following sections describe: (1) an update to the SPT-based case history database, (2) the distributions of the case history data processed using the revised MSF relationship and binned into varying ranges of fines content, earthquake magnitude, and overburden stress, and (3) the findings of this examination.

6.2 Update to SPT-based case history database

The SPT-based case history database examined herein is the database from Idriss and Boulanger (2010) with the following changes and additions.

Two no-liquefaction cases were removed from the database because the field documentation on their performance was found to be insufficient to warrant their inclusion in the database (see discussion by Youd et al. 2013 and closure by Boulanger et al. 2013,). The two cases were:

- 1979 Imperial Valley earthquake, Wildlife B site
- 1987 Superstition Hills earthquake, McKim Ranch A site

An additional 24 cases from the 1999 Kocaeli and 1999 Chi-Chi earthquakes were compiled by D. W. Wilson and the authors (2013, personal communication) and added to the database. These case histories are listed in Table 6.1.

The tables in Idriss and Boulanger (2010) and Boulanger et al. (2012) had typographical errors in the computed CSR values for 10 cases. The actual CSR values, as contained in the original database, can be computed using the published input parameters and equations. The affected cases were:

- 1944 M=8.1 Tohnankai earthquake, Ienaga site
- 1977 M=7.4 Argentina earthquake, San Juan B-3
- 1978 M=6.5 Miyagiken-Oki earthquake, Nakamura Dyke N-4
- 1978 M=7.7 Miyagiken-Oki earthquake , Nakamura Dyke N-4
- 1981 M=5.9 Westmorland earthquake, Wildlife B
- 1983 M=7.7 Nihonkai-Chubu earthquake, Takeda Elementary School
- 1989 M=6.9 Loma Prieta earthquake, Miller Farm CMF3
- 1994 M=6.7 Northridge earthquake, Balboa Blvd. Unit C
- 1994 M=6.7 Northridge earthquake, Potrero Canyon C1
- 1994 M=6.7 Northridge earthquake, Wynne Ave. Unit C1

The authors appreciate the efforts of K. Mengyun (2013, personal communication) in bringing these typographic errors to our attention.

Table 6.1. Additional case histories (Wilson, Boulanger, and Idriss 2013, personal communication)

Earthquake	Site	Mag. (M)	a_{max} (g)	Liq?	Avg depth (m)	Depth to GWT (m)	σ_{vc} (kPa)	σ'_{vc} (kPa)	$(N_m)_{aver}$	$(N_1)_{60}$	C_B	C_E	C_N	C_R	C_S	FC (%)	$(N_1)_{60,cs}$	r_d	K_σ	MSF	CSR	CSR for M=7.5, σ=1	Primary source of data
1999 M=7.5 Kocaeli - Aug 17	Building C1 & C2	7.51	0.4	Yes	4.0	1.5	71	46	7.0	11.3	1	1.12	1.45	1	1	28	16.6	0.97	1.09	1.00	0.387	0.355	Bray et al. (2004), PEER (2000a)
1999 M=7.5 Kocaeli - Aug 17	Building C3	7.51	0.4	No	5.1	1.5	91	56	14.0	19.0	1	1.07	1.27	1	1	67	24.5	0.96	1.09	1.00	0.407	0.373	Bray et al. (2004), PEER (2000a)
1999 M=7.5 Kocaeli - Aug 17	Site B, Building B1	7.5	0.4	Yes	2.8	1.8	51	41	3.0	4.0	1	0.82	1.63	1	1	90	9.5	0.98	1.08	1.00	0.316	0.293	Bray et al. (2004), PEER (2000a)
1999 M=7.5 Kocaeli - Aug 17	Site D, Building D1	7.5	0.4	Yes	2.5	1.7	46	38	2.9	4.2	1	0.85	1.70	1	1	59	9.8	0.99	1.09	1.00	0.310	0.285	Bray et al. (2004), PEER (2000a)
1999 M=7.5 Kocaeli - Aug 17	Site E, Buildings E1 & E2: Sand	7.5	0.4	Yes	2.0	0.5	38	23	7.0	10.8	1	0.90	1.70	1	1	4	10.8	0.99	1.10	1.00	0.427	0.388	Bray et al. (2004), PEER (2000a)
1999 M=7.5 Kocaeli - Aug 17	Site E, Buildings E1 & E2: Silt	7.5	0.4	Yes	3.0	0.5	56	32	5.5	9.3	1	0.99	1.70	1	1	60	14.9	0.98	1.10	1.00	0.454	0.413	Bray et al. (2004), PEER (2000a)
1999 M=7.5 Kocaeli - Aug 17	Site F, Building F1	7.5	0.4	Yes	2.4	1.9	44	39	4.4	6.6	1	0.90	1.64	1	1	80	12.1	0.99	1.10	1.00	0.289	0.264	Bray et al. (2004), PEER (2000a)
1999 M=7.5 Kocaeli - Aug 17	Site G, Buildings G2 & G3	7.5	0.4	Yes	2.7	0.6	50	29	6.7	10.4	1	0.91	1.70	1	1	76	15.9	0.98	1.10	1.00	0.438	0.399	Bray et al. (2004), PEER (2000a)
1999 M=7.5 Kocaeli - Aug 17	Site H, Building H1	7.5	0.4	Yes	2.4	1.7	44	37	11.0	16.6	1	0.97	1.56	1	1	15	19.9	0.99	1.10	1.00	0.305	0.277	Bray et al. (2004), PEER (2000a)
1999 M=7.5 Kocaeli - Aug 17	Site I, Building I2 & I2	7.5	0.4	Yes	4.8	0.8	88	48	6.8	9.9	1	1.02	1.43	1	1	79	15.4	0.96	1.08	1.00	0.454	0.420	Bray et al. (2004), PEER (2000a)
1999 M=7.5 Kocaeli - Aug 17	Site J, Building J2 & J2	7.5	0.4	Yes	2.9	0.6	53	31	6.1	8.7	1	0.84	1.70	1	1	71	14.3	0.98	1.10	1.00	0.436	0.397	Bray et al. (2004), PEER (2000a)
1999 M=7.5 Kocaeli - Aug 17	Degirmendere DN-1	7.5	0.4	Yes	9.6	1.7	174	97	14.9	16.5	1	1.08	1.02	1	1	11	18.3	0.90	1.01	1.00	0.422	0.420	Youd et al. (2009)
1999 M=7.5 Kocaeli - Aug 17	Degirmendere DN-2	7.5	0.4	No	3.6	2.5	65	54	14.6	18.1	1	0.94	1.31	1	1	13	20.4	0.98	1.08	1.00	0.303	0.280	Youd et al. (2009), Cetin et al. (2004)
1999 M=7.5 Kocaeli - Aug 17	Yalova Harbor	7.5	0.3	Yes	5.1	0.8	93	51	10.2	14.4	1	1.04	1.36	1	1	19	18.7	0.96	1.09	1.00	0.340	0.314	Cetin et al. (2004)
1999 M=7.6 Chi-Chi - Sept 20	Wufeng - Site A1	7.6	0.65	No	7.4	1.1	147	85	12.6	16.5	1	1.25	1.08	0.97	1	24	21.5	0.94	1.03	0.97	0.686	0.686	Chu et al. (2008), Chu (2006), PEER (2000b)
1999 M=7.6 Chi-Chi - Sept 20	Wufeng - Site C (WCS-1)	7.6	0.67	Yes	2.8	1.3	55	41	6.0	8.4	1	0.88	1.59	1	1	21	13.1	0.99	1.09	0.98	0.585	0.543	Chu et al. (2004), PEER (2000b)
1999 M=7.6 Chi-Chi - Sept 20	Wufeng - Site C (WCS-2)	7.6	0.67	Yes	2.8	1.3	55	41	2.2	4.6	1	1.25	1.69	1	1	18	7.3	0.99	1.08	0.99	0.584	0.548	Chu et al. (2004), PEER (2000b)
1999 M=7.6 Chi-Chi - Sept 20	Wufeng - Site B (WBS-1)	7.6	0.67	Yes	3.3	1.5	65	47	7.9	12.1	1	1.25	1.42	0.86	1	29	17.4	0.98	1.09	0.98	0.587	0.549	Chu (2006), PEER (2000b)
2000 M=7.6 Chi-Chi - Sept 20	Yuanlin BH40	7.6	0.18	Yes	4.8	1.2	92	56	9.4	12.9	1	1.05	1.31	1	1	33	18.4	0.97	1.07	0.98	0.185	0.176	Chu (2006), PEER (2000b)
2001 M=7.6 Chi-Chi - Sept 20	Yuanlin BH28	7.6	0.18	Yes	5.9	2.3	111	76	4.1	5.3	1	1.10	1.16	1	1	45	10.9	0.96	1.03	0.99	0.163	0.161	Chu (2006), PEER (2000b)
2002 M=7.6 Chi-Chi - Sept 20	Yuanlin BH30	7.6	0.18	Yes	3.9	1.1	73	46	4.9	7.3	1	1.01	1.49	1	1	46	12.9	0.98	1.08	0.98	0.181	0.170	Chu (2006), PEER (2000b)
2003 M=7.6 Chi-Chi - Sept 20	Yuanlin BH31	7.6	0.18	No	6.6	4.2	120	96	3.7	4.3	1	1.13	1.03	1	1	47	10.0	0.95	1.00	0.99	0.138	0.139	Chu (2006), PEER (2000b)
2004 M=7.6 Chi-Chi - Sept 20	Yuanlin BH10	7.6	0.18	No	7.1	2.0	131	81	8.7	11.3	1	1.16	1.13	1	1	9	11.9	0.94	1.02	0.98	0.179	0.178	Chu (2006), PEER (2000b)
2005 M=7.6 Chi-Chi - Sept 20	Yuanlin BH27	7.6	0.18	No	4.3	0.4	80	41	2.9	4.8	1	1.03	1.62	1	1	54	10.4	0.97	1.08	0.99	0.220	0.205	Chu (2006), PEER (2000b)

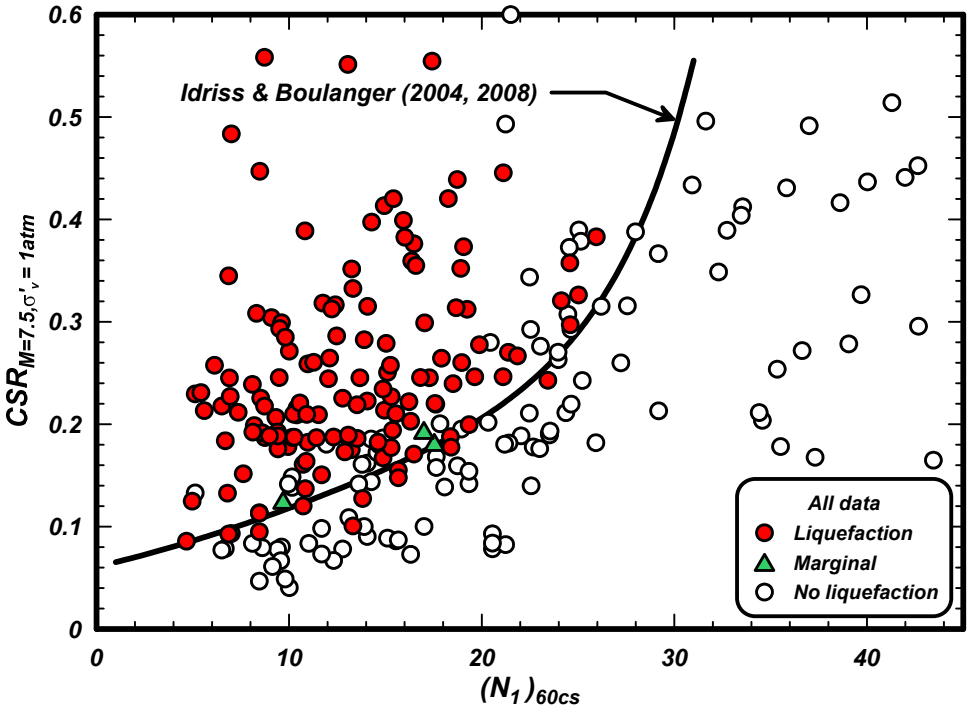

Figure 6.1. Curves of $CRR_{M=7.5,\sigma'v=1atm}$ versus $(N_1)_{60cs}$ for the updated database processed with the Idriss and Boulanger (2008) procedures

The updated case history data processed using the procedures in Idriss and Boulanger (2008) are plotted along with the Idriss-Boulanger (2008) deterministic triggering curve in Figure 6.1. A total of 9 liquefaction case histories plot below the curve and 29 no-liquefaction cases plot above the curve.

6.3. Correlation with updated database and analysis framework

The updated case history database processed with the revised MSF relationship is plotted along with the Idriss-Boulanger (2008) deterministic triggering curve in Figure 6.2. There are now fewer liquefaction cases plotting below the triggering curve (6 versus 9) and more no-liquefaction cases plotting above the triggering curve (30 versus 29) as a result of using the revised MSF relationship.

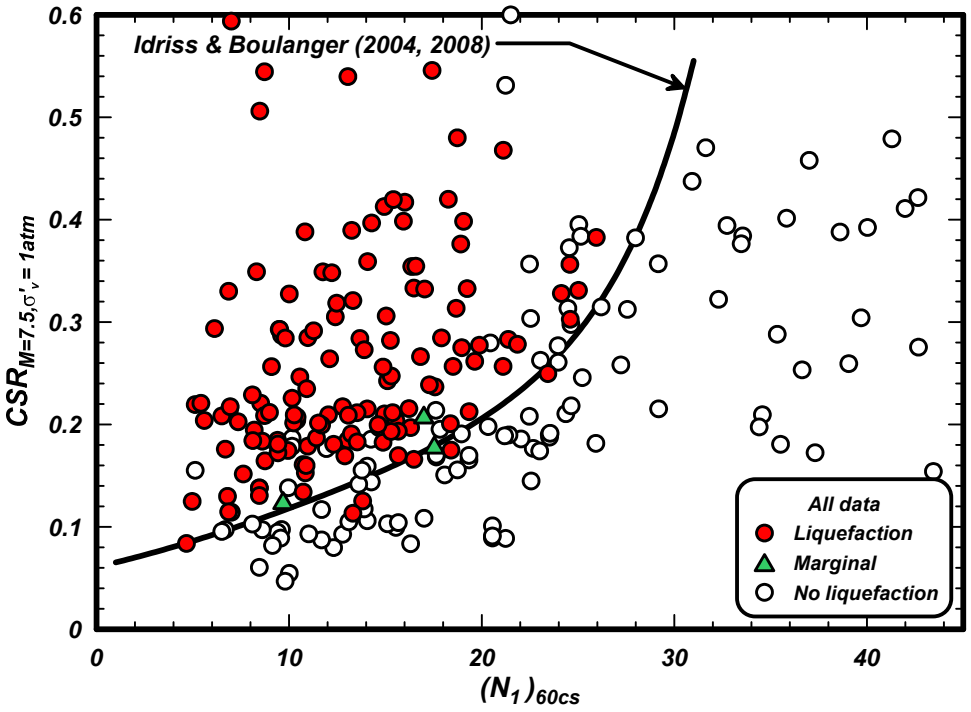

Figure 6.2. Curves of $CRR_{M=7.5,\sigma'v=1atm}$ versus $(N_1)_{60cs}$ for the data processed with the Idriss and Boulanger (2008) procedures with the revised MSF relationship

6.4. Variation with fines content

The reprocessed case histories are plotted for different bins of FC in Figures 6.3: (a) FC ≤ 5%, (b) 5% < FC ≤ 15%, (c) 15% < FC ≤ 35%, and (d) 35% < FC. For these respective bines, there are 3, 2, 1, and 0 liquefaction points below the triggering curve and 9, 6, 8, and 7 no-liquefaction points above the triggering curve. The reprocessed data are good agreement with the triggering curve across all bins, with no apparent bias with respect to FC.

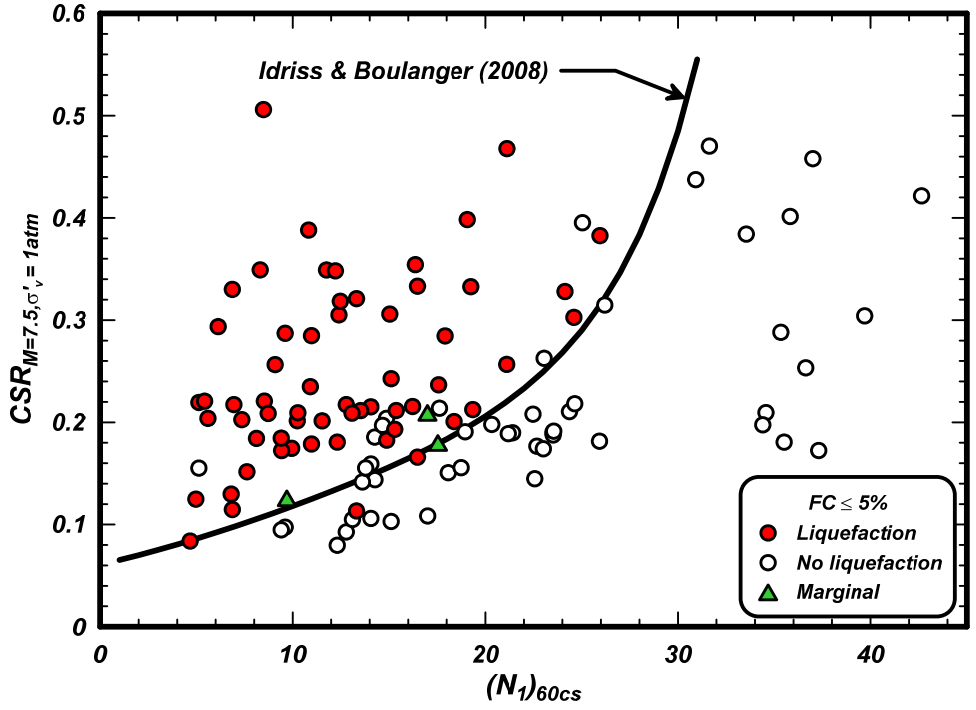

(a)

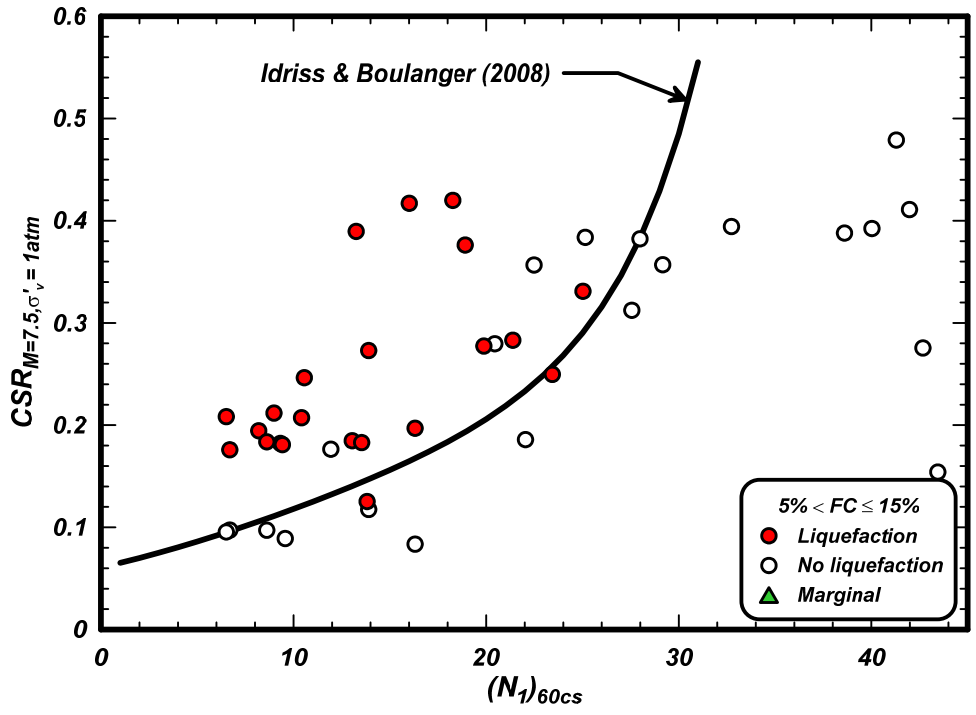

(b)

Figure 6.3a-b. Distribution of case history data with different fines contents and processed with the revised MSF relationship

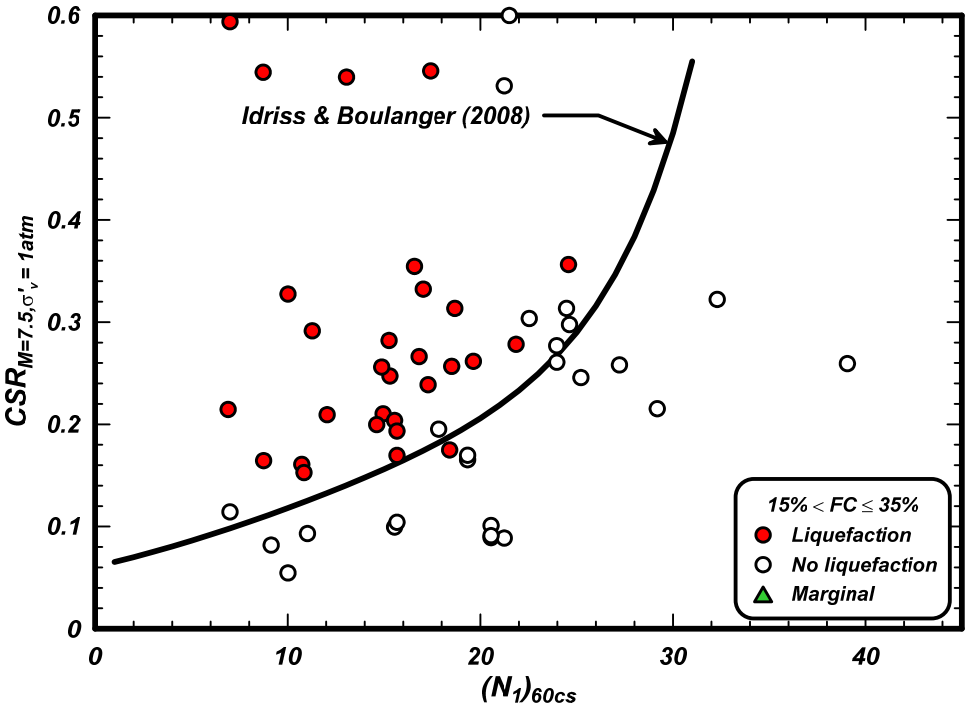

(c)

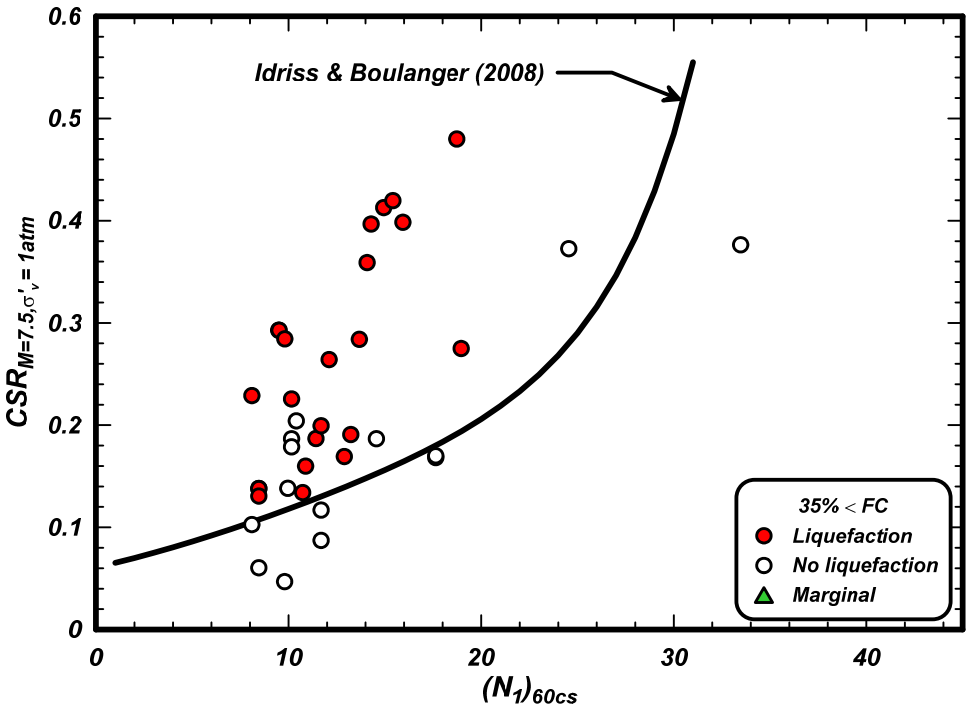

(d)

Figure 6.3c-d. Distribution of case history data with different fines contents and processed with the revised MSF relationship

6.5. Variation with earthquake magnitude

The reprocessed case histories are plotted for different bins of M in Figures 6.4: (a) $M \leq 6.25$, (b) $6.25 < M \leq 6.75$, (c) $6.75 < M \leq 7.25$, (d) $7.25 < M \leq 7.75$, and (e) $7.75 < M$. The reprocessed data are in reasonable agreement with the triggering curve across all bins, with no apparent bias with respect to M.

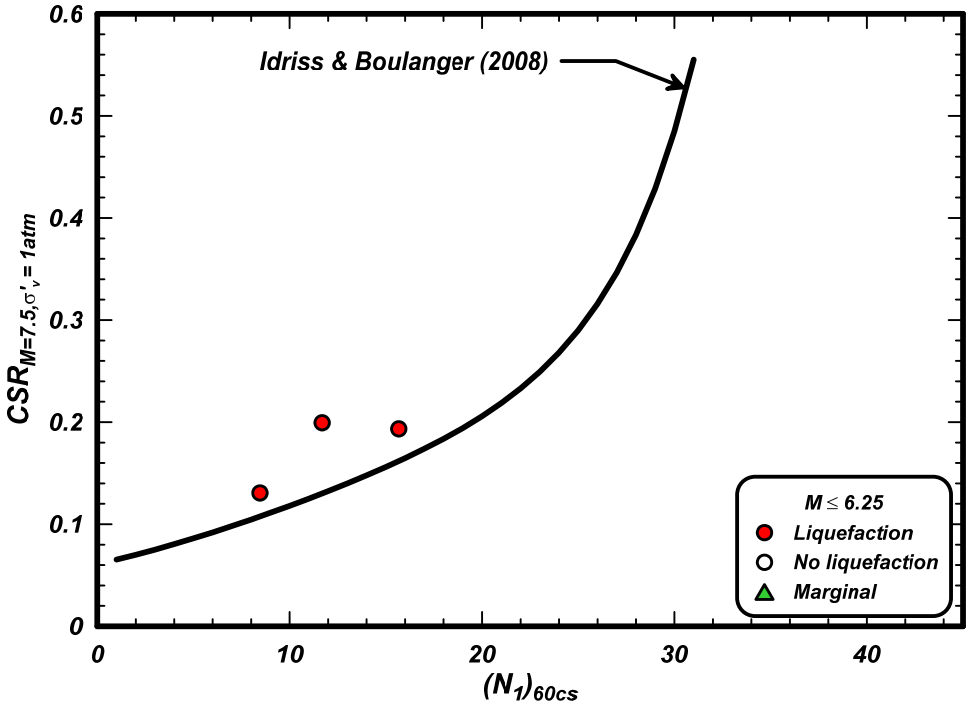

(a)

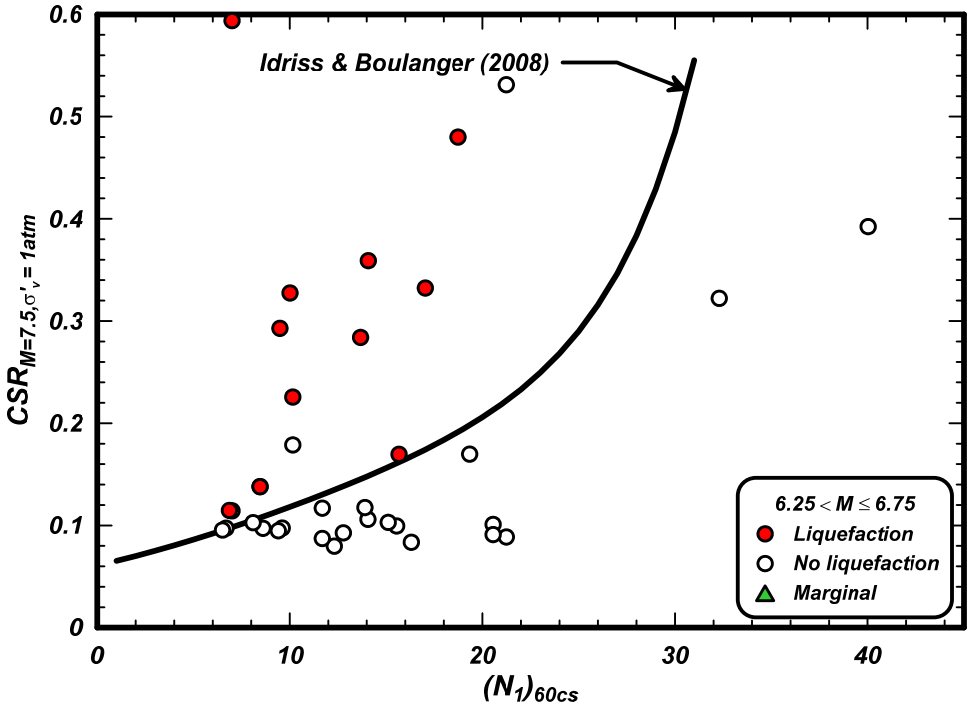

(b)

Figure 6.4a-b. Distribution of case history data with different earthquake magnitudes and processed with the revised MSF relationship

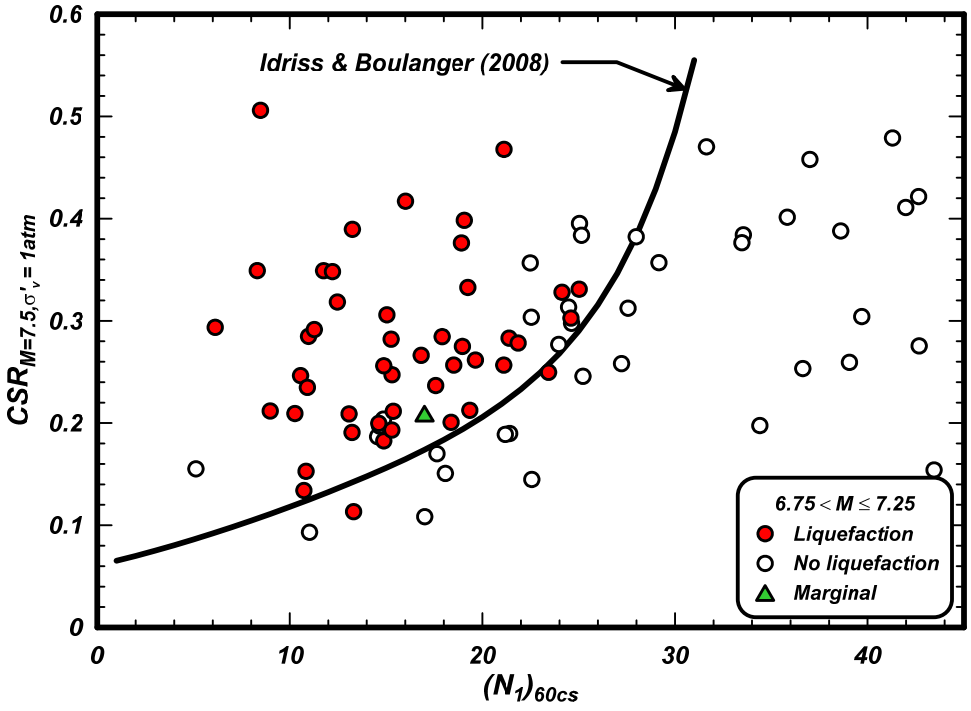

(c)

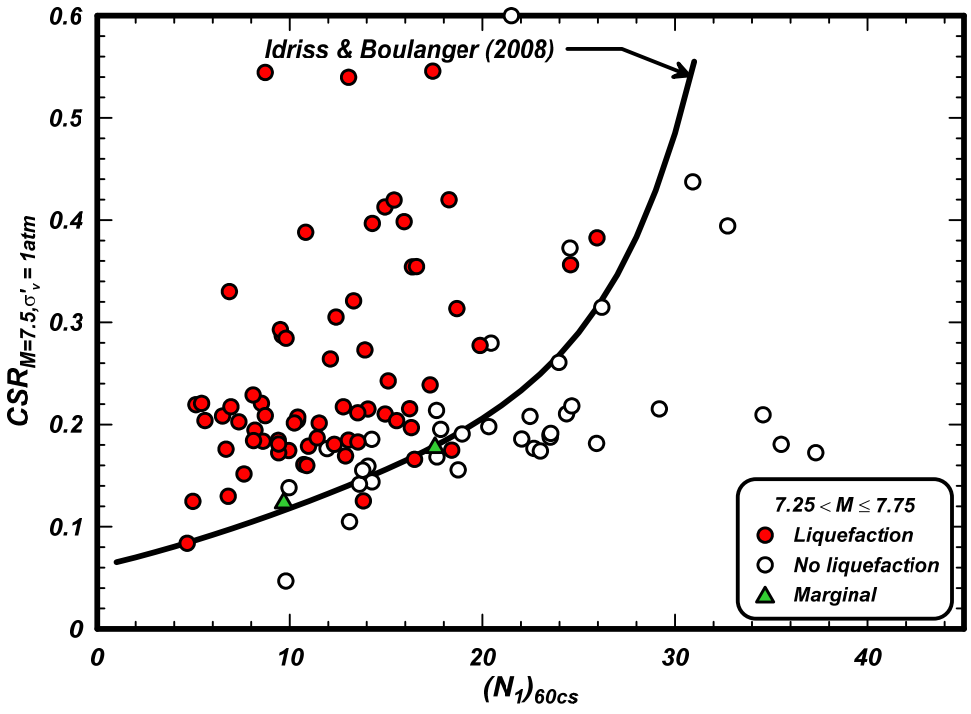

(d)

Figure 6.4c-d. Distribution of case history data with different earthquake magnitudes and processed with the revised MSF relationship

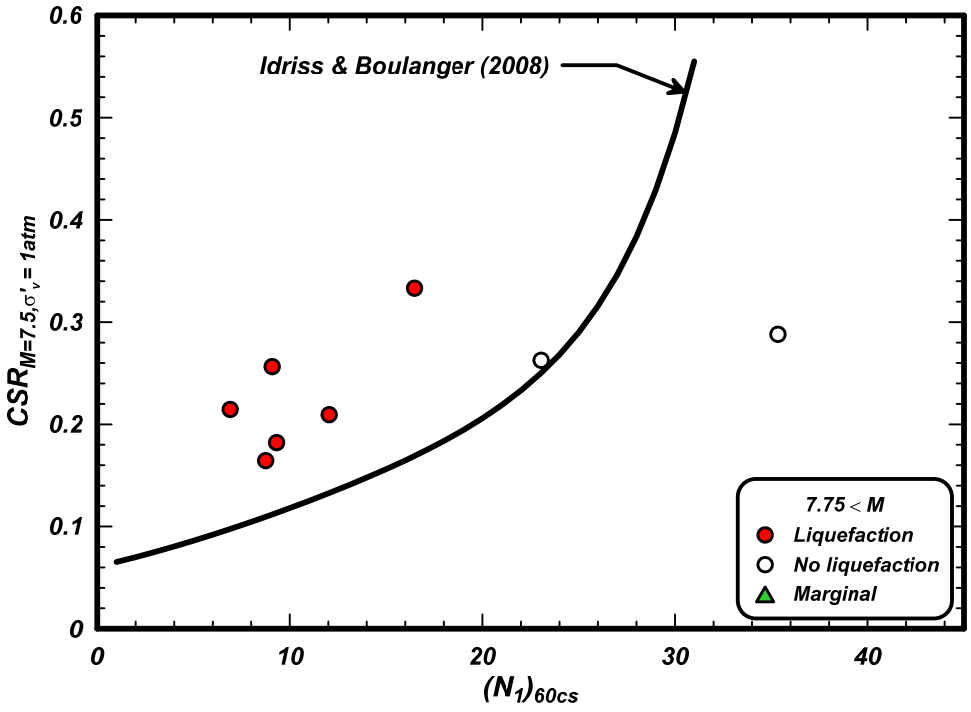

(e)

Figure 6.4e. Distribution of case history data with different earthquake magnitudes and processed with the revised MSF relationship

6.6. Variation with effective overburden stress

The reprocessed case histories are plotted for different bins of σ'_v in Figures 6.5: (a) $\sigma'_v \leq 40$ kPa, (b) 40 kPa $< \sigma'_v \leq 80$ kPa, (c) 80 kPa $< \sigma'_v \leq 120$ kPa, and (d) 120 kPa $< \sigma'_v$. The reprocessed data do not equally constrain the triggering curve across these four bins, with the data for the higher stresses falling slightly higher relative to the triggering curve. These data are not, however, sufficient in quantity to suggest the need for any adjustments to the current correlation.

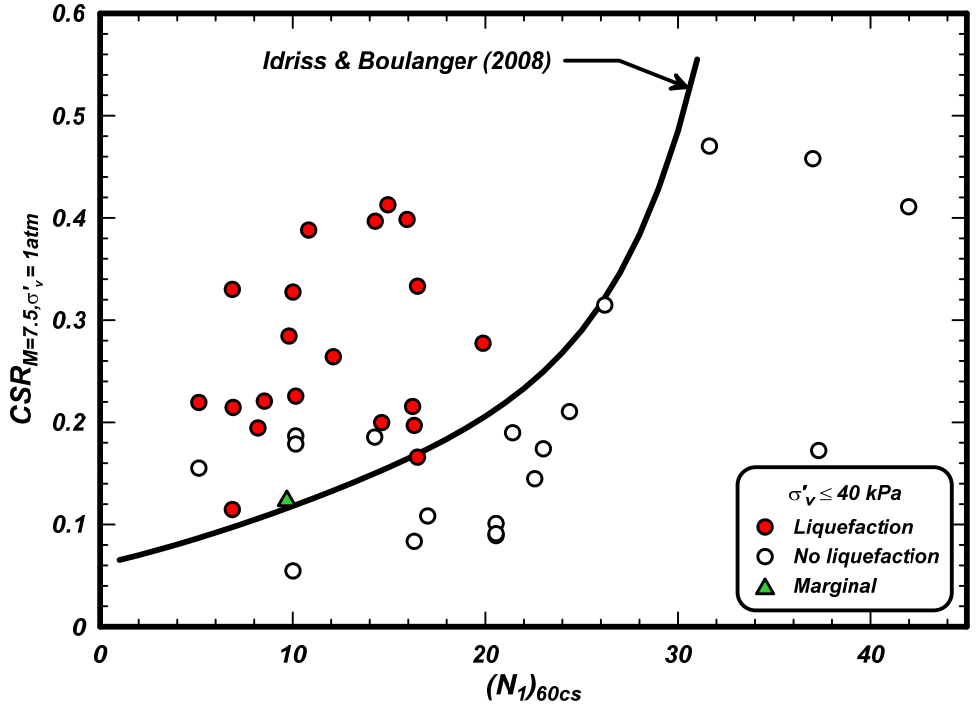

(a)

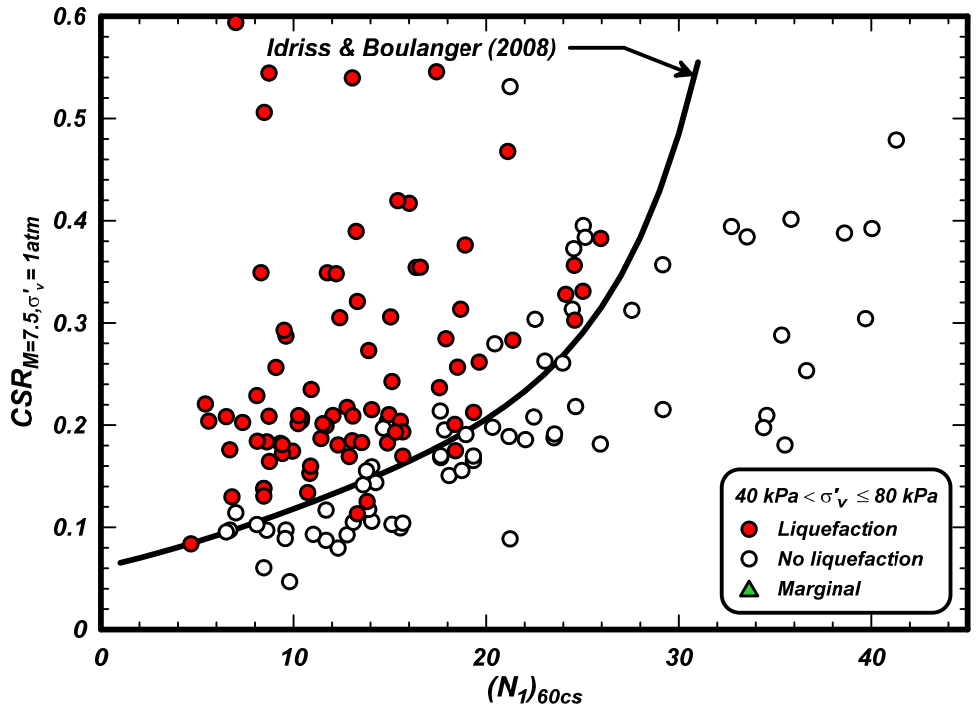

(b)

Figure 6.5a-b. Distribution of case history data with different σ'_v and processed with the revised MSF relationship

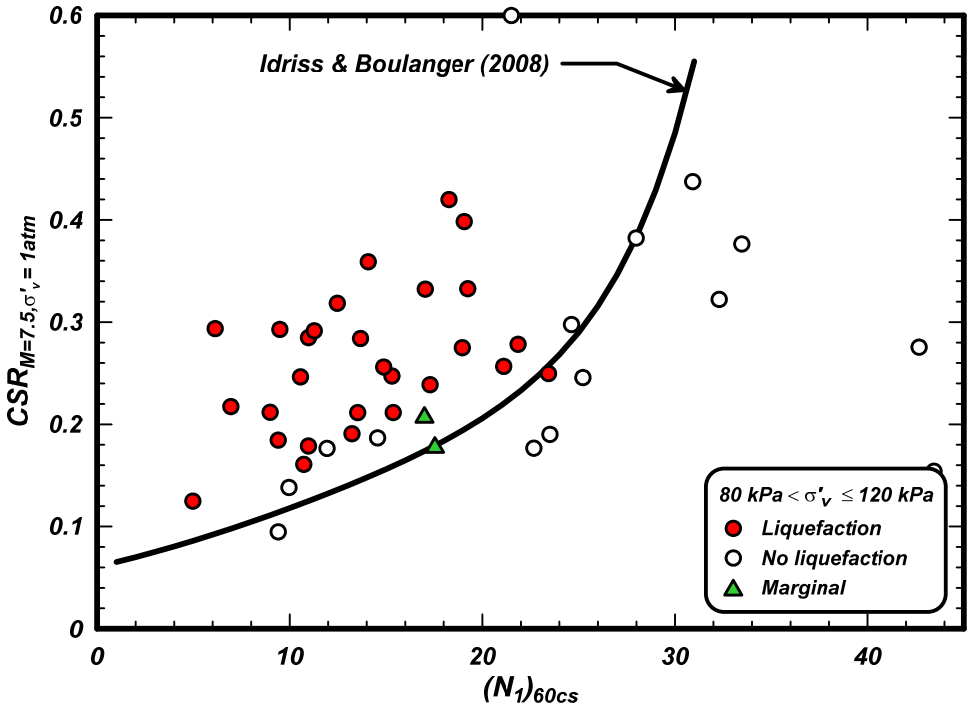

(c)

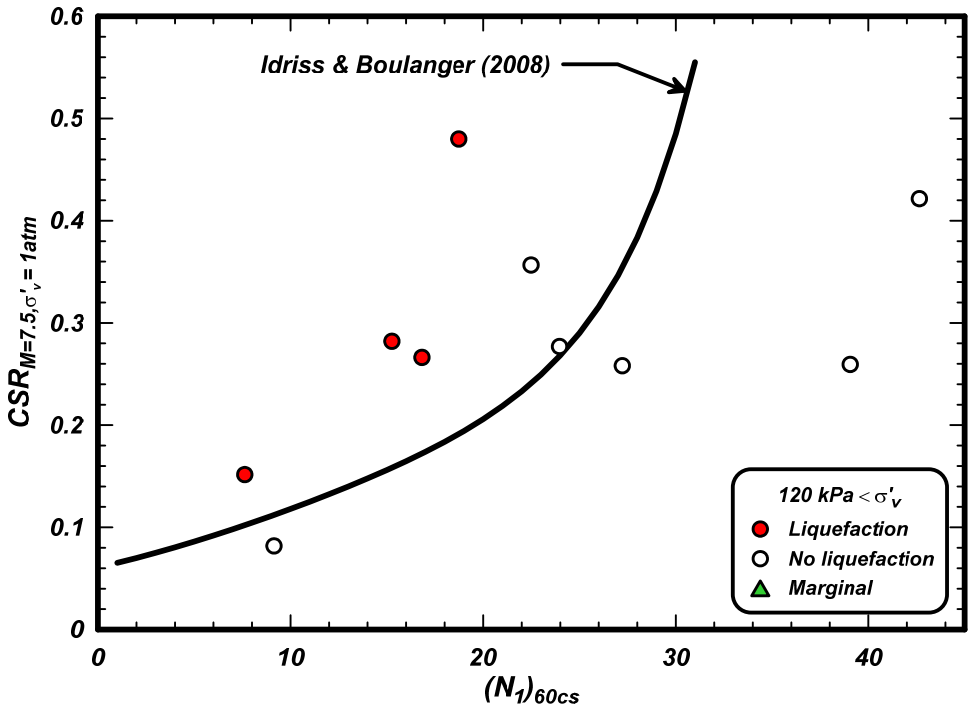

(d)

Figure 6.5c-d. Distribution of case history data with different σ'_v and processed with the revised MSF relationship

6.7. Summary

The SPT-based case history database by Idriss and Boulanger (2010) was updated to remove two no-liquefaction cases based on additional information regarding their field documentation (Youd et al. 2013, Boulanger et al. 2013) and add 24 cases from the 1999 Kocaeli and 1999 Chi-Chi earthquakes.

The SPT-based case histories were reprocessed using the revised MSF relationship developed in Appendix A and summarized in Section 2 of this report.

The reprocessed SPT-based database was shown to be in good agreement with the triggering curve recommended by Idriss and Boulanger (2008). This indicates that the SPT database supports implementation of the revised MSF relationship in the SPT-based liquefaction triggering procedures.

7. OTHER CONSIDERATIONS IN DEVELOPMENT OF TRIGGERING MODELS

7.1 Equivalent q_c/N_{60} ratios

Idriss and Boulanger (2004) evaluated the consistency of their deterministic SPT- and CPT-based liquefaction triggering correlations for clean sand using correlations relating penetration resistances [q_{c1N} and $(N_1)_{60}$] to relative density and relative state parameter index. That evaluation demonstrated that: (1) the shapes of the SPT- and CPT-based correlations were consistent, (2) the q_c/N_{60} ratios implied by the correlations were toward the upper range of empirically observed q_c/N_{60} ratios, and (3) q_c/N_{60} ratios should be expected to decrease with increasing relative density.

The consistency of the probabilistic CPT-based triggering correlation (Section 6) with the previously derived probabilistic SPT-based triggering correlation by Boulanger and Idriss (2012a) was similarly evaluated, including the calculation of q_c/N_{60} ratios for common values of $CRR_{M=7.5,\sigma'=1atm}$ and P_L. The q_c/N_{60} ratios for clean sands are obtained at common $CRR_{M=7.5,\sigma'=1atm}$ values, which uniquely define corresponding q_{c1Ncs} and $(N_1)_{60cs}$ values. The resulting q_c/N_{60} ratios for clean sands are plotted versus $(N_1)_{60}$ in Figure 7.1 for P_L = 15, 50, and 85%. For P_L = 50%, the q_c/N_{60} ratio varies between 5.6 and 7.6, with the lower ratios occurring at both the lower and upper ranges of $(N_1)_{60cs}$. For P_L = 85%, the q_c/N_{60} ratios are slightly lower, with values varying between about 4.0 and 6.5. For P_L = 15%, the q_c/N_{60} ratios are slightly greater, with values ranging between 5.6 and 8.0. The spread in the q_c/N_{60} ratios for different P_L values is greatest for loose sands, whereas the q_c/N_{60} ratio trends toward a value of about 5.6 at $(N_1)_{60} \approx 30$ for all three P_L values. These q_c/N_{60} ratios are reasonably consistent with the empirical data for q_c/N_{60} ratios, although they tend to fall toward the upper range of the empirical data (Figure 7.1). The q_c/N_{60} ratios are greatest for the P_L = 15% curves and lowest for the P_L = 85% curves. The deterministic liquefaction triggering correlations are based on P_L = 16%, and thus the q_c/N_{60} ratios obtained from the deterministic triggering correlations similarly will fall toward the upper range of the empirical data for q_c/N_{60} ratios.

The dependency of q_c/N_{60} ratios on the relative density of clean sands has been demonstrated empirically by Suzuki et al. (1998) and Niven et al. (2005) and is evident in other published datasets. For example, the data from Suzuki et al. (1998) for sands with 0-10% fines, as plotted in Figure 7.1, show that q_c/N_{60} ratios range from about 4 to 10 for loose sands [$(N_1)_{60} \leq 10$] and from about 3.5 to 6 for dense sands [$30 \leq (N_1)_{60} \leq 50$]. Similar trends are evident in individual data sets, such as the data set compiled from sites involving frozen sand sampling by Mayne (2005, personal communications).

The comparison of q_c/N_{60} ratios for clean sands raises the question of whether the liquefaction triggering correlations should be expected to produce q_c/N_{60} ratios that are closer to the median values of the empirical data. If the expectation is that they should, then the question becomes whether there is an independent basis for some combination of shifting the SPT correlations to the right and/or shifting the CPT correlations to the left. If no basis for shifting the liquefaction triggering correlations can be identified, then the question is whether there is a mechanistic explanation for why the liquefaction triggering correlations produce q_c/N_{60} ratios near the upper range of the empirical data. Answering the latter question is hindered by the fact there are currently no well-developed mechanistic models that can connect fundamental soil characteristics (e.g., grain crushability, compressibility, dilatancy) to their simultaneous effects on q_c, N_{60}, and $CRR_{M=7.5,\sigma'=1atm}$ values. One possible hypothesis would be that certain soil characteristics (e.g., high crushing resistance and low compressibility) may correlate with higher-than-average q_c values while having lesser effects on $CRR_{M=7.5,\sigma'=1atm}$ or N_{60} values, such that the liquefaction case histories that control the positions of the triggering correlations tend to be soils which produce higher-than-average q_c/N_{60} ratios. Additional research is necessary before these questions and

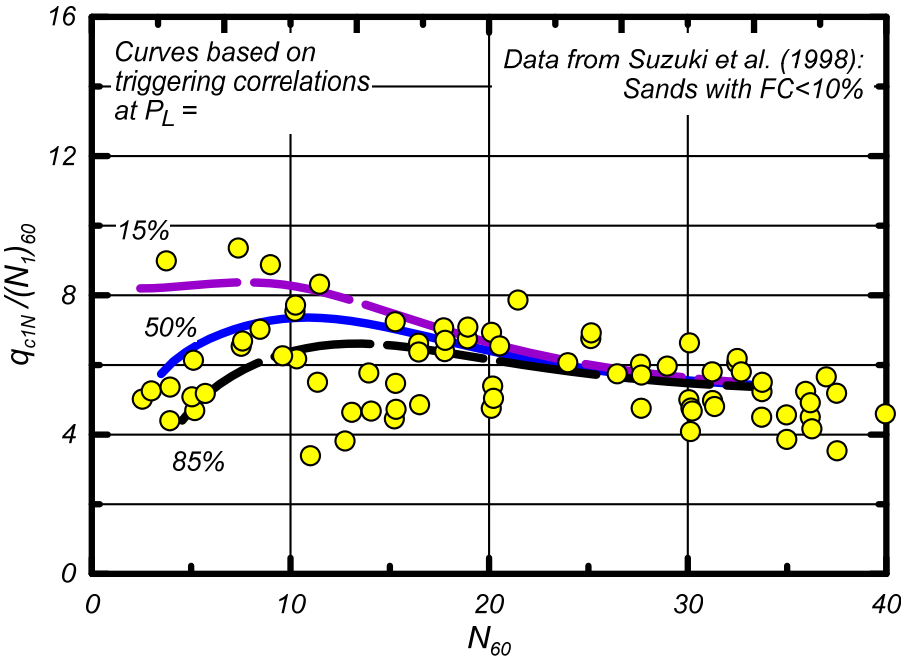

Figure 7.1. Ratio of q_{cN}/N_{60} as a function of N_{60} in sands with FC ≤ 10% (data from Suzuki et al. 1998)

related hypotheses can be addressed. In the meantime, the current probabilistic SPT and CPT based liquefaction triggering correlations are considered to be reasonably consistent because they were developed using consistent procedures and practices and the implied q_c/N_{60} ratios are within the range of the empirical data.

The variation of q_c/N_{60} ratios with FC was also examined in detail, as these ratios provide an important supplemental guide to the form of the FC corrections in the liquefaction triggering correlations (i.e., the Δq_{c1N} and $\Delta(N_1)_{60}$ functions). Values of q_c/N_{60} were computed for varying FC with common values of $CRR_{M=7.5,\sigma'=1atm}$, P_L, and $(N_1)_{60}$. The computed q_c/N_{60} ratios are plotted versus FC in Figure 7.2, along with the empirical data for cohesionless soils from Suzuki et al. (1998). The computed q_c/N_{60} ratios track the empirical data reasonably well, with the lower q_c/N_{60} ratios being obtained for denser soils and the q_c/N_{60} ratios decreasing toward a value of about 4.0 as FC increased to values greater than about 50%.

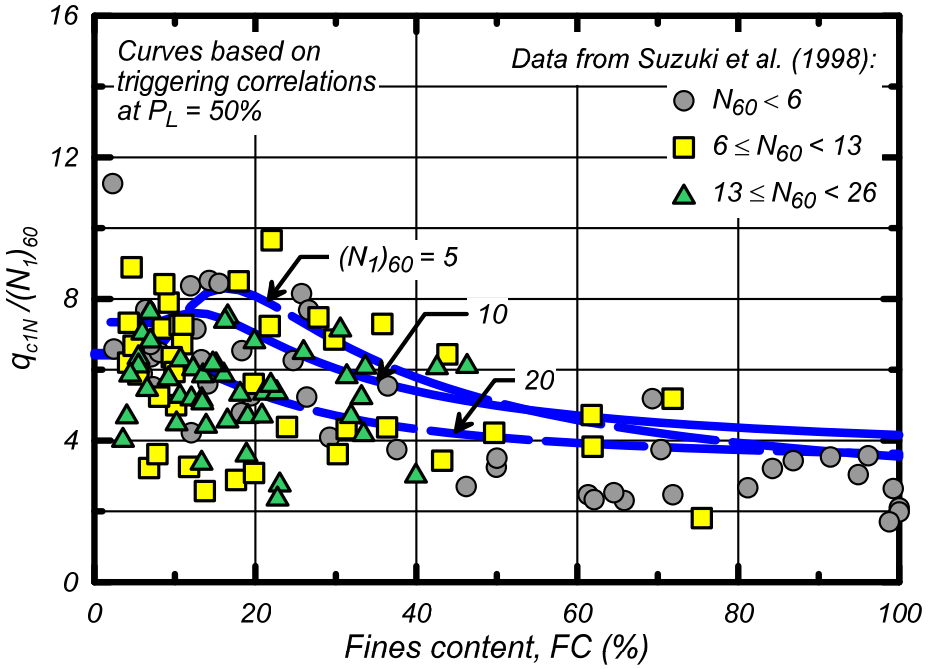

Figure 7.2. Ratio of q_{cN}/N_{60} as a function of FC (data from Suzuki et al. 1998)

7.2. CRR versus relative state parameter

Consistency between the CPT-based and SPT-based triggering correlations was examined in terms of the relationships they imply between $CRR_{M=7.5,\sigma'=1atm}$ and relative state parameter index, ξ_R (Boulanger 2003a) for clean sand. Values for ξ_R were estimated from penetration resistances [q_{c1N} and $(N_1)_{60}$] using the correlations in Idriss and Boulanger (2008). The resulting relationships between $CRR_{M=7.5,\sigma'=1atm}$ and ξ_R are shown in Figure 7.3 for P_L = 15, 50, and 85%. The curves obtained from the CPT and SPT relationships overlap across the full range of ξ_R values, with the differences between curves for individual comparable P_L values being relatively small given the uncertainty in correlations between penetration resistance and ξ_R.

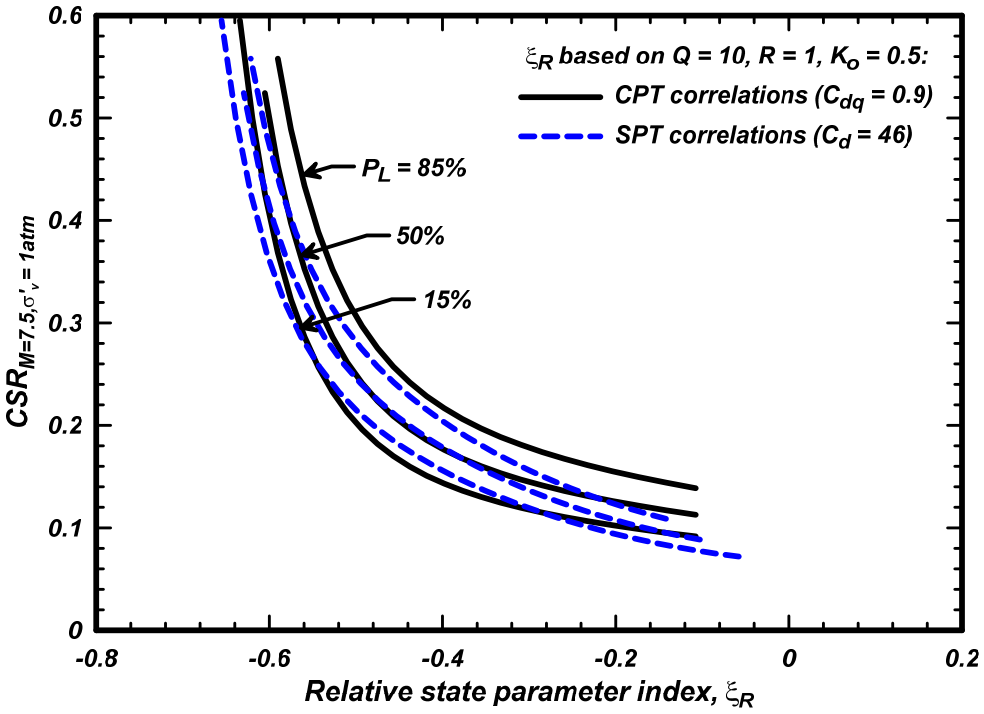

Figure 7.3. Comparison of the CPT-based and SPT-based probabilistic curves after mapping the penetration resistances to equivalent relative state parameter indices

7.3. Comparison to experimentally and theoretically derived models

Mitchell and Tseng (1990) used published calibration chamber cone data for three clean sands to validate a numerical cavity expansion analysis method, performed laboratory characterization tests (including determination of CRR) for four clean sands, and combined the numerical cavity expansion analyses with the lab data to produce a $CRR_{M=7.5,\sigma'=1atm}$ versus q_{c1N} correlation. The resulting correlations, as shown in Figure 7.4, largely fall within the bounds of the P_L = 15% to 85% curves derived in the previous section; e.g., 14 of the 17 points developed by Mitchell and Tseng (1990) fall between the P_L = 15-85% curves.

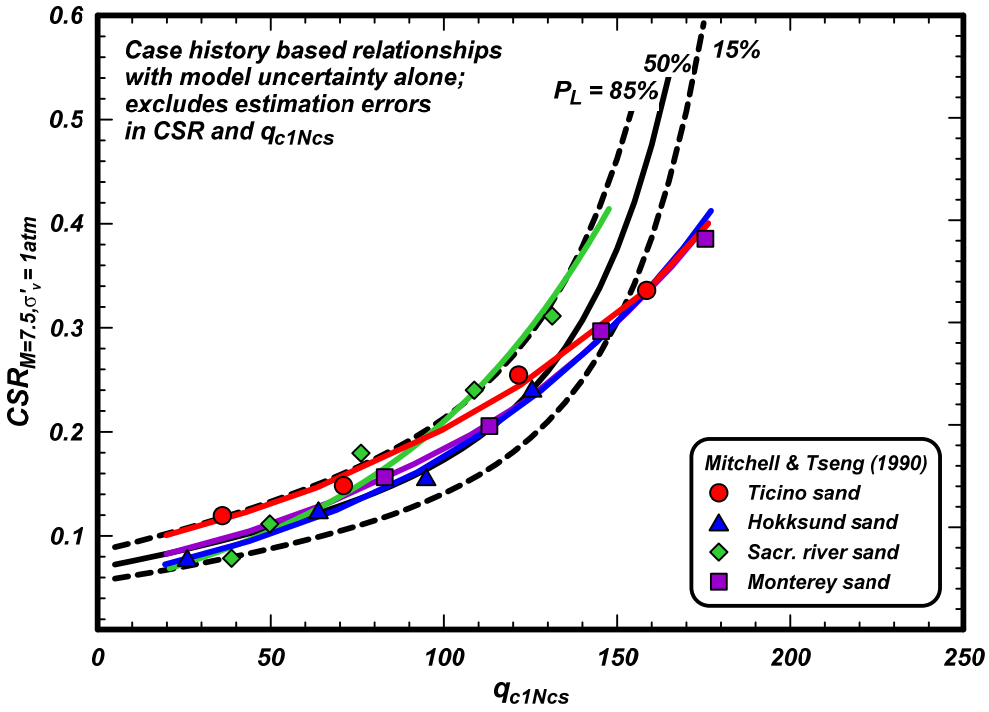

Figure 7.4. Comparison of the probabilistic curves with those derived by Mitchell and Tseng (1990) for four sands based on laboratory test data, calibration chamber test data, and numerical analyses

Carraro et al. (2003) used a similar approach with an improved numerical model to evaluate the effect of nonplastic fines (silica flour) on the $CRR_{M=7.5,\sigma'=1atm}$ versus q_{c1N} correlation. They also found their clean sand relationship to be consistent with case-history-based empirical correlations, but they observed that the correlation shifted to the right with increasing fines content (up to 15% nonplastic fines), which is inconsistent with the trends derived based on analyses of case histories. The analyses by Carraro et al. (2003) assumed fully drained cone penetration resistances, whereas the presence of even 15% fines can significantly impede drainage during cone penetration. Numerical analyses of cone penetration under drained and undrained conditions for silty and clayey sands show that undrained penetration resistances are expected to be lower than those for drained conditions over the range of densities of most concern (e.g., Jaeger 2012).

Kokusho et al. (2012) performed undrained cyclic triaxial tests on specimens of sands with fines, in which a miniature cone penetrometer was pushed to also obtain a measure of cone penetration resistance. The silty and clayey fines had a PI of about 6, and the specimens were prepared with fines contents of 0, 5, 10, 20, 30, and 100%. They concluded that for non-cemented specimens, there was a relatively unique relationship between the CRR and q_{cN} that is independent of FC. The specimens were globally undrained when the cone penetrometer was pushed into it, but the penetration process was likely locally partially drained or essentially drained around the cone tip based on its small diameter (d = 6 mm) and the slow penetration rate (v ≈ 2 mm/s). For example, assuming that the silty sand specimens had a coefficient of consolidation (c_v) of about 1 cm^2/s, then the normalized penetration velocity would be $V = vd/c_v = 0.12$ which would indicate a largely drained penetration process around the cone tip (Randolph 2004, DeJong and Randolph 2012, DeJong et al. 2012). The trends identified by Kokusho et al. (2012) are consistent with those of Carraro et al. (2003), and suggest that resolving differences in trends between the case histories and laboratory test results will require a better understanding of the effects of drainage conditions during cone penetration in silty sands and silts in the laboratory and in the field.

8. SUMMARY AND CONCLUSIONS

An updated examination of CPT-based and SPT-based liquefaction triggering procedures is presented in this report. The primary focus was on the CPT-based procedures, but an examination of the SPT-based procedures was necessitated by a revision in the magnitude scaling factor (MSF) relationship common to both procedures.

The approach used to develop these CPT-based and SPT-based procedures was to synthesize experimental, theoretical, and case history findings. This iterative approach was particularly valuable for arriving at reasonable relationships that are consistent with the cumulative available information while overcoming the unavoidable limitations in each individual source of information.

The liquefaction triggering analysis framework for the CPT-based and SPT-based procedures includes four key functional terms (C_N, K_σ, MSF, and r_d) which form the basis for how the model will effectively interpolate within, and extrapolate beyond, the range of conditions constrained by the case history data. An understanding of the theoretical and experimental bases for each of these functional terms is particularly vital for projects involving conditions that are not well constrained by the case history data. The functional terms used herein and their theoretical/experimental bases were briefly reviewed.

The revised MSF relationship incorporates functional dependency on the soil characteristics [using q_{c1Ncs} as the index for the CPT procedures and $(N_1)_{60cs}$ for the SPT procedures] as well as on earthquake magnitude. The revised MSF was based on the examination of cyclic testing results for a range of soil types and denseness, analyses of strong ground motion records, and the selection of a MSF function form guided by a number of other considerations. The revised MSF relationship was found to improve the agreement between the revised CPT-based and SPT-based liquefaction triggering correlations and their respective case history databases.

A number of CPT-based case histories were reviewed in detail to illustrate several issues important to the interpretation of case histories, including the importance of a geologic understanding of the site and the methodology used for selecting representative CPT q_{c1Ncs} values from critical strata. In general, the appropriateness of any averaging of q_{cN} values for a specific stratum in forward analyses or case history interpretations depends on the spatial characteristics of the stratum (e.g., thickness, lateral extent, continuity), the mode of deformation (e.g., reconsolidation settlement, lateral spreading, slope instability), and the spatial dimensions of the potential deformation mechanisms relative to the strata of concern.

The distributions of the CPT-based case history data (Table 3.1) with respect to the major parameters and the liquefaction triggering correlation were examined. The case history data do not adequately cover certain ranges of parameters and thus provide little or no empirical constraint on liquefaction triggering correlations for some ranges of conditions that are of interest to practice. In particular, the case history data are lacking for depths greater than about 10-12 m, for combinations of high FC and high q_{c1Ncs} values, and for earthquake magnitudes significantly smaller or larger than 7.5.

A revised CPT-based liquefaction triggering correlation was developed by processing the updated CPT case history database using the revised MSF relationship and the other components of the Idriss and Boulanger (2008) liquefaction triggering procedure. The revised correlation was shown to exhibit no apparent trends or biases, relative to the case history data, with respect to fines content, earthquake magnitude, or effective overburden stress. The SPT case history database by Idriss and Boulanger (2010) was similarly reexamined using the new MSF relationship; the results showed that the new MSF relationship similarly improved the agreement between SPT case history data and the liquefaction triggering correlation by Idriss and Boulanger (2008).

The revised CPT-based liquefaction triggering procedure included a recommended relationship and approach for estimating FC and soil classifications from the I_c index when site specific sampling and lab testing data are not available. For analyses in the absence of site-specific soil sampling and lab testing data, it would be prudent to perform parametric analyses to determine if reasonable variations in the FC and soil classification parameters have a significant effect on the final engineering recommendations. It is suggested that liquefaction analyses be repeated using C_{FC} = -0.29, 0.0, and 0.29 in Equation 2.30 to evaluate the sensitivity to FC estimates and using I_c values of 2.4, 2.6, and 2.8 for screening out clay-like soils to evaluate sensitivity to this parameter. The results of such analyses can be used to illustrate the importance of site-specific sampling and testing for a given project, while recognizing that some amount of sampling and testing should always be required for high risk/high consequence projects.

A probabilistic CPT-based liquefaction triggering correlation was developed using the updated case history database, revised MSF relationship, and a maximum likelihood approach. Measurement and estimation uncertainties in CSR and q_{c1Ncs}, the potential effects of false positives and false negatives in the case history database, and the effects of the choice-based sampling bias in the case history database were accounted for. The results of sensitivity analyses showed that the position of the most likely triggering curve was well constrained by the data and that the magnitude of the total error term was also reasonably constrained. The most likely value for the standard deviation of the error term in the triggering correlation was, however, found to be dependent on the uncertainties assigned to CSR and q_{c1Ncs} and the potential presence of false negatives and false positives in the case history database. Despite this and other limitations, the results of the sensitivity study appear to provide reasonable bounds on the effects of different interpretations on the positions of the triggering curves for various probabilities of liquefaction. The probabilistic relationship for liquefaction triggering proposed herein is considered a reasonable approximation in view of these various findings.

Probabilistic liquefaction hazard analyses need to consider the uncertainties in the seismic hazard, the site characterization, and the liquefaction triggering model. The uncertainty in the liquefaction triggering model is much smaller than the uncertainty in the seismic hazard, and will often be smaller than the uncertainty in the site characterization. For this reason, the seismic hazard analysis and the site characterization efforts are often the more important components of any probabilistic assessment of liquefaction hazards.

The SPT-based liquefaction triggering procedure by Idriss and Boulanger (2010) and Boulanger and Idriss (2012a) was reexamined using the updated analysis framework and including a few additions to the case history database. The agreement between the SPT-based procedures and case histories was good, so no revisions were recommended to these established procedures.

The CPT-based and SPT-based liquefaction triggering correlations were shown to: (1) be reasonably consistent with the empirical expectations for q_c/N_{60} ratios, including their dependence on denseness and fines content, (2) to produce reasonably consistent relationships between CRR and the relative state parameter index, and (3) to be in reasonable agreement with the CRR-q_{c1N} relationships derived for clean sands by Mitchell and Tseng (1990) based on results of calibration chamber tests, cyclic laboratory tests, and cone penetration analyses.

It is hoped that the findings presented in this report will contribute to more accurate evaluations of liquefaction hazards across the range of conditions encountered in practice. It is also hoped that this report will serve as a helpful resource for practicing engineers and researchers working in the field of soil liquefaction.

ACKNOWLEDGMENTS

The authors are grateful for information and insights provided over the years by numerous colleagues regarding liquefaction case histories and analysis procedures. For this report, specific information on certain case histories was provided by Drs. Michael Bennett, Thomas Holzer, and Rob Kayen. Professor Russell Green and his coauthors provided advance copies of their work examining CPT data from Christchurch. Additional comments and suggestions regarding different components of the report were provided by Professors Jonathan Bray, Misko Cubrinovski, Jason DeJong, Russell Green, James K. Mitchell, and Jonathan Stewart, Drs. Mike Beaty, Dave Gillette, Thomas Holzer, Lelio Mejia, and Peter Robertson, and Mr. Adam Price. The comments and suggestions received from these valued colleagues helped significantly improve the work presented herein. The authors are, however, solely responsible for the data, interpretations, and recommendations presented in this report.

Portions of the work presented herein were derived from studies supported by the California Department of Water Resources (DWR) and the National Science Foundation (grants CMMI-1138203 and CMMI-1300518). Any opinions, findings, or recommendations expressed in this material are those of the authors and should not be interpreted as necessarily representing the official policies, either expressed or implied, of either organization.

REFERENCES

Abdel-Haq, A., and Hryciw, R. D. (1998). "Ground settlement in Simi Valley following the Northridge earthquake." Journal of Geotechnical and Geoenvironmental Engineering, 124(1), 80-89.

Abrahamson, N., Atkinson, G., Boore, D., Bozorgnia, Y., Campbell, K., Chiou, B., Idriss, I. M., Silva, W., and Youngs, R. (2008). "Comparisons of the NGA ground-motion relations." Earthquake Spectra, 24(1), 45-66.

Ambraseys, N. N. (1988). "Engineering seismology." Earthquake Eng. and Structural Dynamics 17(1), 1–105.

Ancheta, T. D., Darragh, R. B., Stewart, J. P., Seyhan, E., Silva, W. J., Chiou, B. S. J., Wooddell, K. E., Graves, R. W., Kottke, A. R., Boore, D. M., Kishida, T., and Donahue, J. L. (2014). "NGA-West 2 database." Earthquake Spectra, EERI, http://dx.doi.org/10.1193/070913EQS197M.

Andrus, R. D. and Youd, T. L. (1987). "Subsurface Investigation of a Liquefaction-Induced Lateral Spread Thousand Springs Valley, Idaho." Misc. paper GL-87-8, U.S. Army Corps of Engineers.

Andrus, R. D., Stokoe, K. H., II, and Roesset, J. M. (1991). "Liquefaction of gravelly soil at Pence Ranch during the 1983 Borah Peak, Idaho Earthquake." Soil dynamics and earthquake engineering, Vol. 5, Computational Mechanics Publications and Elsevier Applied Science, London.

Arango, I. (1996). "Magnitude scaling factors for soil liquefaction evaluations." J. Geotechnical Eng., ASCE 122(11), 929–36, 1996.

Arulanandan, K., Douglas, B. J., Qu, Y. Z., Junfei, X., Chengchun, W., and Qizhi, H. (1982). "Evaluation of earthquake induced liquefaction in Tientsin during the Tangshan Earthquake P. R. C." Proc., United States-People's Republic of China Bilateral Workshop on Earthquake Engineering, E-3-1–E-3-42.

Arulanandan, K., Yogachandran, C., Meegoda, N. J., Ying, L., and Zhauji, S. (1986). "Comparison of the SPT, CPT, SV and Electrical Methods of Evaluating Earthquake Induced Liquefaction Susceptibility in Ying Kou City During the Haicheng Earthquake." Use of In Situ Tests in Geotechnical Engineering, Geotechnical Special Publication No. 6, 389-415.

Baecher, G. B., and Christian, J. T. (2003). Reliability and Statistics in Geotechnical Engineering. John Wiley and Sons, Ltd., 619 pp.

Bennett, M. J., and Tinsley, J. C, III (1995). Geotechnical data from surface and subsurface samples outside of and within liquefaction-related ground failures caused by the October 17, 1989, Loma Prieta earthquake, Santa Cruz and Monterey Counties, California. U.S. Geological Survey, Open-File Report 95-663, 360 pp.

Bennett, M. J., McLaughlin, P. V., Sarmiento, J. S., and Youd, T. L. (1984). Geotechnical investigation of liquefaction sites, Imperial Valley, California. U.S. Geological Survey, Open-File Report 84-252, 103 pp.

Berrill, J. B., Bienvenu, V. C., and Callaghan, M. W. (1988). "Liquefaction in the Buller Region in the 1929 and 1968 earthquakes." Bulletin of the New Zealand Society for Earthquake Engineering, 21(3), 174-189.

Bennett, M. J., Ponti, D. J., Tinsley, J. C., III, Holzer, T. L., and Conaway, C. H. (1998). Subsurface geotechnical investigations near sites of ground deformations caused by the January 17, 1994, Northridge, California, earthquake. U.S. Geological Survey, Open-file report 98-373, 148 pp.

Boore, D. M., Watson-Lamprey, J., and Abrahamson, N. A. (2006). "Orientation-independent measures of ground motion." Bulletin of the Seismological Society of America, 96(4A), 1502-1511.

Boulanger, R. W. (2003a). "Relating K_α to relative state parameter index." Journal of Geotechnical and Geoenvironmental Engineering, ASCE, 129(8), 770-773.

Boulanger, R. W. (2003b). High overburden stress effects in liquefaction analyses, *J. Geotechnical and Geoenvironmental Eng.,* ASCE **129**(12), 1071–082.

Boulanger, R. W., and Idriss, I. M. (2007). "Evaluation of cyclic softening in silts and clays." J. Geotechnical and Geoenvironmental Eng., ASCE 133(6), 641–52.

Boulanger, R. W., and Idriss, I. M. (2012a). "Probabilistic SPT-based liquefaction triggering procedure." Journal of Geotechnical and Geoenvironmental Engineering, ASCE, 138(10), 1185-1195.

Boulanger, R. W., and Idriss, I. M. (2012b). "Evaluation of overburden stress effects on liquefaction resistance at Duncan Dam." Canadian Geotechnical Journal, 49, 1052-1058.

Boulanger, R. W., and Seed, R. B. (1995). "Liquefaction of sand under bi-directional monotonic and cyclic loading." Journal of Geotechnical Engineering, ASCE, 121(12), 870-878.

Boulanger, R. W., Idriss, I. M., and Mejia, L. H. (1995). "Investigation and evaluation of liquefaction related ground displacements at Moss Landing during the 1989 Loma Prieta earthquake." Report No. UCD/CGM-95/02, Center for Geotechnical Modeling, Department of Civil & Environmental Engineering, University of California, Davis, 231 pp., May.

Boulanger, R. W., Mejia, L. H., and Idriss, I. M. (1997). Liquefaction at Moss Landing during Loma Prieta earthquake, *J. Geotechnical and Geoenvironmental Eng.*, ASCE **123**(5), 453–67.

Boulanger, R. W., Wilson, D. W., and Idriss, I. M. (2012). "Examination and re-evaluation of SPT-based liquefaction triggering case histories." Journal of Geotechnical and Geoenvironmental Engineering, ASCE, 138(8), 898-909.

Boulanger, R. W., Wilson, D. W., and Idriss, I. M. (2013). Closure to "Examination and reevaluation of SPT-based liquefaction triggering case histories." Journal of Geotechnical and Geoenvironmental Engineering, ASCE, 138(8), 2000-2001.

Bray, J. D., Sancio, R. B., Durgunoglu, T., Onalp, A., Youd, T. L., Stewart, J. P., Seed, R. B, Cetin, O. K, Bol, E., Baturay, M. B., Christensen, C., and Karadayilar, T. (2004). "Subsurface characterization of ground failure sites in Adapazari, Turkey. Journal of Geotechnical and Geoenvironmental Engineering, ASCE, 130(7), 673-685.

Campanella, R.G., Gillespie, D., and Robertson, P.K. (1982). "Pore pressure during cone penetration testing." Proc. Of the 2nd European Symposium on Penetration Testing, ESPOT II. Amsterdam. A.A. Balkema, 507 - 512.

Carr, K., and Berrill, J. (2004). "Liquefaction case histories from the west coast of the south island, New Zealand." 13th World Conference on Earthquake Engineering, Vancouver, B.C., Canada, August 1-6, paper 1325.

Carraro, J. A. H., Bandini, P., and Salgado, R. (2003). "Liquefaction resistance of clean and nonplastic silty sands based on cone penetration resistance." Journal of Geotechnical and Geoenvironmental Engineering, ASCE, 129(11), 965-976.

Carter, L., Green, R., Bradley, B., and Cubrinovski, M. (2013). "The influence of near-fault motions on liquefaction triggering during the Canterbury earthquake sequence." New Zealand – Japan Workshop on Soil Liquefaction during Recent Large-Scale Earthquakes, Dec 2-3, University of Auckland, NZ.

Cetin, K. O., and Bilge, H. T. (2012). "Performance-based assessment of magnitude (duration) scaling factors." Journal of Geotechnical and Geoenvironmental Engineering, ASCE, 138: 324-334.

Cetin, K. O., and Seed, R. B. (2004). "Nonlinear shear mass participation factor (r_d) for cyclic shear stress ratio evaluation." Soil Dynamics and Earthquake Engineering, Elsevier, 24: 103-113.

Cetin, K. O., Seed, R. B., Moss, R. E. S., Der Kiureghian, A. K., Tokimatsu, K., Harder, L. F., and Kayen, R. E. (2000). *Field Performance Case Histories for SPT-Based Evaluation of Soil Liquefaction Triggering Hazard,* Geotechnical Engineering Research Report No. UCB/GT-2000/09, Geotechnical Engineering, Department of Civil Engineering, University of California at Berkeley.

Cetin, K. O., Der Kiureghian, A., Seed, R. B. (2002). "Probabilistic models for the initiation of seismic soil liquefaction." Structural Safety, 24: 67-82.

Cetin, K. O., Seed, R. B., Der Kiureghian, A., Tokimatsu, K., Harder, L. F., Kayen, R. E., and Moss, R. E. S. (2004a). Standard penetration test-based probabilistic and deterministic assessment of seismic soil liquefaction potential, *J. Geotechnical and Geoenvironmental Eng.*, ASCE **130**(12), 1314–340.

Cetin, K. O., Youd, T. L., Seed, R. B., Bray, J. D., Stewart, J. P., Durgunoglu, H. T., Lettis, W., and Yilmaz, M. T. (2004b). "Liquefaction-induced lateral spreading at Izmit Bay during the Kocaeli (Izmit) – Turkey earthquake." Journal of Geotechnical and Geoenvironmental Engineering, 130(12), 1300–1313.

Chameau, J.-L. A., Clough, G. W., and Frost, J. D. (1998). "Liquefaction characteristics of San Francisco bayshore fills." The Loma Prieta, California, Earthquake of October 17, 1989 – Liquefaction. Thomas L. Holzer, editor, U.S. Geological Survey Professional Paper 1551-B, 314 pp.

Chiou, B., Darragh, R., Gregor, N., and Silva, W. (2008). "NGA project strong-motion database." Earthquake Spectra, EERI, 24(1), 23-44.

Christensen, S. A. (1995). "Liquefaction of Cohesionless Soils in the March 2, 1987 Edgecumbe Earthquake, Bay of Plenty, New Zealand, and Other Earthquakes." Masters of Engineering Thesis, Department of Civil Engineering, University of Canterbury, Christchurch, New Zealand.

Christian, J. T., and Swiger, W. F. (1975). "Statistics of liquefaction and SPT results." Journal of Geotechnical Engineering Div., ASCE, 101(GT11), 1135-1150.

Chu, D. B. (2006). "Case studies of soil liquefaction of sands and cyclic softening of clays induced by the 1999 Taiwan Chi-Chi earthquake." Ph.D. dissertation, Dept. of Civil and Environmental Engineering, Univ. of California, Los Angeles.

Chu, D. B., Stewart, J. P., Lee, S., Tsai, J. S., Lin, P. S., Chu, B. L. , Seed, R. B., Hsu, S. C. Yu, M. S., Wang, M. C. H. (2004). "Documentation of soil conditions at liquefaction and non-liquefaction sites from 1999 Chi–Chi (Taiwan) earthquake." Soil Dynamics and Earthquake Engineering, 24: 647–657

Chu, D. B., Stewart, J. P., Boulanger, R. W., and Lin, P. S. (2008). "Cyclic softening of low-plasticity clay and its effect on seismic foundation performance." J. Geotechnical and Geoenvironmental Eng., ASCE, 134(11), 1595-1608.

Cox, B. R., Boulanger, R. W., Tokimatsu, K., Wood, C., Abe, A., Ashford, S., Donahue, J., Ishihara, K., Kayen, R., Katsumata, K., Kishida, T., Kokusho, T., Mason, B., Moss, R., Stewart, J., Tohyama, K., and Zekkos, D. (2013). "Liquefaction at strong motion stations and in Urayasu City during the 2011 Tohoku-Oki earthquake." Earthquake Spectra, EERI, 29(S1), S55-S80.

Cubrinovski, M., Rees, S., and Bowman, E. (2010). "Effects of non-plastic fines on liquefaction resistance of sandy soils." Earthquake Engineering in Europe. Geotechnical, Geological, and Earthquake Engineering, Springer, Vol. 17, 125-144.

Dahl, K. R. (2011). Evaluation of seismic behavior of intermediate and fine-grained soils. Doctoral thesis, University of California, Davis, CA.

Dahl, K, R., DeJong, J. T., Boulanger, R. W., Pyke, R., and Wahl, D. (2014). "Characterization of an alluvial silt and clay deposit for monotonic, cyclic and post-cyclic behavior." Canadian Geotechnical Testing Journal, DOI: 10.1139/cgj-2013-0057.

DeAlba, P., Seed, H. B., and Chan, C. K. (1976). "Sand liquefaction in large scale simple shear tests." J. Geotechnical Eng. Div., ASCE 102(GT9), 909–27.

DeJong, J. T. and Randolph, M. F. (2012). "Influence of partial consolidation during cone penetration on estimated soil behavior type and pore pressure dissipation measurements." Journal of Geotechnical and Geoenvironmental Engineering, ASCE, 138(7), 777-788, DOI: 10.1061/(ASCE)GT.1943-5606.0000646.

DeJong, J. T., Jaeger, R. A., Randolph, M. F., Boulanger, R. W., and Wahl, D. (2012). "Variable penetration rate cone testing for characterization of intermediate soils." Geotechnical and Geophysical Site Characterization 4 (ISC'4), Coutinho and Mayne, eds., Taylor and Francis Group, London, 25-42.

Diaz-Rodriquez, J. A. (1984). "Liquefaction in the Mexicali Valley During the Earthquake of June 9, 1980." Eighth World Conference on Earthquake Engineering EERI, San Francisco, 223-230.

Diaz-Rodriquez, J. A., and Armijo-Palacio, G. (1991). "Liquefaction potential of fine cohesionless soils using the CPT." Soils and Foundations, 31(3), 111-119.

Douglas, B. J., Olson, R. S., and Martin, G. R. (1981). "Evaluation of the cone penetrometer test for SPT liquefaction assessment." Preprint 81 544, Session on In Situ Testing to Evaluate Liquefaction Susceptibility, ASCE National Convention, St. Louis, MO, October.

Draper, N. R., and Smith, H. (1998). Applied regression analysis. John Wiley & Sons, Inc., 3rd edition.

Earth Technology Corporation (1985). "In Situ Testing II, Peoples Republic of China." Report 84-141-13, prepared for NSF, Long Beach, CA 90807, July.

Engdahl, E. R., and Villasenor, A. (2002). "Global seismicity: 1900-1999." International Handbook of Earthquake and Engineering Seismology, Intl. Assoc. Seismol. And Phys. Earth's Interior, Committee on Education, Vol. 81A, 665-690.

Farrar, J. A. (1990). "Study of In Situ Testing for Evaluation of Liquefaction Resistance." R-90-06, U.S. Department of the Interior, Bureau of Reclamation, Research and Laboratory Services Division, Geotechnical Services Branch, Denver Office.

Golesorkhi, R. (1989). *Factors Influencing the Computational Determination of Earthquake-Induced Shear Stresses in Sandy Soils*, Ph.D. thesis, University of California at Berkeley, 395 pp.

Green, R. A., and Terri, G. A. (2005). "Number of equivalent cycles concept for liquefaction evaluations—revisited." J. Geotechnical and Geoenvironmental Eng., ASCE 131(4), 477–88.

Green, R. A., Cubrinovski, M., Cox, B., Wood, C., Wotherspoon, L., Bradley, B., and Mauer, B. (2014). "Select liquefaction case histories from the 2010-2011 Canterbury earthquake sequence." Earthquake Spectra, Earthquake Engineering Research Institute, http://dx.doi.org/10.1193/030713EQS066M.

Holzer, T. L. (1998). The Loma Prieta, California, Earthquake of October 17, 1989 – Liquefaction. Thomas L. Holzer, editor, U.S. Geological Survey Professional Paper 1551-B, 314 pp.

Holzer, T. L., and Bennett, M. J. (2007). Geologic and hydrogeologic controls of boundaries of lateral spreads: Lessons from USGS liquefaction case histories, *Proceedings, First North American Landslide Conference,* Schaefer, V. R., Schuster, R. L., and Turner, A. K., eds., Association of Engineering Geologists Special Publication 23, 502-522.

Holzer, T. L., and Youd, T. L. (2007). "Liquefaction, Ground Oscillation, and Soil Deformation at the Wildlife Array, California. Bulletin of the Seismological Society of America, 97(3), 961-976.

Holzer, T. L., Tinsley, J. C., III, Bennett, M. J., and Mueller, C. S. (1994). "Observed and predicted ground deformation – Miller Farm Lateral Spread, Watsonville, California." Proceedings, 5th U.S.-Japan Workshop on Earthquake Resistant Design of Lifeline Facilities and Countermeasures Against Soil Liquefaction. National Center for Earthquake Engineering Research, Report NCEER-94-0026, 79-99.

Holzer, T. L., Bennett, M. J., Ponti, D. J., and Tinsley, J. C., III (1999). "Liquefaction and soil failure during 1994 Northridge earthquake." J. Geotechnical and Geoenvironmental Engineering, ASCE, 125(6), 438-452.

Hyde, A., Higuchi, T., and Yasuhara, K. (2006). "Liquefaction, cyclic mobility, and failure of silt." Journal of Geotechnical and Geoenvironmental Engineering, ASCE, 132(6), 716-735.

Idriss, I. M. (1999). An update to the Seed-Idriss simplified procedure for evaluating liquefaction potential, in *Proceedings, TRB Workshop on New Approaches to Liquefaction*, Publication No. FHWA-RD-99-165, Federal Highway Administration, January.

Idriss, I. M., and Boulanger, R. W. (2003). Relating K_α and K_σ to SPT blow count and to CPT tip resistance for use in evaluating liquefaction potential, in *Proceedings of the 2003 Dam Safety Conference*, ASDSO, September 7–10, Minneapolis, MN.

Idriss, I. M., and Boulanger, R. W. (2004). Semi-empirical procedures for evaluating liquefaction potential during earthquakes, in *Proceedings, 11th International Conference on Soil Dynamics and*

Earthquake Engineering, and 3rd International Conference on Earthquake Geotechnical Engineering, D. Doolin et al., eds., Stallion Press, Vol. 1, pp. 32–56.

Idriss, I. M., and Boulanger, R. W. (2008). *Soil liquefaction during earthquakes*. Monograph MNO-12, Earthquake Engineering Research Institute, Oakland, CA, 261 pp.

Idriss, I. M., and Boulanger, R. W. (2010). "SPT-based liquefaction triggering procedures." Report UCD/CGM-10/02, Department of Civil and Environmental Engineering, University of California, Davis, CA, 259 pp.

Ishihara, K. (1985). "Stability of natural deposits during earthquakes." in Proceedings, 11th International Conference on Soil Mechanics and Foundation Engineering, San Francisco, A. A. Balkema, Rotterdam, pp. 321–376.

Ishihara, K., and Koga, Y. (1981). "Case studies of liquefaction in the 1964 Niigata earthquake." Soils and Foundations, 21(3), 35-52.

Jaeger, R.A. (2012). "Numerical and Experimental Study on Cone Penetration in Sands and Intermediate Soils", PhD Dissertation, University of California Davis.

Juang, C. H., Jiang, T., and Andrus, R. D. (2002). "Assessing probability-based methods for liquefaction potential evaluation." J. Geotechnical and Geoenvironmental Engineering, ASCE, 128(7), 580-589.

Kayen, R.E. and Mitchell, J. K. (1998). "Arias Intensity Assessment of Liquefaction Test Sites on the East Side of San Francisco Bay Affected by the Loma Prieta, California, Earthquake of 17 October 1989," in M.I. El-Sabh, S. Venkatesh, C. Lomnitz and T.S. Murty, eds., Earthquake and Atmospheric Hazards: Preparedness Studies. Kluwer Academic Publishers, The Netherlands, p 243-265.

Kayen, R. E., Mitchell, J. K., Seed, R. B., and Nishio, S. (1998). "Soil liquefaction in the east bay during the earthquake." *The Loma Prieta, California, Earthquake of October 17, 1989 – Liquefaction*. Thomas L. Holzer, editor, U.S. Geological Survey Professional Paper 1551-B, B61-B86.

Kishida, H. (1966). "Damage to reinforced concrete buildings in Niigata City with Special reference to foundation engineering." Soils and Foundations, Japanese Society of Soil Mechanics and Foundation Engineering, 6(1),71–86.

Kishida, T., and Tsai, C.-C. (2014). "Seismic demand of the liquefaction potential with equivalent number of cycles for probabilistic seismic hazard analysis." Journal of Geotechnical and Geoenvironmental Engineering, ASCE, 10.1061/(ASCE)GT.1943-5606.0001033.

Kishida, T., Boulanger, R. W., Abrahamson, N. A., Driller, M. W., and Wehling, T. M. (2009). "Seismic response of levees in Sacramento-San Joaquin Delta." Earthquake Spectra, EERI, 25(3), 557-582.

Kokusho, T., Ito, Y., Nagao, Y., and Green, A. R. (2012). "Influence of non/low-plastic fines and associated aging effects on liquefaction resistance." Journal of Geotechnical and Geoenvironmental Engineering, ASCE, 138(6), 747-756.

Kondoh, M., Sasaki, Y., and Matsumoto, H. (1987). "Effect of fines contents on soil liquefaction strength (part 1)." Proc. Annual Meeting of the Japanese Society of Soil Mechanics and Foundation Engineering (in Japanese), Public Works Research Institute, Ministry of Construction, Tsukuba, Japan.

Kulhawy, F. H. and Trautmann, C. H. (1996). "Estimation of in-situ test uncertainty." Uncertainty in the Geologic Environment, Madison, WI, ASCE: 269–286.

Liao, S. S. C., and Lum, K. Y. (1998). "Statistical analysis and application of the magnitude scaling factor in liquefaction analysis." Geotechnical Earthquake Engineering and Soil Dynamics III, ASCE, 1:410–21.

Liao, S. C., and Whitman, R. V. (1986). Overburden correction factors for SPT in sand, *J. Geotechnical Eng.*, ASCE **112**(3), 373–77.

Liao, S. S. C., Veneziano, D., and Whitman, R. V. (1988). "Regression models for evaluating liquefaction probability." J. Geotech. Eng. Div., ASCE, 114(4), 389–411.

Liu, A. H., Stewart, J. P., Abrahamson, N. A., and Moriwaki, Y. (2001). "Equivalent number of uniform stress cycles for soil liquefaction analysis." J. Geotechnical and Geoenvironmental Eng., ASCE 127(12), 1017–026.

Maki, I. P., Boulanger, R. W., DeJong, J. T., and Jaeger, R. A. (2014). "Overburden normalizations of CPT data in sands to clays." Third International Symposium on Cone Penetration Testing, Las Vegas, NV, paper 2-34.

Manski, C. F., and Lerman, S. R. (1977). "The estimation of choice probabilities from choice-based samples." Econometrica, 45(8): 1977-1998.

Marcuson, W. F., and Bieganousky, W. A. (1977a). Laboratory standard penetration tests on fine sands, *J. Geotechnical Eng. Div.*, ASCE **103**(GT6), 565–88.

Marcuson, W. F., and Bieganousky, W. A. (1977b). SPT and relative density in coarse sands, *J. Geotechnical Eng. Div.*, ASCE **103**(GT11), 1295–309.

Miner, M. A. (1945). “Cumulative damage in fatigue.” Transactions, ASME 67, A159–A164.

Mitchell, J. K., and Tseng, D. J. (1990). "Assessment of liquefaction potential by cone penetration resistance", Proc., H. Bolton Seed Memorial Symposium, BiTech Publishers, Vol. 2, 335-350.

Mitchell, J. K., Lodge, A. L., Coutinho, R. Q., Kayen, R. E., Seed, R. B., Nishio, S., and Stokoe, K. H., II (1994). Insitu test results from four Loma Prieta earthquake liquefaction sites: SPT, CPT, DMT and shear wave velocity. Earthquake Engineering Research Center, University of California at Berkeley, Report No. UCB/EERC-94/04, 186 pp.

Montgomery, J., Boulanger, R. W., and Harder, L. F., Jr. (2012). "Examination of the K_σ overburden correction factor on liquefaction resistance." Report No. UCD/CGM-12-02, Center for Geotechnical Modeling, Department of Civil and Environmental Engineering, University of California, Davis, CA, 44 pp.

Moss, R. E. S., Seed, R. B., Kayen, R. E., Stewart, J. P., Youd, T. L., and Tokimatsu, K. (2003). "Field case histories for CPT-based in situ liquefaction potential evaluation." Geoengineering Research Rep. UCB/GE-2003/04.

Moss, R. E. S., Collins, B. D., and Whang, D. H. (2005). “Retesting of liquefaction/nonliquefaction case histories in the imperial valley.” Earthquake Spectra, 21(1), 179–196.

Moss, R. E. S., Seed, R. B., Kayen, R. E., Stewart, J. P., Der Kiureghian, A., and Cetin, K. O. (2006). CPT-based probabilistic and deterministic assessment of in situ seismic soil liquefaction potential, *J. Geotechnical and Geoenvironmental Eng.*, ASCE **132**(8), 1032–051.

Moss, R. E. S., Kayen, R. E., Tong, L.-Y., Liu, S.-Y., Cai, G.-J., and Wu, J. (2009). "Re-investigation of liquefaction and nonliquefaction case histories from the 1976 Tangshan earthquake." Rep. No. 209/102, Pacific Earthquake Engineering Research (PEER) Center, Berkeley, CA.

Moss, R. E. S., Kayen, R. E., Tong, L.-Y., Liu, S.-Y., Cai, G.-J., and Wu, J. (2011). "Retesting of liquefaction and nonliquefaction case histories from the 1976 Tangshan earthquake." Journal of Geotechnical and Geoenvironmental Engineering, ASCE, 137(4), 334-343.

Nguyen, T., Shao, L., Gingery, J., and Robertson, P. (2014). "Proposed modification to CPT-based liquefaction method for post-vibratory ground improvement." Geo-Congress 2014 Technical Papers: pp. 1120-1132. doi: 10.1061/9780784413272.109

Niven, E., Robertson, P., Sego, D., and Woeller, D. (2005). "On the use of the SPT and CPT in loose sands." Canadian Geotechnical Conference, Canadian Geotechnical Society.

Okamura, M., Ishihara, M., and Oshita, T. (2003). "Liquefaction resistance of sand deposit improved with sand compaction piles." Soils and Foundations, Japanese Geotechnical Society, 43(5), 175-187.

Olsen, R. S. (1997). "Cyclic liquefaction based on the cone penetrometer test." in Proceedings, NCEER Workshop on Evaluation of Liquefaction Resistance of Soils, National Center for Earth-quake Engineering Research, State University of New York at Buffalo, Report No. NCEER-97-0022, pp. 225–76.

Ooi, E. T. C. (1987). "Investigation of Liquefaction in the Buller Region." Masters Thesis, University of Canterbury, Christchurch, New Zealand.

O'Rourke, T. D. (1998). "An overview of geotechnical and lifeline earthquake engineering." Proc., Geotechnical Earthquake Engineering and Soil Dynamics – III, ASCE, 1392-1426.

Palmgren, A. (1924). "Die lebensdauer von kugella geru." ZVDI, 68(14), 339–341.

Park, S.-S., and Kim, Y.-S. (2013). "Liquefaction resistance of sands containing plastic fines with different plasticity." Journal of Geotechnical and Geoenvironmental Engineering, ASCE, 139(5), 825-830.

Pass, D. G. (1994). *Soil characterization of the deep accelerometer site at Treasure Island, San Francisco, California*. MS thesis in Civil Engineering, University of New Hampshire, May.

PEER (2000a). "Documenting Incidents of Ground Failure Resulting from the Aug. 17, 1999, Kocaeli, Turkey Earthquake." http://peer.berkeley.edu/publications/turkey/adapazari/index.html (last accessed 9/2013).

PEER (2000b). "Documentation of Soil Conditions at Liquefaction Sites from 1999 Chi-Chi, Taiwan Earthquake." http://peer.berkeley.edu/lifelines/research_projects/3A02/ (last accessed 9/2013).

Pillai, V. S., and Byrne, P. M. (1994). "Effect of overburden pressure on liquefaction resistance of sand." Canadian Geotechnical Journal, 31, 53-60.

Pillai, V. S., and Stewart, R. A. (1994). "Evaluation of liquefaction potential of foundation soils at Duncan Dam." Canadian Geotechnical Journal, 31, 951-966.

Phoon, K. K. and Kulhawy, F. H. (1999). "Characterization of geotechnical variability." Canadian Geotechnical Journal 36(4): 612–624.

Porcella, R., Etheredge, E., Maley, R., and Switzer, J. (1987). Strong-motion data from the Superstition Hills Earthquakes of 0154 and 1315 (GMT), November 24, 1987. US Geological Survey Open-File Report 87-672, December, 60 pp.

Randolph, M. F. (2004). "Characterisation of soft sediments for offshore applications." Proc., Int. Conf. on Geotechnical and Geophysical Site Characterization, ISC-2, Millpress, The Netherlands, 209–232.

Rees, S. D. (2010). "Effects of fines on the undrained behavior of Christchurch sandy soils." Ph.D. thesis, University of Canterbury, Christchurch, New Zealand, May, 300 pp.

Robertson, P.K. (1990). "Soil classification using the cone penetration test." Canadian Geotechnical J. 27(1), 151–58.

Robertson, P. K. (2009). "Interpretation of cone penetration tests – a unified approach." Canadian Geotechnical Journal, 46: 1337-1355.

Robertson, P. K., and Wride, C. E. (1997). "Cyclic liquefaction and its evaluation based on SPT and CPT." in Proceedings, NCEER Workshop on Evaluation of Liquefaction Resistance of Soils,

Robertson, P. K., and Wride, C. E. (1998). "Evaluating cyclic liquefaction potential using the cone penetration test." Canadian Geotechnical J. 35(3), 442–59.

Robinson, K., Cubrinovski, M., and Bradley, B.A. (2013). "Comparison of actual and predicted measurements of liquefaction-induced lateral displacements from the 2010 Darfield and 2011 Christchurch Earthquakes." Proc. 2013 Conference of the New Zealand Society for Earthquake Engineering (NZSEE 2013), Wellington, New Zealand, 26-28 April.

Sancio, R. B. (2003). Ground failure and building performance in Adapazari, Turkey. Ph.D. thesis, University of California, Berkeley, 790 pp.

Salgado, R., Boulanger, R. W., and Mitchell, J. K. (1997a). Lateral stress effects on CPT liquefaction resistance correlations, *J. Geotechnical and Geoenvironmental Eng.*, ASCE **123**(8), 726–35.

Salgado, R., Mitchell, J. K., and Jamiolkowski, M. (1997b). Cavity expansion and penetration resistance in sands, *J. Geotechnical and Geoenvironmental Eng.*, ASCE **123**(4), 344–54.

Seed, H. B., and Idriss, I. M. (1967). "Analysis of liquefaction: Niigata earthquake." Proc., ASCE, 93(SM3), 83-108.

Seed, H. B., and Idriss, I. M. (1971). "Simplified procedure for evaluating soil liquefaction potential." *J. Soil Mechanics and Foundations Div.*, ASCE **97**(SM9), 1249–273.Seed, H. B., and Idriss, I. M. (1982). *Ground Motions and Soil Liquefaction During Earthquakes*, Earthquake Engineering Research Institute, Oakland, CA, 134 pp.

Seed, H. B., and Idriss, I. M. (1981). "Evaluation of Liquefaction Potential of Sand Deposits Based on Observations of Performance in Previous Earthquakes." Preprint 81 544, Session on In Situ Testing to Evaluate Liquefaction Susceptibility, ASCE National Convention, St. Louis, MO, October.

Seed, H. B., Idriss, I. M., Makdisi, F., and Banerjee, N. (1975). Representation of irregular stress time histories by equivalent uniform stress series in liquefaction analyses. Report No. EERC 75-29, Earthquake Engineering Research Center, University of California at Berkeley, CA, October.

Seed, H. B., Tokimatsu, K., Harder, L. F. Jr., and Chung, R. (1984). The influence of SPT procedures in soil liquefaction resistance evaluations. Earthquake Engineering Research Center, University of California, Berkeley, Report No. UCB/EERC-84/15, 50 pp.

Seed, H. B., Tokimatsu, K., Harder, L. F. Jr., and Chung, R. (1985). "Influence of SPT procedures in soil liquefaction resistance evaluations." Journal of Geotechnical Engineering, ASCE, 111(12), 1425-1445.

Shibata, T., and Teparaksa, W. (1988). "Evaluation of liquefaction potentials of soils using cone penetration tests." Soils and Foundations, Tokyo, Japan, 28(2), 49–60.

Silver, M. L., Chan, C. K., Ladd, R.S., Lee, K. L., Tiedemann, D. A., Townsend, F. C., Valera, J. E. and Wilson, J. H. (1976). "Cyclic triaxial strength of standard test sand." Journal of ASCE, 102, GT5, 511-523.

Skempton, A. W. (1986). "Standard penetration test procedures and the effects ins ands of overburden stress, relative density, particle size, aging and overconsolidation." Geotechnique, 36(3), 425-47.

Stark, T. D., and Olson, S. M. (1995). "Liquefaction resistance using CPT and field case histories." J. Geotechnical Eng., ASCE 121(12), 856–69.

Stewart, J. P., Abrahamson, N. A., Atkinson, G. M., Baker, J. W., Boore, D. M., Bozorgnia, Y., Campbell, K. W., Comartin, C. D., Idriss, I. M., Lew, M., Mehrain, M., Moehle, J. P., Naeim, and Sabol, T. A. (2011). "Representation of bidirectional ground motions for design spectra in building codes." Earthquake Spectra, EERI, 27(3), 927-937.

Suzuki, Y., Tokimatsu, K., Taya, Y., and Kubota, Y. (1995). "Correlation between CPT data and dynamic properties of in situ frozen samples." in Proceedings, 3rd International Conference on Recent Advances in Geotechnical Earthquake Engineering and Soil Dynamics, Vol. I, St. Louis, MO.

Suzuki, Y., Koyamada, K., and Tokimatsu, K. (1997). "Prediction of liquefaction resistance based on CPT tip resistance and sleeve friction." in Proceedings, 14th International Conference on Soil Mechanics and Foundation Engineering, Hamburg, Germany, Vol. 1, pp. 603–06.

Suzuki Y., Sanematsu, T., and Tokimatsu, K. (1998). "Correlation between SPT and seismic CPT." In: Robertson PK, Mayne PW (eds.), in Proceedings, Conference on Geotechnical Site Characterization, Balkema, Rotterdam, pp. 1375–380.

Suzuki, Y., Tokimatsu, K., Moss, R. E. S., Seed, R. B., and Kayen, R. E. (2003). "CPT-based liquefaction case histories from the 1995 Hyogoken-Nambu (Kobe) earthquake, Japan." Geotech. Engrg. Res. Rept. No. UCB/GE-2003/03, May.

Tatsuoka, F., Ochi, K., Fujii, S., and Okamoto, M. (1986). "Cyclic undrained triaxial and torsional shear strength of sands for different sample preparation methods." Soils and Foundations, JSSMFE, 26(3), 23-41.

Toki, S., Tatsuoka, F., Miura, S., Yoshimi, Y., Yasuda, S. and Makihara, Y. (1986). "Cyclic undrained triaxial strength of sand by a cooperative test program." Soils and Foundations, 26, 117-128.

Tokimatsu, K., Tamura, S., Suzuki, H., and Katsumata, K. (2012). "Building damage associated with geotechnical problems in the 2011 Tohoku Pacific Earthquake." Soils and Foundations, Japanese Geotechnical Society, 52(5): 956-974.

Toprak, S., and Holzer, T. L. (2003). "Liquefaction potential index: Field assessment." Journal of Geotechnical and Geoenvironmental Engineering, ASCE, 129(4), 315-322.

Toprak, S., Holzer, T. L., Bennett, M. J., Tinsley, J. C. (1999). "CPT- and SPT-based probabilistic assessment of liquefaction potential." Proceedings of Seventh US Japan Workshop on Earthquake Resistant Design of Lifeline Facilities and Counter-measures Against Liquefaction, T. D. O'Rourke, J. P. Bardet, and M. Hamada, eds., Report MCEER-99-0019, MCEER, NY.

Towhata, I., Gunji, K., Hernandez, Y. A., and Yamada, S. (2013). "Laboratory tests on cyclic undrained behavior of loose sand with cohesionless silt and its application to assessment of seismic performance of subsoil." New Zealand – Japan Workshop on Soil Liquefaction during Recent Large-Scale Earthquakes, Dec 2-3, University of Auckland, NZ, paper 8.

Van Ballegooy, S., Malan, P., Lacrosse, V., Jacka, M. W., Cubrinovski, M., Bray, J. D., O'Rourke, T. D., Crawford, S. A., and Cowan, H. (2014). "Assessment of liquefaction-induced land damage for residential Christchurch." Earthquake Spectra, Earthquake Engineering Research Institute, in-press.

Worden, C. B., Wald, D. J., Allen, T. I., Lin, K., and Cua, G. (2010). "Integration of macroseismic and strong-motion earthquake data in ShakeMap for real-time and historic earthquake analysis." USGS web site, http://earthquake.usgs.gov/earthquakes/shakemap/.

Yoshimi, Y., Tokimatsu, K., Kaneko, O., and Makihara, Y. (1984). Undrained cyclic shear strength of a dense Niigata sand, *Soils and Foundations*, Japanese Society of Soil Mechanics and Foundation Engineering **24**(4), 131–45.

Yoshimi, Y., Tokimatsu, K., and Hosaka, Y. (1989). "Evaluation of liquefaction resistance of clean sands based on high-quality undisturbed samples." Soils and Foundations, 29(1), 93-104.

Youd, T. L. (2013). Discussion of "Examination and reevaluation of SPT-based liquefaction triggering case histories." Journal of Geotechnical and Geoenvironmental Engineering, ASCE, 138(8), 2000-2001.

Youd, T. L., and Bennett, M. J. (1983). "Liquefaction sites, Imperial Valley, California." Journal of the Geotechnical Engineering Division, ASCE, 109(3), 440-457.

Youd, T. L., and Carter, B. L. (2005). "Influence of soil softening and liquefaction on spectral acceleration." Journal of Geotechnical and Geoenvironmental Engineering, ASCE, 131(7), 811-825.

Youd, T. L, and Noble, S. K. (1997). "Liquefaction criteria based on statistical and probabilistic analyses." Proceedings of the NCEER workshop on evaluation of liquefaction resistance of soils, Technical Report NCEER-97-022, 201–205.

Youd, T. L., Idriss, I. M., Andrus, R. D., Arango, I., Castro, G., Christian, J. T., Dobry, R., Finn, W. D. L., Harder, L. F., Hynes, M. E., Ishihara, K., Koester, J. P., Liao, S. S. C., Marcuson, W. F., Martin, G. R., Mitchell, J. K., Moriwaki, Y., Power, M. S., Robertson, P. K., Seed, R. B., and Stokoe, K. H. (2001). Liquefaction resistance of soils: summary report from the 1996 NCEER and 1998 NCEER/NSF workshops on evaluation of liquefaction resistance of soils, *J. Geotechnical and Geoenvironmental Eng.,* ASCE 127(10), 817–33.

Youd, T. L., DeDen, D. W., Bray, J. D., Sancio, R., Cetin, K. O., and Gerber, T. M. (2009). "Zero-displacement lateral spreads, 1999 Kocaeli, Turkey, earthquake." J. Geotechnical and Geoenvironmental Eng., ASCE, 135(1), 46-61.

Zhao, J. X., Dowrick, D. J., and McVerry, G. H. (1997). "Attenuation of Peak Ground Accelerations in New Zealand Earthquakes." Bulletin of the New Zealand National Society for Earthquake Engineering, 30(2), 133-158.

Zhou, S. (1980). "Evaluation of the liquefaction of sand by static cone penetration test." in Proceedings, 7th World Conference on Earthquake Engineering, Istanbul, Turkey, Vol. 3, 156-162.

Zhou, S. G., and Zhang, S. M. (1979). "Liquefaction investigation in Tangshan District." Report to Ministry of Railway, China (in Chinese).

Ziotopoulou, K., and Boulanger, R. W. (2012). "Constitutive modeling of duration and overburden effects in liquefaction evaluations." 2nd International Conference on Performance-Based Design in Earthquake Geotechnical Engineering, ISSMGE, Taormina, Italy, May 28-30, paper no. 03.10, 467-482.

APPENDIX A:

MAGNITUDE SCALING FACTOR

APPENDIX A:

MAGNITUDE SCALING FACTOR

A.1. Introduction

Magnitude scaling factor (MSF) relationships are used in liquefaction triggering correlations to approximately account for how the characteristics of the irregular cyclic loading produced by different magnitude earthquakes affect the potential for triggering of liquefaction. MSF relationships depend on the characteristics of both the imposed loading and the soil's loading response, as expected for any type of fatigue problem. MSF relationships developed for sands (e.g., Seed et al. 1975, Idriss 1999, Liu et al. 2001, Green and Terri 2005) have mostly been developed using typical properties for clean sands, such that the MSF relationships do not include functional dependence on any soil property. The MSF relationship developed by Boulanger and Idriss (2007) for cyclic softening analyses of clays similarly used typical properties for clays and plastic silts, and thus also did not included functional dependence on any soil property. Cetin and Bilge (2012) introduced MSF relationships that depended on the failure criterion (strain or pore pressure ratio based) and dilational response of the soil (which depends on relative density and overburden stress). Kishida and Tsai (2014) presented a MSF relationship which includes functional dependence on the soil parameter (b) which describes the slope of the relationship between cyclic resistance ratio (CRR) and number of uniform loading cycles to failure (N). The strong effect of soil properties on MSF relationships is illustrated in Figures A.1 and A.2 showing the MSF relationships from Boulanger and Idriss (2007) and Kishida and Tsai (2014).

The purpose of the MSF relationship as a functional component in a liquefaction analysis framework is to account for the primary influencing variables while maintaining sufficient simplicity for implementation in practice. Fundamentally, the MSF is known to be physically affected by numerous factors, including the earthquake source characteristics, distance from the site to the source, soil profile characteristics, and depth in the soil profile (e.g., Liu et al. 2001, Green and Terri 2005), but the inclusion of all dependencies may not be warranted in practice. The benefits of progressively including additional influencing variables in an MSF relationship can instead be evaluated by the degree to which it: (1) reduces bias or dispersion between the liquefaction case history data and the liquefaction triggering correlation, or (2) is considered important for extending the correlation beyond the range of conditions covered by the case history data.

This Appendix presents the development of the revised MSF relationship used in the liquefaction analysis framework described in Section 2 of this report. The MSF relationship was revised to include functional dependence on an index of the soil properties in addition to the earthquake magnitude M. The following sections describe the procedure used for weighting of irregular loading cycles, a review of cyclic testing literature to evaluate how the parameter b varies with soil type or other factors, the effect of the parameter b on the equivalent number of loading cycles, and the synthesis of those results into an MSF relationship suitable for implementation in practice. The revised MSF relationship was used in the processing of the CPT-based and SPT-based case histories, as described in the body of this report. The fits between the case history data and the updated liquefaction triggering procedures are presented in Sections 4 and 6 for the CPT and SPT, respectively.

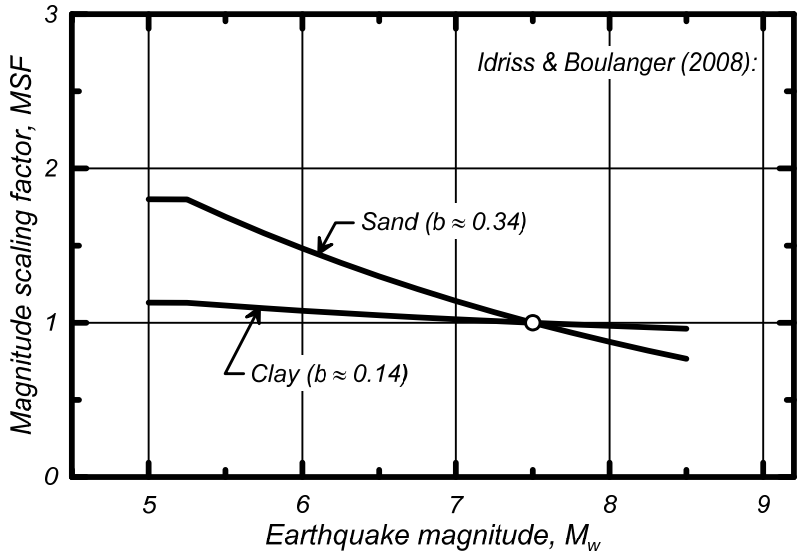

Figure A.1. MSF relationships for clay and sand (Boulanger and Idriss 2007)

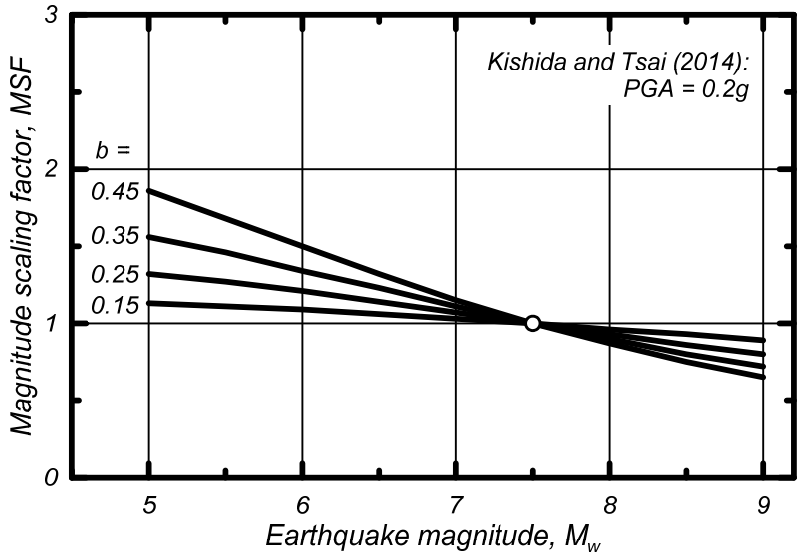

Figure A.2. MSF relationships by Kishida and Tsai (2014)

A.2. Weighting of irregular loading cycles

Seed et al. (1975) introduced a weighting scheme for converting an irregular cyclic loading history to some equivalent number of uniform loading cycles. This weighting scheme, which has been used in later studies (e.g., Idriss 1999, Liu et al. 2001, Boulanger and Idriss 2007, Kishida and Tsai 2014), was shown by Green and Terri (2005) to be similar to the Palmgren-Miner cumulative damage hypothesis (Palmgren 1924, Miner 1945) for high-cycle fatigue of metals. A key parameter in these procedures is the slope of the relationship between the CRR and number of uniform loading cycles to failure (N). The CRR versus N relationship, over the range of N values important to earthquake loading, can often be reasonably approximated using a power law as,

$$CRR = a \cdot N^{-b} \tag{A.1}$$

where the fitting parameter b describing the slope of the relationship. For two individual stress cycles having magnitudes CSR_A and CSR_B, the relative number of cycles to cause failure at these two stress ratios can be obtained from the above relationship as,

$$\frac{N_A}{N_B} = \left(\frac{CSR_B}{CSR_A} \right)^{1/b} \tag{A.2}$$

The damage from one cycle of stress at CSR_B would then be equivalent to the damage from X_A cycles at CSR_A if their numbers of cycles are an equal fraction of the number of cycles to failure at their respective CSRs. This leads to the expression,

$$X_A = \left(\frac{CSR_B}{CSR_A} \right)^{1/b} \left(1 \, cycle \, at \, CSR_B \right) \tag{A.3}$$

This expression can be used to convert individual stress cycles into an equivalent number of uniform cycles at some reference stress level. The total number of equivalent uniform cycles at a reference stress level can then be determined for a wide range of earthquake ground motions, from which a representative number of equivalent uniform cycles can be obtained for a given earthquake magnitude (N_M). The MSF can then be determined as,

$$MSF = \frac{CSR_M}{CSR_{M=7.5}} = \left(\frac{N_{M=7.5}}{N_M} \right)^b \tag{A.4}$$

where $N_{M=7.5}$ is the number of uniform cycles for M = 7.5.

The effect of b on the MSF relationships was previously illustrated in Figures A.1 and A.2. The MSF relationship derived by Idriss (1999) for sands used b = 0.34 based on cyclic test data by Yoshimi et al. (1984) for samples of Niigata sand obtained using frozen sampling techniques. The MSF relationship by Boulanger and Idriss (2007) for clays and plastic silts used b = 0.135 for clays and plastic silts based on a compilation of cyclic testing data. The smaller b value for clays and plastic silts results in a much flatter MSF relationship than was obtained for sands, as shown in Figure A.1.

The MSF relationships by Kishida and Tsai (2014) in Figure A.2 can be compared to those of Idriss (1999) and Boulanger and Idriss (2007) in Figure A.1. The Kishida-Tsai MSF relationships are based on analyses of more than 3500 ground motion records for site class D conditions from the PEER strong ground motion database and include functional dependence on the peak ground acceleration, a spectral ratio parameter describing the shape of the acceleration response spectra, the earthquake magnitude, the parameter b, and the period of the soil layer. The Kishida-Tsai MSF curves shown in Figure A.2 are based on a strike-slip earthquake, a peak ground acceleration of 0.20 g, and the expected value for the spectral shape based on a ground motion prediction equation. The Kishida-Tsai MSF for b = 0.15 is in good agreement with the Boulanger-Idriss MSF for the similar value of b = 0.135. The Kishida-Tsai MSF for b = 0.35 is, however, a bit flatter than the Idriss MSF for b = 0.34.

The difference in MSF curves for b ≈ 0.35 in Figure A.2 can be explained as follows. Kishida and Tsai's (2014) results indicated that the equivalent number of loading cycles for b = 0.35 and M = 5.25 would be about 5 to 6. Idriss (1999) considered the case where a small M event is dominated by a single pulse (taken as ¾ cycles), from which he computed an equivalent number of uniform cycles at 65% of the peak stress of 2.7. For design purposes, Idriss chose to use this minimum loading case to anchor the MSF at M = 5.25. For M = 7.5, the two studies obtained similar numbers of equivalent uniform loading cycles; 17.3 by Kishida and Tsai versus 15 by Idriss. The difference in the MSF curves can now be explained using Equation A.4 and seeing that at M = 5.25; the ratio $N_{M=7.5}/N_M$ is smaller for the results by Kishida and Tsai (17.3/5.5 ≈ 3.1) than from Idriss (15/2.7 ≈ 5.6). These MSF differences are not large, however, considering the large uncertainty in the estimated numbers of equivalent uniform loading cycles and other ground motion characteristics as described in Kishida and Tsai (2014).

A.3. Experimental data for b values

For clean sands, experimental data compiled from the literature shows that the b value tends to increase with increasing CRR (for the same number of cycles to failure) or relative density. Results of cyclic tests on sands obtained using frozen sampling techniques are summarized in Figures A.3 and A.4. The data obtained by Yoshimi et al. (1989) for five sites show b values of 0.34 for the densest site (curve D in Figure A.3), values of 0.41, 0.27 and 0.13 for the sites with intermediate strengths (curves C3, C1, and B), and a value of 0.15 for the weakest site (curve A). The sand from Duncan Dam (Pillai and Stewart 1994, Figure A.3) also has very low cyclic strengths and the lowest b value of 0.08. The data obtained by Okamura et al. (2003; Figure A.4) at a site treated by sand compaction piles similarly show a consistent variation with denseness of the sand; the densest and strongest sands had b values of 0.45, 0.50, and 0.54, whereas the looser and weaker sands had b values of 0.13, 0.15, and 0.21.

Cyclic tests on reconstituted samples of clean sand show similar trends to those from frozen samples. For example, the cyclic tests by Silver et al. (1976) for D_R = 60% Monterey sand show intermediate cyclic strengths with a b value of 0.22, whereas the cyclic tests by Toki et al. (1986) for D_R = 50% Toyoura sand show much smaller cyclic strengths with a smaller b value of 0.10 (Figure A.5). The cyclic direct simple shear tests by Boulanger and Seed (1995) for reconstituted sand showed b values of 0.17 and 0.15 at D_R of 35% and 45%, respectively, but a higher b value of 0.27 for D_R of 55% (Figure A.6). The cyclic shaking table tests by DeAlba et al. (1976) for reconstituted sand at D_R ranging from 54% to 90% are a notable exception, in that they show b values of 0.21 to 0.25 without any apparent trend with D_R (Figure A.7).

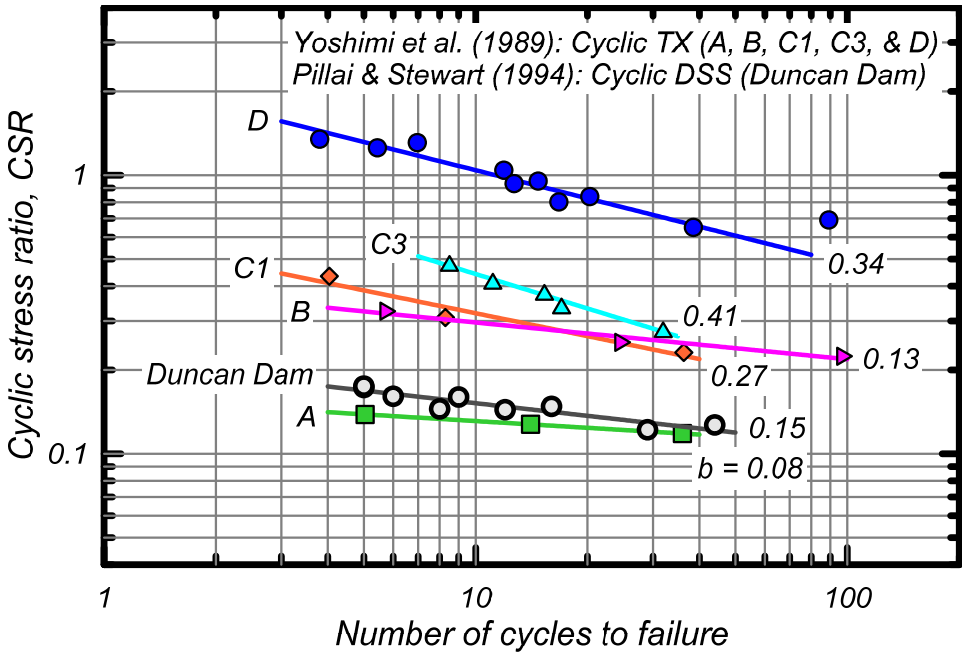

Figure A.3. Cyclic tests on sands obtained by frozen sampling techniques – data from Yoshimi et al. (1989) and Pillai and Stewart (1994)

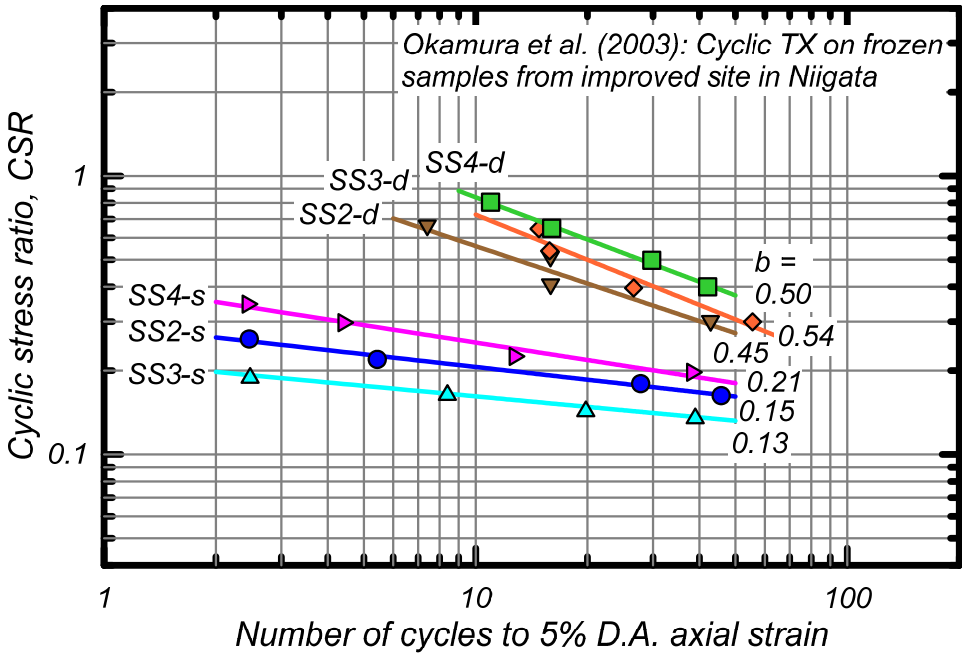

Figure A.4. Cyclic tests on sands obtained by frozen sampling techniques – data from Okamura et al. (2003)

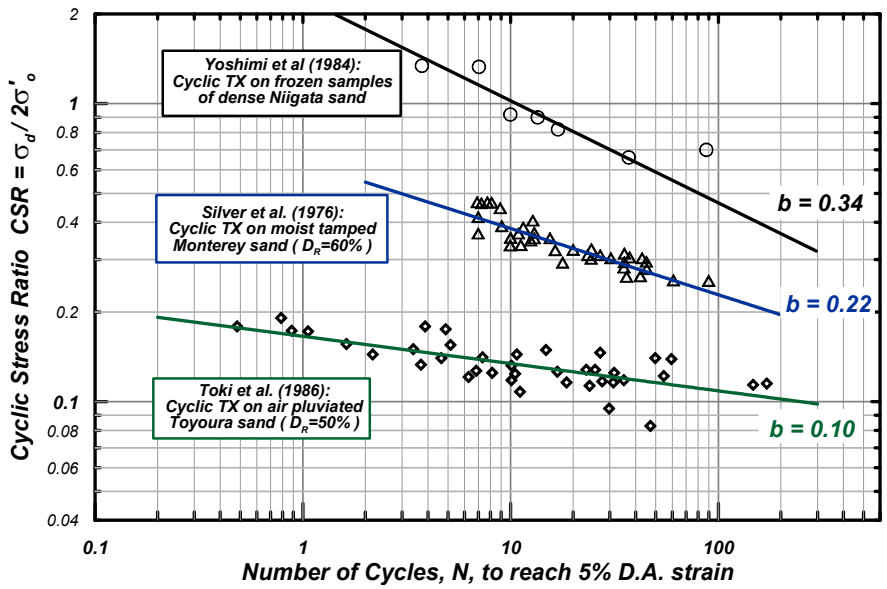

Figure A.5. Cyclic tests on reconstituted sands by Toki et al. (1986) and Silver et al. (1976) with the data on frozen sand sample by Yoshimi et al. (1984) for comparison.
(from Ziotopoulou and Boulanger 2012)

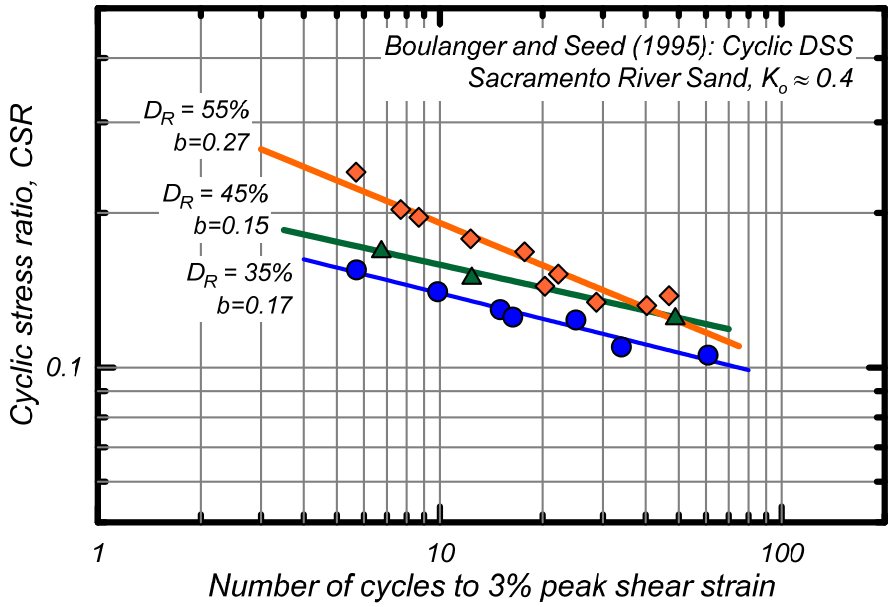

Figure A.6. Cyclic simple shear tests on reconstituted clean sand by Boulanger and Seed (1995)

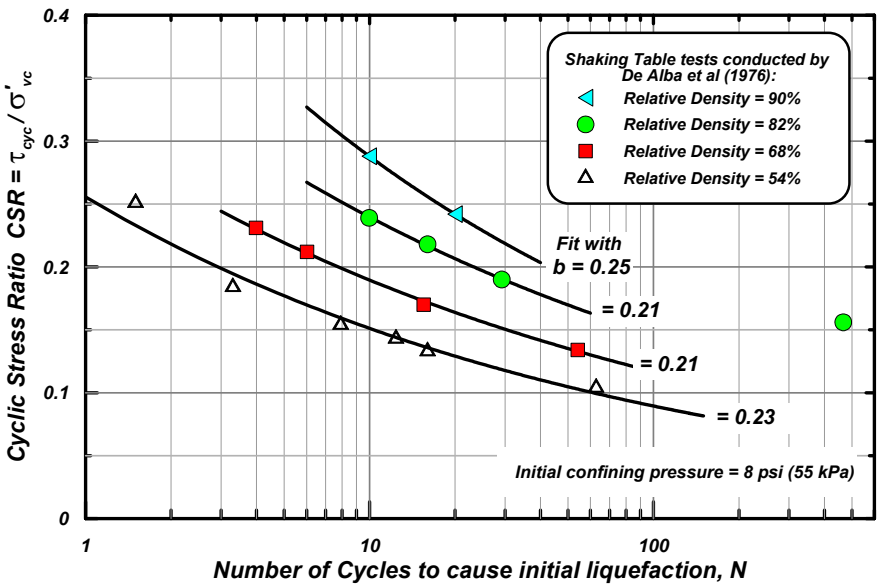

Figure A.7. Cyclic tests on clean sand by De Alba et al. (1976)
(from Ziotopoulou and Boulanger 2012)

Cyclic triaxial and cyclic torsional shear tests on Toyoura and Sengenyama sands by Tatsuoka et al. (1986) demonstrate a number of other factors affecting the shape and slope of the CRR versus N curves. For example, their results for cyclic torsional shear tests and cyclic triaxial tests indicated that the cyclic triaxial tests tended to produce steeper curves at lower numbers of cycles than were obtained in the cyclic torsional shear tests. This trend is, however, opposite to Seed et al.'s (1975) observation that cyclic triaxial tests gave flatter curves than obtained using simple shear tests. The results of Tatsuoka et al. also showed that the slope increased with increasing values for the failure strain used to define the CRR, which suggests that magnitude duration effects may be different when evaluating the potential for large strains and deformations versus evaluating the onset of triggering alone (e.g., a shear strain of about 3%). Furthermore, their results showed that the cyclic strength curves became more strongly curved at low numbers of cycles as the relative density of the specimens increased and the failure strain criterion increased. This latter observation is illustrated by their results in Figure A.8 for cyclic torsional shear tests on Sengenyama sand air pluviated to relative densities ranging from 40-95% and plotted for a failure strain criterion of 15% double-amplitude shear strain. The curves for the denser specimens are more strongly curved than a power law fit can approximate, showing that the b parameter will depend on the range of cycles over which it is fit (the average values listed on the figure are based on a power fit over the range of the data provided). Lastly, these and other results by Tatsuoka et al. (1986) also show effects of the sample preparation method, the consolidation stress conditions, and the specific sand being tested.

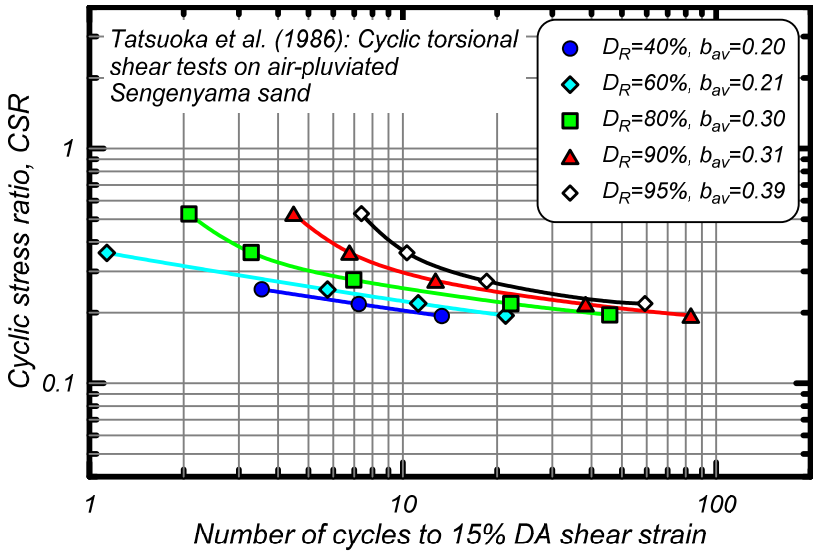

Figure A.8. Cyclic stress ratio to cause 15% double-amplitude shear strain in anisotropically-consolidated cyclic undrained torsional shear tests (after Tatsuoka et al. 1986)

Cyclic tests on reconstituted silty sands with nonplastic fines have also shown similar trends. Cyclic triaxial tests on Ottawa sand with 0, 5, 10, and 15% nonplastic fines by Carraro et al. (2003) showed b values ranging from 0.09 to 0.44, with the b values generally increasing with increasing value of CRR (for the same number of cycles to failure) regardless of FC (Figure A.9). Similarly, cyclic triaxial tests on reconstituted Fitzgerald bridge sand with 1, 10, 20, and 30% nonplastic fines by Rees (2010) showed b values ranging from 0.22 to 0.4,with the b values generally increasing with increasing value of CRR (for the same number of cycles to failure) regardless of FC (Figure A.10). Cyclic torsional shear tests by Towhata et al. (2013) on loose Tokyo Bay sand ejecta with 0, 10, 20, 30, 40, 60, and 80% nonplastic fines prepared with similar compaction energies showed b values of about 0.07-0.23 with no apparent trend with respect to FC (Figure A.11). Cyclic direct simple shear tests Dahl et al. (2014) on undisturbed samples of a normally consolidated, silty sand and sandy silt stratum (FC = 35-77%) showed a b value of about 0.14 (Figure A.12).

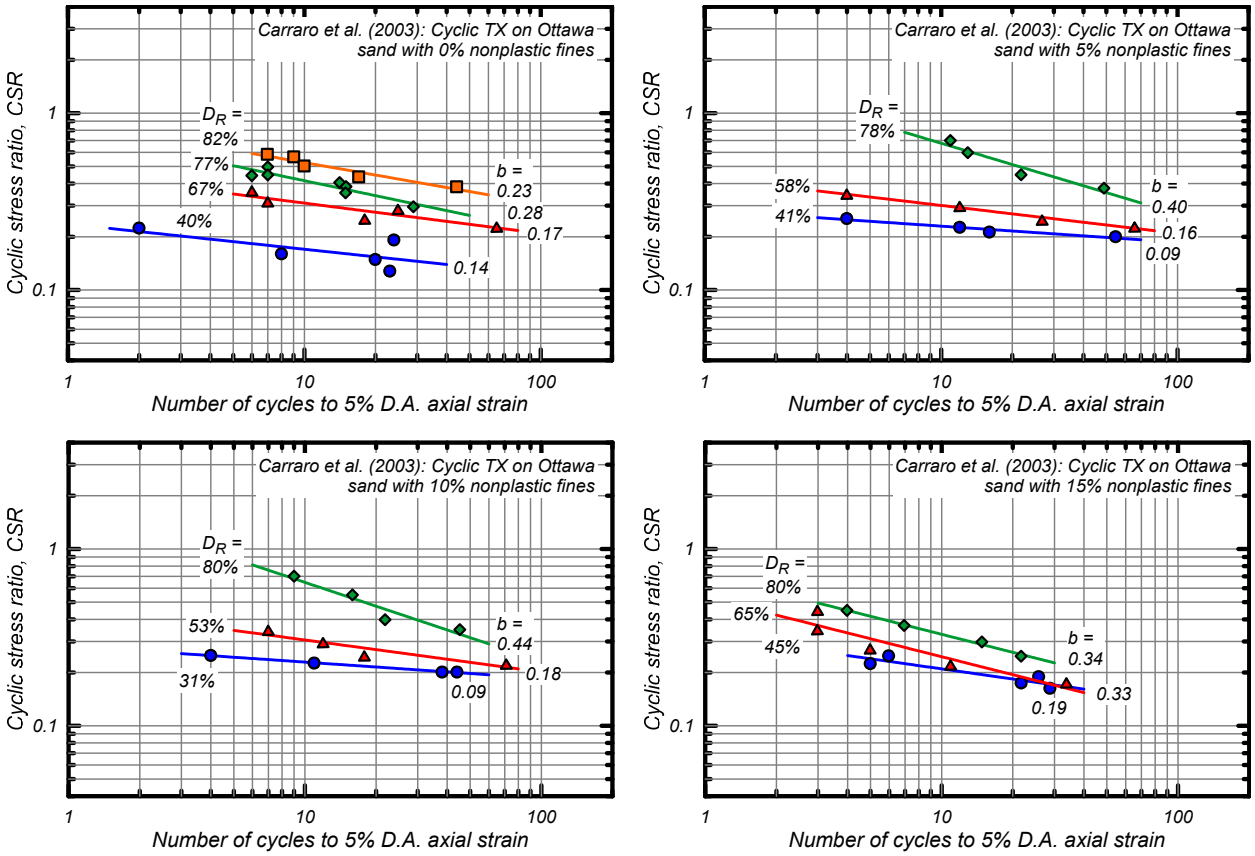

Figure A.9. Cyclic stress ratio to cause 5% double-amplitude shear strain for Ottawa sand with 0, 5, 10, and 15% nonplastic fines (after Carraro et al. 2003)

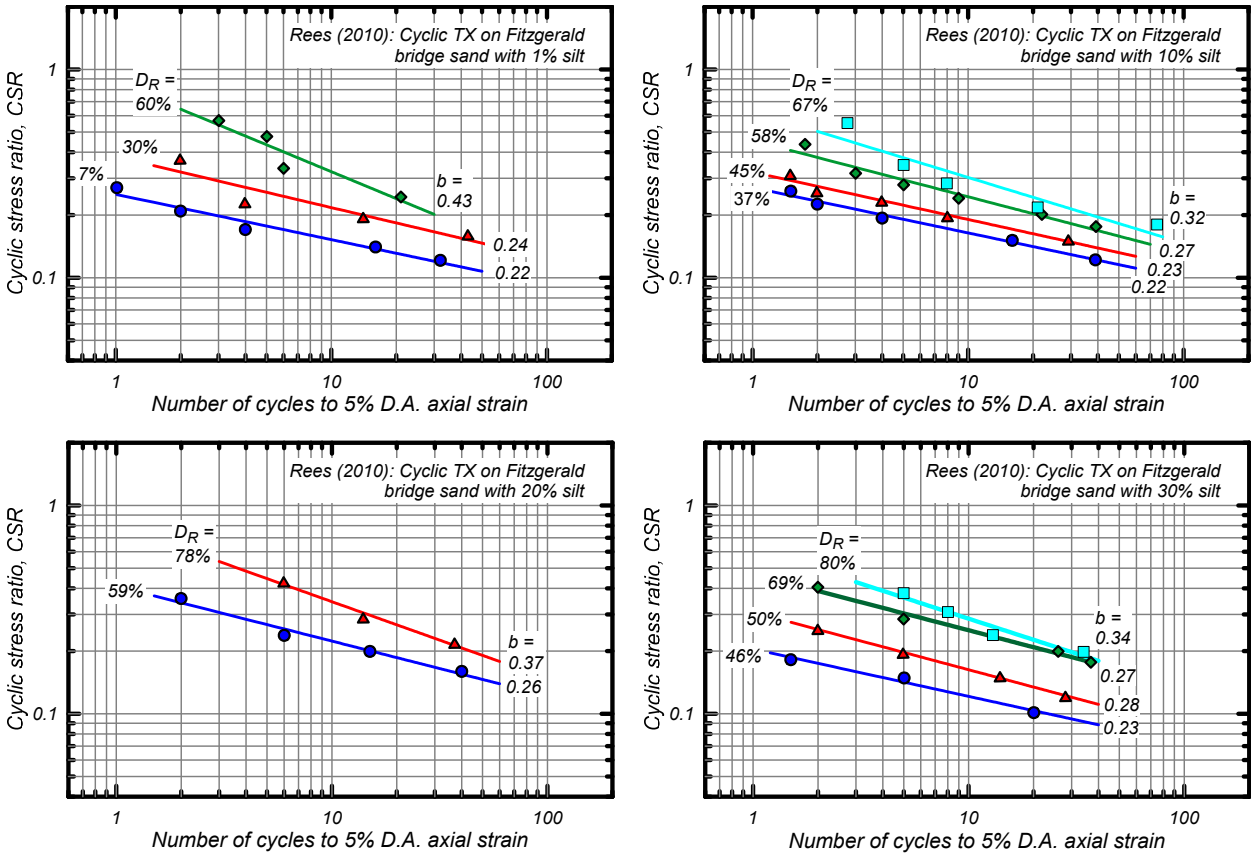

Figure A.10. Cyclic stress ratio to cause 5% double-amplitude shear strain for Fitzgerald bridge sand with 1, 10, 20 and 30% nonplastic fines (after Rees 2010)

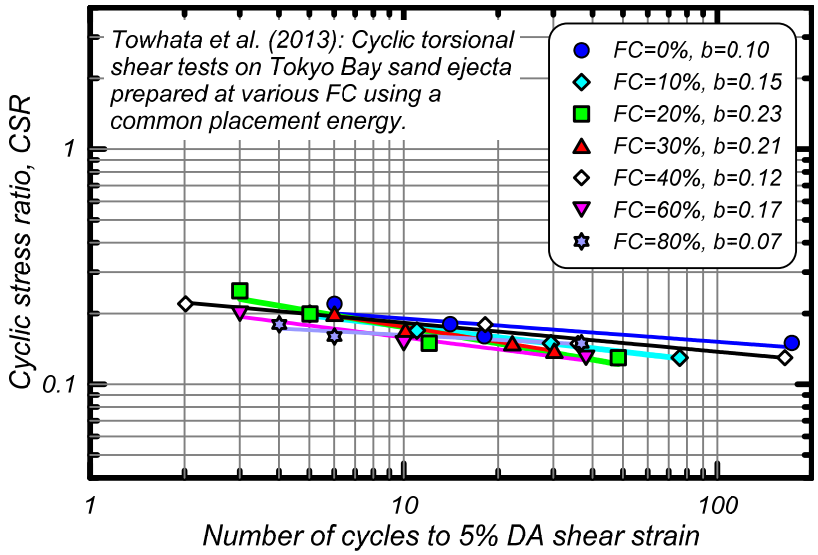

Figure A.11. Cyclic stress ratio to cause 5% double-amplitude shear strain for Tokyo Bay sand ejecta with 0-80% nonplastic fines (after Towhata et al. 2013)

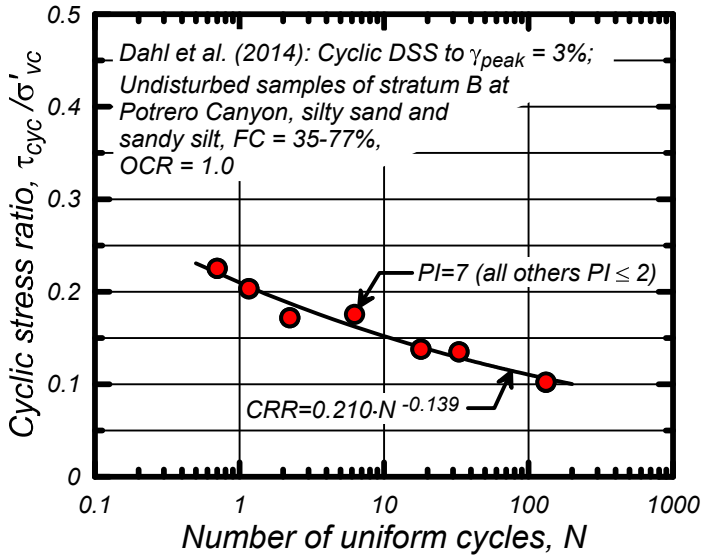

Figure A.12. Cyclic stress ratio to cause 3% single-amplitude shear strain for undisturbed samples of a silty sand and sandy silt with 35-77% fines (after Dahl et al. 2014)

Cyclic tests on reconstituted clayey sands with low-plasticity fines have shown similar trends as well. Cyclic tests by Kokusho et al. (2012) on a sand with 0, 5, 10, and 20% silty and clayey fines (PI = 6) produced b values of about 0.08 to 0.13 when loose ($D_R \approx 30\%$) and about 0.17 to 0.28 when dense ($D_R \approx 70\%$). Cyclic triaxial tests by Kondoh et al. (1987) on Sengenyama sand with 30% Kaolin prepared at overconsolidation ratios (OCR) of 1, 2, and 4 showed b values of 0.14, 0.22, and 0.28, respectively; the increase of b value with increasing OCR may reflect increases in density as well as the effects of OCR. Cyclic tests by Park and Kim (2013) on sand with FC = 10% with the fines having PI values of 8, 18, 50, and 377 produced b values of about 0.14 for loose specimens and about 0.19 for dense specimens. Isotropically and anisotropically consolidated cyclic triaxial tests by Hyde et al. (2006) on sedimented specimens of a low plasticity silt (powdered limestone; PI = 6) showed a b value of 0.23 for cases with shear stress reversal and 0.28 for cases with no shear stress reversal.

Dahl (2011) compiled cyclic test data for a wide range of plastic fine-grained soils, from which the b values were examined for any trend with regard to FC or fines PI. For example, the cyclic test data for six different clays shown in Figure A.13 have b values of 0.10 to 015. The full dataset from Dahl is summarized in Figure A.14; the distinction between Groups A and B are based on issues of sampling disturbance, with sampling disturbance being less of a concern for the Group A soils. These data show considerable scatter, but the general trend is that the average b value is between 0.1 and 0.135 for FC from 45 to 100% and PI from 2 to 30.

The preceding examples of laboratory test data illustrate how the slopes of the cyclic strength curves can vary with denseness (or state), FC, fines plasticity, failure strain, number of cycles to failure (i.e., slope is not constant), and test device. There is significant variability in the slopes obtained in these various studies and in the observed effects of each of the above factors. The dominant factor does, however, appear to be the denseness (or state) of the soil, and thus its influence on MSF relationships is explored further in the following sections.

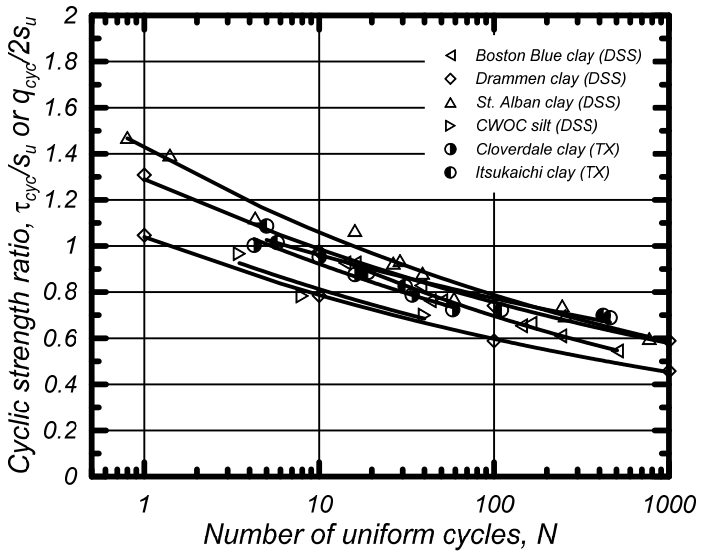

Figure A.13. Cyclic stress ratio to cause 3% single-amplitude shear strain for a set of fine-grained soils; b values range from 0.10 to 0.15 (from Boulanger and Idriss 2007)

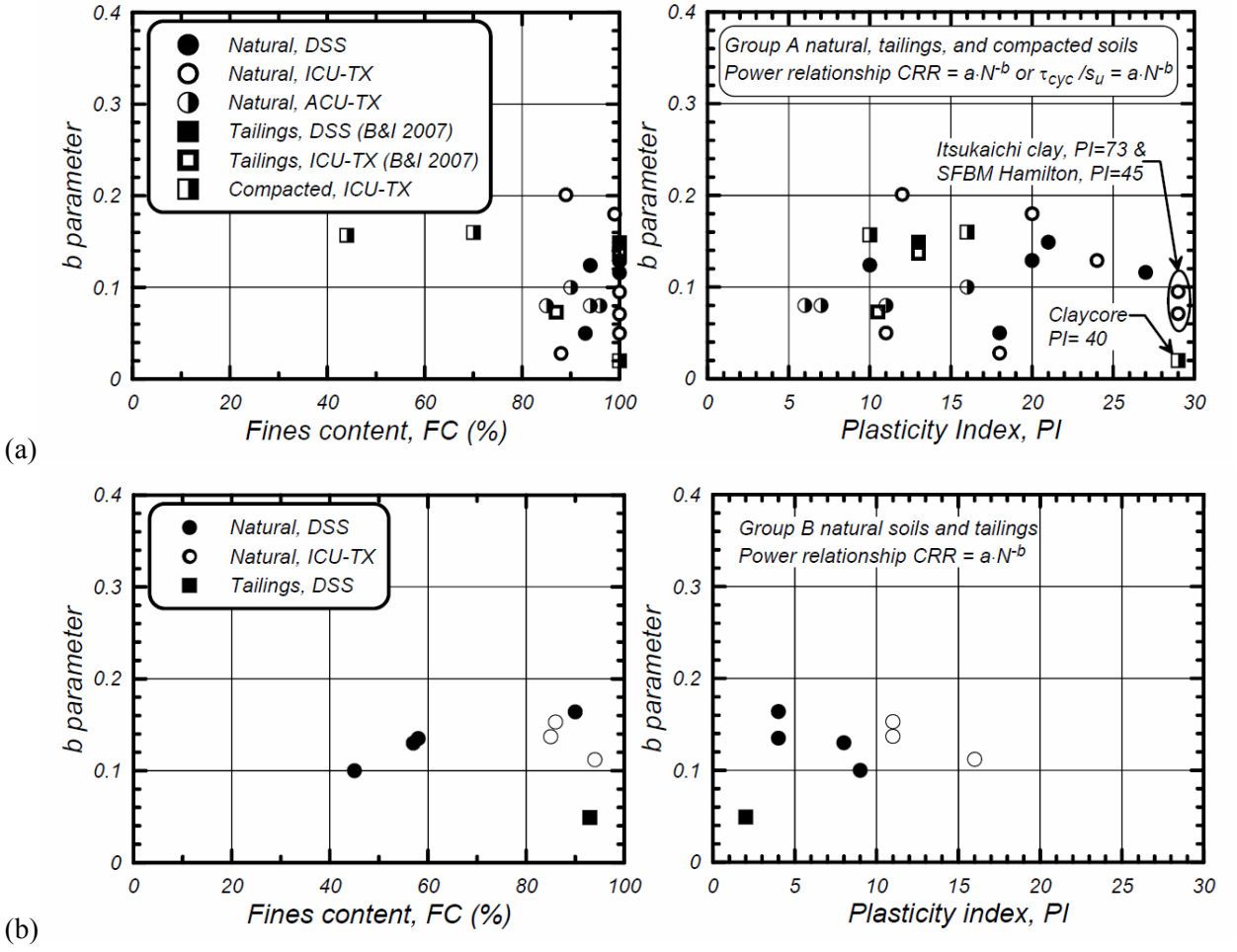

Figure A.14. Variation of b with FC and PI for fine-grained soils: (a) Group A soils, and (b) Group B soils. (from Dahl 2011)

A.4. Effect of b value on the number of equivalent loading cycles and MSF

The effect of b on the number of equivalent uniform loading cycles is illustrated in Figure A.15 for earthquakes with M ≈ 7.5. This figure shows $N_{M=7.5}$ computed for b values of 0.06 to 0.40 for a set of 42 motions at category D sites with peak ground accelerations (PGA) of 0.11 to 0.51 g during M = 7.3-7.6 earthquakes. At any given value of b, the $N_{M=7.5}$ values varied by factors of 2 to 3. The geometric mean values for $N_{M=7.5}$ were relatively constant at about 15 for b values of 0.2 to 0.5, and then increased rapidly for b values progressively smaller than about 0.2. Also shown on this figure is the trend in mean values obtained by Kishida and Tsai (2014) based on their analyses of more than 3500 ground motion recordings at category D sites from the PEER strong ground motion database. These results, and those presented previously by Boulanger and Idriss (2007) and Dahl (2011), and in good agreement.

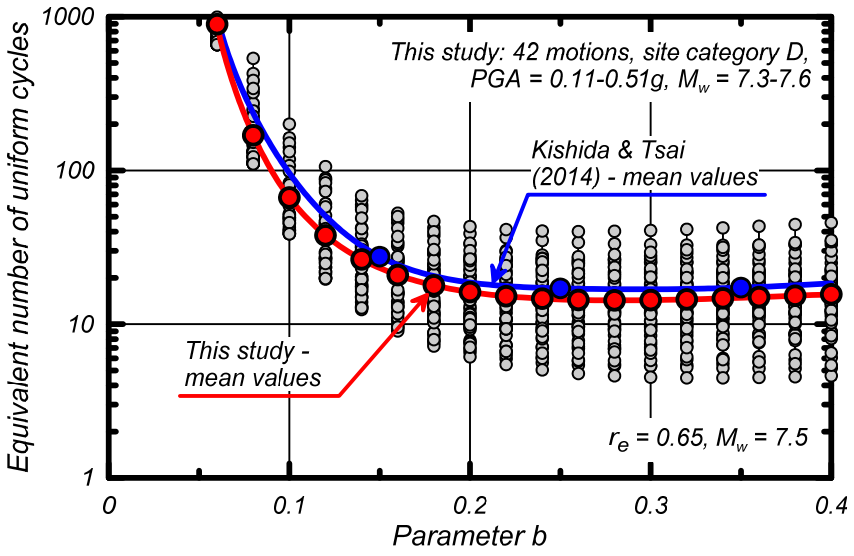

Figure A.15. Variation in number of equivalent uniform cycles with parameter b for M ≈ 7.5

The maximum value that the MSF can obtain for a small magnitude earthquake (MSF_{max}) corresponds to the case where the motion is dominated by a single strong acceleration pulse. Such a pulse could be one-sided such that it corresponds to ½ of a full cycle, or it could be symmetric so it corresponds to a full cycle. If this single pulse scenario is represented by ¾ of a cycle at its peak stress, then the equivalent number of uniform cycles at 65% of the peak stress would be (Idriss and Boulanger 2008),

$$N_{min} = \left(\frac{1.0}{0.65}\right)^{1/b} \left(\frac{3}{4} cycle\right) \tag{A.5}$$

This minimum number of equivalent cycles can be used to compute the upper limit on MSF as,

$$MSF_{max} = \left(\frac{N_{M=7.5}}{N_{min}}\right)^{b} \tag{A.6}$$

The value of MSF_{max} for a given value of b can be determined using the above equations with the $N_{M=7.5}$ results from Figure A.15. The resulting relationship between MSF_{max} and b is shown in Figure A.16. The values of MSF_{max} = 1.8 at b = 0.34 and MSF = 1.09 at b = 0.135 are consistent with the MSF_{max} values derived for sand by Idriss (1999) and for clays and plastic silts by Boulanger and Idriss (2007), respectively, as shown previously in Figure A.1. Idriss (1999) and Boulanger and Idriss (2007) assigned the MSF_{max} value to M = 5.25 events, and so the MSF values at M = 5.25 from Kishida and Tsai's (2014) results in Figure A.2 are also included on this figure for comparison. Kishida and Tsai's $MSF_{M=5.25}$ values become progressively smaller than the plotted MSF_{max} values with increasing b value, for the reasons discussed previously.

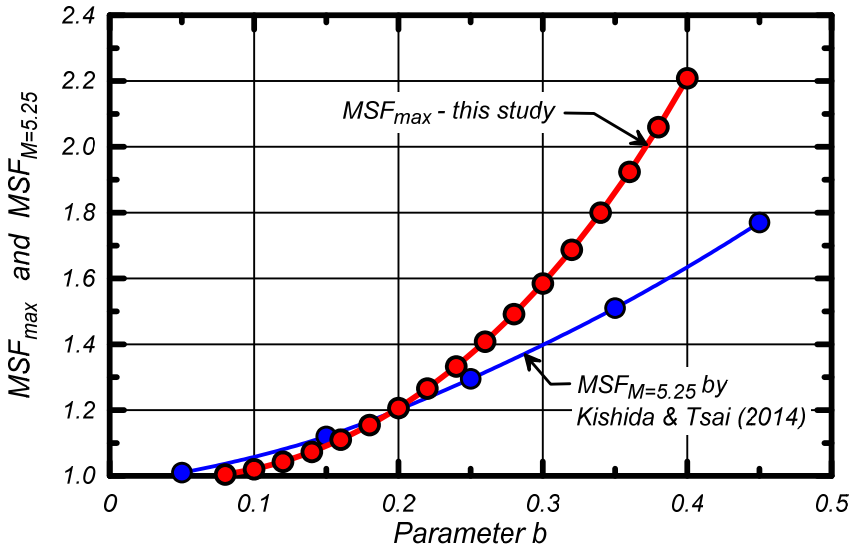

Figure A.16. Variation of MSF_{max} with parameter b

The MSF relationships used by Idriss and Boulanger (2008), as shown in Figure A.1, can be rewritten in a more general form as,

$$MSF = 1 + \left(MSF_{max} - 1\right)\left(\frac{exp\left(\frac{-M}{4}\right) - exp\left(\frac{-7.5}{4}\right)}{exp\left(\frac{-5.25}{4}\right) - exp\left(\frac{-7.5}{4}\right)}\right) \tag{A.7}$$

where they used MSF_{max} = 1.8 for sand and MSF_{max} = 1.09 for clay and plastic silt, and the form of the equation is based on MSF_{max} occurring at M = 5.25. With the fixed terms expressed numerically, the above equation becomes,

$$MSF = 1 + \left(MSF_{max} - 1\right)\left(8.64\, exp\left(\frac{-M}{4}\right) - 1.325\right) \tag{A.8}$$

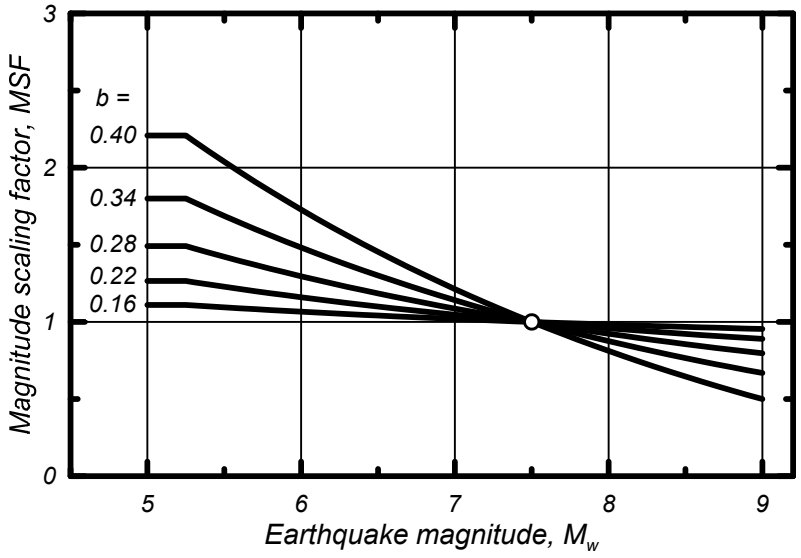

Figure A.17. Variation in the MSF relationship with parameter b

This form of the MSF relationship, coupled with a relationship between MSF_{max} and b, allows generation of MSF curves for different values of b. For example, the MSF_{max} versus b relationship shown in Figure A.16 can be used to generate the MSF curves shown in Figure A.17. These MSF curves have slightly greater dependency on M (i.e., slightly steeper curves) than those by Kishida and Tsai (2014), which were shown previously in Figure A.2.

A.5. Relating MSF to CPT penetration resistances

The last step in deriving a revised MSF for CPT-based or SPT-based liquefaction triggering procedures requires relating the parameter MSF_{max} (via the parameter b) to some combination of soil characteristics (e.g., FC, PI), CPT parameters (e.g., q_{c1N}, q_{c1Ncs}, I_c), or SPT parameters (e.g., $(N_1)_{60}$, $(N_1)_{60cs}$). The experimental data reviewed in the previous section suggests that a key parameter affecting the parameter b is the dilatancy or dilation angle for the soil; i.e., denser and stronger soils have greater CRR values and greater b values. This trend appears to hold independently of FC. The presence of fines causes CPT- and SPT-based triggering curves to shift upward (or leftward), with this upward shift attributed to the effects of the fines on the penetration resistance primarily (Cubrinovski et al. 2010). For this reason, the parameters q_{c1Ncs} and $(N_1)_{60cs}$ were preferred over q_{c1N}, $(N_1)_{60}$, or I_c as the indicator variables for dilatancy and b values.

The MSF_{max} values computed for b values from the laboratory test data reviewed in the previous section is plotted versus equivalent values of q_{c1Ncs} in Figure A.18 and equivalent $(N_1)_{60cs}$ values in Figure A.19. The equivalent q_{c1Ncs} and $(N_1)_{60cs}$ values in these figures were determined as the values for which the applicable triggering correlation produces the same $CRR_{M=7.5,\sigma'=1}$ value as obtained from the laboratory test data. This approach is consistent with the assumption of CPT or SPT based triggering correlations that those factors which affect penetration resistances also affect the cyclic strengths in reasonably proportional ways. The results of the cyclic laboratory tests were first converted to equivalent field conditions using the adjustment factors summarized in Idriss and Boulanger (2008). Alternative estimates for equivalent q_{c1Ncs} and $(N_1)_{60cs}$ values were obtained through various correlations between soil characteristics and penetration resistances, but such approaches were difficult to apply to all laboratory

data due to insufficient information for estimating penetration resistances and did not change the general trends or reduce the significant scatter observed between the MSF_{max} values and estimated penetration resistances. The MSF_{max} values remain close to about 1.1 up to q_{c1Ncs} values of about 40, after which they increase sharply with increasing q_{c1Ncs} or $(N_1)_{60cs}$. The data points for field samples obtained using frozen sampling techniques and for reconstituted soil specimens are reasonably consistent given the significant scatter in the data.

The specification of relationship between MSF_{max} and q_{c1Ncs} or $(N_1)_{60cs}$ values is not well constrained by the data in Figures A.18 and A.19 alone, and thus a number of other factors were considering in guiding the form of these relationships. First, MSF_{max} was set equal to 1.8 at $q_{c1Ncs} \approx 160$ and $(N_1)_{60cs} \approx 28$ to be consistent with the clean sand relationship Idriss (1999) developed based on the frozen sampling test data for dense Niigata sands by Yoshimi et al. (1984). Second, MSF_{max} was kept close to 1.10 for very low penetration resistances to: (1) be consistent with the values expected for low-plasticity silts based on the b values compiled by Dahl (2011) and summarized previously in Figure A.14, and (2) not be smaller than the MSF_{max} value of 1.09 developed for plastic fine-grained soils by Boulanger and Idriss (2007). Third, the scenario of a loose low-plasticity silt having a low penetration resistance was considered; e.g., for q_{c1N} in the range of 20, the resulting q_{c1Ncs} value would be about 70-80 (Figure 2.7) and this would produce an MSF_{max} close to about 1.2, which was considered reasonable for this type of soil. Fourth, the adopted MSF_{max} relationships were used to produce a family of curves showing CRR versus number of loading cycles for a range of penetration resistances, for the purpose of ensuring that the curves smoothly shift rather than pinch sharply together (further discussed and illustrated below). Fifth, the relationships between MSF_{max} and q_{c1Ncs} or $(N_1)_{60cs}$ were developed to be consistent as illustrated in Figure A.20 and described below. Sixth, the resulting MSF relationships were evaluated based on how well they reduced any apparent biases or misfits between the CPT-based and SPT-based case histories and their respective correlations. This process required several iterations, with each successive adjustment guided by consideration of all of the above factors.

The relationship between MSF_{max} and q_{c1Ncs} or $(N_1)_{60cs}$ values was re-examined using the ground motion regression results of Kishida and Tsai (2014) to describe the variation of $MSF_{M=5.25}$ with the parameter b. The results of this re-examination are plotted in Figure A.21 and A.22 showing $MSF_{M=5.25}$ versus q_{c1Ncs} and $(N_1)_{60cs}$ values, respectively. Kishida and Tsai's values for $MSF_{M=5.25}$ are smaller than the values of MSF_{max} for the same b value (Figure A.16), and thus use of their relationship lowers the data points for the same penetration resistance.

The adopted relationships between MSF_{max}, q_{c1Ncs}, and $(N_1)_{60cs}$ are given by,

$$MSF_{max} = 1.09 + \left(\frac{q_{C1Ncs}}{180} \right)^3 \leq 2.2 \tag{A.9}$$

$$MSF_{max} = 1.09 + \left(\frac{(N_1)_{60cs}}{31.5} \right)^2 \leq 2.2 \tag{A.10}$$

These MSF_{max} relationships, as plotted in Figures A.18 and A.19, A.21, and A22 are considered reasonable approximations of the available data. The consistency of the CPT-based and SPT-based forms is illustrated in Figure A.20 showing their respective MSF_{max} values versus the values of $CRR_{M=7.5,\sigma'=1atm}$ obtained from their respective deterministic correlations (Sections 4 and 6).

The resulting MSF relationships for different values of q_{c1Ncs} and $(N_1)_{60cs}$ are shown in Figure A.23. As expected, the MSF for very low penetration resistances (loose soils) is relatively flat and the MSF for high penetration resistances (dense soils) is similar to those previously used for clean sands.

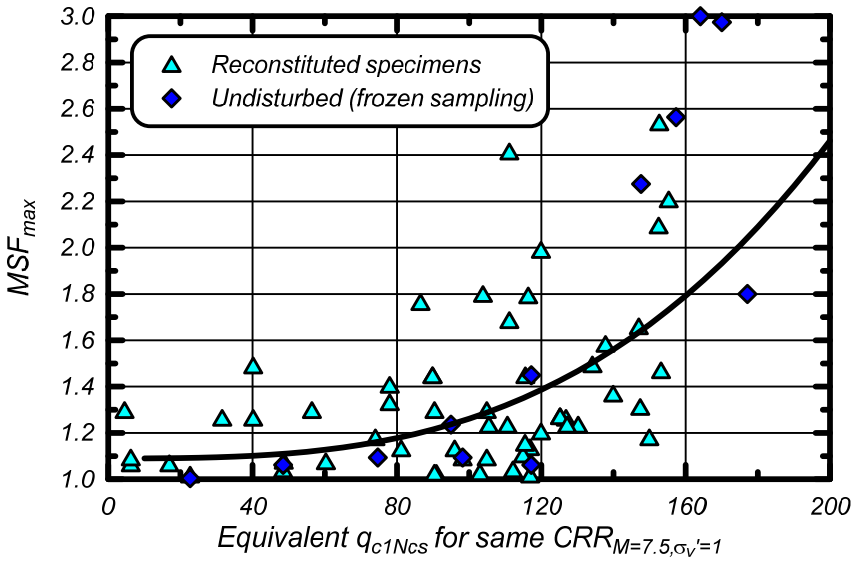

Figure A.18. Variation in MSF_{max} with equivalent q_{c1Ncs} for cohesionless soils

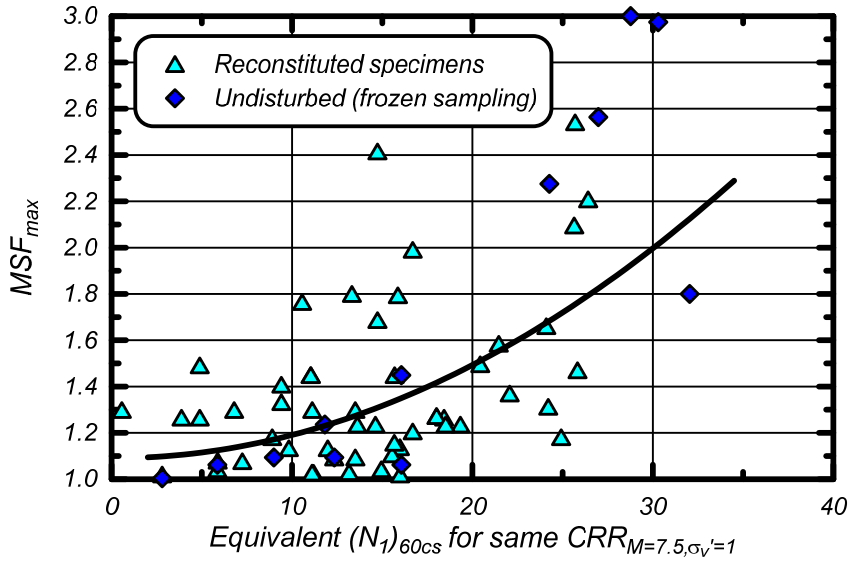

Figure A.19. Variation in MSF_{max} with equivalent $(N_1)_{60cs}$ for cohesionless soils

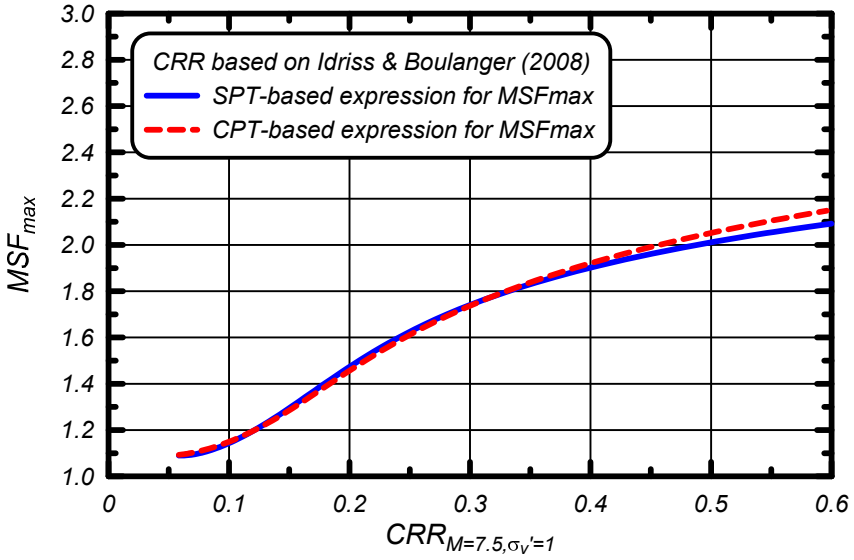

Figure A.20. Comparison of the SPT- and CPT-based equations for MSF_{max}

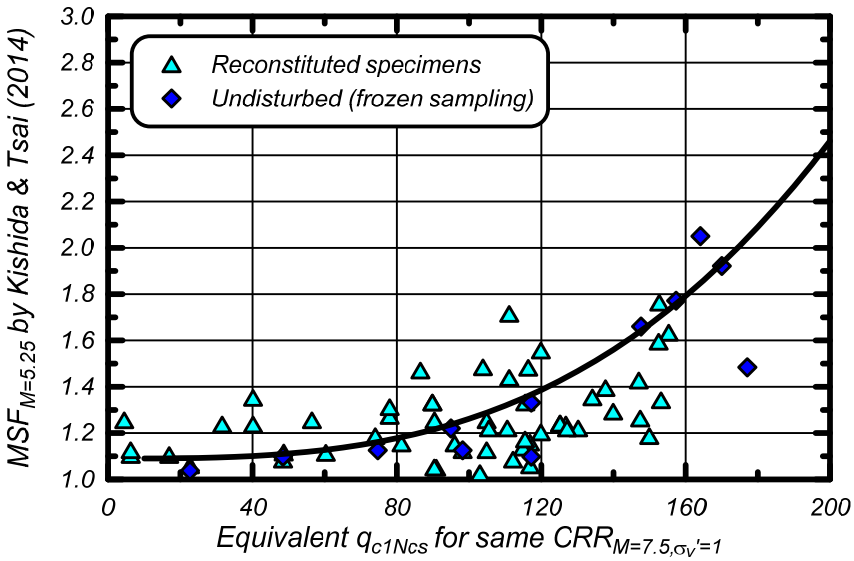

Figure A.21. Variation in $MSF_{M=5.25}$, computed using Kishida and Tsai's (2014) results, with equivalent q_{c1Ncs} for cohesionless soils

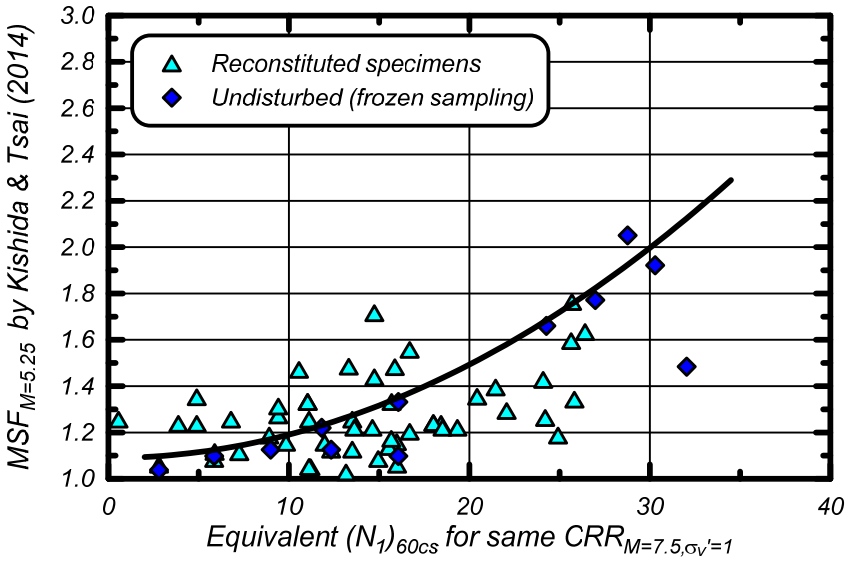

Figure A.22. Variation in $MSF_{M=5.25}$, computed using Kishida and Tsai's (2014) results, with equivalent $(N_1)_{60cs}$ for cohesionless soils

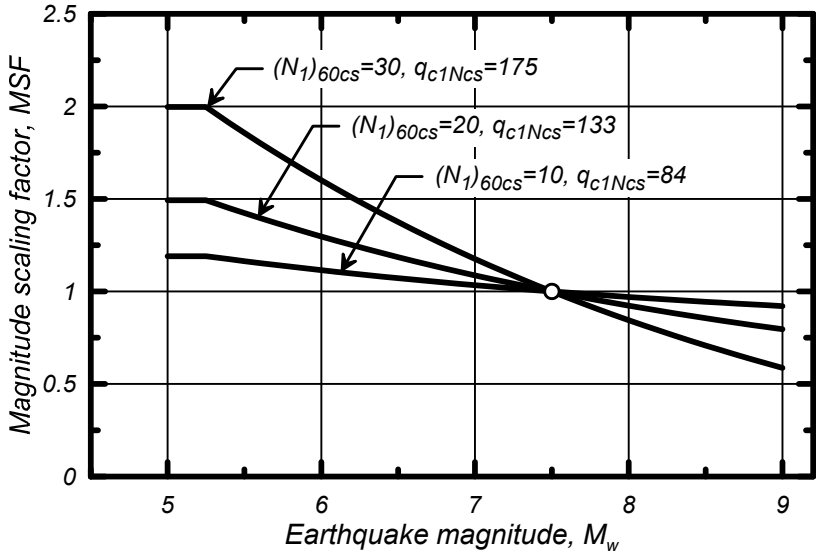

Figure A.23. Variation in the MSF relationship with q_{c1Ncs} and $(N_1)_{60cs}$ for cohesionless soils

The revised MSF relationship in combination with the liquefaction triggering correlations defines the expected CRR – N curves for sands at different penetration resistances. For example, curves of CRR versus N cycles are shown in Figure A.24 for a range of q_{c1Ncs} values. These curves are shown from 1 to 200 cycles to illustrate that the curves remain separated despite their differences in slopes; i.e., the curves will intersect at some extremely large number of loading cycles because they do not explicitly incorporate any strain threshold limits or lower limits on the CSR values below which liquefaction is not possible regardless of the number of loading cycles. This limitation is, however, not of practical significance for the current application.

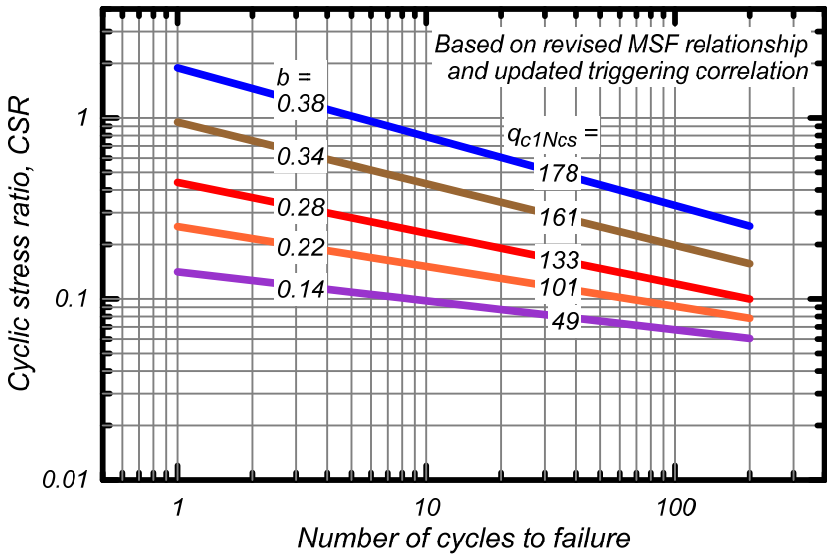

Figure A.24. Variation in CRR versus number of cycles based on the updated triggering correlation and the revised MSF relationship

The fit between the revised CPT-based and SPT-based liquefaction triggering correlations and their respective case history databases is shown in Sections 4 and 6 of the report. The revised MSF relationships were found to improve the degree of fit for both databases, providing support for assumed functional forms for this relationship. The case history data are not, however, sufficient to constrain the shape of the MSF relationships to any significant degree. In this regard, the inclusion of some dependency of the MSF on soil characteristics was an improvement over having no such dependency, even though the form of this dependency was necessarily guided by subjective judgments.

The revised MSF relationship is considerably flatter than the relationships by Ambraseys (1988) and Arango (1996). These two earlier studies concluded that the liquefaction case history database supported these steeper MSF relationships. However, the updated CPT-based and SPT-based case histories databases presented in Sections 4 and 6 were shown to be more consistent with the flatter revised MSF relationship derived herein. This difference in findings may reflect the expanded datasets from the past two to three decades and the effects of revisions to other components of the liquefaction triggering analysis framework. It is also noteworthy that Arango's (1996) MSF relationship was based on an energy-based analogy, in which CSR cycles were weighted by an exponent of 0.5. Arango's approach would therefore be expected to produce results consistent with the current framework when using b = 0.50, which would explain why Arango's relationship is much steeper than recommended herein.

A.6. Summary

A revised MSF relationship for CPT-based and SPT-based liquefaction triggering analyses was described which incorporates functional dependency on the soil characteristics [using q_{c1Ncs} as the index for the CPT procedures and $(N_1)_{60cs}$ for the SPT procedures] as well as on earthquake magnitude. The revised MSF is based on the examination of cyclic testing results for a broad range of soil types and densities, analyses of strong ground motion records to develop relationships for the equivalent number of loading cycles for different soil properties (including the work of Kishida and Tsai 2014), and the development of an MSF correlation whose form was guided by a number of other considerations. The revised MSF relationship

builds upon and utilizes findings from Idriss (1999), Boulanger and Idriss (2007), Dahl (2011), and Kishida and Tsai (2014).

The revised MSF relationship was found to improve the degree of fit between the revised CPT-based and SPT-based liquefaction triggering correlations and their respective case history databases (Sections 4 and 6 of this report). This improvement in fit with the liquefaction case histories provides support for having the MSF component of the liquefaction analysis framework include functional dependency on soil characteristics in addition to earthquake magnitude.

Additional studies are needed for further improving the models used to represent magnitude scaling effects in liquefaction triggering analyses, as these are important for extending the liquefaction triggering analyses to situations involving either small or large earthquake magnitudes. Improvements may come from refining the functional dependency on soil type (e.g., FC, fines plasticity, state) and failure criterion (see Cetin and Bilge 2012), or from improvements to the weighting function for irregular loading or the inclusion of function dependency on factors such as distance to the fault, directivity, site conditions, or depth in a soil profile (see Liu et al. 2001, Green and Terri 2005, Carter et al. 2013). For critical projects, future studies may also demonstrate the utility of site-specific adjustments, such as may be possible with advanced laboratory testing of undisturbed field samples to determine the soil parameter b in combination with detailed seismic hazard analyses to better define the loading.